Novel Metal Template Strategies for the Construction of Rotaxanes and Catenanes

Roy T. McBurney

Degree of Doctor of Philosophy

School of Chemistry

The University of Edinburgh

December 2008

Dedicated to My Family

Contents

Abstract and Layout of Thesis

The template synthesis of rotaxanes and catenanes has allowed a detailed study of their intrinsically novel and interesting properties. A key strategy has been the deployment of transition metal ions with their well-defined coordination geometries allowing high-yielding and facile preparation of interlocked architectures. Knowledge of how to exploit the coordination sphere of metal ions and the design of ligands for the creation of intermediates that are pre-disposed to undergo 'stoppering' or 'clipping' has been a crucial requirement for this approach. This Thesis is in three parts describing the use of three dimensional, two dimensional and one dimensional coordination geometries in the synthesis of interlocked architectures.

Firstly, the octahedral coordination geometry of cobalt(III) was utilized to organize dianionic pyridine-2,6-dicarboxamido ligands in a mutually orthogonal arrangement such that ring closing metathesis macrocyclizations gave access to interlocked or entwined products. A 'figure-of-eight' complex was obtained from a double macrocyclizations, whereas a catenate was accessed through a single macrocyclization. The topology of the isomers was proved by X-ray crystallography. An analogous [2]rotaxane was synthesized and the interlocked nature of the rotaxane demonstrated by ^{1}H NMR spectroscopy and mass spectrometry.

Secondly, an "active" metal template strategy, in which the metal ion plays a dual role – acting to both organize ligands and catalyze mechanical bond formation – allowed rotaxanes be constructed using the square planar coordination geometry and Lewis acidic nature of a palladium(II) complex. The interlocked nature of the rotaxane was proved by X-ray crystallography, demonstrating that a nitrile group present in the thread acted as a "station" for the Pd(II)-macrocycle. This observation led to the construction of a two "station" degenerate molecular shuttle in which the dynamics of translocation were controlled by reagent addition and observed by ^{1}H NMR techniques.

Lastly, the linear coordination geometry of gold(I) was successfully used as a template for construction of rotaxanes and catenanes via a 'clipping' strategy. The linear coordination geometry and the interlocked nature of the gold(I)-catenate was

proved by X-ray crystallography, the rotaxane architecture was proved by ^{1}H NMR spectroscopy and mass spectrometry.

Chapters Two, Three and Four are in the form of articles that have been published in peer-reviewed journals, and are reproduced, in their published format, in the Appendix. No attempt has been made to rewrite the published work; as a consequence the numbering of compounds, whilst consistent within each Chapter, is not consistent throughout this Thesis. Another consequence is that the many failed synthetic routes have been left out. I hope the reader will forgive these omissions as well as the slight repetition that occurs in the introduction and bibliography of each chapter. Additionally, preceding each Chapter is a brief synopsis that places the work in context and acknowledges the contributions of my fellow researchers.

Declaration

The scientific work described in this Thesis was carried out in the School of Chemistry at the University of Edinburgh between September 2005 and June 2008. Unless otherwise stated, it is the work of the author and has not been submitted in whole or in support of an application for another degree or qualification at this or any other University or institute of learning.

Signed.....

Date .....

Lectures and Meetings Attended and Presentations Given

1. **Organic Research Seminars**, School of Chemistry, University of Edinburgh, UK, 2005–2008.
   Oral presentations:
   i) "*Towards a Pybox Macrocycle for Interlocked Architecture Formation"*, April, 2006.
   ii) "*Studies Towards The Active-Template Synthesis of Rotaxanes"*, December, 2006.

2. **School of Chemistry Visiting Speaker Colloquia**, School of Chemistry, University of Edinburgh, UK, 2005–2008.

3. **School of Chemistry, Organic Section Firbush Symposium**, Firbush Point Centre, University of Edinburgh, UK, April 2007.
   Poster presentation: **"***The 'Active-Template' Approach to Interlocked Architectures: A Quantitative [2]Rotaxane Synthesis via Pd-Catalysed Michael Addition*".

4. **Young(-ish) Giants of Chemistry**, a scientific conference in honor of Prof. Sir J. Fraser Stoddart's 65th Birthday, Edinburgh, June, 2007.
   Poster presentation: **"***The 'Active-Template' Approach to Interlocked Architectures: A Quantitative [2]Rotaxane Synthesis via Pd-Catalysed Michael Addition*".

5. **II International Symposium on Macrocyclic and Supramolecular Chemistry (ISMSC)**, Salice Terme (Pavia), Italy, June, 2007.
   Poster presentation: **"***The 'Active-Template' Approach to Interlocked Architectures: A Quantitative [2]Rotaxane Synthesis via Pd-Catalysed Michael Addition*".

6. **36th Scottish Regional Meeting of the Organic Division of the Royal Society of Chemistry**, Glasgow, December, 2007.
   Poster presentation: *"Active Template Synthesis of Rotaxanes and Molecular Shuttles via Four-Component Pd^{II}-Catalysed Michael Additions"*, 3rd Prize.

7. **School of Chemistry, Organic Section Firbush Symposium**, Firbush Point Centre, University of Edinburgh, UK, April 2008.
   Oral presentation: "*Metal-Template Strategies for Interlocked Architecture Formation"*, 1st Prize.

8. **Graduate School of Chemistry Postgraduate Seminar Afternoon**, University of Edinburgh, UK, 2nd May, 2008.
   Oral presentation: *"Metal-Template Strategies for Interlocked Architecture Formation"*, Runner-up prize.

9. **RSC Inorganic Reaction Mechanisms/Coordination Chemistry Meeting,** Edinburgh, 18th-20th June, 2008.
   Oral presentation: *"Metal-Template Strategies for Interlocked Architecture Formation"*.

10. **III International Symposium on Macrocyclic and Supramolecular Chemistry (ISMSC)**, Las Vegas, U.S.A., 11th-18th July, 2008.
    Poster presentation: "*Gold(I) Catenane and Rotaxane Synthesis"*.

11. **USIC 2008**, Strathclyde University, Glasgow, 11th September, 2008.
    Poster presentation: *"Getting Harder: Catenane and Rotaxane Formation Using a Trivalent Transition Metal Template"*, 1st Prize.

12. **Supra-Nano 2008**, University of Birmingham, 16th-18th December, 2008.
    Poster presentation: *"Getting Harder: Catenane and Rotaxane Formation Using a Trivalent Transition Metal Template"*, 2nd Prize

Acknowledgements

I would like to thank my main supervisor Prof. Dave Leigh, whom I am eternally gratefully to, firstly for giving me the opportunity to work in his group, secondly for providing an excellently resourced laboratory in which to carry out my Ph.D studies, and thirdly for the all the knowledge passed on how to survive in the academic world. I would also like to thank Dr. Paul Lusby, my second supervisor, for his rigorous scientific approach and for helping develop my scientific skills.

My fiancée, Siân, for all that she has done for me, without her I would not have finished my first degree, let alone have written this. I would also like to thank my parents for their continuous support throughout both degrees.

During an organic chemistry Ph.D much practical work is required, necessitating two opposable thumbs. Thus, I must thank Dr. Gary Keenan at Edinburgh Royal Infirmary who stitched my thumb back together (three permanent stitches in the tendon), the result of a lively aqueous work-up one Saturday morning in August 2006. Paul Iannerelli must also be thanked for driving me to the ERI on the above occasion (and on the second occasion too!) and for cleaning up the mess (my blood, aqueous and organic layers, glass, etc.!

Visualization of interlocked architectures is key to proving their topology; as such I am deeply indebted to Prof. Alex Slawin at St. Andrews for solving all my crystal structures presented in this Thesis. Without the input, guidance and enthusiasm of the following people Steve Goldup, James Crowley, Vincent Aucagne, Euan Kay, Ai-Lan Lee, Barney Walker, Anne-Marie Fuller, Drew Thompson, Steve Mason, Monica Alvarez, and Laure-Emmanuelle Perret-Aebi, I would still be struggling away making starting materials. Sarah Pike for her camaraderie in Lab 99, and for not complaining too much when Metallica was put on the stereo. My Ph.D peers Mark Symes, Aurelien Viterisi and Kevin Hänni for stimulating and equally ridiculous conversations. Special thanks goes to Louise Hogg and Stewart Franklin for synthesizing gargantuan quantities of ‘stopper’ and other intermediates along the way. A thank you also goes out to Derek, Raymond, Kenny and Tim in Stores for

ensuring that all the chemicals and supplies I required were available. I need to extend my thanks to Tim for also driving me to work in the last two months of my stay in Edinburgh, saving me from the hell of Edinburgh's buses!

General Comments on Experimental Data

Unless otherwise stated, all reagents and solvents were purchased from Aldrich Chemicals and used without further purification. Tetrahydrofuran, dichloromethane, chloroform, acetonitrile and *N*,*N*-dimethylformamide were dried using a solvent purification system manufactured by Innovative Technology, Newburyport, MA, USA. 4-[*Tris*(4-*tert*-butylphenyl)methyl]-phenol, 2,6-*bis*(3-(4-hydroxyphenyl)-propyl)-pyridine and 1-(*bis*(4-*tert*-butylphenyl)(4-(pent-4-ynyloxy)phenyl)methyl)-4-*tert*-butylbenzene were prepared according to literature procedures. Unless otherwise stated, all reactions were carried out under an atmosphere of nitrogen at room temperature. Column chromatography was carried out using Silica 60A (particle size 35-70 μm, Fisher, UK) as the stationary phase, and TLC was performed on precoated silica gel plates (0.25 mm thick, 60 F_{254}, Merck, Germany) and observed under UV light. By petrol is meant the fraction of petroleum ether boiling between 40 ºC - 60 ºC. All chemical reactions involving gold(I) complexes were carried out in the absence of light whenever possible. ^{1}H spectra were recorded on Bruker AV 400, Bruker DMX 500 and Bruker AVA 600 instruments whilst all ^{13}C NMR spectra were recorded on a Bruker AV 400 instrument. Chemical shifts are reported in parts per million (ppm) from low to high frequency and referenced to the residual solvent resonance. Coupling constants (*J*) are reported in hertz (Hz). Standard abbreviations indicating multiplicity were used as follows: s = singlet, d = doublet, t = triplet, dd = double doublet, q = quartet, m = multiplet, b = broad, ddd = doublet of double doublets. Melting points (m.p.) were determined using a Sanyo Gallenkamp apparatus and are reported uncorrected. Mass spectrometry was carried out by the services at the University of Edinburgh and the EPSRC National Mass Spectrometry Service Centre, Swansea, UK.

CHAPTER ONE

Metal Template Synthesis of Catenanes, Rotaxanes, Knots and Links

Acknowledgements

Dr. Paul Lusby and Dr. Steve Goldup are gratefully thanked for their proof-reading of this introduction. The "active" metal template section of this introduction formed the basis of a tutorial review, thus I must thank all my fellow contributors for making this review happen: James D. Crowley, Stephen M. Goldup, Ai-Lan Lee, David A. Leigh and Roy T. McBurney, *Chem. Soc. Rev*., **2009**, DOI: 10.1039/b804243h.

Synopsis

There exists a plethora of strategies available for today's synthetic chemist to utilize in the construction of mechanically interlocked and entwined architectures. Rotaxanes, catenanes, knots and Borromean rings have all been successfully accessed via template methods in which metal ions play a pivotal role. The success of this strategy is the application of well-defined metal coordination geometries as templates that gather and organize building blocks such that subsequent covalent capturing reactions generate the interlocked or entwined structures. A major development saw the "passive" role of the metal ion evolve into an "active" role; in addition to gathering and organizing ligands, the metal ion can also catalyze covalent and mechanical bond formation, furnishing the interlocked structure. Furthermore, using the "active" template approach a stoichiometric quantity of the metal template ion is not always required as it is possible for the metal ion to turn over during the catalytic cycle. This introduction focuses on entangled structures based on discreet molecules, specifically catenanes, rotaxanes, knots and links, in which removal of the metal ion template does not cause dissociation of the interlocked sub-components.

1.1 Ordering and Entwining about a Metal Template

1.1.1 Historical Background

Sauvage's achievement of using a metal-ligand coordination geometry as a template for the synthesis of a catenane was a revolutionary step forward.[1] The methodology allowed, for the first time, a feasible synthesis of interlocked and entwined structures. The basis of Sauvage's strategy was the knowledge that metal ions provide an excellent template for the synthesis of macrocycles, first exemplified by the work of Daryle Busch and co-workers. Busch used the square planar coordination geometry of nickel(II) as a template in the synthesis of a tetradentate macrocycle from α-diketone **1** and mercaptoethylamine (**2**) in 70% yield (Scheme 1.1).[2] The Ni(II) ion gathered the newly formed tetradentate ligand (**3**) such that both reactive end-groups were brought close in space, or put another way, Ni(II) forced the ligand into a 270° turn around the metal ion. Here Ni(II) is acting as a kinetic template, as this arrangement of the ligand favors intra-molecular cyclization such that addition of 1,2-*bis*-(bromomethyl)benzene (**4**) to chelate **3-Ni(II)** afforded Ni(II)-macrocyclic complex **5-Ni(II)**.[3]

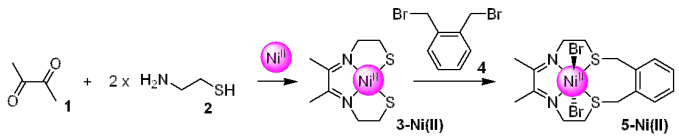

Scheme 1.1. Ni(II) as a kinetic template in the synthesis of tetradentate nitrogen containing macrocycles.[2, 3]

Furthermore, Busch demonstrated what he described as the "thermodynamic template effect", whereby complex mixtures converged into a common product upon the addition of metal ions. The five component self-assembly, using reversible imine-bond formation, of four equivalents of *o*-aminobenzaldehyde **6** and a divalent ion, Cu(II) or Ni(II), produced metallo-macrocycle **7** (Scheme 1.2).[4] Additionally, tridentate macrocycle **8** was isolated.[5] The condensation of ketones and amines in

the presence of metal salts was also exploited by Curtis and Hay in the construction of macrocycles.[6]

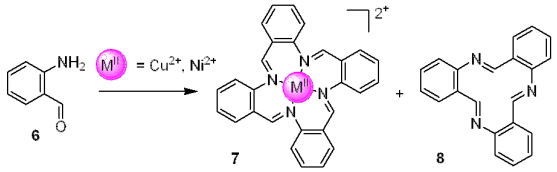

Scheme 1.2. Ni(II) as a thermodynamic template in the synthesis of tri- and tetra-dentate nitrogen containing macrocycles.[4,5]

Busch also demonstrated that metal ions could also be used to gather reactive molecules to form complex three dimensional structures. 2,6-diacetylpyridine (**9**) undergoes condensation, in the presence of Fe(III), with triethylenetetraamine to form a five coordinate complex. The condensation of **9** with tetraethylenepentaamine (**10**) produced hexadentate octahedral complex **11-Fe(III)** (Scheme 1.3).[7]

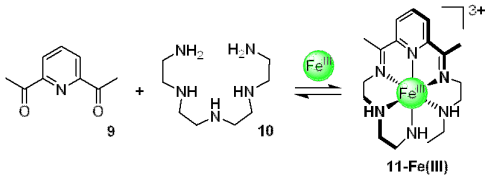

Scheme 1.3. The use of Fe(III) allowed the construction of macrocycle **11-Fe(III)** from 2,6-diacetylpyridine (**9**) and tetraethylenepentaamine (**10**).[7]

The aldehyde-amine condensation in the presence of metal ions has also used by the group of Urbach to form various helicate complexes (Scheme 1.4).[8] With no metal ion present, the condensation between three equivalents of 2-formyl-pyridine (**12**) and one equivalent of *tris*-(aminomethyl)ethane (**13**) led to cross-condensed product **14**. **14** undergoes a rearrangement upon treatment with Fe(II) (but not Co(III), Ni(II), or Zn(II)) to form helicate **15-Fe(II)**. To generate the desired helicates (**15**), the initial condensation was performed in the presence of metal ions, such as Fe(II), Co(III), Ni(II), and Zn(II). Interestingly the same condensation, but using Mn(II) or Cu(II), resulted in **13** condensing with only two pyridyl molecules, generating N_5-complexes **16-Mn(II)** and **16-Cu(II)**.

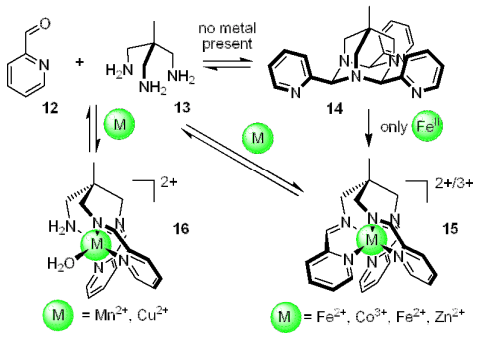

Scheme 1.4. Imine bond formation in the construction of helicates **15** and **16** from 2-formyl-pyridine (**12**) and *tris*-(aminomethyl)ethane (**13**) around various octahedral ions.[8]

Lehn and co-workers have also exploited coordination chemistry for the creation of synthetic helicates. Coordination of two quarterpyridine ligands to two copper(I) ions led to the formation of a simple entwined complex.[9] Larger helicate assemblies were constructed using longer ligands featuring additional bipyridine (bipy) units: homo-duplex tri-,[10a, b] tetra-[10c] and penta-nuclear[10c] helicates and also hetero-duplex helicates[10d] were assembled. Appending nucleosides to helicates was also achieved, with the resultant structures resembling 'inside-out' DNA.[11] More exotic assemblies were formed in conjunction with anion templates. In the presence of chloride ions five-membered circular double helicate **17-Fe(II)** was formed (Scheme 1.5),[12a] while a six-membered circular double helicate was formed in the presence of sulfate anions.[12b]

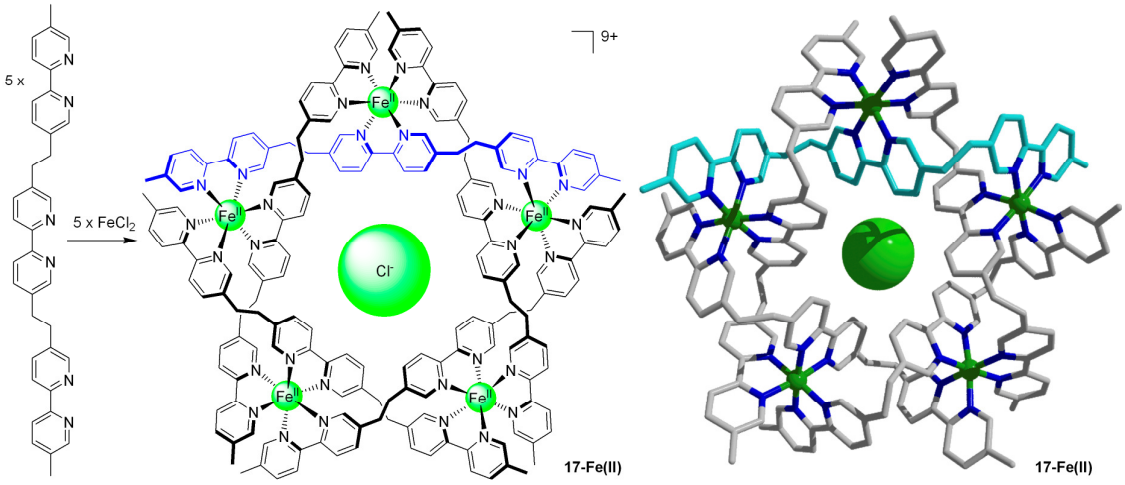

Scheme 1.5. A circular double helicate assembly **17-Fe(II)**, constructed using five Fe(II) ions that organize five polypyridine ligands around an anion template.[12a] The crystal structure (right) revealed the constitution of the complex, one polypyridine ligand is shown in blue and protons and counterions have been omitted for clarity.

1.1.2 Metal-Template Strategies to Mechanically Interlocked and Entwined Molecular Architectures

The predictable nature of metal-ligand coordination geometries coupled with the relative strength of these interactions makes them an attractive proposition for assembling interlocked architectures. Building on this concept, Solokov discussed the possibility of using an octahedral metal ion as a template for the assembly of a catenane.[13] Indeed, the entire range of simple (coordination number ≤ 6, see Figure 1.1 for examples of coordination geometries and the possible modes of coordination) metal-ligand coordination geometries have since been used as templates in the construction of many rotaxanes, catenanes, knots and links.

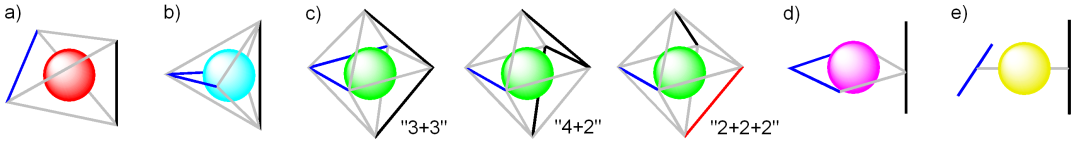

Figure 1.1. The range of simple (coordination number ≤ 6) metal-ligand coordination geometries utilized in the construction of rotaxanes, catenanes, knots and links. Three dimensional (a) tetrahedral with a "2+2" coordination mode, (b) trigonal bipyramidal with a "2+3" mode (c) octahedral with either "3+3", "4+2", or "2+2+2" modes, two dimensional (d) square planar with a "3+1" mode, and one dimensional (e) linear using a "1+1" coordination mode.

Crucial to the synthesis of interlocked architectures is an understanding of the factors lying at the heart of the metal template methodology, as shown in Figure 1.2. The metal ion acts as an anchor to gather and organize ligands around its coordination sphere. This is achieved through coordination of a metal ion to the binding sites present on the ligands (dark blue segments, Figure 1.2). Once arranged about the metal ion, the conformations of the ligands act to generate crossing-points by either (1) the use of structural rigidity, *i.e.* ligands that possess a pre-organized turn, or (2) taking advantage of secondary non-covalent interactions that promote the formation of crossing-points. Establishment of crossing-points positions the reactive termini in an appropriate spatial orientation such that subsequent intra- or inter-ligand cyclizations lead to interlocked or entwined products.

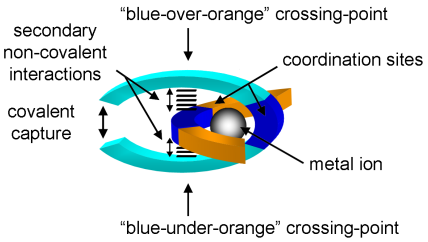

Figure 1.2. A simple diagram illustrating the importance of both the metal ion (grey sphere) acting to gather and organize ligands, and the ligands acting to produce a turn around the metal centre in order to generate crossing-points. Secondary non-covalent interactions help to organize flexible ligands, promoting entwining; rigid ligands possess a structure that completes a pre-organized turn about the metal ion.

1.2 "Passive" Metal Template Synthesis of Rotaxanes and Catenanes

1.2.1 "Passive" Metal Template Strategies

Scheme 1.6 summarizes the main strategies for the construction of catenanes and rotaxanes using a "passive" metal template. The catenane double 'clipping' strategy (Scheme 1.6a, i) involves two intra-ligand macrocyclizations of a pre-interlocked species. The 'threading-followed-by-clipping' strategy (Scheme 1.6a, ii) necessitates that an acyclic component be threaded through a cyclic component, with subsequent intra-ligand cyclization. The 'clipping' strategy for rotaxanes (Scheme 1.6b, i) requires a pre-macrocycle to be coordinated to a thread before cyclization of the pre-macrocycle around the thread. An alternative rotaxane strategy is 'threading-followed-by-stoppering' (Scheme 1.6b, ii) involving the threading of an axle through a cyclic component prior to reactions that install bulky 'stopper' units.

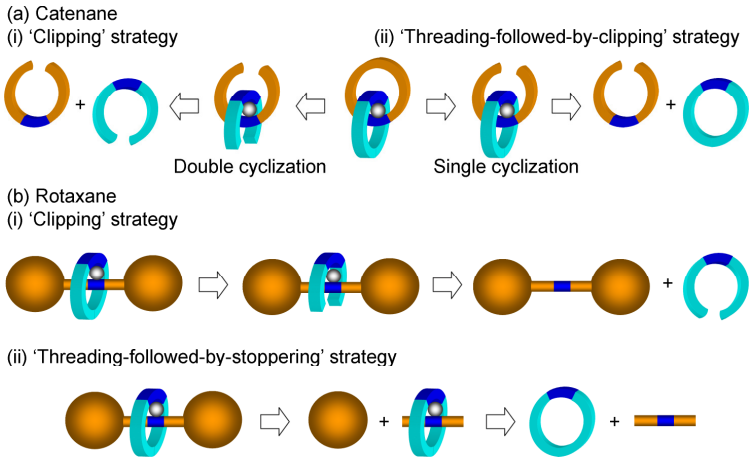

Scheme 1.6. A general overview of the "passive" metal template strategies to rotaxanes and catenanes.

1.2.2 Tetrahedral Geometries

1.2.2.1 Sauvage's Cu(I)-Phen Catenane Strategy

From research into macrocycles based on a 2,9-diphenyl-1,10-phenanthroline (phen) unit,[14] Sauvage and co-workers realized that these ligands in combination with a tetrahedral metal ion, such as copper(I), could be used to construct interlocked structures.[1, 15] The rigid phen ligands proved ideal for this purpose as they are pre-organized for a 120° degree turn about the metal ion. Coordination of two phen ligands to copper(I) results in the ligands adopting a mutually orthogonal alignment. The reactive end-groups are setup to undergo intra-ligand cyclization to afford the interlocked species. Catenate **18-Cu(I)** was accessed in two ways; by a single cyclization of a macrocycle-Cu(I)-phen complex or by double cyclization of a phen-Cu(I)-phen complex. First to be reported was the single cyclization approach; phen-based macrocycle **19** and acyclic ligand **20** were coordinated to Cu(I) generating complex **21-Cu(I)** (Scheme 1.7a).[16a] Single intra-ligand cyclization *via* Williamson alkylation of the phenol end-groups with diiodo-polyether **22** generated catenate **18-Cu(I)** in 42% yield. The second approach followed a double macrocyclization strategy; two equivalents of acyclic phen ligand **23** were complexed to copper(I) to give pre-catenate **23-Cu(I)**. Subsequent double macrocyclizations afforded catenate **18-Cu(I)** in 27% yield (Scheme 1.7b).[16b] The yields reflect the ease with which

catenate **18-Cu(I)** is formed - 27% *via* double cyclization *vs* 42% *via* single cyclization.

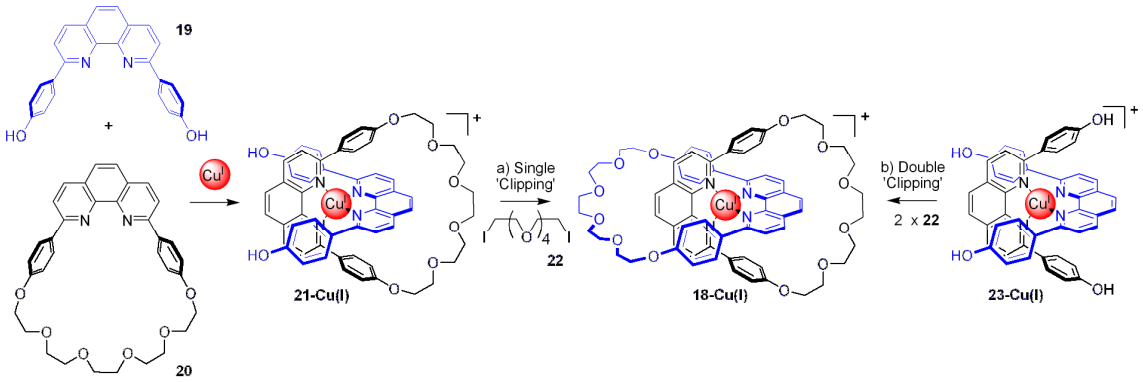

Scheme 1.7. Cu(I)-phen catenate synthesis *via* (a) a single macrocyclization,[16a] and (b) double macrocyclization.[16b]

In 1997, a collaboration between the groups of Sauvage and Grubbs saw a significant advancement in catenane construction with the application of a new olefin metathesis catalyst (**24**) developed by Grubbs.[17] Double intra-ligand RCM macrocyclizations between the terminal olefins of pre-catenate **25-Cu(I)** generated catenate **26-Cu(I)** in 92% yield (Scheme 1.8); single macrocyclizations gave similar yields of catenate.[18]

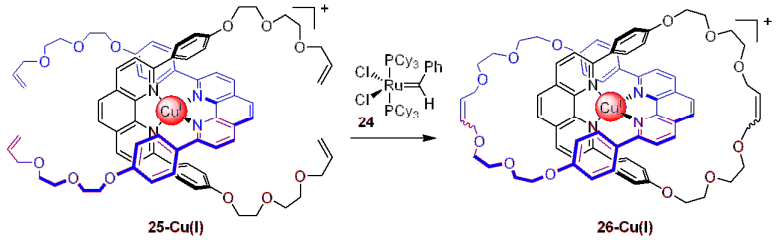

Scheme 1.8. The application of a new olefin metathesis catalyst (**24**) led to the synthesis of catenate **26-Cu(I)** in near quantitative yield.[18]

Catenate **18-Cu(I)** can be demetallated by treatment with potassium cyanide, quantitatively affording metal-free catenand **18** (Scheme 1.9).[16b] Sauvage introduced the nomenclature of naming catenanes derived from a metal template strategy and still containing a metal ion as "catenates", and the demetallated analogues as "catenands". Although ^{1}H NMR analysis and mass spectrometry

evidence of both catenate and catenand pointed toward an interlocked topology, it was X-ray crystallographic analysis that provided the conclusive evidence of the molecular topology.[19] The crystal structure of metal-complexed catenate **18-Cu(I)** (Scheme 1.9, bottom right) shows a distorted tetrahedral geometry around a central Cu(I) ion which is ligated *via* four *N*-donor atoms to the phen units. In contrast, metal-free catenand **18** (Scheme 1.9, top right) adopts a different co-conformation; the two phen units, no longer held together by coordination to Cu(I), have swung to the periphery of the structure and now point away from each other. This is presumably as a result of lone-pair repulsion, although the non-coordinated sub-components are free to rotate in solution, unless bulky groups are incorporated to prevent rotation.[20]

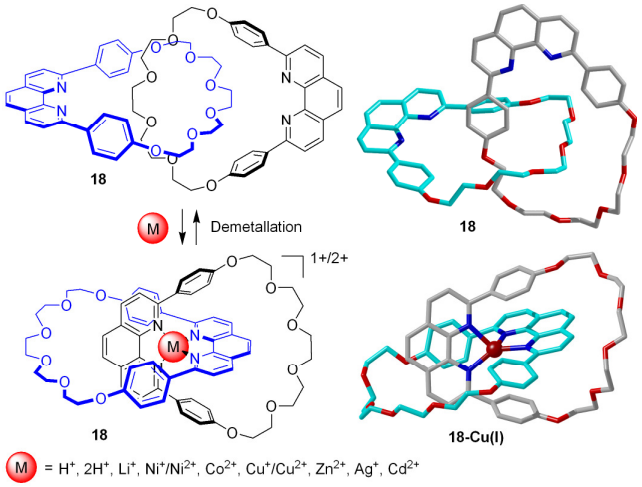

Scheme 1.9. Catenate **18-Cu(I)** was demetallated generating metal-free catenand **18**[16b] to which many other metal ions were complexed in later studies.[21, 22] The crystal structures of both catenate **18-Cu(I)** (bottom right) and catenand **18** (top right) proved the interlocked topology of the molecules.[19] The atoms of one ring are colored blue and the other ring grey, Cu(I) dark red, oxygen red, nitrogen blue, the counter-ion and protons have been omitted for clarity.

It was also shown that the template metal ion could be re-introduced to the catenand (Scheme 1.9). In addition, the catenand could coordinate a range of other metal ions, including Li(I), Co(II), Zn(II), Ag(I), Cd(II),[21a] Ni(I), Ni(II),[21b] Pd(II).[21c] Furthermore, single and double protonation of catenand **18** with perchloric acid led

to a similar co-conformational rearrangement as observed for other catenates (Scheme 1.9).[22]

1.2.2.2 Cu(I)-Phen-Imine Catenane Strategy

Recently Nitschke and co-workers published the synthesis of a novel di-copper(I) catenate which also contained functionalized phen units as chelating groups.[23] However, unlike Sauvage's earlier syntheses - which proceeded *via* kinetically stable intermediates - copper(I) catenate **27-Cu(I)** (Scheme 1.10) was formed under thermodynamic control through the condensation reaction of dianiline **28** and 2,9-diformyl-1,10-phenanthroline (**29**). It is presumed that each Cu(I) ion is datively bonded to two imine nitrogens and two phen nitrogens. Unfortunately, the unique coordination motif could not be verified in the solid-state. Instead, the interlocked nature was proved *via* molecular mechanics calculations, mass spectrometry and NMR studies, in which signals were observed between the phen protons and the alkyl protons located on the adjacent ring. In addition, catenate **27-Cu(I)** was successfully demetallated to afford catenand **30** (Scheme 1.10). This was achieved by first reducing the imine bonds (essential to stop imine metathesis and kinetically fix the interlocked structure) and secondly by reacting with ethylenediaminetetraacetic acid (EDTA) under basic conditions to remove the copper ions.

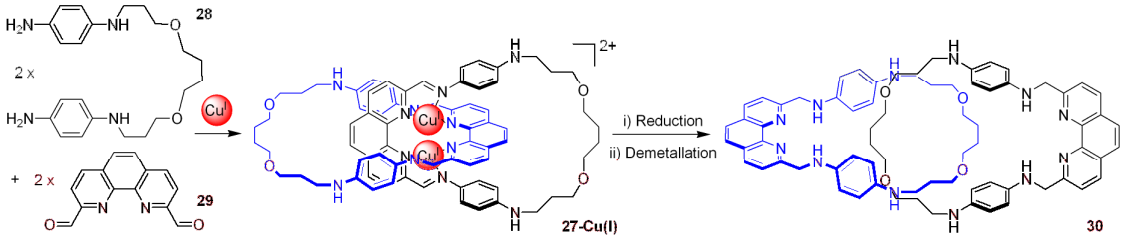

Scheme 1.10. A Cu(I) catenate **27-Cu(I)** constructed around a novel di-copper(I) template that directed imine bond formation between aniline **28** and aldehyde **29**. Reduction of the imines to amines and removal of the metal ions yielded catenand **30**.[23]

Reaction of **29** with a diamine analogue of **28**, that contains a shorter and more flexible amine, resulted in the self-assembly of a macrocycle twisted into a helical structure through the coordination of two copper(I) ions.[24] Demonstrating that

control over product topology could be achieved by appropriate selection of reaction components, based on properties such as rigidity and length.

1.2.2.3 Cu(I) Rotaxane Strategy

Surprisingly, it was not until eight years after the publication of the first copper(I)-phen [2]catenate **18-Cu(I)**[16a] that a [2]rotaxane based on the same motif was published.[25] Gibson and co-workers demonstrated that Sauvage's pre-catenate complex (**21-Cu(I)**) could be alkylated with bulky 'stopper' units to generate, after demetallation with solid-supported cyanide, metal-free [2]rotaxane **31** in 42% yield (Scheme 1.11). The interlocked nature of rotaxane **31** was proved by mass spectrometry and ^{1}H NMR comparison of the compound to macrocycle and the thread side-product.

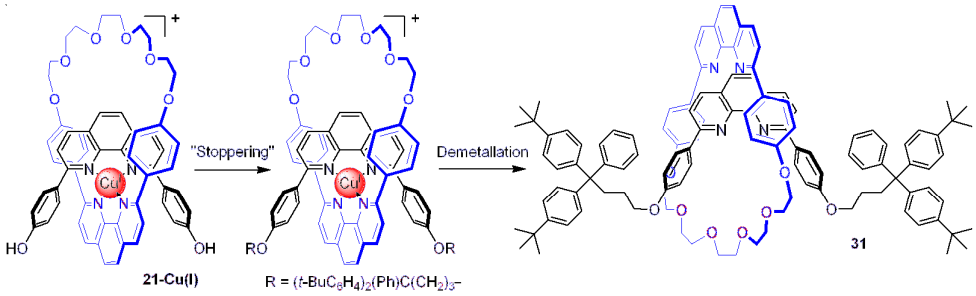

Scheme 1.11. Installation of 'stopper' units onto complex **21-Cu(I)** led the construction of [2]rotaxane **31**.[25]

A year later Sauvage synthesized his first [2]rotaxane.[26] A pre-rotaxane complex was 'stoppered' *via* a reaction in which a second porphyrin unit was installed to generate a rotaxane in 25% yield (Scheme 1.12). Zinc(II) was introduced to the newly formed porphyrin 'stopper' unit to generate trimetallic rotaxane **32-Cu(I)**. Incorporation of metallo-porphyrins has allowed Sauvage to study electron transfer processes in both rotaxane and catenane architectures.[27]

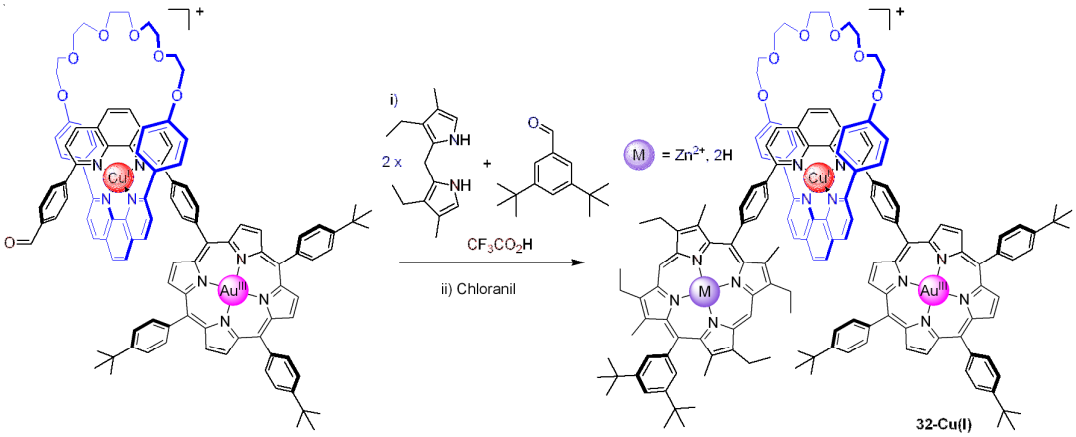

Scheme 1.12. Synthesis of a porphyrin 'stoppered' [2]rotaxane assembled using the Cu(I)-phen motif.[26]

Sauvage has also synthesized rotaxanes by a copper(I) catalyzed azide-alkyne 1,3-cycloaddition (CuAAC) 'stoppering' reaction (Scheme 1.13). Subjecting azide functionalized pre-rotaxane complex **33-Cu(I)** to a CuAAC reaction, in the presence of alkyne functionalized 'stoppers' (**34**), yielded rotaxane **35-Cu(I)** in 62% yield.[28a] A later study saw the replacement of the thread bipy unit with a phen-based unit and as expected the Cu(I)-phen-phen complex proved more stable to the reaction conditions and resulted in an increased yield (67%) of rotaxane obtained.[28b]

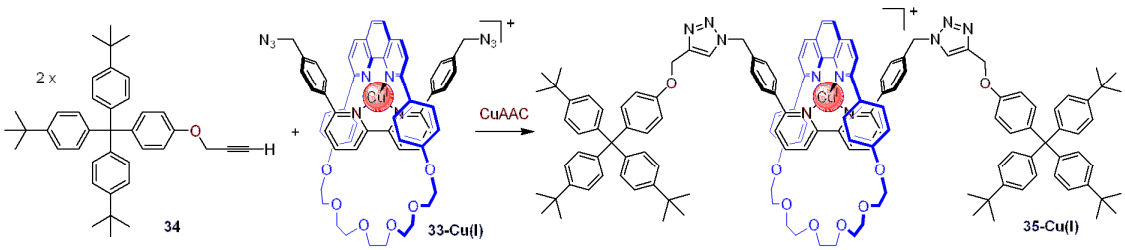

Scheme 1.13. Synthesis of rotaxane **35-Cu(I)** *via* CuAAC reactions between pre-rotaxane **33-Cu(I)** and alkyne 'stopper' **34**.[28a]

1.2.2.4 [*n*]Catenanes and [*n*]Rotaxanes

Sauvage has published a wide body of work exemplifying the versatility of the Cu(I)-phen motif, including its successful application to the synthesis of higher order catenanes and rotaxanes. In 1985 the synthesis of a [3]catenane using Williamson macrocyclization reactions was reported.[29] Exploiting poly-ethylene linkers that

were too short to undergo intra-ligand cyclization, Sauvage hoped to promote a "1+1" inter-molecular reaction to generate the desired [3]catenates, unfortunately the yield was very low (~2%). An alternative approach relied on the oxidative coupling of terminal acetylene groups of threaded complex **36-Cu(I)** to generate [3]catenane **37-Cu(I)** in 58% yield (Scheme 1.14).[30] The synthesis also gave a tri-metallic complex in 22% yield, which was proposed to be a [4]catenate consisting of a central hexayne 66-membered ring interlocked with three 30-membered rings. These catenates were demetalated using KCN and crystal structures of both Cu(I) [3]catenate[31a] **37-Cu(I)** (Scheme 1.14, right) and the corresponding metal-free [3]catenand were published.[31b] Higher order homologues of these catenates were by-products in this synthetic approach. Electrospray mass spectrometry of a crude reaction mixture identified multi-ring [*n*]catenates of up to *n* = 7 (Scheme 1.14).[32]

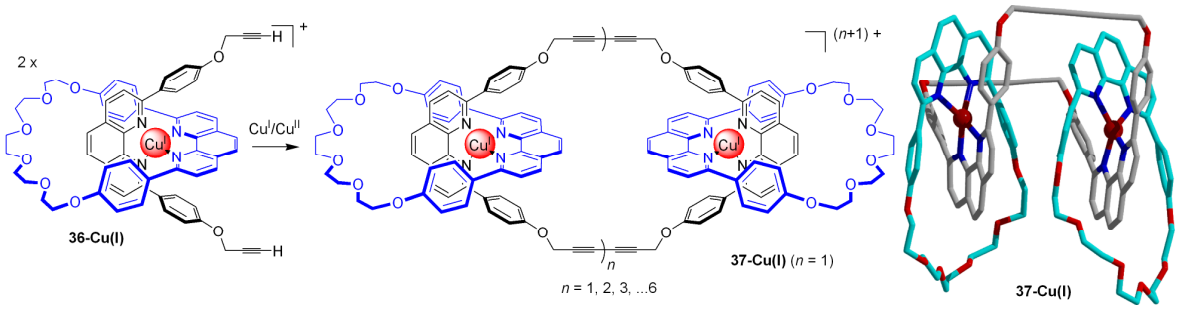

Scheme 1.14. An [*n*]catenate[30] synthesis using oxidative alkyne couplings on pre-catenate **36-Cu(I)** to generate [3]catenate **37-Cu(I)**. Higher order catenanes, up to [7]catenates, were observed by mass spectrometry.[32] The crystal structure of [3]catenate **37-Cu(I)** (right) proved the topology of the interlocked molecule.[31a]

In order to selectively generate [3]catenates, Sauvage and co-workers opted to use a single-cyclization approach. Two small phen-based macrocycles were coordinated using Cu(I) to a *bis*-phen pre-macrocycle featuring terminal alkynes. Again, using a Glaser coupling to 'clip' the central ring, a [3]catenate was generated in 48% yield.[33] RCM reactions were later applied to the synthesis of [3]catenanes by the group of Mayer.[34] Coordination of two Cu(I) ions to a large *bis*-phen macrocycle and two smaller acyclic phen-based ligands possessing terminal olefins generated a

pre-[3]catenate. Subsequent double intra-ligand RCM cyclizations led to a [3]catenate in 71% yield.

The synthesis of [*n*]rotaxanes was achieved through porphyrin formation to install both 'stopper' and central porphyrin groups onto a pre-rotaxane, assembled using the Cu(I)-phen motif.[35] The porphyrin and phen coordination sites could each be selectively remetallated, giving rise to a variety of homo- and hetero-metallic [*n*]rotaxanes.[36]

1.2.2.5 Stimuli Responsive Structures Based on a Cu(I)-Phen Motif

The Cu(I)-phen motif has been used to create structures in which the position of the interlocked sub-components can be controlled. A collaboration between the groups of Sauvage and Stoddart saw the trademark template motifs of both groups incorporated into [2]catenate **38-Cu(I)** (Scheme 1.15)[37] A Cu(I)-phen motif was used to organize the ligands prior to a 'clipping' reaction *via* alkylation to form a new tetrapyridinium macrocycle. Coordination to Cu(I) forces the phen units to be orientated at the centre of the catenate. Upon removal of the metal ion, catenand **38** undergoes a co-conformation rearrangement such that the π-electron rich /π-electron deficient components interact at the centre of the catenane.

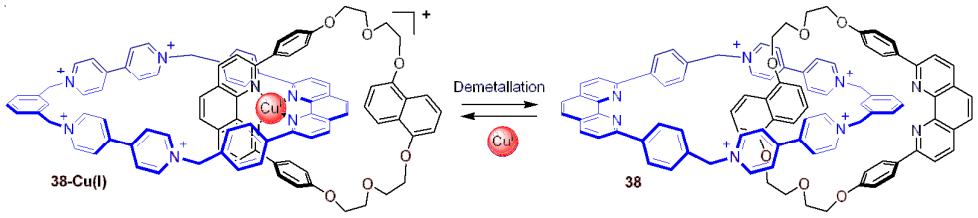

Scheme 1.15. Catenane **38** relies on metallation/demetallation to control the orientation of the macrocyclic rings relative to each other.[37]

Sauvage and co-workers have also synthesized a catenate in which one contains both a phen unit a tridentate terpy unit as a second metal binding site.[38] Here, positional control was achieved by exploiting the Cu(I)/Cu(II) redox couple. In the monovalent state the two phen units ligate the copper ion in its preferred tetrahedral coordination mode (Scheme 1.16, **39-Cu(I)**). Oxidation to the divalent state leads to a co-

conformational rearrangement such that copper(II) is ligated to one phen unit and the terpy unit in a trigonal bipyramidal coordination mode (Scheme 1.15, **39-Cu(II)**).[39]

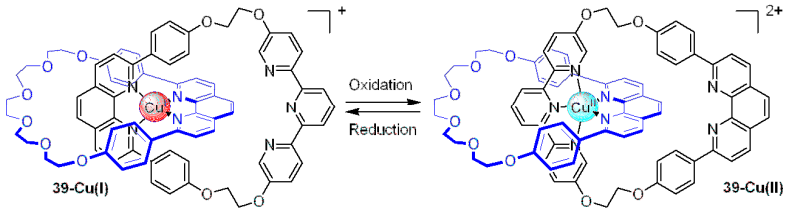

Scheme 1.16. Catenane **39** relies on redox chemistry of Cu(I)/Cu(II) to control the co-conformation of the macrocycles between tetradentate (phen-phen) and pentadentate (phen-terpy) coordination modes.[39]

Incorporating both phen and terpy units into the thread of a rotaxane, Sauvage exploited the same Cu(I)/Cu(II) driven co-conformation positional control in the translational movement of a phen-based macrocycle between the two stations in rotaxane **40-Cu(I)** (Figure 1.3).[40] Furthermore, a rotaxane was synthesized in which the thread contained just one phen unit and the macrocycle contained both phen and terpy units.[41] Using the Cu(I)/Cu(II) redox couple controlled rotation of the macrocycle around the thread was achieved.

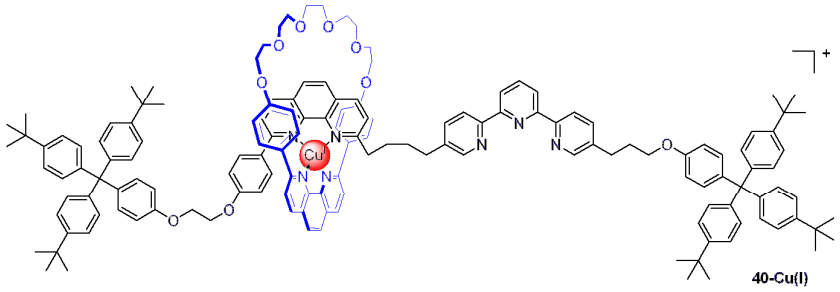

Figure 1.3. Rotaxane **40-Cu(I)** exploits the redox chemistry of Cu(I)/Cu(II) to control the position of the macrocycle on the thread.[40c]

1.2.2.6 Non-Interlocked Assemblies Based on the Cu(I)-Phen Motif

Sauvage's Cu(I)-phen template coordination motif has also been used to construct various non-interlocked assemblies.[42] Phen-based macrocycle **20** was dimerized to create a *bis*-macrocycle. The addition of four equivalents of Cu(I) ions to two equivalents of the *bis*-macrocycle and two equivalents of a *bis*-bipy axle generated

tetramer **41-Cu(I)** (Scheme 1.17).[43] It was hoped that the two threads could be covalently linked, generating a novel class of interlocked architecture, however all attempts were unsuccessful.

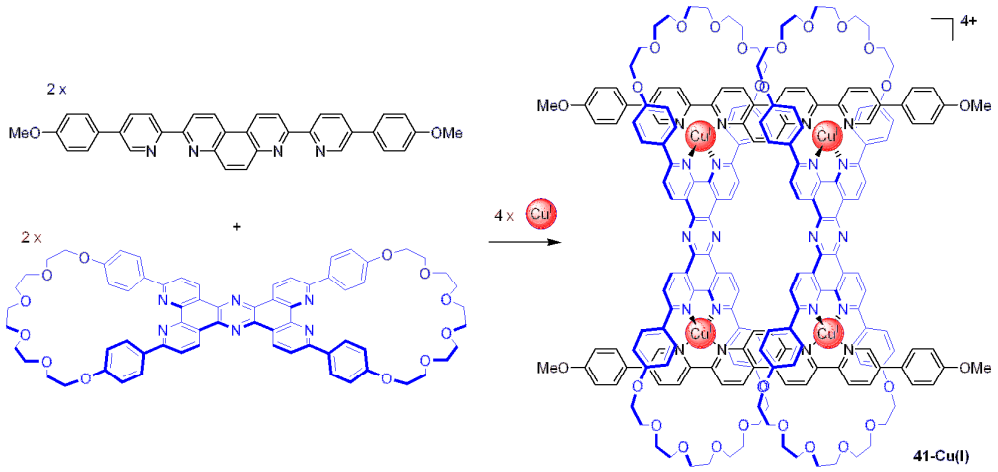

Scheme 1.17. A pseudo-[4]rotaxane **41-Cu(I)** constructed using four Cu(I) ions to coordinate two *bis*-macrocycles and two linear polypyridine axles.[43]

1.2.3 Trigonal Bipyramidal Geometries

The only example of interlocked architectures assembled around a 5-coordinate metal template comes from the Sauvage group. Zinc(II) was used in combination with bidentate and tridentate ligands to assemble catenate **42-Zn(II)** (Scheme 1.18).[44] Complexation of a tridentate terpy-based macrocycle with $Zn(OTf)_2$ yielded **43-Zn(II)**, subsequent coordination to bidentate phen-based ligand **44** afforded pre-catenate **45-Zn(II)**. Intra-ligand RCM macrocyclization, followed by hydrogenation of the newly formed double bond afforded penta-coordinated catenate **42-Zn(II)**. The metal-free catenand was formed by stirring a dichloromethane solution of the catenate with aqueous base. Similar to previous work with the tetrahedral template, catenand **42** was re-metallated with Zn(II) and other metal ions such as Cu(II) and Fe(II).

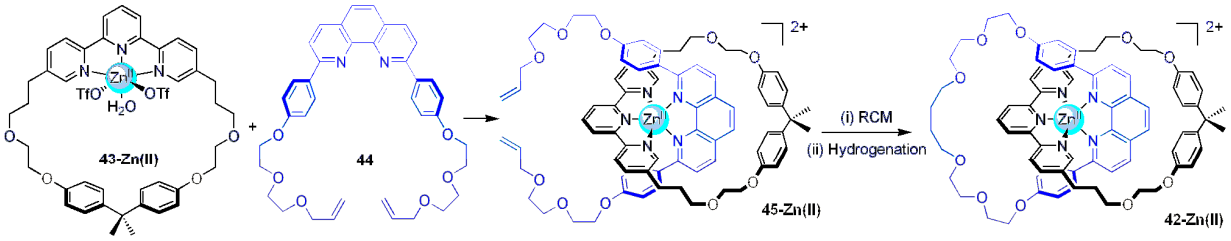

Scheme 1.18. Synthesis of five coordinate Zn(II) catenate **42-Zn(II)** using the combination bidentate phen (**44**) and tridentate terpy (**43**) ligands.[44]

1.2.3 Octahedral Geometries

1.2.3.1 "3+3" Octahedral Strategy

As demonstrated in the tetrahedral section, there are numerous examples of catenanes and rotaxanes assembled around Cu(I) but it took almost a decade before a new template was developed. The first catenane successfully assembled around an octahedral metal ion was published in 1991 by Sauvage.[45] In this "3+3" approach, coordination of Ru(II) to two equivalents of 5,5"-diphenyl terpy-based ligand led to pre-catenate **46-Ru(II)** (Scheme 1.19). A 5,5''-substitution pattern was chosen, in preference to a 6,6"-motif, as it generates a less hindered binding site around the metal ion. Due to solubility issues the phenol groups were initially masked, subsequent methoxy deprotection afforded pre-catenate **47-Ru(II)**. Double intra-ligand cyclization of complex **47-Ru(II)** using Williamson alkylations afforded catenate **48-Ru(II)** in a low yield of 11%. Unfortunately, the stability of the ruthenium catenate prevented demetallation; attempts to make an Fe(II) catenate, which would have been more susceptible to demetallation, proved unsuccessful.

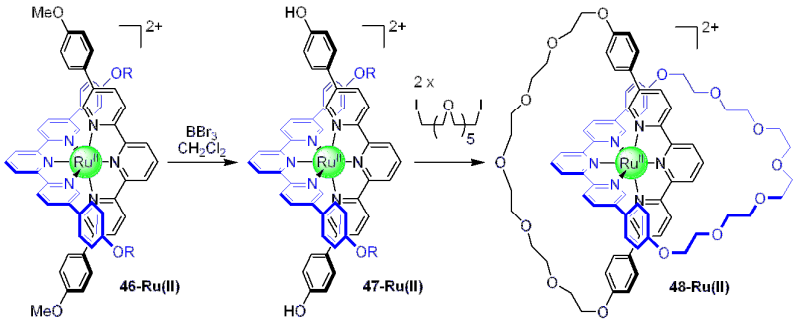

Scheme 1.19. Octahedral template synthesis of catenate **48-Ru(II)** around an octahedral Ru(II) ion using Williamson macrocyclizations on pre-catenate **47-Ru(II)**.[45]

Later efforts to synthesize an iron(II) analogue employing RCM cyclizations to 'clip' pre-catenate **49-Fe(II)**, resulted in the unexpected formation of 'figure-of-eight' complex **50-Fe(II)** (48% yield) which results from the inter- as opposed to intra-ligand cyclization (Scheme 1.20).[46] Building on Sauvage's early octahedral work, Siegel and co-workers also developed an octahedral metal template strategy for assembling catenanes, using both Ru(II) and Fe(II).[47]

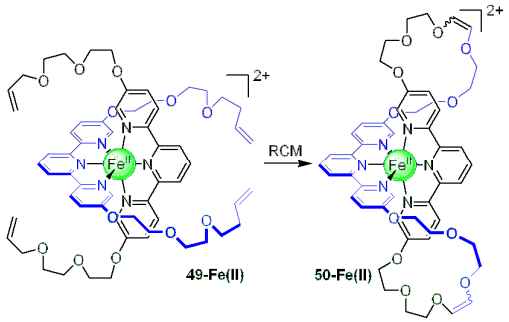

Scheme 1.20. Octahedral template synthesis of an unexpected 'figure-of-eight' complex **50-Fe(II)** from pre-catenate **49-Fe(II)** *via* inter-ligand RCM macrocyclization.[46]

In 2001, the Leigh group reported a simple method for preparing catenates using a variety of divalent octahedral transition metals.[48] Ligand **51** is based on a tridentate 2,6-diiminopyridine coordination motif and thus allows for two distinct strategies in the preparation of catenates. The first approach involved formation of pre-catenate complex **52**, by addition of ligand **51** to a metal salt (Mn(II), Fe(II), Co(II), Ni(II), Cu(II), Zn(II), Cd(II) and Hg(II)). Subsequent double intra-ligand RCM

macrocyclizations between the terminal alkenes generated catenates (**53**) in good yields (Scheme 1.21a). Secondly, a thermodynamic approach was used to assemble catenates through reversible imine bond formation between *bis*-amine **54** and 2,6-diformylpyridine (**55**) in the presence of a metal salt in methanol (Scheme 1.21b). Further study of catenate **53-Zn(II)** revealed the remarkable stability of the metal-complexed catenate, which could not be demetallated using EDTA. Prior reduction of the imine bonds was required to facilitate demetallation, yielding catenand **56** (Scheme 1.21c).

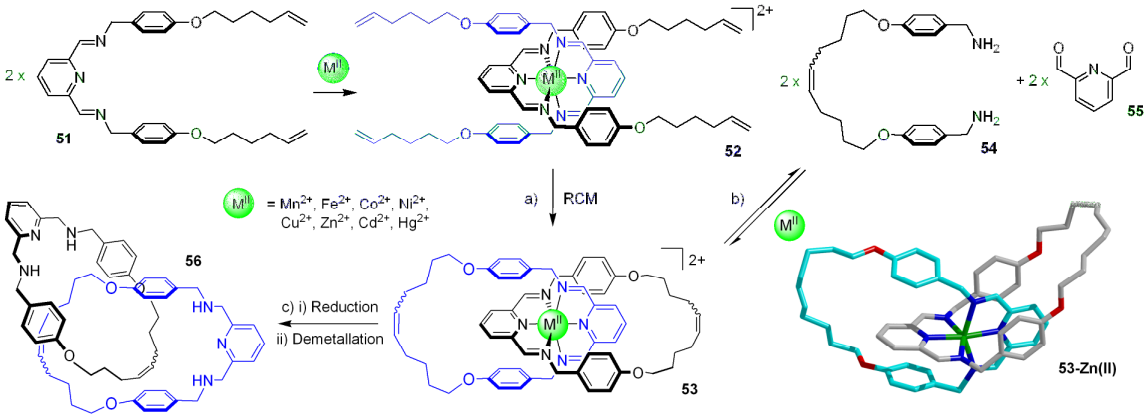

Scheme 1.21. Octahedral catenates (**53**) formed around a wide range of divalent metal ions accessed from either (a) double RCM reactions of pre-catenate **52** or (b) imine-bond formation between amine (**54**) and aldehyde (**55**) based ligands. The crystal structure of **53-Zn(II)** is shown bottom right. (c) Reduction of the imines to amines allowed demetallation to generate catenand **56**.[48]

This "3+3" approach required modification to realize the analogous rotaxanes, as using imine ligand **51** in conjunction with a similar tridentate thread would lead to formation of undesired thread-thread and pre-catenate complexes.[49] Instead *bis*-amine macrocycle (**57**) was coordinated to various divalent metal ions and directed imine-bond formation between 'stopper' aniline **58** and 2,6-diformylpyridine (**55**) through the cavity of the macrocycle to generate rotaxanes (**59**) (Scheme 1.22).

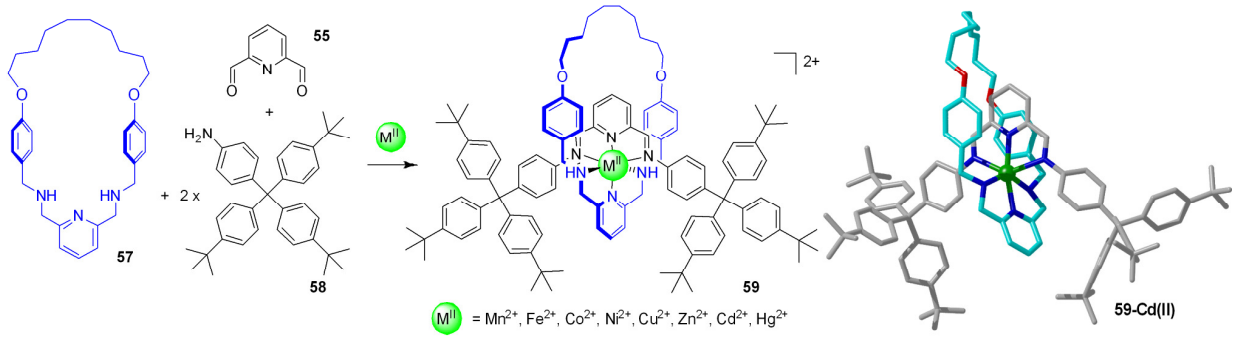

Scheme 1.22. Octahedral amine/imine-based [2]rotaxanes **59** formed through imine bond formation. Shown on the right is the crystal structure of rotaxane **59-Cd(II)**.[49]

The success of this strategy lay in the use of imine bond formation, allowing assembly and disassembly of the many possible structures in order to find the most thermodynamically favored product. It was shown that the other major coordination product, *i.e.* a double-thread complex, converts quantitatively into the rotaxane product in the presence of macrocycle **57**, even when this leads to a mis-match in stoichiometry. This preference was attributed to the presence of π-stacking interactions between the thread and macrocycle in the rotaxane promoting conformations that lead to interlocked products, as demonstrated in crystal structures of both rotaxane **59-Cd(II)** and catenate **53-Zn(II)**. These favorable aromatic interactions are absent in the *bis*-thread complex.

Chapter Two describes the use of a "harder" trivalent metal ion, cobalt(III), in the template directed synthesis of catenanes and rotaxanes using amido-based ligands.

1.2.3.2 "4+2" Octahedral Strategy

In 2003 Sauvage published the synthesis of a catenate assembled using a novel "4+2" octahedral coordination motif.[50] Macrocycle **60-Ru(II)** features two phen units that acts as a tetradentate ligand for Ru(II). Subsequent coordination of acyclic bidentate ligand **61** to macrocycle **60-Ru(II)** generated pre-catenane **62-Ru(II)**. Subsequent RCM macrocyclization afforded catenate **63-Ru(II)** in 68% yield (Scheme 1.23).

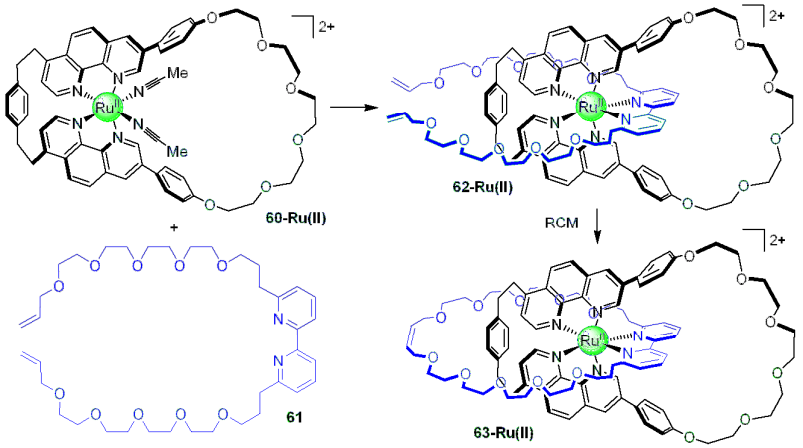

Scheme 1.23. Octahedral "4+2" motif using Ru(II), tetradentate Ru(II) complex **60-Ru(II)**, and bidentate ligand **61**. Mixing **60-Ru(II)** with **61** led to pre-catenate **62-Ru(II)**, subsequent RCM macrocyclization yielded catenate **63-Ru(II)**.[50b]

This new system has shown some versatility; catenanes can be assembled *via* a double macrocyclization approach in which a Ru(II)-[2]catenane was isolated in 46% yield.[51] Structural modification of the poly-ether backbone of the tetradentate macrocycle resulted in an increased yield of Ru(II)-catenate (76% yield).[52] Additionally, using a 4,4'-substituted bipy ligand intra-ligand RCM cyclization of the pre-catenate occurred around the poly-ether chain rather than round the metal-binding site as in previous examples[50b] (34% yield of catenate).[53] This example used rhodium(III), another second-row transition metal ion, as the octahedral template. Unfortunately, this set of ligands has met with limited success when employed with first-row transition metals such as zinc(II) or iron(II).[50b]

In contrast to the previously reported *bis*-terpy catenate **48-Ru(II)**[45] (Scheme 1.19) which could not be demetallated, this new coordination motif has the advantage that Ru(II) can be selectively photochemically de-complexed from just the bipy unit. In the presence of chloride ions, irradiation results in the vacant coordination sites on Ru(II) occupied by two chloride ions. Photochemical decomplexation also occurs in the absence of chloride ions, with the vacant coordination sites occupied by two molecules of acetonitrile.[51] The photo-decomplexed catenanes possess a structure in which although a metal ion is present, only one macrocycle is ligated to it. The octahedral "4+2" approach has also been adapted for rotaxane construction.[54]

1.2.3.3 "2+2+2" Octahedral Strategy

Further investigations into novel ligand design for the synthesis of interlocked architectures led the Sauvage group to create a bidentate ligand based on a bi-isoquinoline unit (Scheme 1.24a). These new ligands place the phenyl rings further from the metal centre resulting in a less sterically congested metal coordination site.[55] In the case of the phen or bipy-based ligands there is a 7 Å distance between the phenyl rings, in the novel bi-isoquinoline ligand the phenyl rings are now separated by 11 Å. Thus an octahedral metal ion can coordinate three bidentate bi-isoquinoline ligands (**64**) to generate a triply entwined complex, such as **65-Ru(II)** in a "2+2+2" approach (Scheme 1.24a).[56] The crystal structure of **65-Ru(II)** revealed this intriguing entwinement around the metal ion which was later exploited to create an interpenetrated structure.[57] Two bi-isoquinoline axles (**66**) terminated with azide functional groups were threaded through the cavity of bi-isoquinoline-based macrocycle **67** to generate complex **68-Fe(II)** (Scheme 1.24b). In an attempt to covalently capture the architecture, four 'stopper' units were installed *via* triazole formation using a CuAAC reaction. Although metal coordinated complex **69-Fe(II)** is extremely stable, upon demetallation the threaded sub-components slowly dissociate from the macrocycle. This is an unfortunate consequence of bi-isoquinoline macrocycle **67** being too large for the 'stoppers' used.

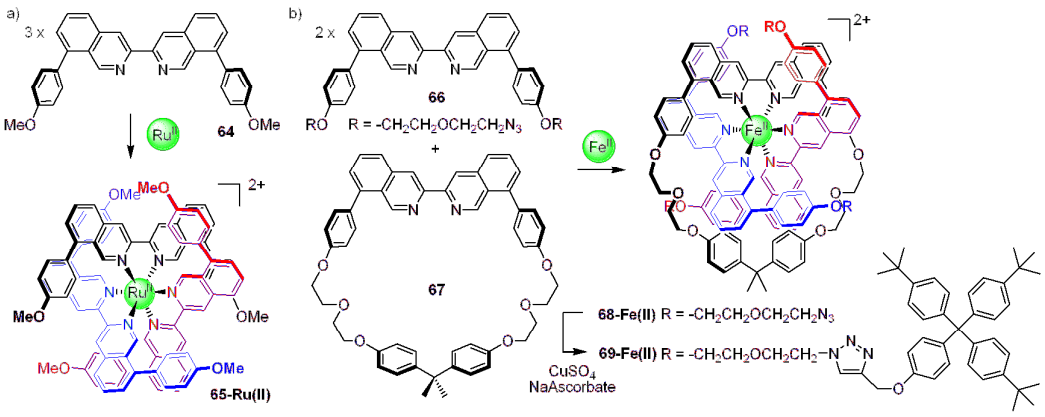

Scheme 1.24. (a) The synthesis of sterically unencumbering bi-isoquinoline ligand **64** allowed a "2+2+2" ligand arrangement about an octahedral metal centre to generate complex **65-Ru(II)**.[56] (b) The formation of a triply entwined complex was later exploited for the synthesis of doubly threaded [3]rotaxane **69-Fe(II)**.[57]

1.2.4 Square Planar Geometries

The first report of using a 2D metal geometry came from Sauvage in the synthesis of a palladium(II)-based pseudo-[2]rotaxane.[58] Here a "3+1" approach was used, in which the macrocycle featured a tridentate terpy unit to which Pd(II) was complexed. Subsequent coordination of a monodentate pyridine-based thread gave a pseudo-rotaxane in quantitative yield.

Rotaxane formation was later achieved using the "3+1" approach with an acyclic pyridine-2,6-dicarboxamide-based Pd(II)-complex (**70-Pd(II)**) and a 2,6-substituted pyridine-based thread (**71**) (Scheme 1.25).[59] The pre-rotaxane complex was stable enough to be isolated in 63% yield before being subjected to RCM macrocyclization. Hydrogenation of the newly formed double bonds allowed saturated Pd(II)-rotaxane **72-Pd(II)** to be isolated in 77% yield. Demetallation with potassium cyanide generated the metal-free rotaxane in 97% yield.

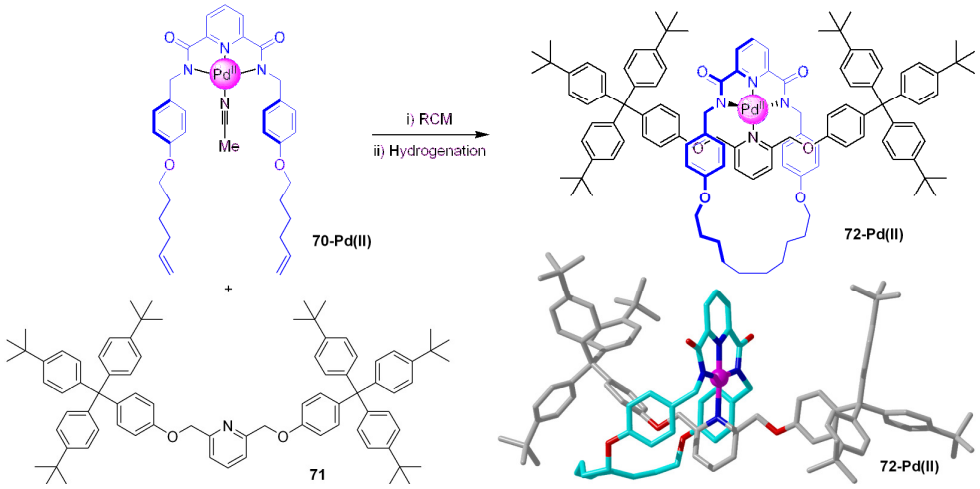

Scheme 1.25. The first interlocked molecule, rotaxane **72-Pd(II)**, to be assembled around a 2D square planar metal ion. The crystal structure is shown bottom right.[59]

The crystal structure of Pd(II)-rotaxane **72-Pd(II)** (Scheme 1.25, bottom right) demonstrated the "3+1" coordination motif around which the rotaxane was assembled and also revealed subtleties about the ligand design. Using a thread with a 3,5-substituted pyridine binding site leads exclusively to non-interlocked products, as

RCM occurs without capturing the thread. This is due to the conformation of the macrocycle, as the benzylic units "kink" the macrocycle away from the fourth coordination site. Replacement of the 2,6-dibenzyl ethers with 2,6-diesters prevented coordination from even occurring.

Another [2]rotaxane synthesis based on the same "3+1" motif with similar ligands but using a 'threading-followed-by-stoppering' strategy, was reported by the groups of Takata and Hirao.[60] Coordination of a monodentate 2,6-substituted pyridine based thread to a tridentate Pd(II)-macrocycle generated a pre-rotaxane. Subsequent 'stoppering' reactions generated the interlocked product in 96% yield. Again, this study demonstrated the importance of the substitution pattern around the pyridine ligand, as a 3,5-substitution led exclusively to non-interlocked products.

The Leigh group later used the demetallated [2]rotaxane synthesized previously[59] to demonstrate the power of interlocked architectures to enforce binding motifs that are either unobserved or unstable in related non-interlocked molecules.[61] This study showed that the mechanically bound molecule could coordinate Pd(II), from both acetate and chloride salts, whereas the analogous non-interlocked ligand could only bind Pd(II) from the acetate salt. Additionally, Cu(II) and Ni(II) were successfully complexed to the rotaxane but not to the non-interlocked ligand.

The robust nature of the square planar Pd(II) methodology was later exemplified in the synthesis of [*n*]rotaxanes.[62] An unsymmetrical thread was used, in which a monodentate pyridine unit (the binding site for Pd(II)-pre-macrocycle **70-Pd(II)**) is located adjacent to one stopper but separated from the second stopper by a long alkyl chain, thus providing space for the macrocycles. Macrocycles were then added to the thread in an iterative manner using the following sequence: (i) complexation; (ii) macrocyclization; (iii) hydrogenation; and (iv) demetallation. After the first iteration, a [2]rotaxane was isolated; after the second iteration, a [3]rotaxane (**73**); the final iteration yielded [4]rotaxane **74** (see Scheme 1.26 for the final iteration). With this approach the only limiting factor in the synthesis of higher order rotaxanes is the length of thread used.[63]

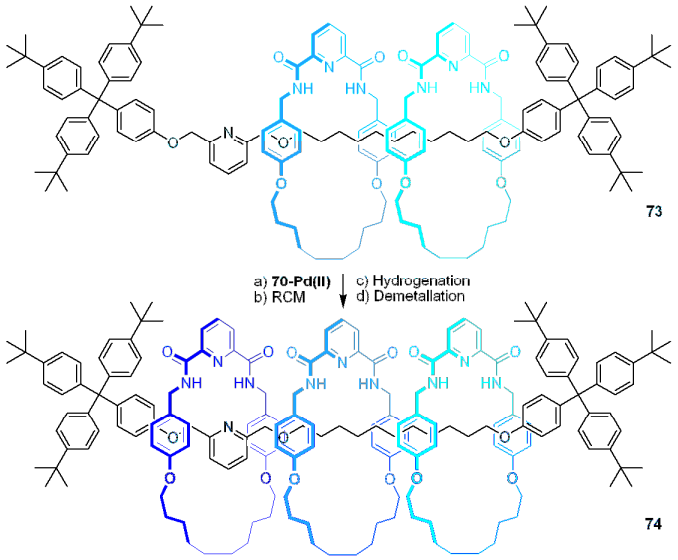

Scheme 1.26. Synthesis of [4]rotaxane **74** from [3]rotaxane **73** *via* (a) coordination of **74** to **70-Pd(II)**; (b) RCM macrocyclization; (c) hydrogenation; and (d) demetallation.[62]

Incorporation of a second heterocycle, a 2,6-substituted DMAP, into a pyridine-based thread allowed the synthesis of a pH-responsive molecular shuttle.[64] Under neutral conditions a Pd(II)-macrocycle preferentially resides on the more basic heterocycle. Protonation and heating at elevated temperatures allowed a new co-conformation to be achieved where the macrocycle now resides over the less basic heterocycle. Upon treatment with base and heating, the original co-conformation was re-established with macrocycle on the DMAP "station". The mechanism of macrocycle translocation is based on competitive binding between the Pd(II)-macrocycle and proton for the most basic heterocycle. The proton exhibits a greater discrimination between the two heterocycles and thus the macrocycle can be translocated to the less basic heterocycle. If the Pd(II)-macrocycle exhibited a greater discrimination between heterocycles, then no translocation would be possible *via* this mechanism.

In an attempt to synthesize [2]catenanes based on the square planar geometry of Pd(II), cyclic complex **75-Pd(II)** was coordinated to acyclic pyridine-2,6-dibenzyl ether-based ligand **76** (Scheme 1.27, left).[65] Subsequent intra-ligand macrocyclization failed to capture the desired interlocked structure, but instead led to 'ring-on-ring' complex **77-Pd(II)**. Next, a double-cyclization approach was

attempted using acyclic ligands **70-Pd(II)** and **76** (Scheme 1.27, middle). Yet again the catenate was not formed, instead 'figure-of-eight' complex **78-Pd(II)** was the isolated product. Finally, using acyclic complex **70-Pd(II)** and monodentate macrocycle **79**, Pd(II)-catenate **80-Pd(II)** was obtained as the major product, in 78% yield (Scheme 1.27, right). The topology and connectivity of all three isomers was proved in the solid state by crystal structure analysis (Scheme 1.27, bottom).

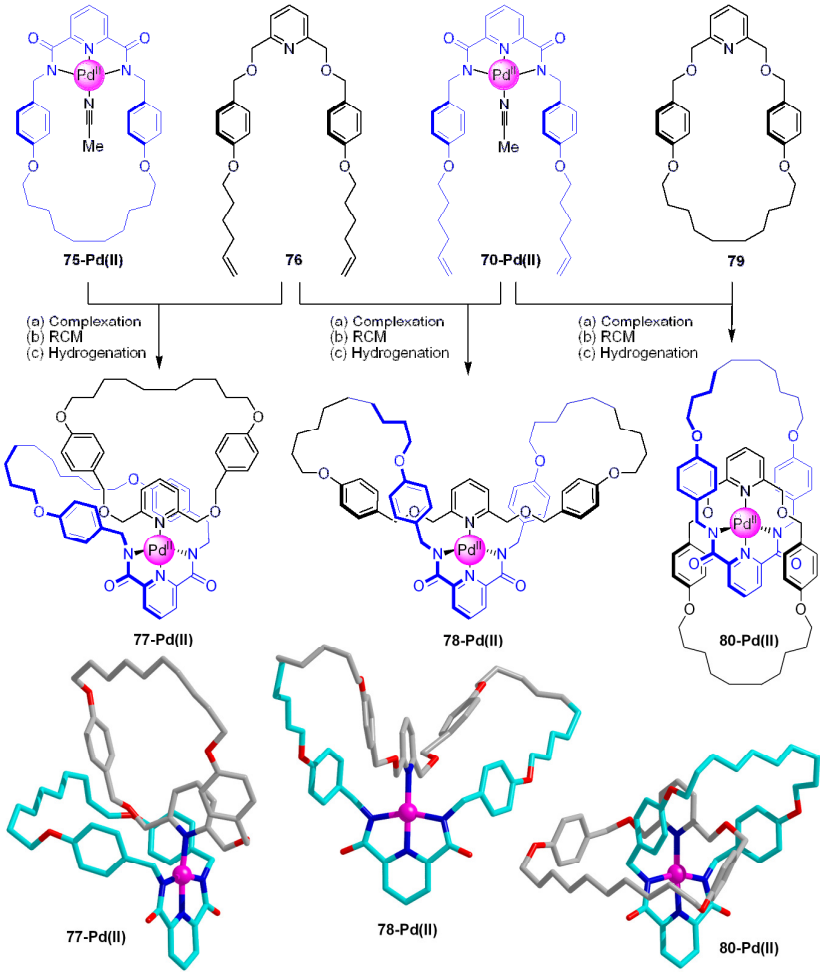

Scheme 1.27. A complete range of topological and connectivity isomers were isolated in a Pd(II)-template synthesis of catenanes. All three isomers were characterized in the solid-state (bottom).[65]

1.2.5 Linear Geometries

Chapter Four describes the use of the 1D linear geometry of gold(I) to construct the both catenanes and rotaxanes.[66]

1.3 Knots

Knots are another interesting class of topological structures.[67] The simplest knot, the trefoil, consists of a single component that has been entwined once around itself to produce a knot. The next simplest knot, named after King Solomon, features two components entwined twice about each other, much like a [2]catenane but with four crossing-points. Schematically, the inner-core of both trefoil and Solomon knots are identical (Scheme 1.28). The termini connected during the cyclization step determine the topological outcome. Inter-ligand cyclizations between "A+Y" and "B+X" termini lead to a trefoil knot (Scheme 1.28a). Whereas intra-ligand cyclizations between "A+B" and "X+Y" lead to the doubly entwined rings of the Solomon knot (Scheme 1.28b). The pioneers in this field have again been the group of Sauvage, using the Cu(I)-phen motif to organize ligands in order to furnish many knotted products.

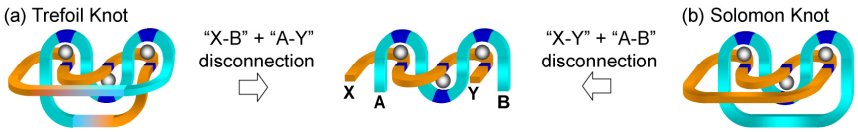

Scheme 1.28. (a) Trefoil and (b) Solomon knots can be formed from a common intermediate, with the topological outcome depending on the termini connected through covalent bond formation.

1.3.1 Molecular Trefoil Knots

The metal-template synthesis of knots[68] was initiated using ligands that possessed two phen coordination units; upon coordination to Cu(I) ions the ligands were organized into a helical arrangement. Covalent capture of the knot was achieved *via* double inter-ligand cyclizations using Williamson alkylations between the four

terminal phenols and two iodo-functionalized 'clipping' units.[69] Although the synthesis of the trefoil knot was a triumph in terms of topologically complexity (elucidation of the crystal structure revealed the non-trivial topological structure, Figure 1.4, right),[70] the isolated yield of knot **81-Cu(I)** (Figure 1.4) was only 3%. ^{1}H NMR analysis of the *bis*-Cu(I) helix showed that a significant amount of a mono-Cu(I)-ligand complex was present, *i.e.* the ligand had folded around itself to act as a tetradentate ligand to Cu(I).

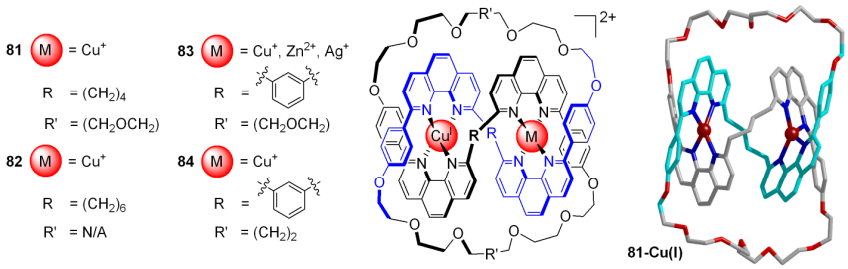

Figure 1.4. The pioneering synthesis of trefoil knots by the Sauvage group: **81-Cu(I)**,[69a] **82-Cu(I)**[71a], **83-Cu(I)**[71b], **83-Cu(I)/Zn(II)**[73] and **83-Cu(I)/Ag(I)**,[73] and **84-Cu(I)**.[74] The crystal structure of **81-Cu(I)** is shown, right.[70]

Modifications to the design of the trefoil knot, most notably to the unit linking the phen groups, led to an improvement in yield. Replacing the four carbon linkage with a six carbon linkage gave an increased 8% yield of knot **82-Cu(I)**[71a] (Figure 1.4), whilst using a rigid 1,3-isothaloyl spacer gave knot **83-Cu(I)**[71b] in a higher 29% yield (the topology of knot **83-Cu(I)** was proved by X-ray analysis).[71c] The utility of RCM reactions in the synthesis of interlocked and entwined molecules was again demonstrated; a di-Cu(I)-knot precursor was synthesized featuring four terminal olefins that when subjected to double RCM macrocyclizations gave knot **84-Cu(I)**, after hydrogenation of the double bonds, in 74% isolated yield.[72]

Due to its enhanced rigidity, knot **83-Cu(I)** proved inert to demetallation at room temperature with cyanide. Nevertheless, the two Cu(I) ions were extracted in a stepwise manner by using KCN in refluxing acetonitrile giving first a mono-copper species and subsequently the metal-free knot ligand. This artifact of the synthesis was exploited for the formation of heterodinuclear copper/zinc **83-Cu(I)/Zn(II)** and copper/silver **83-Cu(I)/Ag(I)** knotted complexes.[73] Metal-free knot **83** was easily

coordinated to two lithium ions.[74] The kinetics of demetallation with cyanide ions was studied for a range of knots: **81-Cu(I)**, a knot similar to **81** but with a $(CH_2)_6$ spacer between phen units, **82-Cu(I)**, and **83-Cu(I)**, and compared to the non-interlocked/non-entwined complexes.[75] It was shown that the kinetics of demetallation strongly depended on topological and steric factors, with the knotted species being several orders of magnitude slower to demetallate than non-interlocked/non-entwined complexes.

The advancement in the synthetic preparation of molecular knots[71b] has allowed resolution of the right- and left-handed trefoil knots.[71c, 76] Anion exchange of the triflate salt of di-copper(I) knot **83-Cu(I)** for a (*S*)-(+)-binaphthylphosphorate salt[77] allowed selective crystallization to occur, yielding first the left-handed (-)-knot. Subsequent recrystallization of the remaining material gave the right-handed (+)-knot. The circular dichroism (CD) spectra of both diastereoisomers gave the expected mirror-image between 280-700 nm. The chiroptical properties of the right-handed (+)-knot were later studied in more detail.[78] More recently, a stereoselective synthesis of a trefoil knot was achieved by using chiral pinene groups adjacent to a bipy coordination unit to direct the synthesis of a left-handed knot.[79] Double RCM cyclizations proceeded smoothly to give the knot in 74% yield. Whilst suitable single crystals could not be grown, the CD spectra showed evidence of the stereoselective knot synthesis.

Sauvage has also used an octahedral Fe(II)-terpy motif in the synthesis of knots (Figure 1.5). Unlike the unsuccessful catenane synthesis using this coordination motif,[46] trefoil knot **85-Fe(II)** was generated in 20% yield using RCM cyclizations.[80]

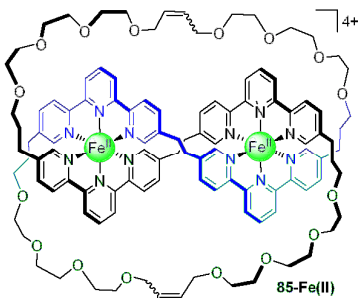

Figure 1.5. Knot **85-Fe(II)** was synthesized around an octahedral *bis*-Fe(II)-terpy template.[80]

An example of an pre-knot structure assembled around a single octahedral metal centre (Scheme 1.29) was reported by Hunter in 2001.[81] A multidentate ligand containing three bipy units coordinated a Zn(II) ion in a manner that entwined the ligand, generating pre-knot complex **107-Zn(II)** (the entwined structure was demonstrated by crystallographic analysis, see Scheme 1.29, left). The folding process is fully reversible; addition of excess chloride ions produced the decomplexed ligand whilst subsequent addition of silver ions regenerates **86-Zn(II)**. Further work revealed that this assembly could be covalently captured *via* a 'clipping' reaction between the two terminal alcohols to yield knot **87-Zn(II)**.[82] The same conditions that demetallated pre-knot **86-Zn(II)**, failed to remove the metal ion from knot **87-Zn(II)**.

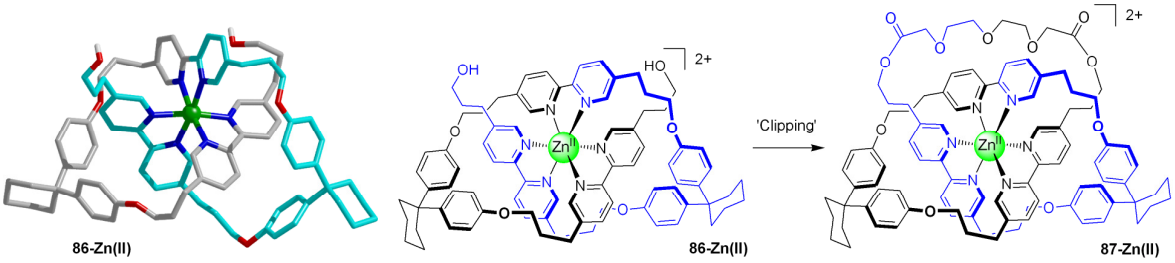

Scheme 1.29. Zn(II) gathered a multi-dentate ligand to form complex **86-Zn(II)**,[81] subsequent 'clipping' yielded knot **87-Zn(II)**.[82]

In a similar fashion to that described for Cu(I)-[*n*]catenates, Sauvage and co-workers coupled acyclic knot-precursors *via* Glaser acetylenic-couplings to produce a composite knot, composed of one molecular chain featuring six crossover points in 3% yield.[83] Extensive 1D and 2D ^{1}H NMR analysis identified the desired metallo-

knotted species in a complex mixture of 'figure-of-eight' macrocycles and macrocycle-knot species. The Sauvage group have tried to synthesize more elaborate structures, such as higher order knots (with the number of crossing points greater than three), and a molecular Star of David, a triply entwined [2]catenane.[84]

1.3.2 Molecular Solomon Knots

Sauvage's group was the first to realize the synthesis of a Solomon knots using a metal-template strategy. The approach employed ligands that each possessed three phen coordination units that upon coordination to three Cu(I) ions generated a pre-knot complex with four crossing-points.[85] Cyclization was achieved *via* intra-ligand Williamson alkylations between two terminal phenol groups and an iodo-functionalized 'clipping' unit. Knot complex **88-Cu(I)** (Figure 1.6) proved unstable, thus purification was attempted after demetallation to yield metal-free knot **88** in 2% yield, also isolated was the singly entwined [2]catenane in 1% yield.

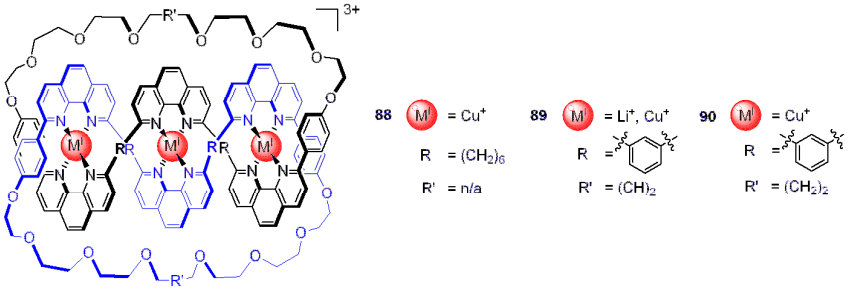

Figure 1.6. Sauvage's first **88-Cu(I)**[85] and improved **89-Li(I)**[87] and **90-Cu(I)**[87] synthesis of Solomon knots.

Characterization of the knot proved, initially, to be very difficult. Although both compounds could be separated by TLC, electrospray MS gave identical spectra. Only extensive interpretation of the ^{1}H NMR spectra of both compounds allowed an assignment to be made. Later it was found that **88** could be differentiated from its isomeric singly entwined [2]catenane using advanced mass spectrometry techniques.[86] The Solomon knot, as a consequence of its more entangled nature and greater strain, was prone to cleavage at higher cone voltages compared to the simple catenane.

An improved synthesis was achieved by taking advantage of quantitative formation of a stable double-stranded tri-lithium(I) helix. Subsequent double intra-component RCM cyclization reactions lead to Solomon knot **89-Li(I)**.[87] Unfortunately, purification issues meant that lithium catenane **89-Li(I)** could not be isolated, instead it was converted to the copper(I) analogue **89-Cu(I)** which allowed isolation of the Solomon knot in a much improved 30% yield. Catalytic hydrogenation gave access to saturated metallo-knot **90-Cu(I)**.

1.4 Borromean Rings

Borromean rings (BRs)[88] consist of three interpenetrating rings with each individual ring not interlocked with respect to any other ring. However, the overall structure is mechanically interlocked such that cleavage of just one ring results in complete disassembly of the overall structure. Two main stepwise metal template strategies have been investigated by synthetic chemists.[89] With an orthogonal depiction (Scheme 1.30a) it is possible to build up the structure *via* a 'ring-in-ring' approach. Starting from one macrocycle (orange), a second macrocycle (blue) can be orientated within the cavity of the orange ring by the use of two metal ions as anchors. A third pre-macrocycle (green) can then be positioned outside the orange ring but through the cavity of the blue ring. Cyclization of the green pre-macrocycle outside the orange ring captures the interlocked molecule. Alternatively, if BRs are depicted as chain rings then a 'rack' strategy can be envisaged (Scheme 1.30b). Three acyclic ligands can form a complex on the addition of two metal ions, cyclization of the green termini leads to a complex resembling half of the overall structure. Thus if two such complexes are fused, by reaction between the correct termini, BRs can be formed.

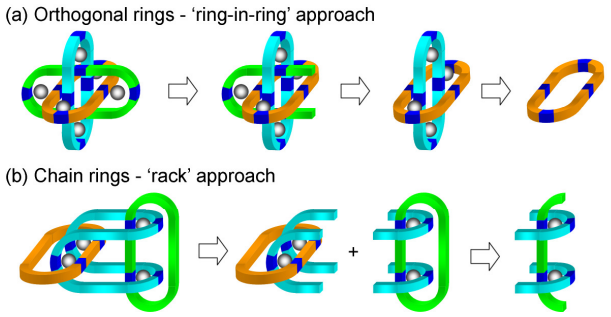

Scheme 1.30. Borromean rings can be represented as (a) orthogonal rings or (b) as a chain rings. Orthogonal rings allow for a stepwise 'ring-in-ring' strategy, whereas chain rings allow for a 'rack' approach.[89]

1.4.1 Studies Toward the Synthesis of Borromean Rings

1.4.1.1 Stepwise 'Ring-in-Ring' Strategies

Stoddart's group was the first to report a 'ring-in-ring' assembly, utilizing ammonium-crown ether interactions.[90] This was followed by two reports which relied on metal-ligand interactions to generate 'ring-in-ring' complexes.[89, 91]

Schmittel's group made use of the tetrahedral Cu(I)-phen motif of Sauvage,[16] with one macrocycle featuring two *endo*-phen units (possessing a 2,9-substitution pattern) and a second macrocycle featuring two *exo*-phen units (possessing a 4,7-substitution pattern). Coordination to Cu(I) formed the desired 'ring-in-ring' complex **91-Cu(I)**, isolated in 79% yield (Figure 1.7).[91] Aside from the phen units no other functionality was built into the macrocycles that could be exploited to generate more complex structures, such as BRs.

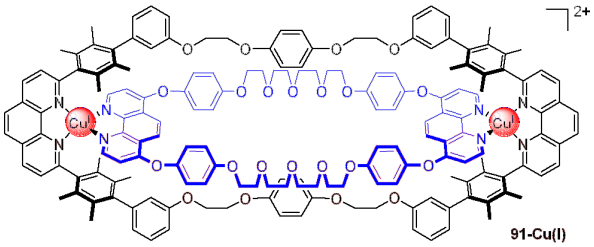

Figure 1.7. A 'ring-in-ring' complex formed using a Cu(I)-phen motif.[91]

Unlike Schmittel's approach,[91] Siegel utilized an octahedral metal-terpy motif to assemble 'ring-in-ring' complex **92-Ru(II)** (Figure 1.8).[89] Siegel's group included two vacant bipy units in one ring for possible coordination to a third ring.

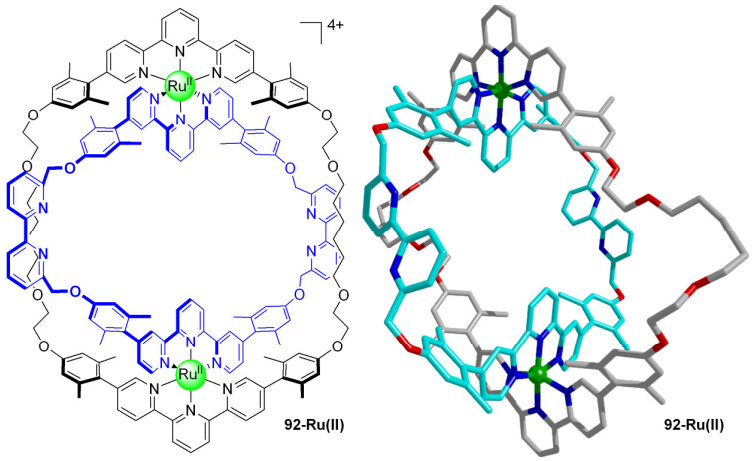

Figure 1.8. A 'ring-in-ring' complex, in which the vacant bipy units allow the possible coordination of a third ring, as a route towards Borromean rings.[89]

1.4.1.2 'Chain Ring' Strategies

A second approach arose from depicting the BRs as chain rings (Scheme 1.30b). Using this strategy Siegel and co-workers constructed basic 'rack' assemblies.[92] Two separate axles were synthesized featuring two tridentate terpy-based coordination units that formed a bimetallic heteroleptic complex with two smaller tridentate units in the presence of Ru(II). In this way complexes **93-Ru(II)** (Figure 1.9a) and **94-Ru(II)** (Figure 1.9b) were accessed. 'Rack' **94-Ru(II)** could possibly be utilized as a pre-cursor for BRs as it contained functionality suitable covalent derivatization. Unfortunately, no successful stepwise syntheses of BRs have been reported using either 'ring-in-ring' or 'rack' strategies.

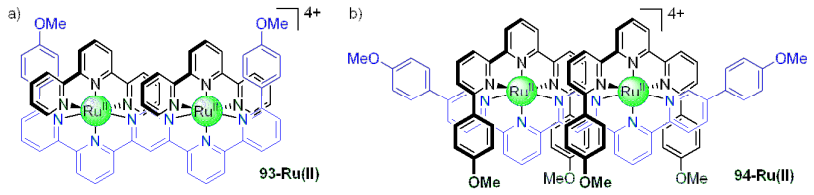

Figure 1.9. 'Rack' complexes (a) **93-Ru(II)** and (b) **94-Ru(II)** as basic building blocks for a 'rack' strategy towards Borromean rings.[92]

1.4.2 Molecular Borromean Rings

The synthesis of molecular BRs was finally achieved in 2004 using an 18-component one-pot self-assembly approach.[93, 94] Stoddart and co-workers designed their BR to be the most thermodynamically favored product, exploiting many non-covalent interactions. Furthermore the use of dynamic covalent chemistry and labile Zn(II)-nitrogen coordination allowed the system to reach a thermodynamic minimum through continual error-correction steps. Six Zn(II) ions direct the self-assembly of six bidentate bipy-based ligands, **95**, and six 2,6-diformylpyridine ligands (**55**) in the construction of BRs in near quantitative yield (Scheme 1.31). The impressive structure of **96-Zn(II)** was confirmed upon elucidation of the X-ray crystal structure (Scheme 1.31, right). The solid-state structure demonstrated how the newly-formed imine bonds helped create a tridentate coordination unit that in conjunction with a bipy unit coordinated to the octahedral metal ions (the sixth coordination site was occupied by a TFA anion). The crystal structure also illustrated that other non-covalent interactions play a part in the assembly process, evidenced by the fact that each bipy unit is flanked by a pair of phenolic rings at a distance ideally suited for π-stacking.

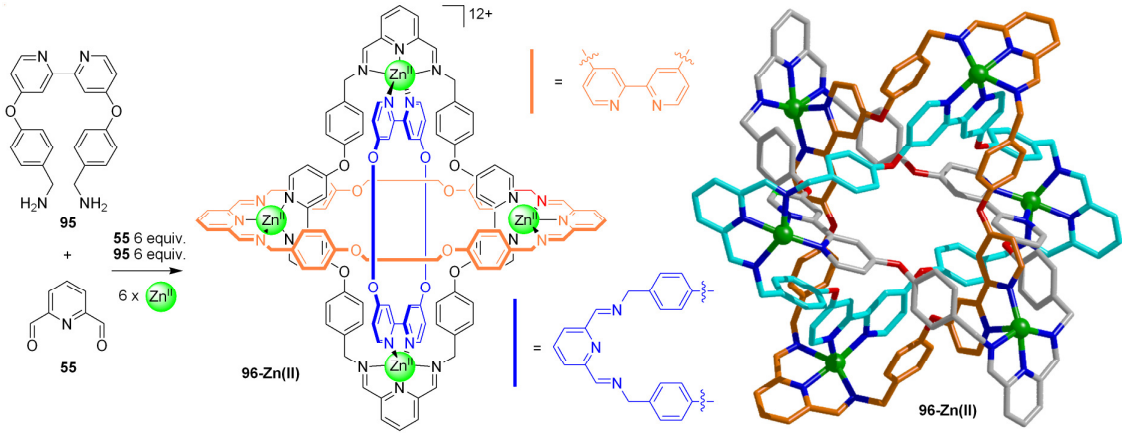

Scheme 1.31. Borromean rings **96-Zn(II)** synthesized from *bis*-aldehyde **55** and *bis*-amine **95** based ligands. The rings of one macrocyclic ring are shown in grey, second ring in light blue, and third ring in orange, zinc(II) green, the anions occupying the sixth coordination site have been omitted for clarity, nitrogen blue and oxygen red.[94a]

The synthetic simplicity of this approach to BRs belies the extremely tough synthetic challenge that vexed chemists following stepwise 'ring-in-ring' or 'rack' strategies. In fact, the level of synthetic ability necessary to construct these BRs has made it an excellent education tool for undergraduate students. The synthetic procedure was modified such that BRs could be constructed from commercially available starting materials in seven 4-hour laboratory sessions, with the final BR synthesis proceeding in 90% yield.[95]

The dynamic behavior of the BRs has been probed by halogen labeling of the 2,6-pyridinediformyl unit (**55**). Hexa-bromine and hexa-chlorine labeled BRs were synthesized separately. When mixed together complete exchange to a statistical mixture was found to have occurred after five days in a methanolic solution at 60 °C in the presence of a few drops of trifluoroacetic acid.[96] Further studies have shown that Borromeands are stable in the absence of the Zn(II) ions following reduction of the imines to amines, 'fixing' the interlocked nature of the molecule.[97] Partial cleavage of the imine bonds occurs during the reduction step. Accordingly, those BRs disassociated into their constituent rings and an acyclic ligand. Performing the reduction at elevated temperatures, only individual macrocyclic rings and linear ligands were obtained.

Derivatization of BRs was achieved through the functionalization of the pyridine rings. The self-assembly approach tolerated substitution in the *para*-position on the pyridyl rings; 4-acetoxymethylphenyl, 4-methylthiophenyl, 4-pentenyloxy, and *p*-tolylpentenyloxy were all be incorporated into BRs.[98] BRs formed with 4-pentenyloxy proved amenable to olefin cross metathesis with styrene, in which the dominant product was found to be generated from five cross metatheses.[98b] Incorporating chiral units, (*R,R*) or (*S,S*), into the bipy-amine fragment resulted in the formation of chiral BRs composed of either twelve (R) or (*S*) units.[99] The crystal structure of the (*R*)-BR showed that the Zn(II) metal centers were distorted substantially from their ideal octahedral geometry, suggesting that the stereogenic centers exerted a great influence on the metal centers.

Stoddart and co-workers subsequently synthesized BRs using another transition metal ion template, Cu(II).[100] Intriguingly, when a mixed metal template of Zn(II) and Cu(II) was subjected to the same reaction conditions instead of the expected formation of BRs, a Solomon knot (a doubly entwined catenane) was formed (Scheme 1.32). In the Solomon knot, only four equivalents of ligands **55** and **117** are incorporated into the knot. However, the Solomon knot can only be accessed by using equimolar amounts of Zn(II) and Cu(II). The reasons as to why the Solomon knot is produced remain unclear. In contrast to BRs, formed under thermodynamic control, the Solomon knots are generated in a kinetically controlled crystallization process. Instead of forming a 'ring-in-ring' complex, as in the case of BRs, the macrocyclic rings in the Solomon knot entwine about each other to create four crossing-points that result in the knot (Scheme 1.32).

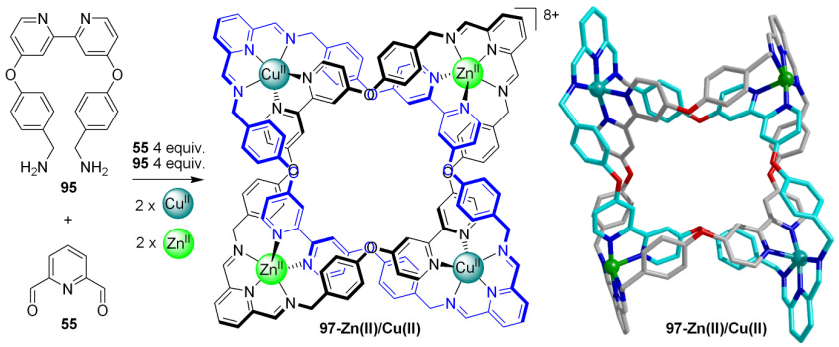

Scheme 1.32. Solomon knot **97-Zn(II)/Cu(II)** was synthesis (Scheme 1.32).[100a] Zn(II) is shown in green, Cu(II) teal, anions occupying the sixth coordination site have been omitted.

1.5 "Active" Metal Template

As described above, many metal-ligand coordination geometries have been successfully utilized in the construction of interlocked and entwined architectures. In all these template-directed syntheses, the metal ion is essentially a "passive" glue holding the organic ligands together prior to covalent capture. Thus, in all such "passive" metal template strategies the metal ion must be present in stoichiometric quantities.

A major advance saw the use of sub-stoichiometric quantities of metal ion, in an "active" metal template synthesis of interlocked architectures. Here, the metal ion plays a dual role; firstly acting to gather and organize ligands, and secondly to catalyze covalent bond formation between two 'half-threads' through the cavity of a macrocycle yielding the interlocked product (Scheme 1.33a). Once the rotaxane has been formed, it is possible for the metal ion to turn over, re-entering the catalytic cycle in the production of more rotaxane (Scheme 1.33b).

Additionally, in order to assemble the interlocked structure, "passive" metal template strategies require well-defined coordination sites in each of the organic sub-components that "live-on" after mechanical bond formation. In the "active" template strategy, organization and reaction of 'half-thread' units is achieved *via* the metal ions interaction with the terminal functional groups (dark blue segments, Scheme

1.32) present on the 'half-threads' during covalent bond forming step. As such, this novel strategy only requires a permanent coordination site on the macrocycle as the functionality used in covalent bond formation can "disappear" during the reaction.

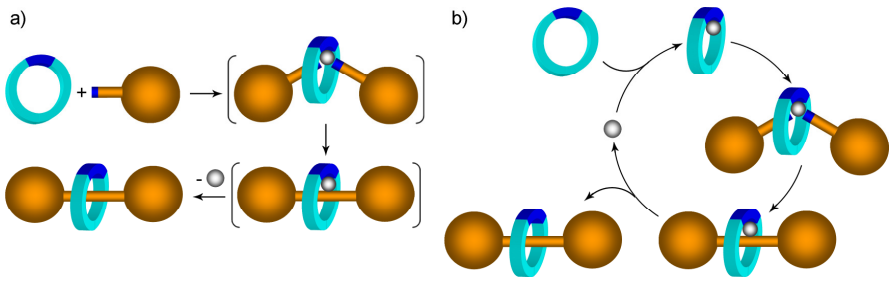

Scheme 1.33. Overview of the "active" metal template strategy. (a) The metal ion plays a dual role; first by gathering and organizing the ligands, and secondly by catalyzing covalent bond formation between 'half-threads' through the cavity of a macrocycle. (b) As the metal ion is able to turn over, sub-stoichiometric quantities of metal ion can be used.

1.5.1 Cu(I) Catalyzed Azide-Alkyne 1,3-Cycloaddition Synthesis of Rotaxanes

The first "active" metal template was reported in 2006 by the Leigh group. A copper(I) catalyzed azide-alkyne 1,3-cycloaddition (CuAAC) was employed to synthesize rotaxanes.[101] Macrocycle **79** coordinated Cu(I) and the Cu(I)-complex then catalyzed triazole formation between alkyne (**34**) and azide (**98**) 'half-threads' (Scheme 1.34). In the presence of a stoichiometric quantity of Cu(I) an excellent yield, 94%, of rotaxane **100** was reported. Remarkably, addition of just three equivalents of pyridine, as a competing ligand for Cu(I), allowed the reaction to proceed catalytically with only 20 mol% of Cu(I), generating rotaxane **100** in 82% yield.

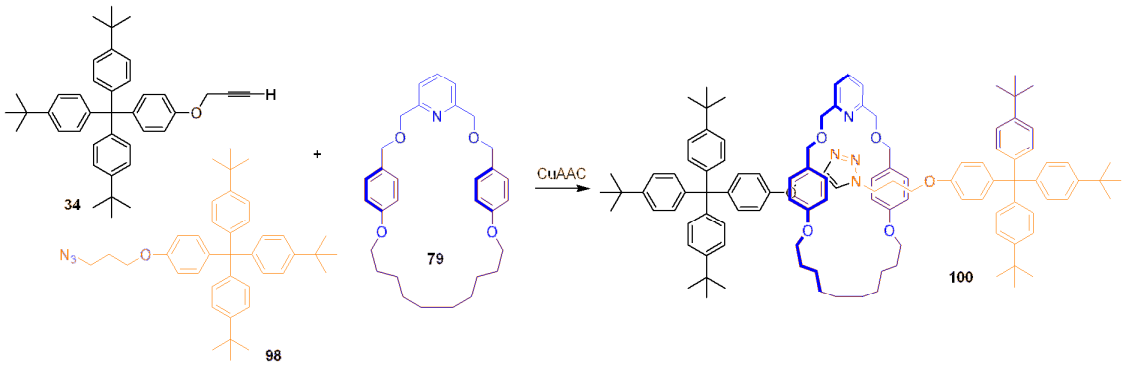

Scheme 1.34. CuAAC synthesis of rotaxane **100** from alkyne **34** and azide **98** 'half-threads'. A stoichiometric quantity of Cu(I) yielded rotaxane in 94% and a sub-stoichiometric quantity (20 mol%) produced rotaxane in 82%.[101]

A more in depth study of the CuAAC mechanism followed, in which a variety of structurally related macrocycles were tested in the CuAAC reaction.[102] These studies demonstrated that the CuAAC reaction tolerates a wide-range of mono-dentate macrocycles, and to a much lesser extent bidentate macrocycles, but not tridentate macrocycles. Unexpectedly, a [3]rotaxane (**102**) was isolated from a reaction that used a large excess of a pyridine-2,6-biphenyl-based macrocycle **101** (Scheme 1.35, the structure of **102** was confirmed in the solid-state).

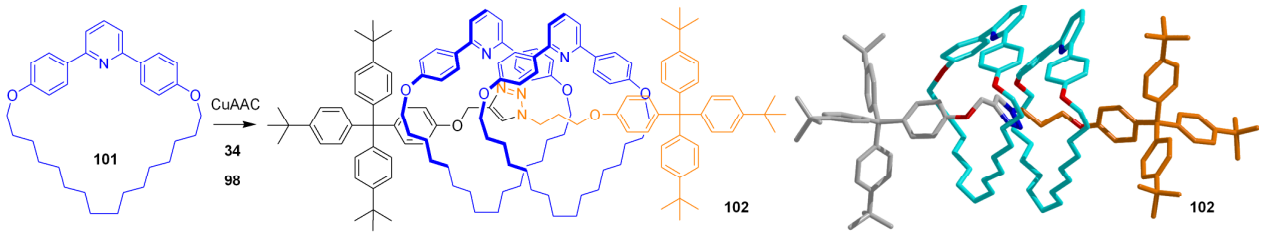

Scheme 1.35. A large excess of macrocycle **101** unexpectedly yielded [3]rotaxane **102**, which was characterized in the solid state (right).[102]

The experimental observations allowed a mechanism to be postulated (Scheme 1.36). Complexation of one Cu(I) ion to the macrocycle *via* *N*-donor coordination to the pyridine unit generated complex **103-Cu(I)**. As mono-dentate macrocycles led to the formation of [3]rotaxanes as well as [2]rotaxanes, it was postulated that this occurred *via* a doubly bridged bi-metallic *bis*-macrocyclic intermediate, **104-Cu(I)**. Bi-dentate macrocycles, on the other hand (Scheme 1.36, **105-Cu(I)**), for steric reasons cannot

achieve the doubly bridged *bis*-macrocyclic arrangement necessary for [3]rotaxane formation and thus only yield [2]rotaxanes. Rotaxane formation is the result of complexes **104-Cu(I)** and **105-Cu(I)** undergoing 1,3-cycloadditions to generate a triazole, a covalent bond, and concurrently the rotaxane architecture, a mechanical bond.

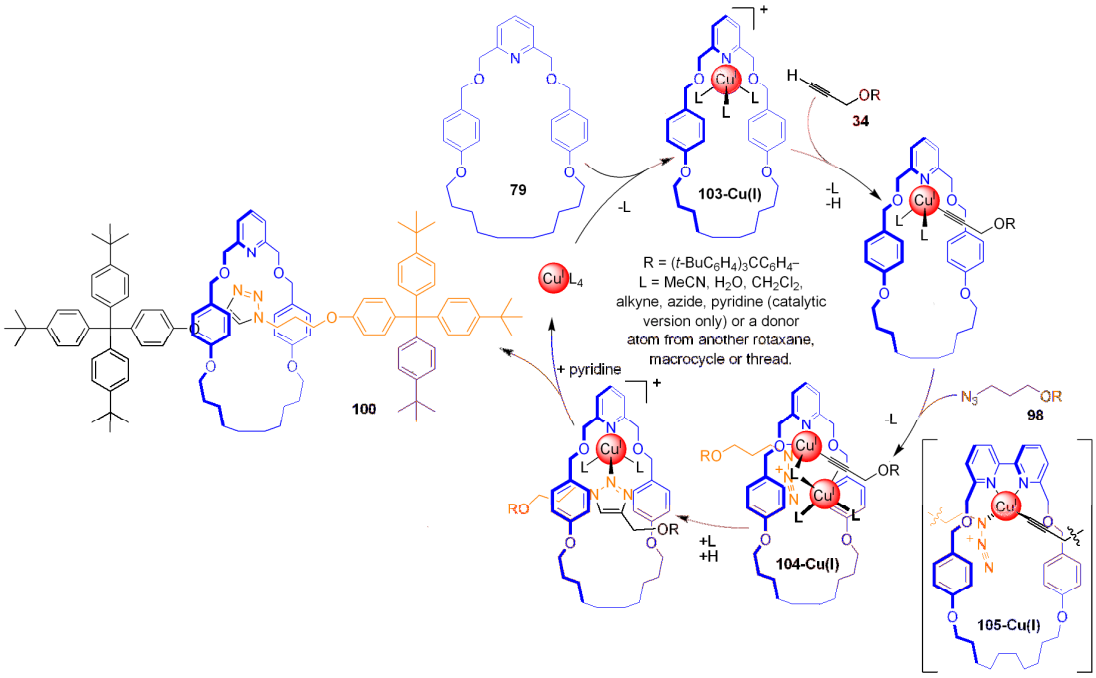

Scheme 1.36. Postulated mechanism of the CuAAC reaction leading to rotaxane **100**.[101, 102]

1.5.2 Rotaxane Synthesis through Alkyne Couplings

The next reports of "active" template reactions came from Saito and co-workers, who utilized an oxidative alkyne dimerization to generate rotaxanes.[103] The oxidative homo-coupling of aryl-alkyne 'half-thread' **106** mediated by Cu(I)-macrocycle **107-Cu(I)** generated rotaxane **108** in 72% yield (Scheme 1.37). The authors also reported rotaxane formation *via* C-S bond formation, using aryl iodide and thiol functionalized 'half-threads' in the presence of macrocycle **85-Cu(I)**, although, in this case, large excesses of 'half-threads' (>10 equivalents) were necessary to produce any rotaxane (27% yield).

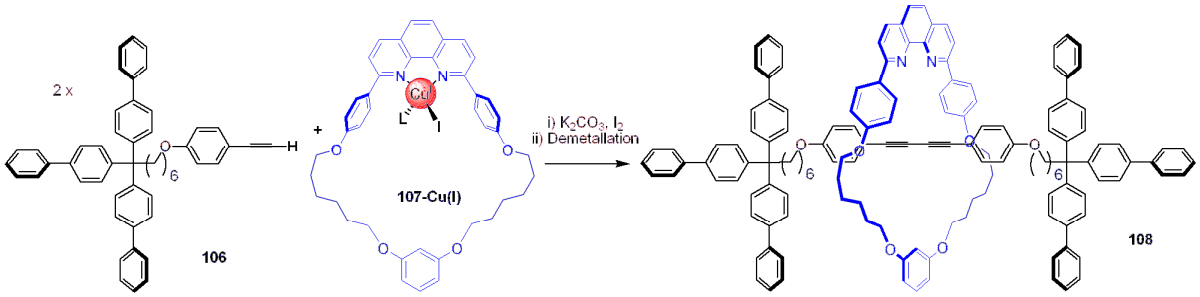

Scheme 1.37. A Cu(I) oxidative homo-coupling of aryl-alkyne 'half-thread' **106** to generate rotaxane **108** in 72% yield.[103]

The Leigh group also reported the use of palladium(II) in alkyne homo-couplings.[104] Both stoichiometric and sub-stoichiometric (10 and 5 mol%) quantities of Pd(II) resulted in good conversions of alkyne functionalized 'half-thread' **109**, in the presence of macrocycle **79**, to rotaxane **110**. The mechanism of rotaxane formation is thought to proceed *via* stereoretentive transmetallation of the *trans* chlorides present in complex **111-Pd(II)** with copper(I)-acetylide 'half-threads' **109-Cu(I)** (Scheme 1.38). Isomerization of *trans*-**112-Pd(II)** to *cis*-**112-Pd(II)** and reductive elimination generated rotaxane **110**. Pd(0) underwent oxidation to Pd(II) and re-entered in the catalytic cycle to generate more rotaxane.

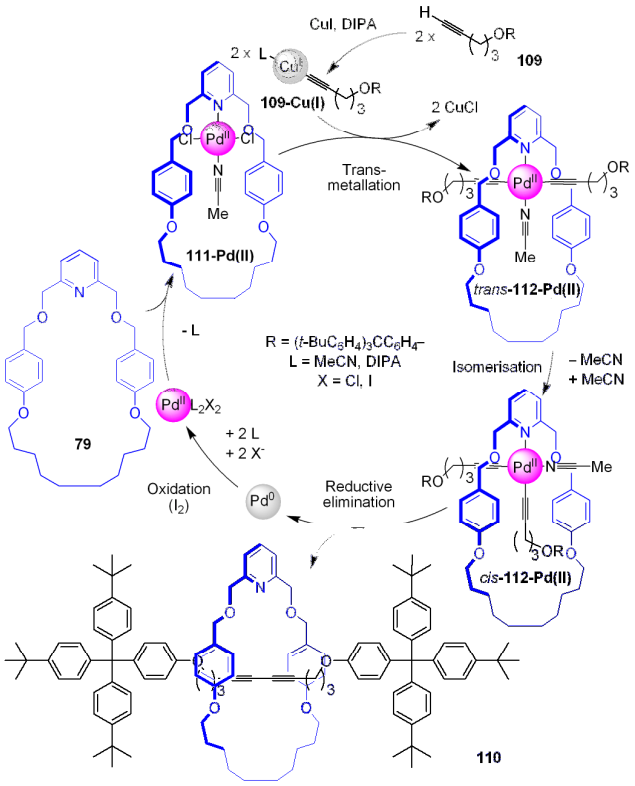

Scheme 1.38. A Pd(II)-catalyzed homo-coupling of alkyne 'half-thread' **109** in the presence of pyridine-based macrocycle **79** led to [2]rotaxane **110**.[104a]

Cross-couplings of alkynes were also achieved using the Cadiot-Chodkiewicz reaction.[105] Carrying out the reaction with one equivalent of preformed copper acetylide 'half-thread' **113-Cu(I)** and one equivalent of bromoacetylene 'half-thread' **114** in the presence of one equivalent of a bipy-based macrocycle **115** led to hetero-coupled rotaxane **116** in 85% yield. The reaction is proposed to proceed *via* coordination of a pre-formed Cu(I)-acetylide **113-Cu(I)** to bidentate macrocycle **115** (Scheme 1.39). Oxidative addition of bromo-acetylene **114** to Cu(I)-complex **117-Cu(I)** occurs on the opposite face of the macrocycle to produce intermediate **118-Cu(III)**. Reductive elimination of complex **118-Cu(III)** furnishes hetero-coupled rotaxane **116**.

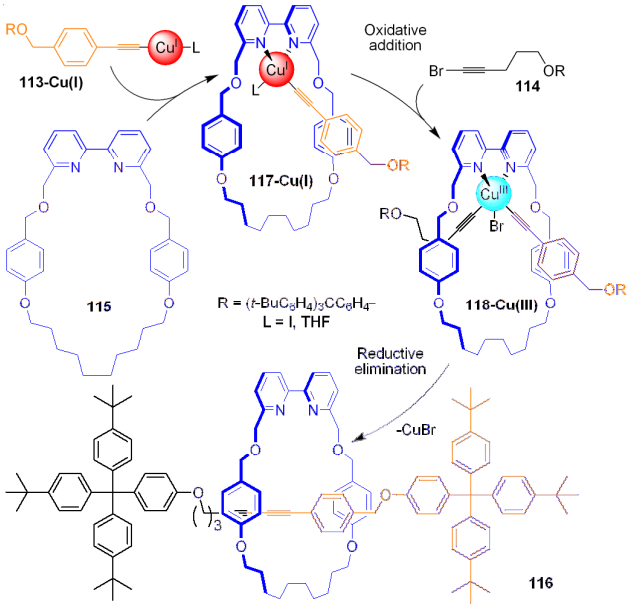

Scheme 1.39. Cadiot-Chodkiewicz "active" metal template synthesis of rotaxanes.[105]

To further demonstrate the utility of this "active" template reaction, a two "station" molecular shuttle (**119**, Scheme 1.40) was synthesized. Weak inter-component interactions were used to bias the position of a macrocycle on the thread. In the neutral form, the bipy macrocycle was predominantly located over the aniline "station" *via* the aniline proton participating in a single contact hydrogen bonding motif to one *N*-donor of the bipy unit. Addition of either *p*-TsOH acid or LiI, led to translocation of the macrocycle to the DMAP "station". The proton or metal ion was involved in binding to two *N*-donors, one from the macrocycle and one from the DMAP "station" (**119-M$^+$**). The molecular shuttle was reset to its neutral state by either washing with Na_2CO_3, in the case of the protonated shuttle, or an aqueous wash to remove the metal salt.

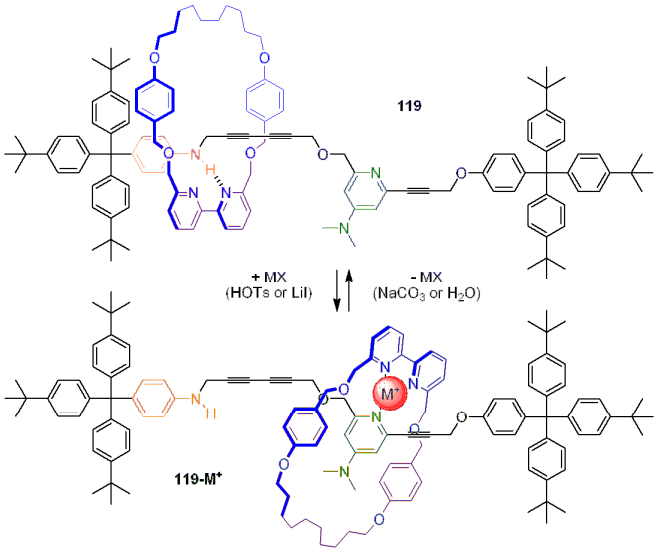

Scheme 1.40. Cadiot-Chodkiewicz synthesis of molecular shuttle **119**, in which control over the macrocycle's position was achieved *via* metallation or protonation.[105]

1.5.3 Rotaxanes *via* Oxidative Heck Reactions

The Leigh group also investigated palladium catalyzed cross-coupling reactions.[106] Attempts at constructing rotaxanes using Pd(0)-catalyzed reactions proved unsuccessful. This was attributed to the inability of the macrocycles, all featured either mono-, bi-, or tridentate *N*-donor ligands, to coordinate to Pd(0). Attention was shifted to Pd(II)-mediated oxidative Heck cross-couplings. Complex **120-Pd(II)** was formed *in situ* by addition of a catalytic quantity (10 mol%) of $Pd(OAc)_2$ to macrocycle **115**. Addition of aryl-boronic acid **121** and alkene **122** 'half-threads' and an oxidant lead to the formation of rotaxane **123**. Good yields of rotaxanes were obtained when using just 1 mol% of $Pd(OAc)_2$. The reaction proved tolerant to a variety of alkene functionalized 'half-threads' and electron-poor boronic acid 'half-threads'.

The proposed mechanism for rotaxane construction is shown in Scheme 1.41. Transmetallation of boronic acid **121** with macrocyclic-Pd(II) complex **120-Pd(II)**, followed by π-coordination to alkene 'half-thread' **122** leads to complex **124-Pd(II)** that features the two 'half-threads' coordinated on opposite faces of the macrocycle. Migratory insertion and subsequent *β*-hydride elimination forms both the covalent

bond and concurrently the mechanical bond generating rotaxane **123**. Pd(0) is oxidized back to Pd(II) and re-enters the catalytic cycle.

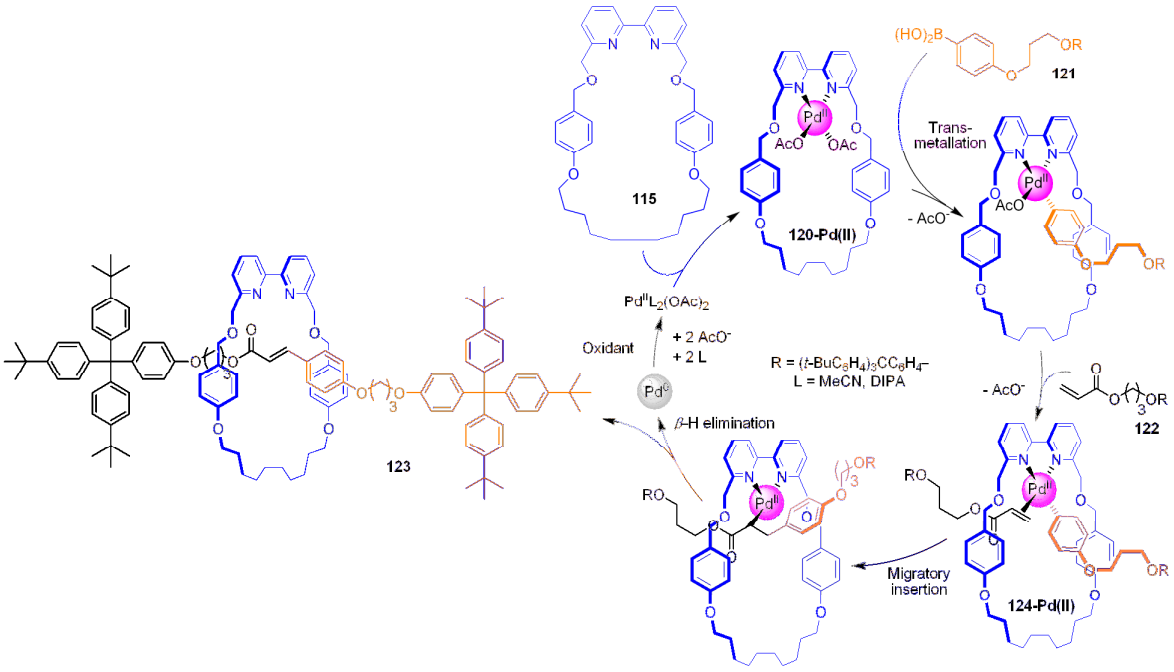

Scheme 1.41. The oxidative Heck reaction between boronic acid and alkene functionalized 'half-threads' generated a variety of [2]rotaxanes in good yields with sub-stoichiometric quantities of Pd(II).[106]

1.5.4 Pd(II)-Promoted Synthesis of Rotaxanes

Chapter Three describes how the "active" template methodology was extended to Lewis-acid catalysis, namely Pd(II)-mediated Michael additions.[107]

1.6 Summary and Outlook

From it's origins in the synthesis of macrocycles, the metal template strategy has grown to encompass the construction of rotaxanes, catenanes, knots and links. Sauvage's pioneering work using the template effect of copper(I) to organize phen ligands provided a practical basis for all subsequent metal template strategies in the construction of interlocked and entwined architectures. In the process, the methods

used for covalent capture have also evolved from the use of Williamson alkylations, to RCM, imine formation, and CuAAC reactions. Even the role of the metal ion has evolved, from acting to passively gather and organize the ligands prior to covalent capture, to, in recent reports, actively catalyzing mechanical bond formation. The "active" template approach, demonstrated through various homo- and hetero-couplings, using a variety of metal ions has provided a new route to interlocked architectures.

1.7 References

[1] (a) D. B. Amabilino, J. F. Stoddart, *Chem. Rev.* **1995**, *95*, 2725-2828; (b) G. A. Breault, C. A. Hunter, P. C. Mayers, *Tetrahedron* **1999**, *55*, 5265-5293; (c) T. J. Hubin, D. H. Busch, *Coord. Chem. Rev.* **2000**, *200*, 5-52.

[2] M. C. Thompson, D. H. Busch, *J. Am. Chem. Soc.* **1962**, *84*, 1762-1963.

[3] M. C. Thompson, D. H. Busch, *J. Am. Chem. Soc.* **1964**, *86*, 3651-3656.

[4] G. A. Melson, D. H. Busch, *J. Am. Chem. Soc.* **1964**, *86*, 4834-4837.

[5] G. A. Melson, D. H. Busch, *J. Am. Chem. Soc.* **1965**, *87*, 1706-1710.

[6] (a) N. F. Curtis, R. W. Hay, *Chem. Commun.* **1966**, 524-525; (b) N. F. Curtis, *Coord. Chem. Rev.* **1968**, *3*, 3-47.

[7] J. D. Curry, D. H. Busch, *J. Am. Chem. Soc.* **1964**, *86*, 592-594.

[8] S. O. Wandiga, J. E. Sarneski, F. L. Urbach, *Inorg. Chem.* **1972**, *11*, 1349-1355.

[9] J.-M. Lehn, J.-P. Sauvage, J. Simon, R. Ziessel, C. Piccini-Leopardi, G. Germain, J.-P. Declercq, M. Van Meersche, *New J. Chem.* **1983**, *7*, 413-420.

[10] (a) J.-M. Lehn, A. Rigault, J. Siegel, J. Harrowfield, B. Chevrier, D. Moras, *Proc. Natl. Acad. Sci. U. S. A.* **1987**, *84*, 2565-2569; (b) T. M. Garrett, U. Koert, J.-M. Lehn, A. Rigault, D. Meyer, J. Fischer, *J. Chem. Soc., Chem. Commun.* **1990**, 557-558; (c) J.-M. Lehn, A. Rigault, *Angew. Chem.* **1988**, *100*, 1121-1122; *Angew. Chem. Int. Ed. Engl.* **1988**, *27*, 1095-1097; (d) B. Hasenknopf, J.-M. Lehn, G. Baum, D. Fenske, *Proc. Natl. Acad. Sci. U. S. A.* **1996**, *93*, 1397-1400.

[11] U. Koert, M. M. Harding, J.-M. Lehn, *Nature* **1990**, *346*, 339-342.

[12] (a) B. Hasenknopf, J.-M. Lehn, B. O. Kneisel, G. Baum, D. Fenske, *Angew. Chem.* **1996**, *108*, 1987-1990; *Angew. Chem. Int. Ed. Engl.* **1996**, *35*, 1838-1840; (b) B. Hasenknopf, J.-M. Lehn, N. Boumediene, A. Dupont-Gervais, A. Van Dorsselaer, B. Kneisel, D. Fenske, *J. Am. Chem. Soc.* **1997**, *119*, 10956-10962.

[13] V. I. Sokolov, *Uspekhi Khimii* **1973**, *42*, 1037-1059.

[14] (a) C. O. Dietrich-Buchecker, P. A. Marnot, J. P. Sauvage, *Tetrahedron Lett.* **1982**, *23*, 5291-5294; (b) C. O. Dietrich-Buchecker, P. A. Marnot, J.-P. Sauvage, J. R. Kirchhoff, D. R. McMillin, *J. Chem. Soc., Chem. Commun.* **1983**, 513-515; (c) C. O. Dietrich-Buchecker, J. P. Sauvage, *Tetrahedron Lett.* **1983**, *24*, 5091-5094.

[15] For reviews, see: (a) C. O. Dietrich-Buchecker, J.-P. Sauvage, *Chem. Rev.* **1987**, *87*, 795-810; (b) J.-P. Sauvage, *Acc. Chem. Res.* **1990**, *23*, 319-327; (c) J.-C. Chambron, C. Dietrich-Buchecker, C. Hemmert, A.-K. Khemiss, D. Mitchell, J.-P. Sauvage, J. Weiss, *Pure Appl. Chem.* **1990**, *62*, 1027-1034; (d) J.-C. Chambron, C. O. Dietrich-Buchecker, J.-F. Nierengarten, J.-P. Sauvage, *Pure Appl. Chem.* **1994**, *66*, 1543-1550; (e) J.-C. Chambron, C. O. Dietrich-Buchecker, V. Heitz, J.-F. Nierengarten, J.-P. Sauvage, C. Pascard, J. Guilhem, *Pure Appl. Chem.* **1995**, *67*, 233-240.

[16] (a) C. O. Dietrich-Buchecker, J.-P. Sauvage, J. P. Kintzinger, *Tetrahedron Lett.* **1983**, *24*, 5095-5098; (b) C. O. Dietrich-Buchecker, J.-P. Sauvage, J.-M. Kern, *J. Am. Chem. Soc.* **1984**, *106*, 3043-3045.

[17] (a) P. Schwab, M. B. France, J. W. Ziller, R. H. Grubbs, *Angew. Chem.* **1995**, *107*, 2179-2181; *Angew. Chem. Int. Ed. Engl.* **1995**, *34*, 2039-2041; (b) P. Schwab, R. H. Grubbs, J. W. Ziller, *J. Am. Chem. Soc.* **1996**, *118*, 100-110.

[18] (a) B. Mohr, M. Weck, J.-P. Sauvage, R. H. Grubbs, *Angew. Chem.* **1997**, *109*, 1365-1367; *Angew. Chem. Int. Ed. Engl.* **1997**, *36*, 1308-1310; (b) M. Weck, B. Mohr, J.-P. Sauvage, R. H. Grubbs, *J. Org. Chem.* **1999**, *64*, 5463-5471.

[19] M. Cesario, C. O. Dietrich-Buchecker, J. Guilhem, C. Pascard, J. P. Sauvage, *J. Chem. Soc., Chem. Commun.* **1985**, 244-247.

[20] C. O. Dietrich-Buchecker, J.-P. Sauvage, J. Weiss, *Tetrahedron Lett.* **1986**, *27*, 2257-2260.

[21] (a) A.-M. Albrecht-Gary, C. Dietrich-Buchecker, Z. Saad, J.-P. Sauvage, *J. Am. Chem. Soc.* **1988**, *110*, 1467-1472; (b) C. O. Dietrich-Buchecker, J.-M. Kern, J.-P. Sauvage, *J. Chem. Soc., Chem. Commun.* **1985**, 760-762; (c) A. J. Blake, C. O. Dietrich-Buchecker, T. I. Hyde, J.-P. Sauvage, M. Schröder, *J. Chem. Soc., Chem. Commun.* **1989**, 1663-1665.

[22] M. Cesario, C. O. Dietrich, A. Edel, J. Guilhem, J.-P. Kintzinger, C. Pascard, J.-P. Sauvage, *J. Am. Chem. Soc.* **1986**, *108*, 6250-6254.

[23] M. Hutin, C. A. Schalley, G. Bernardinelli, J. R. Nitschke, *Chem. Eur. J.* **2006**, *12*, 4069-4076.

[24] Using the same imine-pyridine motif this work has been applied to molecular wires, see: (a) D. Schultz, F. Biaso, A. R. M. Shahi, M. Geoffroy, K. Rissanen, L. Gagliardi, C. J. Cramer, J. R. Nitschke, *Chem. Eur. J.* **2008**, *14*, 7180-7185; and foldamer assemblies: (b) N. Delsuc, M. Hutin, V. E. Campbell, B. Kauffmann, J. R. Nitschke, I. Huc, *Chem. Eur. J.* **2008**, *14*, 7140-7143.

[25] C. Wu, P. R. Lecavalier, Y. X. Shen, H. W. Gibson, *Chem. Mater.* **1991**, *3*, 569-572.

[26] J.-C. Chambron, V. Heitz, J.-P. Sauvage, *J. Chem. Soc., Chem. Commun.* **1992**, 1131-1133.

[27] For electron transfer between porphyrin 'stoppers', see: (a) J.-C. Chambron, V. Heitz, J.-P. Sauvage, *J. Am. Chem. Soc.* **1993**, *115*, 12378-12384; (b) J.-C. Chambron, A. Harriman, V. Heitz, J.-P. Sauvage, *J. Am. Chem. Soc.* **1993**, *115*, 6109-6114; For reviews, see: (c) J.-C. Chambron, S. Chardon-Noblat, A. Harriman, V. Heitz, J.-P. Sauvage, *Pure Appl. Chem.* **1993**, *65*, 2343-2349. (d) J.-C. Chambron, J. P. Collin, J. O. Dalbavie, C. O. Dietrich-Buchecker, V. Heitz, F. Odobel, N. Solladié, J.-P. Sauvage, *Coord. Chem. Rev.* **1998**, *180*, 1299-1312. (e) L. Flamigni, V. Heitz, J.-P. Sauvage in *Non-Covalent Multi-Porphyrin Assemblies Synthesis And Properties: Structure And Bonding*, *Vol. 121*, **2006**, pp. 217-261; For electron transfer between porphyrin 'stoppers' and porphyrins appended to a macrocycle in rotaxane architectures, see: (f) M. Linke, J.-C. Chambron, V. Heitz, J.-P. Sauvage, *J. Am. Chem. Soc.* **1997**, *119*, 11329-11330; (g) M. Andersson, M. Linke, J.-C. Chambron, J. Davidsson, V. Heitz, J.-P. Sauvage, L. Hammarström, *J. Am. Chem. Soc.* **2000**, *122*, 3526-3527; (h) M.-J. Blanco, J.-C. Chambron, V. Heitz, J.-P. Sauvage, *Org. Lett.* **2000**, *2*, 3051-3054; (i) M. Andersson, M. Linke, J.-C. Chambron, J. Davidsson, V. Heitz, L. Hammarström, J.-P. Sauvage, *J. Am. Chem. Soc.* **2002**, *124*, 4347-4362.

[28] (a) P. Mobian, J.-P. Collin, J.-P. Sauvage, *Tetrahedron Lett.* **2006**, *47*, 4907-4909; (b) S. Durot, P. Mobian, J.-P. Collin, J.-P. Sauvage, *Tetrahedron* **2008**, *64*, 8496-8503.

[29] J.-P. Sauvage, J. Weiss, *J. Am. Chem. Soc.* **1985**, *107*, 6108-6110.

[30] C. O. Dietrich-Buchecker, A. Khemiss, J.-P. Sauvage, *J. Chem. Soc., Chem. Commun.* **1986**, 1376-1378.

[31] (a) C. O. Dietrich-Buchecker, J. Guilhem, A. K. Khemiss, J.-P. Kintzinger, C. Pascard, J.-P. Sauvage, *Angew. Chem.* **1987**, *99*, 711-714; *Angew. Chem. Int. Ed. Engl.* **1987**, *26*, 661-663; (b) J. Guilhem, C. Pascard, J.-P. Sauvage, J. Weiss, *J. Am. Chem. Soc.* **1988**, *110*, 8711-8713.

[32] F. Bitsch, C. O. Dietrich-Buchecker, A.-K. Khémiss, J.-P. Sauvage, A. Van Dorsselaer, *J. Am. Chem. Soc.* **1991**, *113*, 4023-4025.

[33] J.-M. Kern, J.-P. Sauvage, J.-L. Weidmann, *Tetrahedron* **1996**, *52*, 10921-10934.

[34] M. Gupta, S. Kang, M. F. Mayer, *Tetrahedron Lett.* **2008**, *49*, 2946-2950.

[35] (a) J.-C. Chambron, V. Heitz, J.-P. Sauvage, *J. Am. Chem. Soc.* **1993**, *115*, 12378-12384; (b) N. Solladié, J.-C. Chambron, C. O. Dietrich-Buchecker, J.-P. Sauvage, *Angew. Chem.* **1996**, *108*, 957-960; *Angew. Chem. Int. Ed. Engl.* **1996**, *35*, 906-909.

[36] N. Solladié, J.-C. Chambron, J.-P. Sauvage, *J. Am. Chem. Soc.* **1999**, *121*, 3684-3692.

[37] D. B. Amabilino, C. O. Dietrich-Buchecker, A. Livoreil, L. Pérez-García, J.-P. Sauvage, J. F. Stoddart, *J. Am. Chem. Soc.* **1996**, *118*, 3905-3913.

[38] A. Livoreil, C. O. Dietrich-Buchecker, J.-P. Sauvage, *J. Am. Chem. Soc.* **1994**, *116*, 9399-9400.

[39] (a) F. Baumann, A. Livoreil, W. Kaim, J.-P. Sauvage, *Chem. Commun.* **1997**, 35-36; (b) A. Livoreil, J.-P. Sauvage, N. Armaroli, V. Balzani, L. Flamigni, B. Ventura, *J. Am. Chem. Soc.* **1997**, *119*, 12114-12124.

[40] (a) J.-P. Collin, P. Gaviña, J.-P. Sauvage, *Chem. Commun.* **1996**, 2005-2006; (b) P. Gaviña, J.-P. Sauvage, *Tetrahedron Lett.* **1997**, *38*, 3521-3524; (c) N. Armaroli, V. Balzani, J.-P. Collin, P. Gaviña, J.-P. Sauvage, B. Ventura, *J. Am. Chem. Soc.* **1999**, *121*, 4397-4408; (d) N. Weber, C. Hamann, J.-M. Kern, J.-P. Sauvage, *Inorg. Chem.* **2003**, *42*, 6780-6792; (e) I. Poleschak, J.-M. Kern, J.-P. Sauvage, *Chem. Commun.* **2004**, 474-476; (f) U. Létinois-Halbes, D. Hanss, J. M. Beierle, J.-P. Collin, J.-P. Sauvage, *Org. Lett.* **2005**, *7*, 5753-5756; (g) F. Durola, J.-P. Sauvage, *Angew. Chem.* **2007**, *119*, 3607-3610; *Angew. Chem. Int. Ed.* **2007**, *46*, 3537-3540; For a comprehensive set of reviews see: (h) J.-P. Sauvage, *Acc. Chem. Res.* **1998**, *31*, 611-619; (i) J.-C. Chambron, J.-P. Sauvage, *Chem. Eur. J.* **1998**, *4*, 1362-1366; (j) M.-J. Blanco, M. C. Jiménez, J.-C. Chambron, V. Heitz, M. Linke, J.-P. Sauvage, *Chem. Soc. Rev.* **1999**, *28*, 293-305; J.-P. Collin, C. Dietrich-Buchecker, P. Gaviña, M. C. Jimenez-Molero, J.-P. Sauvage, *Acc. Chem. Res.* **2001**, *34*, 477-487; (k) L. Raehm, J.-P. Sauvage *in Molecular Machines and Motors: Structure and Bonding*, *Vol. 99*, **2001**, pp. 55-78; (l) C. Dietrich-Buchecker, M. C. Jimenez-Molero, V. Sartor, J.-P. Sauvage, *Pure Appl. Chem.* **2003**, *75*, 1383-

1393; (m) J.-P. Sauvage, *Chem. Commun.* **2005**, 1507-1510; (n) S. Bonnet, J.-P. Collin, M. Koizumi, P. Mobian, J.-P. Sauvage, *Adv. Mater.* **2006**, *18*, 1239-1250; (o) B. Champin, P. Mobian, J.-P. Sauvage, *Chem. Soc. Rev.* **2007**, *36*, 358-366; (p) E. Baranoff, F. Barigelletti, S. Bonnet, J.-P. Collin, L. Flamigni, P. Mobian, J.-P. Sauvage in *Photofunctional Transition Metals Complexes: Structure And Bonding*, *Vol. 123*, **2007**, pp. 41-78; (q) E. R. Kay, D. A. Leigh, F. Zerbetto, *Angew. Chem.* **2007**, *119*, 72-196; *Angew. Chem. Int. Ed.* **2007**, *46*, 72-191; (r) S. Bonnet, J.-P. Collin, *Chem. Soc. Rev.* **2008**, *37*, 1207-1217.

[41] L. Raehm, J.-M. Kern, J.-P. Sauvage, *Chem. Eur. J.* **1999**, *5*, 3310-3317.

[42] (a) M. C. Jiménez, C. Dietrich-Buchecker, J.-P. Sauvage, A. De Cian, *Angew. Chem.* **2000**, *112*, 1351-1354; *Angew. Chem. Int. Ed.* **2000**, *39*, 1295-1298; (b) T. Kraus, M. Buděšínský, J. Cvačka, J.-P. Sauvage, *Angew. Chem.* **2006**, *118*, 264-267; *Angew. Chem. Int. Ed.* **2006**, *45*, 258-261.

[43] (b) J.-P. Collin, J. Frey, V. Heitz, E. Sakellariou, J.-P. Sauvage, C. Tock, *New J. Chem.* **2006**, *30*, 1386-1389; (c) J. Frey, C. Tock, J.-P. Collin, V. Heitz, J.-P. Sauvage, K. Rissanen, *J. Am. Chem. Soc.* **2008**, *130*, 11013-11022.

[44] C. Hamann, J.-M. Kern, J.-P. Sauvage, *Inorg. Chem.* **2003**, *42*, 1877-1883.

[45] J.-P. Sauvage, M. Ward, *Inorg. Chem.* **1991**, *30*, 3869-3874.

[46] N. Belfrekh, C. Dietrich-Buchecker, J.-P. Sauvage, *Inorg. Chem.* **2000**, *39*, 5169-5172;

[47] J. C. Loren, P. Gantzel, A. Linden, J. S. Siegel, *Org. Biomol. Chem.* **2005**, *3*, 3105-3116.

[48] D. A. Leigh, P. J. Lusby, S. J. Teat, A. J. Wilson, J. K. Y. Wong, *Angew. Chem.* **2001**, *113*, 1586-1591; *Angew. Chem. Int. Ed.* **2001**, *40*, 1538-1543.

[49] L. Hogg, D. A. Leigh, P. J. Lusby, A. Morelli, S. Parsons, J. K. Y. Wong, *Angew. Chem.* **2004**, *116*, 1238-1241; *Angew. Chem. Int. Ed.* **2004**, *43*, 1218-1221.

[50] For a review see: (a) J.-C. Chambron, J.-P. Collin, V. Heitz, D. Jouvenot, J.-M. Kern, P. Mobian, D. Pomeranc, J.-P. Sauvage, *Eur. J. Org. Chem.* **2004**, 1627-1638; (b) P. Mobian, J.-M. Kern, J.-P. Sauvage, *J. Am. Chem. Soc.* **2003**, *125*, 2016-2017.

[51] F. Arico, P. Mobian, J.-M. Kern, J.-P. Sauvage, *Org. Lett.* **2003**, *5*, 1887-1890.

[52] P. Mobian, J.-M. Kern, J.-P. Sauvage, *Helv. Chim. Acta* **2003**, *86*, 4195-4213.

[53] P. Mobian, J.-M. Kern, J.-P. Sauvage, *Inorg. Chem.* **2003**, *42*, 8633-8637.

[54] (a) D. Pomeranc, D. Jouvenot, J.-C. Chambron, J.-P. Collin, V. Heitz, J.-P. Sauvage, *Chem. Eur. J.* **2003**, *9*, 4247-4254; (b) J.-P. Collin, D. Jouvenot, M. Koizumi, J.-P. Sauvage, *Eur. J. Inorg. Chem.* **2005**, 1850-1855.

[55] F. Durola, J.-P. Sauvage, O. S. Wenger, *Chem. Commun.* **2006**, 171-173.

[56] F. Durola, L. Russo, J.-P. Sauvage, K. Rissanen, O. S. Wenger, *Chem. Eur. J.* **2007**, *13*, 8749-8753.

[57] A. I. Prikhod'ko, F. Durola, J.-P. Sauvage, *J. Am. Chem. Soc.* **2008**, *130*, 448-449.

[58] C. Hamann, J.-M. Kern, J.-P. Sauvage, *Dalton Trans.* **2003**, 3770-3775.

[59] A.-M. Fuller, D. A. Leigh, P. J. Lusby, I. D. H. Oswald, S. Parsons, D. B. Walker, *Angew. Chem.* **2004**, *116*, 4004-4008; *Angew. Chem. Int. Ed.* **2004**, *43*, 3914-3918.

[60] Y. Furusho, T. Matsuyama, T. Takata, T. Moriuchi, T. Hirao, *Tetrahedron Lett.* **2004**, *45*, 9593-9597.

[61] D. A. Leigh, P. J. Lusby, A. M. Z. Slawin, D. B. Walker, *Angew. Chem.* **2005**, *117*, 4633-4640; *Angew. Chem. Int. Ed.* **2005**, *44*, 4557-4564.

[62] A.-M. L. Fuller, D. A. Leigh, P. J. Lusby, *Angew. Chem.* **2007**, *119*, 5103-5107; *Angew. Chem. Int. Ed.* **2007**, *46*, 5015-5019.

[63] For another [*n*]rotaxane synthesis in which *n* binding sites are required in the thread in order to generate a [*n*]rotaxane, see: J. Wu, K. C.-F. Leung, J. F. Stoddart, *Proc. Natl. Acad. Sci. U. S. A.* **2007**, *104*, 17266-17271.

[64] J. D. Crowley, D. A. Leigh, P. J. Lusby, R. T. McBurney, L.-E. Perret-Aebi, C. Petzold, A. M. Z. Slawin, M. D. Symes, *J. Am. Chem. Soc.* **2007**, *129*, 15085-15090.

[65] A.-M. L. Fuller, D. A. Leigh, P. J. Lusby, A. M. Z. Slawin, D. B. Walker, *J. Am. Chem. Soc.* **2005**, *127*, 12612-12619.

[66] S. M. Goldup, D. A. Leigh, P. J. Lusby, R. T. McBurney, A. M. Z. Slawin, *Angew. Chem.* **2008**, *120*, 7107-7111; *Angew. Chem. Int. Ed.* **2008**, *47*, 6999-7003.

[67] For a review and discussion on knots, see: E. E. Fenlon, *Eur. J. Org. Chem.* **2008**, *30*, 5023-5035.

[68] C. Dietrich-Buchecker, J. P. Sauvage, *New J. Chem.* **1992**, *16*, 277-285.

[69] (a) C. O. Dietrich-Buchecker, J.-P. Sauvage, *Angew. Chem.* **1989**, *101*, 192-194; *Angew. Chem. Int. Ed. Engl.* **1989**, *28*, 189-192; (b) C. O. Dietrich-

Buchecker, J.-P. Sauvage, J.-P. Kintzinger, P. Maltèse, C. Pascard, J. Guilhem, *New J. Chem.* **1992**, *16*, 931-942.

[70] C. O. Dietrich-Buchecker, J. Guilhem, C. Pascard, J.-P. Sauvage, *Angew. Chem.* **1990**, *102*, 1202-1204; *Angew. Chem. Int. Ed. Engl.* **1990**, *29*, 1154-1156.

[71] (a) C. O. Dietrich-Buchecker, J.-F. Nierengarten, J.-P. Sauvage, *Tetrahedron Lett.* **1992**, *33*, 3625-3628; (b) C. O. Dietrich-Buchecker, J.-P. Sauvage, A. De Cian, J. Fischer, *J. Chem. Soc., Chem. Commun.* **1994**, 2231-2232; (c) C. O. Dietrich-Buchecker, G. Rapenne, J.-P. Sauvage, A. De Cian, J. Fischer, *Chem. Eur. J.* **1999**, *5*, 1432-1439.

[72] C. Dietrich-Buchecker, G. Rapenne, J.-P. Sauvage, *Chem. Commun.* **1997**, 2053-2054.

[73] C. O. Dietrich-Buchecker, J.-P. Sauvage, N. Armaroli, P. Ceroni, V. Balzani, *Angew. Chem.* **1996**, *108*, 1190-1193; *Angew. Chem. Int. Ed. Engl.* **1996**, *35*, 1119-1121.

[74] C. Dietrich-Buchecker, N. G. Hwang, J.-P. Sauvage, *New J. Chem.* **1999**, *23*, 911-914.

[75] M. Meyer, A.-M. Albrecht-Gary, C. O. Dietrich-Buchecker, J.-P. Sauvage, *J. Am. Chem. Soc.* **1997**, *119*, 4599-4607.

[76] G. Rapenne, C. Dietrich-Buchecker, J.-P. Sauvage, *J. Am. Chem. Soc.* **1996**, *118*, 10932-10933.

[77] J. Jacques, C. Fouquey, *Org. Synth* **1989**, *67*, 1-12.

[78] S. C. J. Meskers, H. Dekkers, G. Rapenne, J.-P. Sauvage, *Chem. Eur. J.* **2000**, *6*, 2129-2134.

[79] L.-E. Perret-Aebi, A. von Zelewsky, C. Dietrich-Buchecker, J.-P. Sauvage, *Angew. Chem.* **2004**, *116*, 4582-4585; *Angew. Chem. Int. Ed.* **2004**, *43*, 4482-4485.

[80] G. Rapenne, C. Dietrich-Buchecker, J.-P. Sauvage, *J. Am. Chem. Soc.* **1999**, *121*, 994-1001.

[81] H. Adams, E. Ashworth, G. A. Breault, J. Guo, C. A. Hunter, P. C. Mayers, *Nature* **2001**, *411*, 763-763.

[82] P. C. Mayers, *Ph. D. Thesis, University of Sheffield, UK* **1997**.

[83] R. F. Carina, C. Dietrich-Buchecker, J.-P. Sauvage, *J. Am. Chem. Soc.* **1996**, *118*, 9110-9116.

[84] C. Dietrich-Buchecker, B. Colasson, D. Jouvenot, J.-P. Sauvage, *Chem. Eur. J.* **2005**, *11*, 4374-4386.

[85] (a) J.-F. Nierengarten, C. O. Dietrich-Buchecker, J.-P. Sauvage, *J. Am. Chem. Soc.* **1994**, *116*, 375-376; (b) J.-F. Nierengarten, C. O. Dietrich-Buchecker, J.-P. Sauvage, *New J. Chem.* **1996**, *20*, 685-693.

[86] C. Dietrich-Buchecker, E. Leize, J.-F. Nierengarten, J.-P. Sauvage, A. Van Dorsselaer, *J. Chem. Soc., Chem. Commun.* **1994**, 2257-2258.

[87] C. Dietrich-Buchecker, J. P. Sauvage, *Chem. Commun.* **1999**, 615-616.

[88] BRs were first synthesized using DNA, see: (a) C. D. Mao, W. Q. Sun, N. C. Seeman, *Nature* **1997**, *386*, 137-138; Seeman had earlier used DNA to create knots, see: (b) S. M. Du, N. C. Seeman, *J. Am. Chem. Soc.* **1992**, *114*, 9652-9655.

[89] J. C. Loren, M. Yoshizawa, R. F. Haldimann, A. Linden, J. S. Siegel, *Angew. Chem.* **2003**, *115*, 5880-5883; *Angew. Chem. Int. Ed.* **2003**, *42*, 5702-5705.

[90] S.-H. Chiu, A. R. Pease, J. F. Stoddart, A. J. P. White, D. J. Williams, *Angew. Chem.* **2002**, *114*, 280-284; *Angew. Chem. Int. Ed.* **2002**, *41*, 270-274.

[91] M. Schmittel, A. Ganz, D. Fenske, *Org. Lett.* **2002**, *4*, 2289-2292.

[92] M. Benaglia, F. Ponzini, C. R. Woods, J. S. Siegel, *Org. Lett.* **2001**, *3*, 967-969.

[93] (a) K. S. Chichak, S. J. Cantrill, A. R. Pease, S. H. Chiu, G. W. V. Cave, J. L. Atwood, J. F. Stoddart, *Science* **2004**, *304*, 1308-1312; (b) S. J. Cantrill, K. S. Chichak, A. J. Peters, J. F. Stoddart, *Acc. Chem. Res.* **2005**, *38*, 1-9.

[94] C. A. Schalley, *Angew. Chem.* **2004**, *116*, 4499-4501; *Angew. Chem. Int. Ed.* **2004**, *43*, 4399-4401.

[95] C. D. Pentecost, N. Tangchaivang, S. J. Cantrill, K. S. Chichak, A. J. Peters, J. F. Stoddart, *J. Chem. Educ.* **2007**, *84*, 855-859.

[96] K. S. Chichak, S. J. Cantrill, J. F. Stoddart, *Chem. Commun.* **2005**, 3391-3393.

[97] A. J. Peters, K. S. Chichak, S. J. Cantrill, J. F. Stoddart, *Chem. Commun.* **2005**, 3394-3396.

[98] (a) K. S. Chichak, A. J. Peters, S. J. Cantrill, J. F. Stoddart, *J. Org. Chem.* **2005**, *70*, 7956-7962; (b) C. R. Yates, D. Benitez, S. I. Khan, J. F. Stoddart, *Org. Lett.* **2007**, *9*, 2433-2436.

[99] C. D. Pentecost, A. J. Peters, K. S. Chichak, G. W. V. Cave, S. J. Cantrill, J. F. Stoddart, *Angew. Chem.* **2006**, *118*, 4205-4210; *Angew. Chem. Int. Ed.* **2006**, *45*, 4099-4104.

[100] (a) C. D. Pentecost, K. S. Chichak, A. J. Peters, G. W. V. Cave, S. J. Cantrill, J. F. Stoddart, *Angew. Chem.* **2007**, *119*, 222-226; *Angew. Chem. Int. Ed.* **2007**, *46*, 218-222; For a review on the reversible imine bond and its application in the template directed synthesis of interlocked molecules, see: (b) C. D. Meyer, C. S. Joiner, J. F. Stoddart, *Chem. Soc. Rev.* **2007**, *36*, 1705-1723.

[101] V. Aucagne, K. D. Hänni, D. A. Leigh, P. J. Lusby, D. B. Walker, *J. Am. Chem. Soc.* **2006**, *128*, 2186-2187.

[102] V. Aucagne, J. Berná, J. D. Crowley, S. M. Goldup, K. D. Hänni, D. A. Leigh, P. J. Lusby, V. E. Ronaldson, A. M. Z. Slawin, A. Viterisi, D. B. Walker, *J. Am. Chem. Soc.* **2007**, *129*, 11950-11963.

[103] S. Saito, E. Takahashi, K. Nakazono, *Org. Lett.* **2006**, *8*, 5133-5136.

[104] (a) J. Berná, J. D. Crowley, S. M. Goldup, K. D. Hänni, A.-L. Lee, D. A. Leigh, *Angew. Chem.* **2007**, *119*, 5811-5815; *Angew. Chem. Int. Ed.* **2007**, *46*, 5709-5713; (b) T. M. Swager, R. M. Moslin, *Synfacts* **2007**, 1158.

[105] J. Berná, S. M. Goldup, A.-L. Lee, D. A. Leigh, M. D. Symes, G. Teobaldi, F. Zerbetto, *Angew. Chem.* **2008**, *120*, 4464-4468; *Angew. Chem. Int. Ed.* **2008**, *47*, 4392-4396.

[106] J. D. Crowley, K. D. Hänni, A.-L. Lee, D. A. Leigh, *J. Am. Chem. Soc.* **2007**, *129*, 12092-12093.

[107] S. M. Goldup, D. A. Leigh, P. J. Lusby, R. T. McBurney, A. M. Z. Slawin, *Angew. Chem.* **2008**, *120*, 3429-3432; *Angew. Chem. Int. Ed.* **2008**, *47*, 3381-3384.

CHAPTER TWO

Cobalt(III) Template Synthesis of Catenanes and Rotaxanes

Published as "*Getting Harder: Cobalt(III)-Template Synthesis of Catenanes and Rotaxanes*"

David A. Leigh, Paul J. Lusby, Roy T. McBurney, Alessandra Morelli, Alexandra M. Z. Slawin, Andrew R. Thomson and D. Barney Walker, *J. Am. Chem. Soc.* **2009**, *131*, 3762-3771.

Acknowledgements

The following people are gratefully acknowledged for their practical contribution to this chapter: Ale Morelli for synthesis and crystallization of 'figure-of-eight' complex [Co**L4**]Et_3NCH_2Cl; Paul Lusby for initial synthesis of catenand H_4**L7**; Drew Thomson for initial synthesis of rotaxane H_2**L8**; Barney Walker for crystallization of H_4**L7**; Prof. Alex Slawin solved the X-ray crystal structures of 'figure-of-eight' complex [Co**L4**]Et_3NCH_2Cl, catenand H_4**L7** and catenate [Co**L7**]Et_3NH.

Synopsis

The Leigh group has previously reported on the synthesis of catenanes and rotaxanes using a variety of octahedral divalent metal ions to organize both imine and amine-based ligands. To the best of our knowledge there are no reports in the literature of octahedral trivalent metal templates utilized in the construction of interlocked architectures.

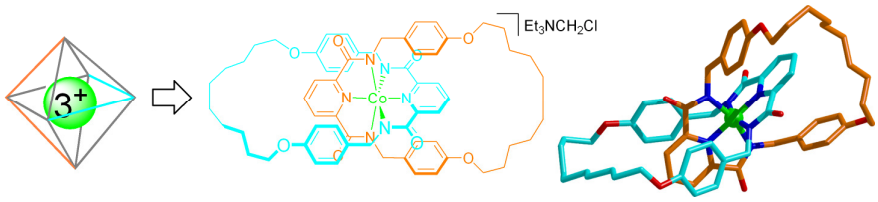

Tridentate dianionic pyridine-2,6-dicarboxamido ligands, each with two terminal alkene groups, coordinate Co(III) in a mutually orthogonal arrangement such that entwined or interlocked molecular architectures are produced by ring closing olefin metathesis. Double macrocyclization of two such ligands bound to Co(III) afford a non-interlocked 'figure-of-eight' complex in 42% yield, the structure determined by X-ray crystallography. Pre-forming one macrocycle and carrying out a single macrocyclization of the second bis-olefin with both ligands attached to the Co(III) template led to the isomeric [2]catenate in 69% yield. The mechanically interlocked structure was confirmed by X-ray crystallography of both the Co(III) catenate and the metal-free catenand. A Co(III)-template [2]rotaxane was assembled in 61% yield by macrocyclization of the bis-olefin ligand about an appropriate dianionic thread. For both catenanes and rotaxanes, removal of the metal ion via reduction under acidic conditions to the more labile Co(II) gave neutral interlocked molecules with well-defined co-conformations stabilized by intercomponent hydrogen bonding.

2.1 Introduction

The use of transition metal ions as templates[1-7] and structural elements[8] were breakthrough strategies in the development of effective methods for the synthesis of mechanically interlocked architectures, but for over fifteen years the Cu(I)-bis-phenanthroline system developed in Strasbourg remained the only reliable metal template route to catenanes and rotaxanes. Recently, however, complimentary and robust methodologies for the construction of rotaxanes and catenanes around other metal-ligand systems, featuring a range of metal coordination geometries and ligand types, have been developed. For example, relatively soft divalent metal ions have been used to template the assembly of catenanes[9a] and rotaxanes[9b] around octahedral metal centers (Figure 2.1a);[10] the two dimensional square planar geometry of palladium(II) has been used to prepare [2]catenanes,[11a] [2]-,[11b, c] [3]-[11d] and [4]rotaxanes[11d] and molecular shuttles;[11e] and the linear coordination mode of gold(I) has been demonstrated to template the assembly of minimally-functionalized building blocks into both catenanes and rotaxanes.[12] The result is that chemists now have a diverse range of mechanically interlocked ligands and complexes that can be investigated from the point of view of their electrochemistry,[2b, 5h, 13] photochemistry,[5l, 10e, 10j, 14] reactivity,[15] selectivity of binding,[13a, 16] and as key structural motifs in prototypes for molecular machines.[17] However, the ability of the metal to template a particular structure remains highly dependent on the nature of both the metal and the ligand system (and their mutual compatibility), and modest changes to either can prevent the building blocks assembling in the desired manner.[11a, b] Furthermore, mechanically interlocked ligands that have been assembled around one type of template (*e.g.* a soft metal ion) are generally not well-suited to binding to other types of metal ion (*e.g.* hard metal ions). Consequently, there is an ongoing need for different types of interlocked ligand motifs which enable different sorts of metal ions to be complexed by them. Herein we revisit the challenge of the template synthesis of mechanically interlocked architectures which bind metal ions with a preferred octahedral coordination geometry, this time utilizing the hard trivalent transition metal ion cobalt(III)[18] to pre-organize two tridentate pyridine 2,6-dicarboxamido ligands in order to construct

both catenanes and rotaxanes. The Co(III) template synthesis has several distinctive features which complement existing methods for interlocked molecule synthesis: (i) it utilizes two similar (rotaxane) or identical (catenane) dianionic ligands in a homotopic binding motif that makes the template complex anionic rather than cationic; (ii) the template is constructed and applied in an unusual three-step process involving, first, assembly of the ligands under thermodynamic control around kinetically labile Co(II), subsequent locking of the ligands on the metal by oxidiation to non-labile Co(III) (after which the desired template complex can be separated from other ligand-metal complexes if necessary), followed by ring closing or cross olefin metathesis to covalently capture the interlocked or entwined structure; (iii) the methodology is high yielding and uses readily prepared building blocks; (iv) removal of the metal ion from the interlocked product generates a free ligand which still exhibits a well-defined co-conformation as a result of intercomponent hydrogen bonding; (v) Co(III) can be reintroduced into the resulting interlocked ligands to form [2]catenane and [2]rotaxane complexes of a hard, kinetically inert to ligand exchange, metal ion.

2.2 Results and Discussion

2.2.1 Ligand design

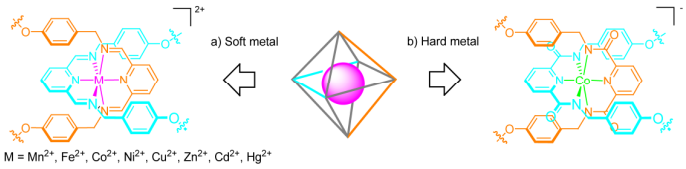

Figure 2.1. Tridentate ligand systems that favor orthogonal *mer* coordination to octahedral metal ions: (a) neutral pyridine-2,6-diimino ligands suitable for chelating 'soft' divalent metal ions; (b) *bis*-anionic pyridine-2,6-dicarboxamido ligands suitable for chelating 'hard' trivalent metal ions.

The basic design of the ligands for Co(III)-mediated assembly is derived from an earlier system successfully used to synthesize interlocked architectures around divalent metal ions (Figure 2.1). In that system, the *mer* coordination of two neutral

tridentate ligands (Figure 2.1a) around a divalent octahedral metal center holds the ligands in an orthogonal arrangement and the shape of the ligands, supported by π-π interactions between the interchelated ligands, subsequently directs interlocking macrocyclization reactions to give high yields of [2]catenates[9a] and [2]rotaxanes[9b] under either kinetic or thermodynamic control. Deprotonated carboxamide (carboxamido) groups are known to be good ligands for hard ions such as Fe(III) and Co(III) and their complexation behavior has been extensively studied because of their significance in key natural processes.[19] It appeared that replacement of the divalent-ion-coordinating imine groups with amides (Figure 2.1b)[20] would facilitate binding to trivalent ions whilst conserving the features—intercomponent π-stacking and preorganized 180˚ degree turn—that induce the terminal groups of each ligands to converge and form the crossover points necessary for catenane and rotaxane formation. We selected ring closing olefin metathesis (RCM) for the reaction to covalently capture the interlocked products, as it is high yielding and tolerant to the demands imposed by macrocyclization to form very large rings (entropy loss and sufficient stability of the reactive intermediate when adoption of a geometry where ring closing can occur is a rare event). Ligand H_2**L1** appeared to have these desired features and, accordingly, the products of a series of single and double macrocyclization reactions of the ligand on a Co(III) template were investigated.

2.2.2. Co(III)-Template 'Figure-of-Eight' Synthesis *via* Double Cross Olefin Metathesis

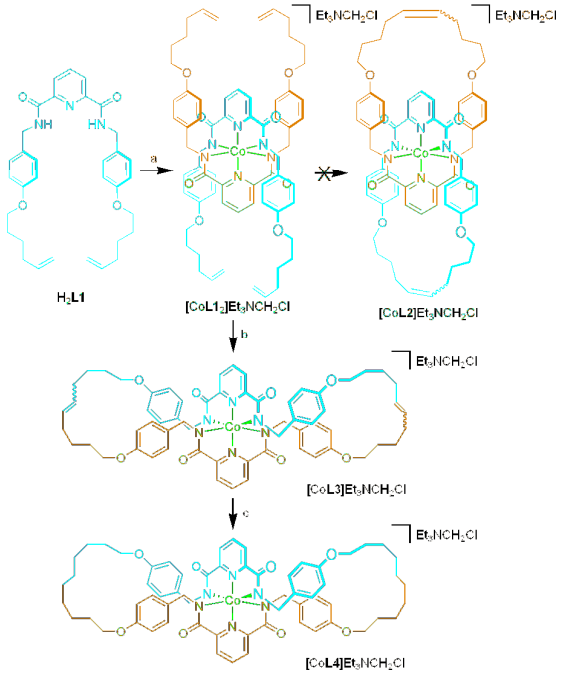

Scheme 2.1. Synthesis of 'figure-of-eight' complex [Co**L4**]$^-$ *via* double cross olefin metathesis of **L2** on a Co(III) template. Reagents and conditions: (a) (i) $Co(OAc)_2{\cdot}(H_2O)_4$, $Et_4N(OAc)$, NaOEt, EtOH, reflux, 1 h, (ii) silica gel, CH_2Cl_2, acetone, Et_3N, 83%; (b) $(Cy_3P)_2Cl_2Ru{=}CHPh$, CH_2Cl_2, 2 d, 42%; (c) Pd/C, MeOH, H_2, 1 d, 85%.

Initially we investigated the olefin metathesis of two molecules of H_2**L1** on a cobalt(III) template, a reaction which could potentially generate a number of different product types and topologies (Scheme 2.1). Since ligand exchange around Co(III) centers is generally slow, it proved convenient to initially assemble the ligands around Co(II) and then to kinetically lock the system by simple air oxidation to Co(III) (the increase in oxidation state is strongly favored by the two doubly-negatively-charged ligands). Reaction of an ethanolic solution of H_2**L1** with a cobalt(II) salt ($Co(OAc)_2{\cdot}(H_2O)_4$), $Et_4N(OAc)$ and NaOEt under anaerobic conditions gave an immediate color change from pink to deep purple. Exposure of the presumed divalent species, [Co$\mathbf{L1}_2$]$^{2-}$, to air resulted in a second color change from purple to green (indicative of oxidation to Co(III)) over *ca.* five minutes. After heating at

reflux for a further 1 h and work up of the reaction, purification by column chromatography on silica gel with acetone:dichloromethane:triethylamine (40:59:1) as eluent, afforded complex [Co**L1**$_2$]Et_3NCH_2Cl in 83% yield (Scheme 2.1, step a). The unexpected countercation is apparently formed ($Et_3N + CH_2Cl_2 \rightarrow Et_3N^+CH_2Cl + Cl^-$) and introduced into the product (cation exchange with Et_4N^+) during the chromatography step.[21] Complex [Co**L1**$_2$]Et_3NCH_2Cl gave a sharp ^{1}H NMR spectrum in CD_2Cl_2 (Figure 2.3a),[22] confirming the structure contained diamagnetic Co(III) rather than paramagnetic Co(II). Comparison of the ^{1}H NMR spectrum with that of the free ligand H_2**L1** (Figure 2.2b) revealed upfield shifts of H_E and H_F, indicative of the π-stacking between the benzylic groups of each ligand intended to favor catenane formation. However, subjecting [Co**L1**$_2$]Et_3NCH_2Cl to olefin metathesis with $(PCy_3)_2Cl_2Ru$=CHPh (Scheme 2.1, step b) led to a 'figure-of-eight' complex [Co**L3**]Et_3NCH_2Cl formed through interligand cross-metathesis.[10b, 23] The structure was confirmed by X-ray crystallography of single crystals of the hydrogenated (H_2, Pd/C, MeOH, Scheme 2.1, step c) complex (Figure 2.3). The X-ray crystal structure shows that in order to accommodate the perpendicular alignment of the tridentate pyridine-2,6-dicarboxamido ligands around the octahedral Co(III) center, the macrocycle adopts a helical conformation which promotes interligand cross metathesis rather than intraligand ring closing metathesis.

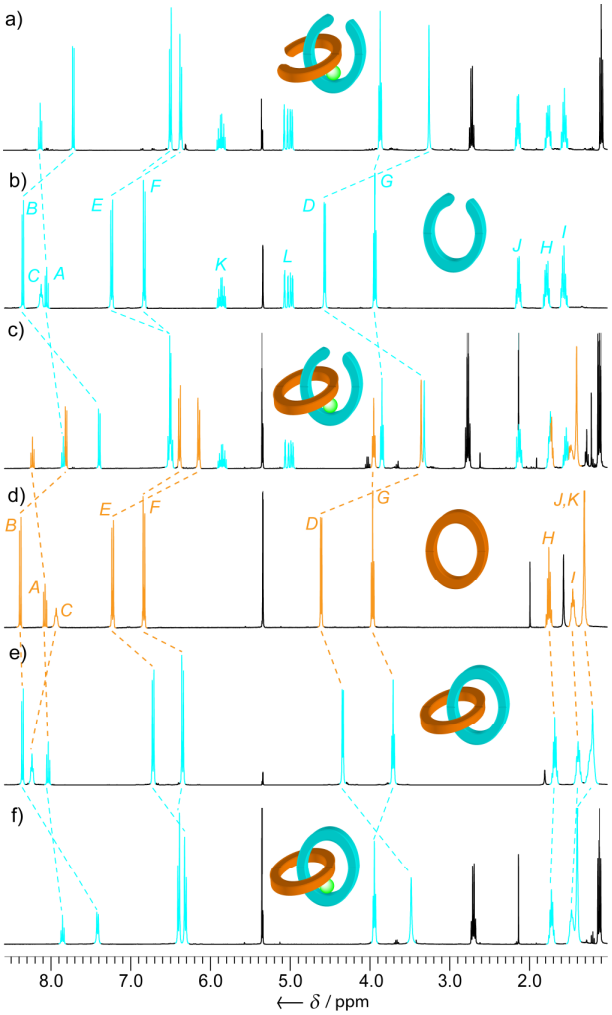

Figure 2.2. ^{1}H NMR spectra (400 MHz, CD_2Cl_2, 300 K) of a) [Co**L1**$_2$]Et_3NCH_2Cl, b) H_2**L1**, c) pre-catenate [**L1**Co**L5**]Et_3NCH_2Cl, d) macrocycle H_2**L5**, e) [2]catenand H_4**L7**, and f) [2]catenate [Co**L7**]Et_3NCH_2Cl. The assignments correspond to the lettering shown in Scheme 2.2.

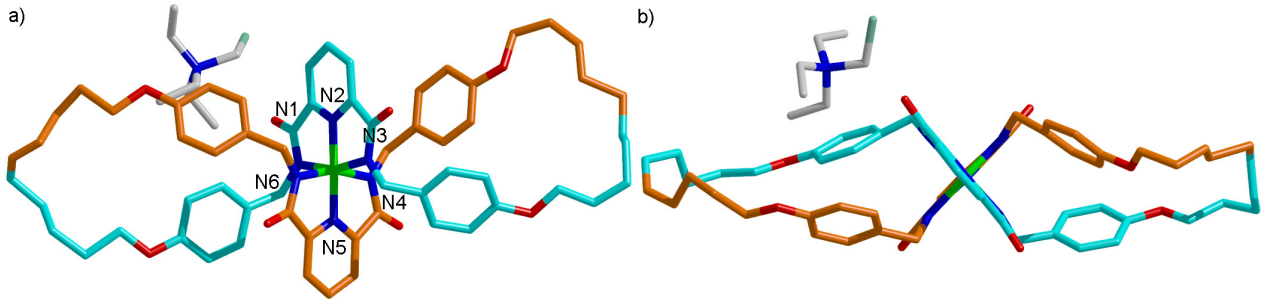

Figure 2.3. X-Ray crystal structure of 'figure-of-eight' complex [Co**L4**]Et_3NCH_2Cl. (a) Side-on view. (b) Viewed down the N2-Co-N5 axis. Selected bond lengths (Å) and angles (°): N1-Co 1.98, N2-Co 1.85, N3-Co 1.94, N4-Co 1.96, N5-Co 1.83, N6-Co 1.96, N1-Co-N3 163.6, N4-Co-N6 163.8, N2-Co-N5 177.1. The hydrogen atoms are omitted for clarity. The carbon atoms are shown in light blue (those originating from one ligand), orange (those originating from the second ligand) and grey (countercation) , cobalt(III) green, oxygen red, nitrogen blue and chlorine olive.

2.2.3 Co(III)-Template [2]Catenate Synthesis *via* Single Macrocyclization

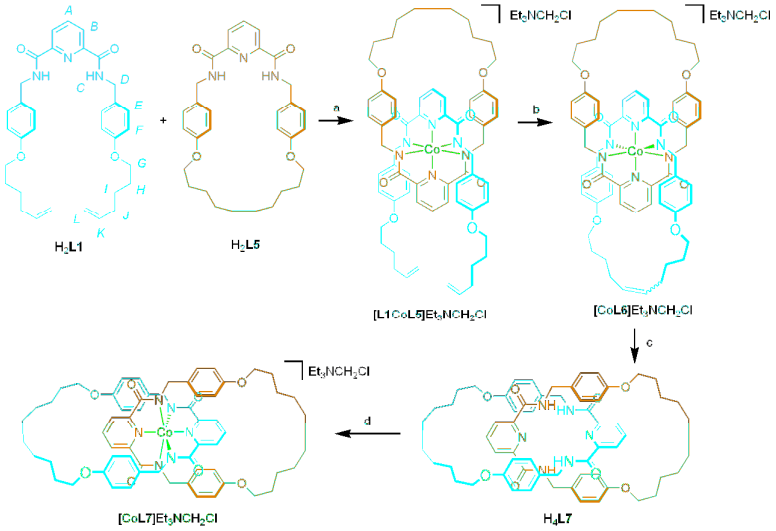

Scheme 2.2. Synthesis of [2]catenate [Co**L7**]$^-$ *via* single macrocyclization of **L1** through **L5** on a Co(III) template. Reagents and conditions: (a) $Co(OAc)_2{\cdot}(H_2O)_4$, $Et_4N(OAc)$, NaOEt, EtOH, reflux, 1 h, 84%; (b) $(PCy_3)_2Cl_2Ru{=}CHPh$, CH_2Cl_2, 2 d, 69%; (c) (i) Pd/C, MeOH, H_2, 1 d, (ii) Zn, AcOH, MeOH, 30 min., 65%; (d) $Co(OAc)_2{\cdot}(H_2O)_4$, $Et_4N(OAc)$, NaOMe, EtOH, reflux, 30 min., 75%.

We next investigated single RCM of a complex consisting of H_2**L1** and the pre-formed macrocycle H_2**L5** held in a mutually orthogonal arrangement by the Co(III)

template. Treatment of an ethanolic solution of H_2**L1**, H_2**L5**, $Co(OAc)_2{\cdot}(H_2O)_4$ and $Et_4N(OAc)$ with NaOEt (4.4 equiv.) (Scheme 2.2, step a) under anaerobic conditions, followed by exposure to air, gave the same series of color changes observed during the formation of $[Co\mathbf{L1}_2]^-$ (Scheme 2.1, step a). The mixed ligand Co(III) complex [**L1**Co**L5**]Et_3NCH_2Cl was isolated after chromatography (again, with cation exchange) in 84% yield. In comparison to the ^{1}H NMR of H_2**L1** (Figure 2.2b) and macrocycle H_2**L5** (Figure 2.2d) a significant shift to lower field is observed for both sets of benzylic aromatic resonances (H_E's and H_F's, Figure 2.2c) in [**L1**Co**L5**]Et_3NCH_2Cl, again indicating the presence of the π-stacking interactions intended to encourage catenane formation. The selectivity of the reaction for the mixed ligand complex [**L1**Co**L5**]$^-$—neither of the homotopic complexes $[\mathbf{L1}_2Co]^-$ or $[\mathbf{L5}_2Co]^-$ are apparent in the product mixture—is a result of the shape and topology of the **L5** macrocycle physically preventing complexes of the type $[\mathbf{L5}_2Co]^-$ from forming. Therefore, the only way in which all the ligands in an equimolar solution of the cobalt ion, $\mathbf{L1}^{2-}$ and $\mathbf{L5}^{2-}$ can be coordinated is through sole formation of the mixed ligand complex. The thermodynamically-driven rearrangement of any initially formed $[\mathbf{L1}_2Co]^{2-}$ likely occurs before the ligands are 'locked' around kinetically inert Co(III), *i.e.* prior to aerobic oxidation.

Ring closing metathesis of [**L1**Co**L5**]Et_3NCH_2Cl under high dilution conditions (Scheme 2.2, step b) proceeded smoothly to give a new Co(III) complex, clearly different by ^{1}H NMR spectroscopy and thin layer chromatography to $[Co\mathbf{L3}]^-$, in 69% yield. Subsequent hydrogenation with H_2 over Pd/C to remove the double bonds (Scheme 2.2, step c, i) resulted in partial abstraction of the Co(III) ion. It was therefore convenient to completely demetallate the structure with activated Zn dust in acetic acid/methanol (Scheme 2.2, step c, ii)[24] prior to isolation, to give the fully reduced neutral molecule H_4**L7** in 65% yield over the two steps. The ^{1}H NMR spectrum H_4**L7** in CD_2Cl_2 (Figure 2.2e) shows shielding of various signals (H_D, H_E, H_F and H_G) with respect to macrocycle H_2**L5** (Figure 2.2d) characteristic of a catenane, an architecture that was confirmed by X-ray crystallography of single crystals grown from a saturated acetonitrile solution (Figure 2.4). In the solid state each macrocycle of the catenand is involved in bifurcated hydrogen bonding to a

molecule of acetonitrile. The alkyl chains of each ring are located in the center of the cavity of the other macrocycle with the amide groups positioned to the outside of each molecule, a very different co-conformation to that required for metal ion template assembly (tridentate chelating groups converging towards the metal ion at the center; alkyl groups to the outside).[25]

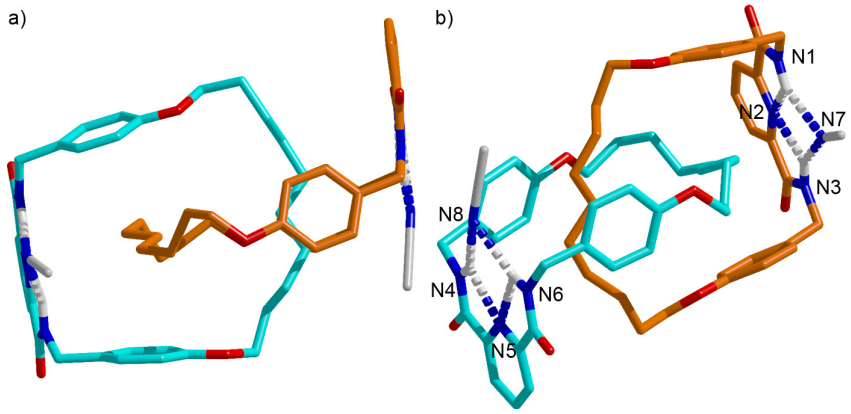

Figure 2.4. X-Ray crystal structure of [2]catenand H_4**L7**.2MeCN viewed (a) in the plane of the pyridine rings and (b) showing the hydrogen bonding networks present. Selected bond lengths (Å) and angles (°): NH1···N2 2.22, NH1···N7 2.32, NH3···N2 2.22, NH3···N7 2.27, NH4···N5 2.24, NH4···N8 2.28, NH6···N5 2.21, NH6···N8 2.40, N1-H1-N2 107.1, N1-H1-N7 145.7, N3-H3-N2 107.3, N3-H3-N7 145.6, N4-H4-N5 105.9, N4-H4-N8 146.7, N6-H6-N5 108.4, N6-H6-N8 143.1. The non-H-bonded hydrogen atoms are omitted for clarity. The carbon atoms are light blue (one macrocycle), orange (the second macrocycle) and grey (acetonitrile), oxygen red and nitrogen blue.

The cobalt(III) cation could be reintroduced into the catenand (Scheme 2.2, step d) to produce the [2]catenate [Co**L7**]Et_3NCH_2Cl in 75% yield. The ^{1}H NMR spectra of [Co**L7**]Et_3NCH_2Cl (Figure 2.2f) shows pronounced π-stacking interaction of resonances H_E and H_F, and a decrease in the shielding for H_G, H_H, H_I, H_J, and H_K compared to H_4**L7** indicating that complexation of the ligand to cobalt(III) fixes the alkyl chains to the outside of the catenate. Single crystals of the Co(III) catenate suitable for X-ray crystallographic analysis were grown by vapor diffusion of Et_2O into a saturated solution of the catenate in CH_2Cl_2. The crystal structure of [Co**L7**]Et_3NH (the countercation again exchanged from the one expected!)[26] (Figure 2.5) shows the octahedral environment of the Co(III) metal center bound to the two

bis-anionic tridentate macrocycles with, as in solution, the alkyl chains of each ring positioned to the outside of the catenate. The off-set π-interactions between the benzyl groups of each macrocycle and the pyridine ring of the other component apparent by ^{1}H NMR are also present in the X-ray crystal structure.

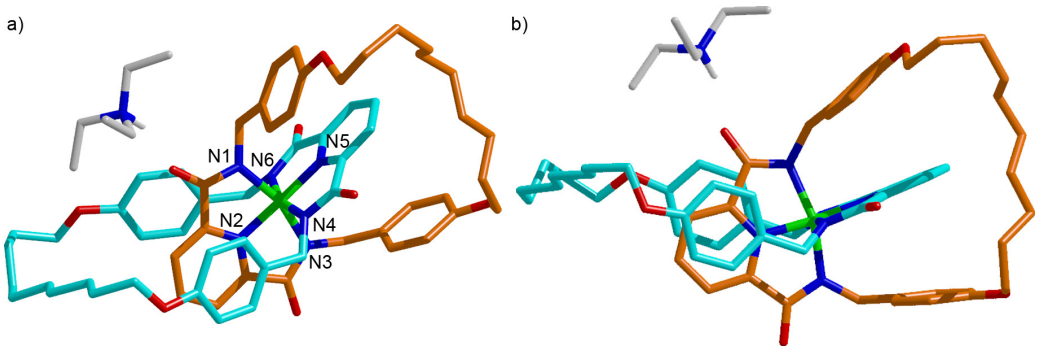

Figure 2.5. X-Ray crystal structure of [2]catenate [Co**L7**]Et_3NH viewed (a) to show the octahedral coordination sphere of the complexed cobalt(III) ion and (b) perpendicular to the plane of the orange ring to show the two sets of intercomponent π-stacking. Selected bond lengths (Å) and angles (°): N1-Co 1.97, N2-Co 1.85, N3-Co 1.95, N4-Co 1.97, N5-Co 1.85, N6-Co 1.97, N1-Co-N3 163.1, N4-Co-N6 163.2, N2-Co-N5 174.2. The hydrogen atoms are omitted for clarity except for the NH of the protonated Et_3N cation. The carbon atoms are shown in light blue (one macrocycle), orange (the second macrocycle) and grey (countercation), cobalt(III) green, oxygen red and nitrogen blue.

2.2.4 Co(III)-Template [2]Rotaxane Synthesis *via* Single Macrocyclization

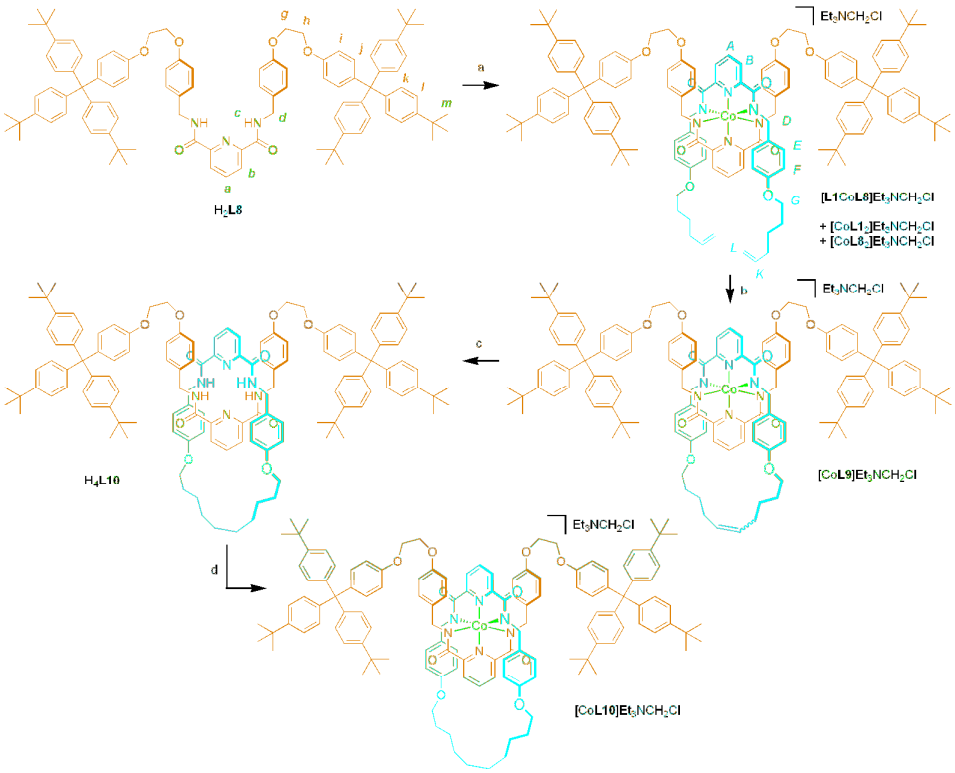

Scheme 2.3. Synthesis of [2]rotaxane [Co**L10**]$^-$ *via* single macrocyclization of **L1** about **L8** on a Co(III) template. Reagents and conditions: (a) H_2**L1**, $Et_4N(OAc)$, $Co(OAc)_2{\cdot}(H_2O)_4$, NaOMe, THF, EtOH, reflux, 1 h, 37%; (b) $(Cy_3P_2)Cl_2Ru$=CHPh, CH_2Cl_2, 2 d, 61%; (c) (i) Zn, AcOH, MeOH, 30 min.; (ii) Pd/C, THF, H_2, 2 d, 83%; (d) $Co(OAc)_2{\cdot}(H_2O)_4$, $Et_4N(OAc)$, NaOMe, EtOH, reflux, 30 min., 16%.

Having established a protocol for the formation of catenanes using pyridine-2,6-dicarboxamide ligands and a Co(III) template, the methodology was applied to the synthesis of a [2]rotaxane (Scheme 2.3). The bis-amide thread H_2**L8** was prepared in four steps (72% overall yield from commercial starting materials, see Experimental Section 2.4) and when subjected to the cobalt-complexation conditions in the presence of H_2**L1** the pre-rotaxane complex [**L1**Co**L8**]Et_3NCH_2Cl could be isolated in 37% yield (Scheme 2.3, step a). Since—unlike macrocycle **L5**—thread **L8** can form a 2:1 complex with Co(III), in this case the ligand assembly reaction was unselective for the mixed-ligand complex and [**L1**Co**L8**]$^-$ needed to be separated *via* column chromatography from [Co$\mathbf{L1}_2$]$^-$ and [Co$\mathbf{L8}_2$]$^-$. The ^{1}H NMR spectrum of

[**L1**Co**L8**]Et_3NCH_2Cl in CD_2Cl_2 (Figure 2.6b) shows the intercomponent π-stacking interactions between $\mathbf{L1}^{2-}$ and $\mathbf{L8}^{2-}$ (shielding of resonances H_E, H_F, H_e, and H_f), which augured well for interlocking occurring under RCM. Indeed, macrocyclization of [**L1**Co**L8**]Et_3NCH_2Cl proceeded smoothly with $(PCy_3)_2Cl_2Ru$=CHPh (Scheme 2.3, step b) to give [Co**L9**]Et_3NCH_2Cl in 61% yield. Following hydrogenation and demetallation (Scheme 2.3, step c) a single organic product was isolated which was confirmed as the metal-free rotaxane, H_4**L10**, by mass spectrometry and ^1H and ^{13}C NMR spectroscopy. The ^1H NMR spectrum of the rotaxane in CD_2Cl_2 (Figure 2.5d) shows shielding of the thread resonances H_d, H_e, H_f, H_g, and H_h and macrocycle resonances H_D, H_E, H_F, and H_G , compared to the non-interlocked components H_2**L8** (Figure 2.5a) and H_2**L5** (Figure 2.2c). In contrast, the amide hydrogen resonances of both the thread and macrocycle are shifted to higher frequency by ~1.5 ppm in the rotaxane indicating that the intercomponent hydrogen bonding observed in solution for the free catenand H_4**L7** also occurs with rotaxane H_4**L10**.

Reintroduction of Co(III) into rotaxane H_4**L10** to give [Co**L10**]Et_3NCH_2Cl (Scheme 2.3, step d) was far more sluggish and low yielding (16% cf 75% for [Co**L7**]$^-$) than the catenane system.[27] As observed in the pre-rotaxane complex [**L1**Co**L5**]Et_3NCH_2Cl, the ^1H NMR spectrum of the Co(III)-complexed rotaxane [Co**L10**]Et_3NCH_2Cl in CD_2Cl_2 (Figure 2.5c) provides evidence (larger shifts) of a significantly stronger π-stacking interaction between the benzylic units of the more flexible thread with the macrocycle's pyridine moiety compared to that between the benzyl groups of the (more rigid) macrocycle and the thread's pyridine unit.

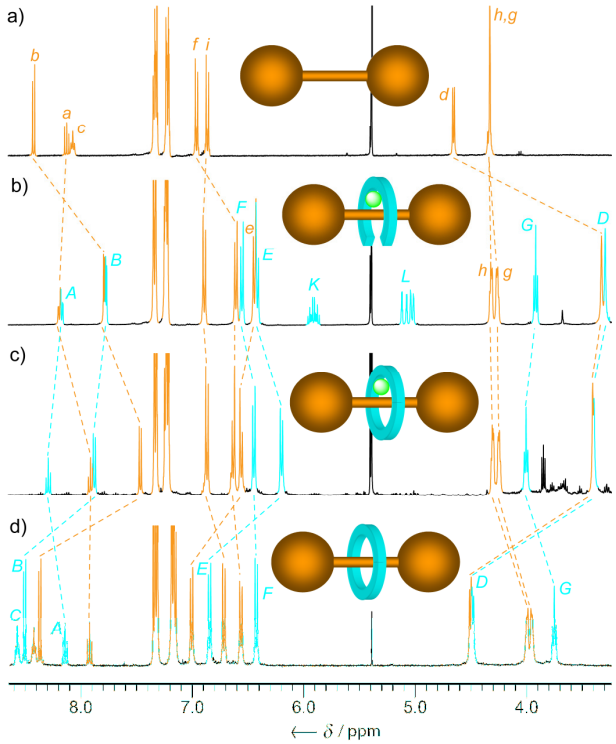

Figure 2.6. ^{1}H NMR spectra (400 MHz, CD_2Cl_2, 300 K) of a) thread H_2**L8** , b) pre-rotaxane [**L1**Co**L8**]Et_3NCH_2Cl, c) Co(II) rotaxane [Co**L10**]Et_3NCH_2Cl, and d) metal-free rotaxane H_4**L10**. The assignments correspond to the lettering shown in Scheme 2.3.

2.3 Conclusions

A [2]catenane, [2]rotaxane and a 'figure-of-eight' complex have been synthesized about a Co(III) template by exploiting the affinity of tridentate pyridine-2,6-biscarboxamido ligands for hard trivalent metal ions. In an unusual three-step template process, the lability of Co(II) coordination allows thermodynamically controlled assembly of the ligands on the metal and subsequent oxidation to Co(III) kinetically traps the template complex. The interlocked or entwined architectures are then covalently captured by cross-metathesis or ring closing metathesis. In each case decomplexation via reduction of the metal to Co(II) and protonation of the anionic ligands generated the metal-free neutral molecules. Cobalt could be re-introduced into the free ligands to form Co(III) complexes that were characterized unambiguously by mass spectrometry, NMR spectroscopy and, in some cases, X-ray crystallography. The methodology allows access to a new class of interlocked

chelating ligand for hard metal cations which adds to the growing toolbox of passive- and active-metal template[28] protocols for catenane and rotaxane synthesis. The binding of different metal types (hard and soft, different oxidation numbers and geometries, etc) may prove useful in the development of new synthetic molecular machine systems.[17]

2.4 Experimental Section

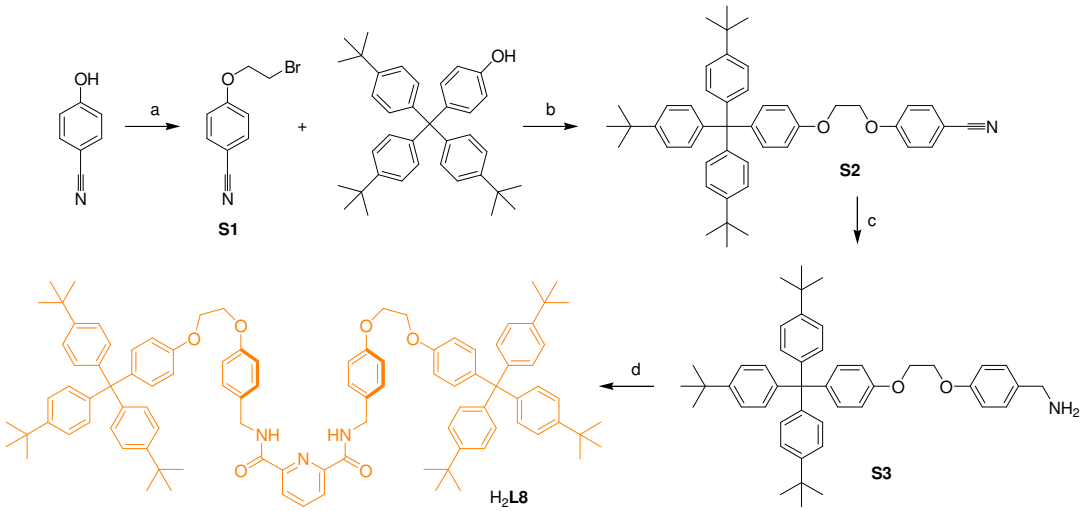

Scheme 2.4. Synthesis of thread H_2**L8** from 4-cyanophenol. Reagents and conditions: (a) $BrCH_2CH_2Br$, K_2CO_3, NaI, butanone, reflux, 18 h, 96%; (b) K_2CO_3, butanone, reflux, 18 h, 87%; (c) $LiAlH_4$, THF, reflux, 3 h, 98%; (d) pyridine-2,6-dicarbonyl dichloride, Et_3N, THF, 0 °C, 2 h, 88%.

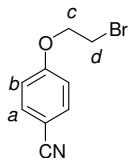

4-Cyano-*β*-phenylethyl bromide – S1[29]

To a solution of 4-cyanophenol (5.95 g, 50.0 mmol) and 1,2-dibromoethane (37.6 g, 200 mmol) in butanone (400 mL) was added K_2CO_3 (69.0 g, 500 mmol) and NaI (0.112 g, 5.00 mmol), the suspension was heated at reflux for 18 h. After cooling, K_2CO_3 was removed by filtration and the solvent was removed under reduced pressure. The crude residue was purified by column chromatography (5:25

EtOAc:CH_2Cl_2) and then recrystallized from hexane to yield the title compound as a colorless crystalline solid (10.90 g, 96%). m.p. = 53 °C (lit = 53 °C); ^{1}H NMR (400 MHz, $CDCl_3$, 300 K): δ = 3.65 (t, *J* = 6.0 Hz, 2H, H_d), 4.33 (t, *J* = 6.0 Hz, 2H, H_c), 6.96 (d, *J* = 8.8 Hz, 2H, H_b), 7.59 (d, *J* = 8.8 Hz, 2H, H_a); ^{13}C NMR (100 MHz, $CDCl_3$, 300 K): δ = 28.4, 67.9, 104.7, 115.3, 119.0, 134.1, 161.3; LRFAB-MS (3-NOBA matrix): *m/z* = 226 $[MH]^+$; HRFAB-MS (3-NOBA matrix): *m/z* = 225.9865 $[MH]^+$ (calcd. for $C_9H_9{}^{79}BrNO$, 225.9867).

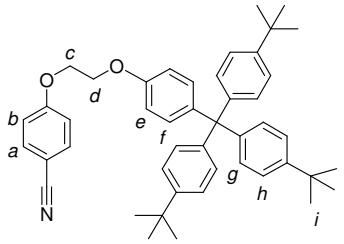

S2

To a solution of 4-tris(4-*tert*-butylphenyl)phenol (4.561 g, 9.05 mmol) and **S1** (6.135 g, 27.17 mmol) in butanone (50 mL) was added K_2CO_3 (12.49 g, 90.5 mmol), the suspension was heated at reflux for 18 h. The solvent was removed under reduced pressure and the crude residue was redissolved in H_2O (100 ml) and extracted into CH_2Cl_2 (3 x 100 ml). The combined organic layers were dried ($MgSO_4$), concentrated under reduced pressure and purified first by column chromatography (CH_2Cl_2) and then precipitated from a hot solution of CH_2Cl_2 by addition of MeOH to yield the title compound as a colorless solid (5.125 g, 87%). m.p. = 239 °C; ^{1}H NMR (400 MHz, $CDCl_3$, 300 K): δ = 1.30 (s, 27H, H_i), 4.32-4.34 (m, 4H, $H_{c,d}$), 6.80 (d, *J* = 8.8 Hz, 2H, H_e), 6.99 (d, *J* = 8.5, 2H, H_b), 7.08 (d, *J*= 8.5 Hz, 6H, H_g), 7.11 (d, *J* = 8.8 Hz, 2H, H_f), 7.23 (d, *J* = 8.5 Hz, 6H, H_h), 7.59 (d, *J* = 8.5 Hz, 2H, H_a); ^{13}C NMR (100 MHz, $CDCl_3$, 300 K): δ = 31.8, 34.7, 63.5, 66.4, 67.3, 104.8, 113.5, 115.8, 119.5, 124.5, 131.1, 132.8, 134.4, 140.8, 144.4, 148.8, 156.6, 162.4; LRFAB-MS (3-NOBA matrix): *m/z* = 649 $[MH]^+$; HRFAB-MS (3-NOBA matrix): *m/z* = 649.3925 $[MH]^+$ (calcd. for $C_{46}H_{51}NO_2$, 649.3920).

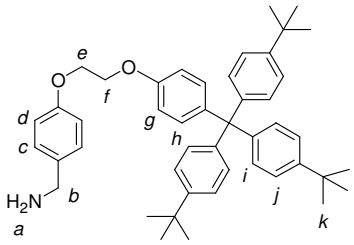

S3

To a solution of **S2** (5.88 g, 9.05 mmol) in THF (100 mL) was added dropwise a solution of $LiAlH_4$ (1.0 M in THF, 37 mL) at 0 °C. The resultant solution was heated at reflux for 3 hours and then allowed to cool to room temperature. The solution was cooled in an ice bath and water (1 mL), 15% aqueous sodium hydroxide solution (1 mL) and water (3 mL) were added cautiously with vigorous stirring. The resultant precipitate was removed by filtration and the filtrate concentrated under reduced pressure to yield the title compound as a colorless solid (5.80 g, 98%). m.p. = 99 °C; ^{1}H NMR (400 MHz, $CDCl_3$, 300 K): δ = 1.34 (s, 27H, H_k), 1.50 (br, 2H, H_a), 3.84 (s, 2H, H_b), 4.34 (s, 4H, $H_{e,f}$), 6.85 (d, J = 8.8 Hz, 2H, H_g), 6.96 (d, J = 8.8 Hz, 2H, H_d), 7.12 (m, 8H, $H_{h,i}$), 7.27 (m, 8H, $H_{c,j}$); ^{13}C NMR (100 MHz, $CDCl_3$, 300 K): δ = 31.8, 34.7, 46.3, 63.5, 66.8, 67.0, 113.6, 115.2, 124.5, 128.7, 131.1, 132.7, 136.4, 140.5, 144.5, 148.7, 156.8, 158.0; LRFAB-MS (3-NOBA matrix): m/z = 654 $[MH]^+$; HRFAB-MS (3-NOBA matrix): m/z = 654.4318 $[MH]^+$ (calcd. for $C_{46}H_{56}NO_2$, 654.4311).

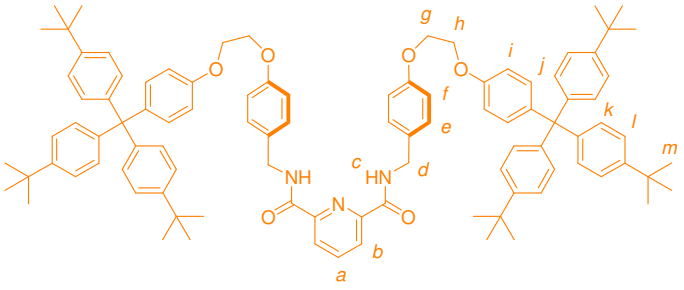

Thread - H_2**L8**

To a solution of **S3** (5.272 g, 8.06 mmol) and Et_3N (3.4 ml, 24.2 mmol) in THF (60 ml) at 0 °C was added *via* syringe a solution of pyridine-2,6-dicarbonyl dichloride (0.783 g, 3.84 mmol) in THF (20 ml). The solution was allowed to warm to room temperature and stirred for 2 h. The reaction mixture was filtered through a plug of

silica and the silica pad was washed with THF several times, the combined THF washings were concentrated under reduced pressure. The crude residue was redissolved in hot CH_2Cl_2 and MeCN was added to the solution to induce precipitation. The suspension was left for 18 h, the precipitate was filtered, washed with cold MeCN, then dried under suction for 3 h to yield the title compound as a colorless powder (4.886 g, 88%). m.p. = 181 °C; ^{1}H NMR (400 MHz, $CDCl_3$, 300 K): δ = 1.29 (s, 54H, H_m), 4.27 (s, 8H, $H_{g,h}$), 4.61 (d, J = 6.1 Hz, 4H, H_d), 6.78 (d, J = 8.9 Hz, 4H, H_i), 6.90 (d, J = 8.6 Hz, 4H, H_f), 7.08 (m, 16H, $H_{j,k}$), 7.21 (d, J = 8.5 Hz, 12H, H_l), 7.26 (d, J = 8.6 Hz, 4H, H_e), 7.88 (t, J = 6.1 Hz, 2H, H_c), 8.04 (t, J = 7.8 Hz, 1H, H_a), 8.40 (d, J = 7.8 Hz, 2H, H_b); ^{13}C NMR (100 MHz, $CDCl_3$, 300 K): δ = 31.8, 34.7, 43.0, 63.1, 66.2, 66.6, 113.1, 114.7, 123.8, 125.3, 129.1, 130.9, 131.0, 132.3, 139.3, 140.5, 144.5, 148.7, 149.2, 156.7, 158.5, 163.9; LRFAB-MS (3-NOBA matrix): m/z = 1439 [MH]$^+$; HRFAB-MS (3-NOBA matrix): m/z = 1438.851 [MH]$^+$ (calcd. for $C_{99}H_{111}N_3O_6$, 1438.851).

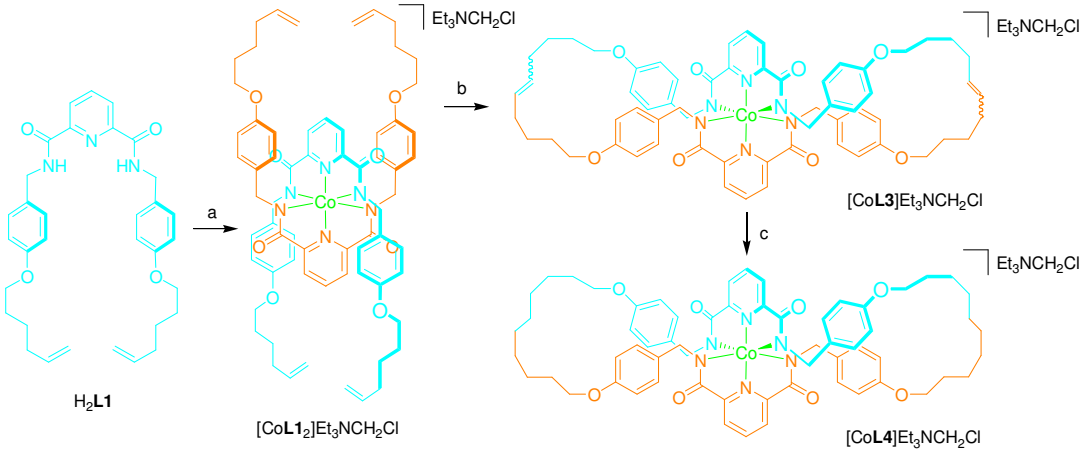

Scheme 2.5. Synthesis of 'figure-of-eight' complex [Co**L4**]Et_3NCH_2Cl from pre-macrocycle H_2**L1**. Reagents and conditions: (a) $Co(OAc)_2{\cdot}(H_2O)_4$, $Et_4N(OAc)$, NaOEt, EtOH, reflux, 1 h, 83%. (b) $(Cy_3P)_2Cl_2Ru$=CHPh, CH_2Cl_2, 2 d, 42%; (c) Pd/C, MeOH, H_2, 1 d; 85%.

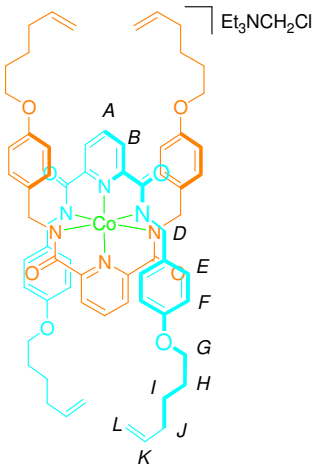

[Co**L1**$_2$]Et_3NCH_2Cl

A suspension of H_2**L1**[11b] (0.993 g, 1.83 mmol), $Et_4N(OAc)$ (0.241 g, 0.92 mmol) and $Co(OAc)_2{\cdot}(H_2O)_4$ (0.229 g, 0.92 mmol) in EtOH (10 ml), was heated at reflux under nitrogen to give a clear, pale pink, solution. To this was added a solution of sodium ethoxide in ethanol, generated by the careful addition of NaH (0.162 g of 60% dispersion in oil, 4.05 mmol) to ethanol, resulting in a color change to deep purple. Upon exposure to air, the color of the solution changed to green over about 5 minutes after which it was refluxed for a further 1 h. The solvent was removed under reduced pressure and the crude residue was purified by column chromatography on silica gel (40:1:59 Me_2CO:Et_3N:CH_2Cl_2 as eluent) to yield the title compound as a green oil (0.979 g, 83%). ^{1}H NMR (400 MHz, CD_2Cl_2, 300 K): δ = 1.09 (t, J = 7.3 Hz, 9H, $H_{NCH2C\underline{H}3}$), 1.55 (m, 8H, H_I), 1.76 (m, 8H, H_H), 2.13 (m, 10H, $H_{J,NC\underline{H}2Cl}$), 2.72 (q, J = 7.3 Hz, 6H, $H_{NC\underline{H}2}$), 3.25 (s, 8H, H_D), 3.86 (t, J = 6.6 Hz, 8H, H_G), 5.02 (m, 8H, H_L), 5.86 (m, 4H, H_K), 6.37 (d, J = 8.7 Hz, 8H, H_E), 6.50 (d, J = 8.7 Hz, 8H, H_F), 7.72 (d, J = 7.7 Hz, 4H, H_B), 8.13 (t, J = 7.7 Hz, 2H, H_A); ^{13}C NMR (100 MHz, CD_2Cl_2, 300 K); δ = 8.9, 25.7, 29.2, 33.8, 46.4, 46.5, 46.6, 68.2, 114.0, 114,4, 114.8, 122.9, 128.4, 133.3, 139.1, 157.6, 158.0, 168.4; LRESI-MS (CH_2Cl_2) m/z = 1138 $[M]^-$, 150 $[N(Et)_3CH_2Cl]^+$.

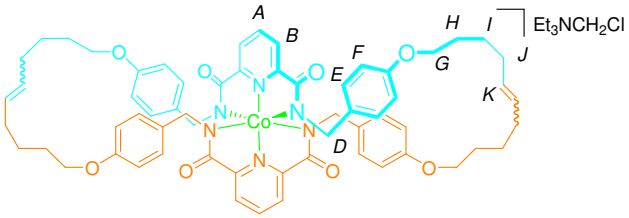

[Co**L3**]Et_3NCH_2Cl

To a solution of pre-catenate [Co**L1**$_2$]Et_3NCH_2Cl (0.500 g, 0.388 mmol) in CH_2Cl_2 (500 ml) was added Grubbs' 1st generation catalyst (0.056 g, 0.068 mmol). The solution was stirred for 2 d in the dark. The solvent was removed under reduced pressure and the crude residue was purified by column chromatography (40:1:59 Me_2CO:Et_3N:CH_2Cl_2) to yield the title compound as a green solid (0.201 g, 42%). m.p. = 172 °C; ^{1}H NMR (400 MHz, $(CD_3)_2CO$, 300 K): δ = 1.15 (t, J = 7.3 Hz, 9H, $H_{NCH2CH3}$), 1.35 (m, 8H, H_J), 1.46 (m, 8H, H_H), 1.62 (m, 12H, $H_{D',I}$), 2.01 (s, 2H, H_{NCH2Cl}), 3.04 (q, J = 7.3 Hz, 6H, $H_{NCH2CH3}$), 3.78 (m, 8H, H_G), 4.12 (t, J = 12.4 Hz, 4H, H_D), 5.24 (m, 4H, H_K), 6.27 (d, J = 1.8 Hz, 8H, H_E), 6.28 (d, J = 1.8 Hz, 8H, H_F), 7.88 (d, J = 7.8 Hz, 4H, H_B), 8.31 (t, J = 7.8 Hz, 2H, H_A); ^{13}C NMR (100 MHz, $(CD_3)_2CO$, 300 K): δ = 27.1 28.6, 32.4, 46.6, 67.5, 114.2, 123.1, 130.3, 130.7, 131.5, 134.1, 135.6, 136.4, 139.8, 157.6, 159.4, 169.3; LRFAB-MS (3-NOBA matrix): m/z = 1082 $[MH_2]^+$.

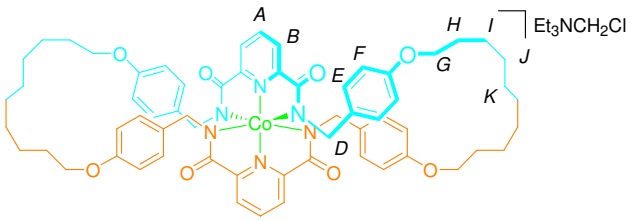

[Co**L4**]Et_3NCH_2Cl

To a solution of [Co**L3**]Et_3NCH_2Cl (0.142 g, 0.1 mmol) in methanol (30 mL) was added 10% w/w Pd/C (0.020 g), the suspension was repeatedly degassed and purged with N_2 before being repeatedly degassed and purged with H_2 and stirred for 18 h under an atmosphere of H_2. The reaction mixture was filtered through celite and the solvent was removed under reduced pressure. The crude mixture was purified by column chromatography (40:1:59 Me_2CO:Et_3N:CH_2Cl_2) to yield the title compound as green solid (0.106 g, 85%). m.p. = 168 °C; ^{1}H NMR (400 MHz, $(CD_3)_2CO$, 300

K): δ = 1.15 (t, J = 7.3 Hz, 9H, $H_{NCH2C\underline{H}3}$), 1.35 (m, 16H, $H_{J,K}$), 1.70 (m, 8H, H_I), 2.01 (s, 2H, $H_{NC\underline{H}2Cl}$), 2.05 (m, 12H, $H_{D',H}$), 3.04 (q, J = 7.3 Hz, 6H, $H_{NC\underline{H}2CH3}$), 3.92 (m, 8H, H_G), 4.29 (d, J = 12.3 Hz, 4H, H_D), 6.25-6.48 (m, 16H, $H_{E,F}$), 7.88 (d, J = 7.7 Hz, 4H, H_B), 8.31 (t, J = 7.7 Hz, 2H, H_A); ^{13}C NMR (100 MHz, $(CD_3)_2CO$, 300 K): δ = 7.5, 25.8, 27.7, 28.4, 28.6, 46.5, 53.3, 67.9, 114.6, 124.2, 130.1, 134.5, 138.1, 141.1, 158.1, 159.2, 169.8; LRFAB-MS (3-NOBA matrix): m/z = 1087 $[MH_2]^+$; HRFAB-MS (3-NOBA matrix): m/z = 1087.474 $[MH_2]^+$ (calcd. for $C_{62}H_{72}CoN_6O_8$, 1087.474).

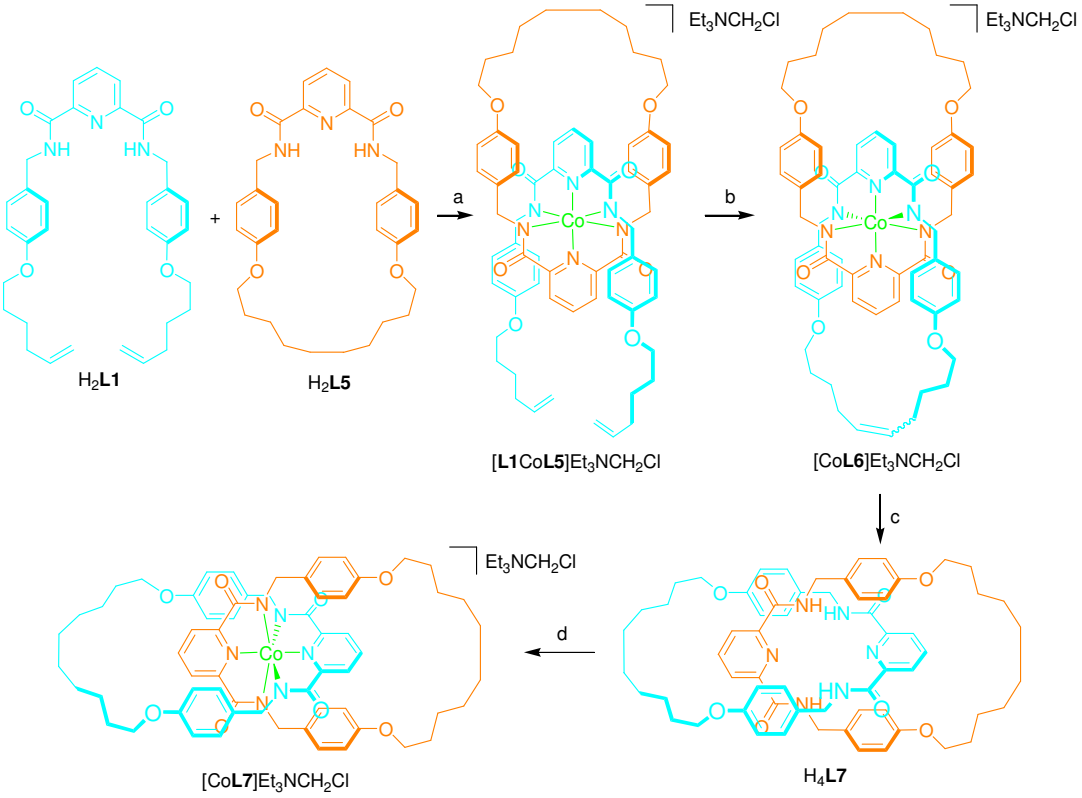

Scheme 2.6. Synthesis of catenanes H_4**L7** and [Co**L7**]Et_3NCH_2Cl from pre-macrocycle H_2**L1** and macrocycle H_2**L5**. Reagents and conditions: (a) $Co(OAc)_2{\cdot}(H_2O)_4$, $Et_4N(OAc)$, NaOEt, EtOH, reflux, 1 h, 84%; (b) $(Cy_3P)_2Cl_2Ru$=CHPh, CH_2Cl_2, 2 d, 69%; (c) (i) Pd/C, MeOH, H_2, 1 d; (ii) Zn, AcOH, MeOH, 30 min., 65%; (d) $Co(OAc)_2{\cdot}(H_2O)_4$, $Et_4N(OAc)$, NaOMe, EtOH, reflux, 30 min., 75%.

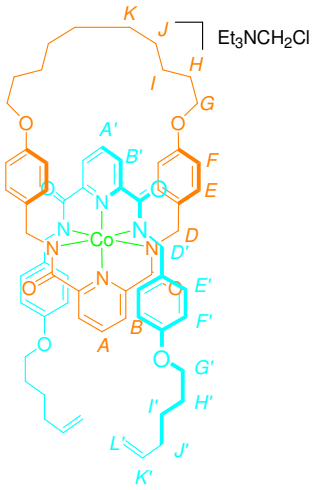

[**L1**Co**L5**]Et_3NCH_2Cl

A suspension of H_2**L1** (0.507 g, 0.936 mmol), H_2**L5**[11a] (0.483 g, 0.936 mmol), $Co(OAc)_2{\cdot}(H_2O)_4$ (0.233 g, 0.936 mmol) and $Et_4N(OAc)$ (0.245 g, 0.936 mmol) was heated at reflux in EtOH (20 ml) under nitrogen to give a clear, pale pink, solution. To this was added a solution of sodium ethoxide in ethanol, generated by the careful addition of NaH (0.165 g of 60% dispersion in oil, 4.12 mmol) to ethanol, resulting in a color change from pink to deep purple. Upon exposure to air, the color changed to green over about 5 minutes after which the solution was refluxed for a further 25 min.. The solvent was removed under reduced pressure and the crude residue was purified by column chromatography on silica gel (40:1:59 Me_2CO:Et_3N:CH_2Cl_2 as eluent) to yield the title compound as green oil (1.130 g, 84%). ^{1}H NMR (400 MHz, CD_2Cl_2, 300 K): δ = 1.12 (t, J = 7.3 Hz, 9H, $H_{NCH2CH3}$), 1.41 (br, 8H, $H_{J,K}$), 1.48 (m, 4H, H_I), 1.54 (m, 4H, $H_{I'}$), 1.74 (m, 8H, $H_{H,H'}$), 2.14 (m, 6H, $H_{J',NCH2Cl}$), 2.77 (q, J = 7.3 Hz, 6H, $H_{NCH2CH3}$), 3.32 (s, 4H, $H_{D'}$), 3.36 (s, 4H, H_D), 3.85 (t, J = 6.6 Hz, 4H, $H_{G'}$), 3.95 (t, J = 6.3 Hz, 4H, H_G), 5.01 (m, 4H, $H_{L'}$), 5.85 (m, 2H, $H_{K'}$), 6.15 (d, J = 8.6 Hz, 4H, H_E), 6.39 (d, J = 8.6 Hz, 4H, H_F), 6.50 (m, 8H, $H_{E',F'}$), 7.39 (d, J = 7.7 Hz, 2H, $H_{B'}$), 7.81 (d, J = 7.8 Hz, 2H, H_B), 7.85 (t, J = 7.7 Hz, 1H, $H_{A'}$), 8.23 (t, J = 7.8 Hz, 1H, H_A); ^{13}C NMR (100 MHz, CD_2Cl_2, 300 K): δ = 9.1, 25.7, 25.9, 28.7, 28.7, 29.2, 29.3, 30.1, 33.9, 46.4, 46.5, 46.6, 67.8, 68.1, 113.9, 114.7, 114.8, 122.4, 123.2, 127.7, 128.3, 132.1, 134.1, 138.7, 139.1, 139.2, 157.2, 157.6, 157.6, 158.3, 168.3, 169.0; LRFAB-MS (3-NOBA matrix): m/z = 1113 $[MH_2]^+$, 150

$[N(Et)_3CH_2Cl]^+$; HRFAB-MS (3-NOBA matrix): *m/z* = 1113.490 $[MH_2]^+$ (calcd. for $C_{64}H_{64}CoN_6O_6$, 1113.490).

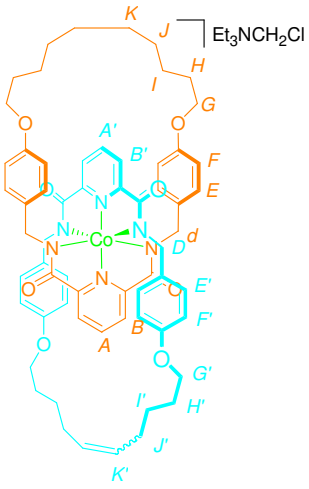

[Co**L6**]Et_3NCH_2Cl

To a solution of pre-catenate [**L1**Co**L5**]Et_3NCH_2Cl (1.130 g, 0.877 mmol) in CH_2Cl_2 (900 ml) was added Grubbs' 1st generation catalyst (0.100 g, 0.121 mmol). The solution was stirred for 2 d in the dark. The solvent was removed under reduced pressure and the crude residue was purified by column chromatography (40:1:59 Me_2CO:Et_3N:CH_2Cl_2) to yield the title compound as a green oil (0.750 g, 69%). ^1H NMR (400 MHz, $(CD_3)_2CO$, 300 K): δ = 1.20 (t, *J* = 7.3 Hz, 9H, $H_{NCH2CH3}$), 1.28 (br, 8H, $H_{J,K}$), 1.39 (m, 8H, $H_{I,I'}$), 1.59 (m, 8H, $H_{H,H'}$), 2.01 (s, 2H, H_{NCH2Cl}), 2.09 (br, 4H, $H_{J'}$), 3.09 (q, *J* = 7.3 Hz, 6H, $H_{NCH2CH3}$), 3.31 (br, 8H, $H_{D,D'}$), 3.84 (m, 8H, $H_{G,G'}$), 5.28 (t, *J* = 4.7 Hz, 1H, $H_{K'cis/trans}$), 5.45 (t, *J* = 3.8 Hz, 1H, $H_{K'cis/trans}$), 6.16 (m, 8H, $H_{E,E'}$), 6.28 (m, 8H, $H_{F,F'}$), 7.38 (m, 4H, $H_{B,B'}$), 7.95 (m, 2H, $H_{A,A'}$).

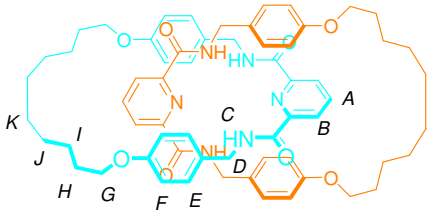

Catenand - H_4**L7**

To a solution of catenate [Co**L6**]Et_3NCH_2Cl (0.698 g, 0.565 mmol) in MeOH (10 ml) was added 10% w/w Pd/C (0.060 g), the suspension was repeatedly degassed and purged with N_2 before being repeatedly degassed and purged with H_2 and stirred for

18 h under an atmosphere of H_2. The reaction mixture was filtered through celite and the solvent was removed under reduced pressure. The crude residue was redissolved in MeOH (5 ml) and AcOH (5 ml) and activated zinc dust (0.050 g) was added, the suspension was stirred for 30 min. under an atmosphere of air. The solvent was removed under reduced pressure and the crude residue was redissolved in $CHCl_3$ (50 ml) and washed with a 17.5% NH_3 solution saturated with EDTA (50 ml). The aqueous layer was extracted with $CHCl_3$ (3 x 50 ml). The combined organic layers were washed with brine (50 ml), dried ($MgSO_4$) and purified by column chromatography (3:7 EtOAc:CH_2Cl_2) to yield the title compound as a colorless solid (0.379 g, 65%). Single crystals suitable for X-ray crystallography were grown from a saturated solution of catenand H_4**L3** in CH_3CN. m.p. = 231 °C; ^{1}H NMR (400 MHz, $CDCl_3$, 300K): δ = 1.25 (br, 16H, $H_{J,K}$), 1.41 (m, 8H, H_I), 1.70 (qt, J = 6.7 Hz, 8H, H_H), 3.62 (t, J = 6.7 Hz, 8H, H_G), 4.39 (t, J = 5.6 Hz, 8H, H_D), 6.23 (d, J = 8.5 Hz, 8H, H_F), 6.67 (d, J = 8.5 Hz, 8H, H_E), 8.02 (t, J = 7.8 Hz, 2H, H_A), 8.29 (t, J = 5.6 Hz, 4H, H_C), 8.40 (d, J = 7.8 Hz, 4H, H_B); ^{13}C NMR (100 MHz, $CDCl_3$, 300 K): δ = 25.3, 28.2, 28.4, 29.0, 43.2, 66.6, 113.9, 125.8, 128.7, 128.9, 138.7, 149.2, 157.5, 163.5; LREI-MS: m/z = 1031 $[M]^+$; HREI-MS m/z = 1030.556 $[M]^+$ (calcd. for $C_{62}H_{74}N_6O_8$, 1030.555).

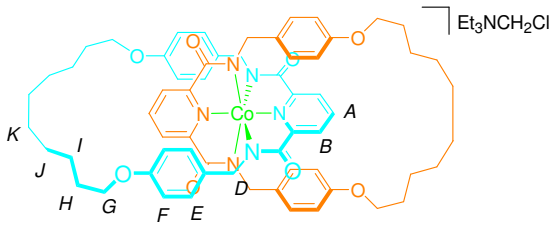

Catenate - [Co**L7**]Et_3NCH_2Cl

To a suspension of catenand H_4**L7** (0.299 g, 0.29 mmol) and $Et_4N(OAc)$ (0.076 g, 0.29 mmol) in EtOH was added $Co(OAc)_2{\cdot}(H_2O)_4$ (0.072, 0.029 mmol). The suspension was heated under nitrogen at reflux to give a clear, pale pink, solution to which NaOMe (0.069 g, 1.28 mmol) was added. The solution was then opened to the air and heated at reflux for 30 min. until only one spot (green) was observed by thin layer chromatography (silica gel, 1:39:60 Et_3N:Me_2CO:CH_2Cl_2). The solvent was removed under reduced pressure and the crude residue was purified by column

chromatography on silica gel (1:39:60 Et_3N:Me_2CO:CH_2Cl_2 then 1:99 Et_3N:Me_2CO as eluent) to yield a green oil. Acetone was added to induce crystallization, then the solvent was removed under reduced pressure to yield the title compound as a green solid (0.268 g, 75%). Single crystals suitable for X-ray crystallography were grown by vapor diffusion of Et_2O into a concentrated solution of catenate [Co**L7**]Et_3NCH_2Cl in CH_2Cl_2. m.p. = 162 °C; ^{1}H NMR (400 MHz, CD_2Cl_2, 300 K): δ = 1.12 (t, *J* = 7.3 Hz, 9H, $H_{NCH2C\underline{H}3}$), 1.40 (br, 16H, $H_{J,K}$), 1.47 (br, 8H, H_I), 1.73 (m, 8H, H_H), 2.14 (s, 2H, $H_{NC\underline{H}2Cl}$), 2.70 (q, *J* = 7.3 Hz, 6H, $H_{NC\underline{H}2CH3}$), 3.48 (s, 8H, H_D), 3.95 (t, *J* = 6.3 Hz, 8H, H_G), 6.31 (d, *J* = 8.6 Hz, 8H, H_E), 6.40 (d, *J* = 8.6 Hz, 8H, H_F), 7.42 (d, *J* = 7.7 Hz, 4H, H_B), 7.85 (t, *J* = 7.7 Hz, 2H, H_A); ^{13}C NMR (100 MHz, CD_2Cl_2, 300 K): δ = 9.1, 25.9, 28.8, 28.9, 29.9, 46.2, 46.3, 46.4, 67.6, 114.4, 122.5, 128.0, 133.0, 138.6, 157.2, 157.8, 169.0; LRESI-MS (CH_2Cl_2): *m/z* = 1085 $[M]^-$; HRESI-MS: *m/z* = 1087.472 $[MH_2]^+$ (calcd. for $C_{62}H_{72}CoN_6O_8$, 1087.473).

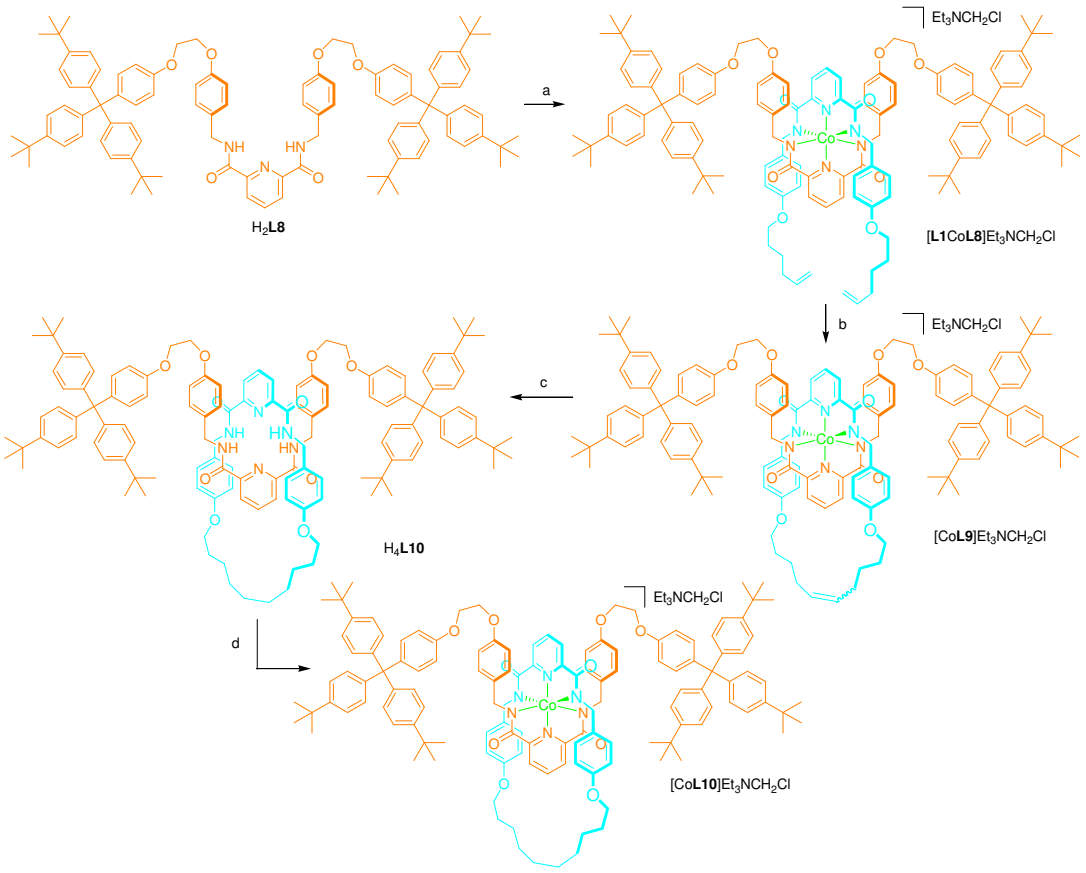

Scheme 2.7. Synthesis of rotaxanes H_4**L10** and [Co**L10**]Et_3NCH_2Cl from pre-macrocycle H_2**L1** and thread H_2**L8**. Reagents and conditions: (a) H_2**L1**, $Et_4N(OAc)$, $Co(OAc)_2{\cdot}(H_2O)_4$, NaOMe, THF, EtOH, reflux, 1 h, 37%; (b) $(Cy_3P_2)Cl_2Ru{=}CHPh$, CH_2Cl_2, 2 d, 61%; (c) (i) Zn, AcOH, MeOH, 30 min.; (ii) Pd/C, THF, H_2, 2 d, 83%; (d) $Co(OAc)_2{\cdot}(H_2O)_4$, $Et_4N(OAc)$, NaOMe, EtOH, reflux, 30 min., 16%.

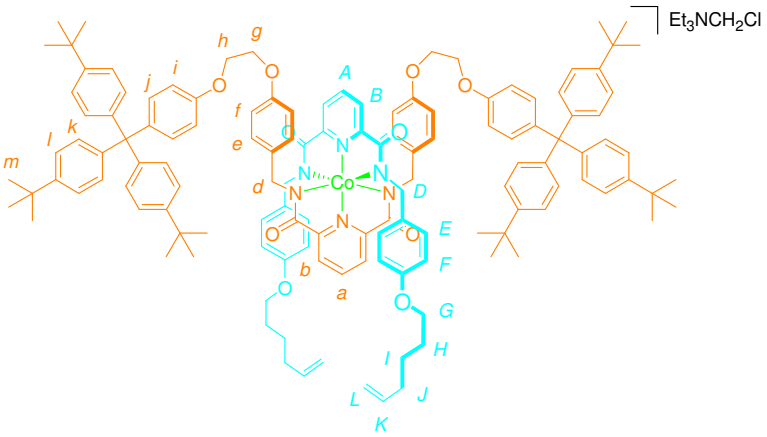

[**L1**Co**L8**]NEt_3CH_2Cl

To a solution of H_2**L1** (0.385 g, 0.71 mmol), H_2**L8** (1.023 g, 0.71 mmol) and $Et_4N(OAc)$ (0.186 g, 0.71 mmol) in EtOH (7 ml) and THF (7 ml) was added a solution of $Co(OAc)_2{\cdot}(H_2O)_4$ (0.177 g, 0.71 mmol) in EtOH (3 ml) and the resulting pale pink solution was heated at reflux under nitrogen for 1 h. NaOMe (0.169 g, 3.124 mmol) was added and the color changed to deep purple and, following exposure to air, to green, accompanied by formation of a suspension. The reaction was heated at reflux for a further 1 h. The solvent was removed under reduced pressure and the crude residue was purified by column chromatography on silica gel (1:19:80 Et_3N:Me_2CO:CH_2Cl_2 then 1:39:60 Et_3N:Me_2CO:CH_2Cl_2 then 1:99 Et_3N:Me_2CO as eluent) to yield the title compound as a green solid (0.573 g, 37%). ^{1}H NMR (400 MHz, CD_2Cl_2, 300 K): δ = 1.11 (t, J = 7.3 Hz, 9H, $H_{NCH2C\underline{H}3}$), 1.33 (br, 56H, $H_{m,NC\underline{H}2Cl}$), 1.55 (m, 4H, H_I), 1.76 (m, 4H, H_H), 2.13 (m, 4H, H_J), 2.78 (q, J = 7.3 Hz, 6H, $H_{NC\underline{H}2CH3}$), 3.25 (br, 4H, H_D), 3.28 (br, 4H, H_d), 3.87 (t, J = 6.6 Hz, 4H, H_G), 4.21 (m, 4H, H_g), 4.27 (m, 4H, H_h), 5.02 (m, 4H, H_L), 5.87 (m, 2H, H_K), 6.38 (m, 8H, $H_{e,E}$), 6.50 (d, J = 8.6 Hz, 4H, H_F), 6.56 (d, J = 8.6 Hz, 4H, H_f), 6.84 (d, J = 8.9 Hz, 4H, H_i), 7.19 (m, 16H, $H_{j,k}$), 7.29 (d, J = 8.6 Hz, 12H, H_l), 7.74 (m, 4H, $H_{b,B}$), 8.14 (m, 2H, $H_{a,A}$); ^{13}C NMR (100 MHz, CD_2Cl_2, 300 K): δ = 8.9, 25.7, 29.2, 31.5, 33.8, 33.9, 34.5, 34.6, 46.5, 46.6, 63.5, 67.0, 67.1, 68.2, 113.6, 114.0, 114.2, 114.7, 123.0, 124.6, 124.7, 128.3, 128.5, 130.8, 132.4, 133.2, 134.0, 139.1, 139.2, 139.3, 140.5, 144.8, 148.8, 156.9, 157.1, 157.6, 158.0, 158.1, 168.3, 168.4; LRESI-MS (CH_2Cl_2): m/z = 2035 $[M]^-$, 150 $[NEt_3CH_2Cl]^+$; HRFAB-MS (3-NOBA matrix): m/z = 2037.063 $[MH_2]^+$ (calcd. for $C_{132}{}^{13}CH_{148}CoN_6O_{10}$, 2037.062).

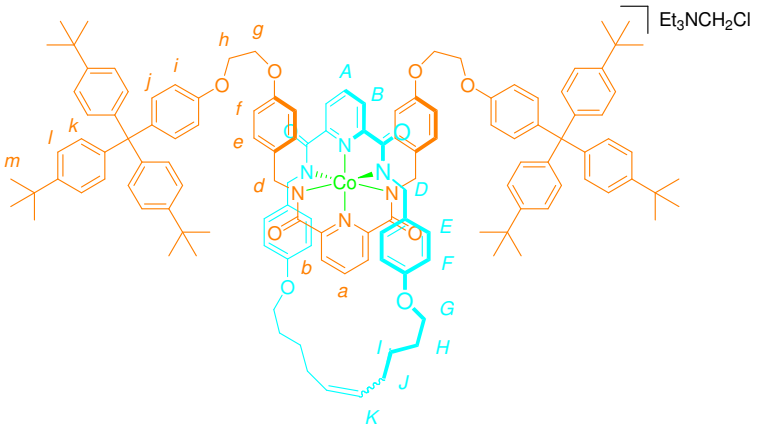

[Co**L9**]NEt_3CH_2Cl

To a solution of [**L1**Co**L8**]NEt_3CH_2Cl (0.261 g, 0.119 mmol) in CH_2Cl_2 (100 ml) was added Grubbs' I (0.020 g, 0.024 mmol). The solution was stirred for 1 d, at which time more Grubbs' 1st generation catalyst was added (0.020 g, 0.024 mmol), the solution was then stirred for a further 2 d. The solvent was removed under reduced pressure and the crude residue was purified by column chromatography (1:39:60 Et_3N:Me_2CO:CH_2Cl_2) to yield the title compound as a green oil (0.156 g, 61%). ^{1}H NMR (400 MHz, CD_2Cl_2, 300 K): δ = 1.14 (t, J = 7.3 Hz, 9H, $H_{NCH2C\underline{H}3}$), 1.29 (s, 2H, $H_{NC\underline{H}2Cl}$), 1.32 (br, 54H, H_m), 1.54 (m, 4H, H_l), 1.74 (m, 4H, H_H), 2.11-2.23 (m, 4H, H_J), 2.79 (q, J = 7.3 Hz, 6H, $H_{NC\underline{H}2CH3}$), 3.36 (m, 8H, $H_{d,D}$), 3.96 (t, J = 6.4 Hz, 4H, H_G), 4.19 (m, 4H, H_g), 4.25 (m, 4H, H_h), 5.47 (t, J = 4.6 Hz, 1H, $H_{Kcis/trans}$), 5.56 (m, 1H, $H_{Kcis/trans}$), 6.12 (m, 4H, H_E), 6.37 (m, 4H, H_F), 6.52 (d, J = 8.6 Hz, 4H, H_e), 6.58 (d, J = 8.6 Hz, 4H, H_f), 6.81 (d, J = 8.9 Hz, 4H, H_i), 7.18 (m, 16H, $H_{j,k}$), 7.28 (d, J = 8.7 Hz, 12H, H_l), 7.40 (d, J = 7.7 Hz, 2H, H_b), 7.85 (m, 3H, $H_{a,B}$), 8.24 (t, J = 7.8 Hz, 1H, H_A); ^{13}C NMR (100 MHz, CD_2Cl_2, 300 K): δ = 8.9, 25.9, 26.0, 28.4, 30.1, 31.5, 32.3, 34.6, 46.5, 63.5, 67.1, 67.8, 67.9, 113.5, 113.9, 114.5, 115.1, 122.5, 123.3, 124.7, 127.7, 129.4, 130.8, 132.1, 132.4, 134.9, 135.0, 138.7, 139.1, 140.5, 144.8, 148.8, 156.8, 157.1, 157.3, 157.6, 158.4, 168.2, 169.0; LRESI-MS (CH_2Cl_2): m/z = 2007 $[M]^-$, 150 $[NEt_3CH_2Cl]^+$; HRFAB-MS (3-NOBA matrix): m/z = 2008.023 $[MH_2]^+$ (calcd. for $C_{130}H_{144}CoN_6O_6$, 2008.026).

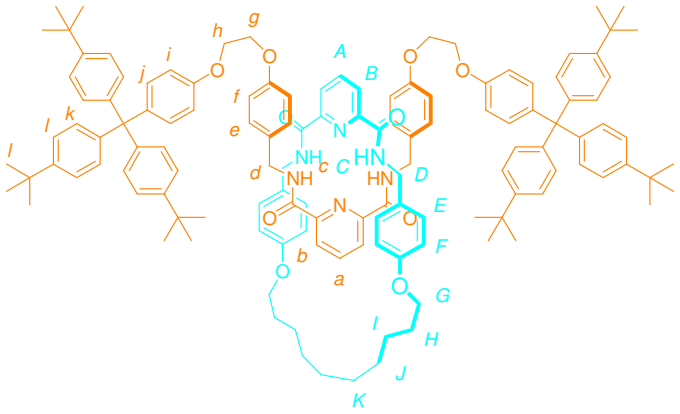

H_4L10

To a solution of [Co**L9**]NEt_3CH_2Cl (0.146 g, 0.0677 mmol) in CH_2Cl_2 (5 ml) and AcOH (5 ml) was added activated zinc dust (0.146 g) and the suspension stirred for 30 min. under an atmosphere of air. The reaction mixture was neutralized with a 17.5% NH_3 solution saturated with Na_4EDTA (50 ml) and the organic phase was extracted into CH_2Cl_2 (3 x 50 ml), the combined organic layers were washed with brine (50 ml), dried ($MgSO_4$) and concentrated under reduced pressure. The crude residue was redissolved in THF (5 ml) and 10% w/w Pd/C was added (0.030 g) the suspension was repeatedly degassed and purged with N_2 before being repeatedly degassed and purged with H_2 and stirred for 2 d under an atmosphere of H_2. The reaction mixture was filtered through celite and the solvent was removed under reduced pressure, then the crude residue was purified by column chromatography (1:9 EtOAc:CH_2Cl_2) to yield the title compound as a colorless solid (0.110 g, 83%). m.p. = 137 °C; ^{1}H NMR (400 MHz, CD_2Cl_2, 300 K): δ = 1.32 (br, 8H, $H_{J,K}$), 1.35 (br, 54H, H_m), 1.42 (m, 4H, H_J), 1.67 (m, 4H, H_I), 3.72 (t, J = 6.6 Hz, 4H, H_G), 3.93 (m, 4H, H_g), 3.95 (m, 4H, H_h), 4.46 (m, 8H, $H_{d,D}$), 6.39 (d, J = 8.6 Hz, 4H, H_F), 6.53 (d, J = 8.6 Hz, 4H, H_f), 6.68 (d, J = 8.9 Hz, 4H, H_i), 6.81 (d, J = 8.6 Hz, 4H, H_E), 6.97 (d, J = 8.6 Hz, 4H, H_e), 7.13 (m, 16H, $H_{j,k}$), 7.29 (d, J = 8.6 Hz, 12H, H_l), 7.89 (t, J = 7.8 Hz, 1H, H_a), 8.11 (t, J = 7.8 Hz, 1H, H_A), 8.33 (d, J = 7.8 Hz, 2H, H_b), 8.39 (t, J = 5.9 Hz, 2H, H_c), 8.47 (d, J = 7.8 Hz, 2H, H_B), 8.54 (t, J = 5.7 Hz, 2H, H_C); ^{13}C NMR (100 MHz, CD_2Cl_2, 300 K): δ = 25.3, 28.1, 28.3, 29.0, 31.4, 34.3, 43.0, 43.3, 63.0, 65.8, 66.0, 66.9, 112.8, 113.9, 114.2, 124.1, 125.5, 125.5, 129.0, 129.1, 129.4, 130.0, 130.6, 132.2, 138.4, 138.9, 140.3, 144.1, 148.3, 149.1, 149.1, 155.9, 157.3, 157.7,

163.5, 163.8; LREI-MS: *m/z* = 1954 $[MH]^+$; HRFAB-MS (3-NOBA matrix): *m/z* = 1954.134 $[MH]^+$ (calcd. for $C_{130}H_{149}N_6O_{10}$, 1954.133).

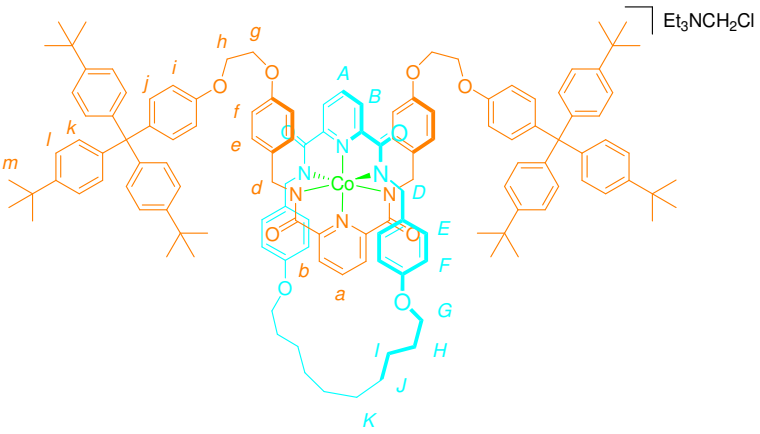

[Co**L10**]NEt_3CH_2Cl

To a solution of rotaxane H_4**L10** (0.110 g, 0.056 mmol) and $Et_4N(OAc)$ (0.015 g, 0.056 mmol) in EtOH (5 ml) and THF (5 ml) was added $Co(OAc)_2{\cdot}(H_2O)_4$ (0.017 g, 0.067 mmol). To this was added NaOMe (0.013 g, 0.246 mmol) and the solution was opened to the air and heated at reflux for a further 1 h. The solvent was removed under reduced pressure and the crude residue was purified by column chromatography on silica gel (1:39:60 Et_3N:Me_2CO:CH_2Cl_2 as eluent) to yield the title compound as a green solid (0.019 g, 16%). ^{1}H NMR (400 MHz, CD_2Cl_2, 300 K): δ = 1.11 (t, *J* = 7.3 Hz, 9H, $H_{NCH2CH3}$), 1.28 (br, 4H, H_K), 1.31 (br, 54H, H_m), 1.41 (br, 4H, H_J), 1.47 (m, 4H, H_I), 1.74 (m, 4H, H_H), 2.14 (s, 2H, H_{NCH2Cl}), 2.76 (q, *J* = 7.3 Hz, 6H, $H_{NCH2CH3}$), 3.35 (m, 8H, $H_{d,D}$), 3.95 (t, *J* = 6.3 Hz, 4H, H_G), 4.20 (m, 4H, H_g), 4.25 (m, 4H, H_h), 6.14 (d, *J* = 8.6 Hz, 4H, H_E), 6.39 (d, *J* = 8.6 Hz, 4H, H_F), 6.51 (d, *J* = 8.7 Hz, 4H, H_e), 6.58 (d, *J* = 8.7 Hz, 4H, H_f), 6.81 (d, *J* = 9.0 Hz, 4H, H_i), 7.18 (m, 16H, $H_{j,k}$), 7.28 (d, *J* = 8.7 Hz, 12H, H_l), 7.41 (d, *J* = 7.58 Hz, 2H, H_b), 7.82 (d, *J* = 7.8 Hz, 2H, H_B), 7.86 (t, *J* = 7.8 Hz, 1H, H_a), 8.24 (t, *J* = 7.8 Hz, 1H, H_A); ^{13}C NMR (100 MHz, CD_2Cl_2, 300 K): δ = 9.2, 25.9, 28.6, 28.7, 29.7, 30.1, 31.5, 34.6, 46.5, 46.5, 62.1, 63.5, 67.0, 67.1, 67.8, 113.5, 113.9. 114.7, 122.5, 123.3, 124.7, 127.7, 129.3, 130.8, 132.0, 132.4, 134.8, 138.8, 139.2, 140.5, 144.8, 148.8, 156.9, 157.1, 157.3, 157.6, 158.3, 168.3, 169.0; LRESI-MS (CH_2Cl_2): *m/z* = 2008 $[M]^-$, 150 $[Et_3NCH_2Cl]^+$; HRFAB-MS (3-NOBA matrix): *m/z* = 2011.047 $[MH_2]^+$ (calcd. for

$C_{130}{}^{13}CH_{146}CoN_6O_{10}$, 2011.047).

Table 2.1. Crystal data and structure refinement for [Co**L4**]Et_3NCH_2Cl.

Identification code	[Co**L4**]Et_3NCH_2Cl	
Empirical formula	$C_{70.50}H_{90}ClCoN_7O_{8.50}$	
Formula weight	1265.88	
Temperature	93(2) K	
Wavelength	0.71073 Å	
Crystal system	Orthorhombic	
Space group	P2(1)2(1)2(1)	
Unit cell dimensions	a = 14.142(4) Å	α = 90°.
	b = 20.476(7) Å	β = 90°.
	c = 23.569(11) Å	γ = 90°.
Volume	6825(4) $Å^3$	
Z	4	
Density (calculated)	1.232 Mg/m^3	
Absorption coefficient	0.350 mm^{-1}	
F(000)	2696	
Crystal size	0.2000 x 0.0800 x 0.0800 mm^3	
Theta range for data collection	1.75 to 25.35°.	
Index ranges	-17 ≤ h ≤ 16, -19 ≤ k ≤ 24, -27 ≤ l ≤ 28	
Reflections collected	42413	
Independent reflections	12213 [R(int) = 0.0716]	
Completeness to theta = 25.35°	98.9%	
Absorption correction	Multiscan	
Max. and min. transmission	1.0000 and 0.8010	
Refinement method	Full-matrix least-squares on F^2	
Data / restraints / parameters	12213 / 0 / 795	
Goodness-of-fit on F^2	1.069	
Final R indices [I>2sigma(I)]	R1 = 0.1006, wR2 = 0.2380	
R indices (all data)	R1 = 0.1349, wR2 = 0.2656	
Absolute structure parameter	0.07(3)	
Extinction coefficient	0.0058(8)	
Largest diff. peak and hole	0.854 and -0.468 e.$Å^{-3}$	

Table 2.2. Crystal data and structure refinement for H_4**L7**.2MeCN.

Identification code	H_4**L7**.2MeCN	
Empirical formula	$C_{66}H_{80}N_8O_8$	
Formula weight	1113.38	
Temperature	93(2) K	
Wavelength	0.71073 Å	
Crystal system	Triclinic	
Space group	P-1	
Unit cell dimensions	a = 10.2200(14) Å	α = 101.182(4)°.
	b = 15.396(3) Å	β = 90.581(4)°.
	c = 19.845(3) Å	γ = 100.776(4)°.
Volume	3005.8(8) $Å^3$	
Z	2	
Density (calculated)	1.230 Mg/m^3	
Absorption coefficient	0.082 mm^{-1}	
F(000)	1192	
Crystal size	0.2000 x 0.2000 x 0.2000 mm^3	
Theta range for data collection	2.03 to 25.35°.	
Index ranges	$-12 \le h \le 12$, $-12 \le k \le 18$, $-23 \le l \le 23$	
Reflections collected	19162	
Independent reflections	10447 [R(int) = 0.0210]	
Completeness to theta = 25.35°	94.9%	
Absorption correction	Multiscan	
Max. and min. transmission	1.0000 and 0.7850	
Refinement method	Full-matrix least-squares on F^2	
Data / restraints / parameters	10447 / 4 / 758	
Goodness-of-fit on F^2	1.043	
Final R indices [I>2sigma(I)]	R1 = 0.0432, wR2 = 0.1057	
R indices (all data)	R1 = 0.0519, wR2 = 0.1124	
Extinction coefficient	0.0031(7)	
Largest diff. peak and hole	0.689 and -0.308 e.$Å^{-3}$	

Table 2.3. Crystal data and structure refinement for [Co**L7**]Et_3NH.

Identification code	[Co**L7**]Et_3NH	
Empirical formula	$C_{68}H_{86}CoNO_8$	
Formula weight	1188.37	
Temperature	93(2) K	
Wavelength	0.71073 Å	
Crystal system	Monoclinic	
Space group	P2(1)/c	
Unit cell dimensions	a = 15.4921(6) Å	α= 90°.
	b = 19.1721(8) Å	β= 100.176(2)°.
	c = 21.3192(9) Å	γ = 90°.
Volume	6232.5(4) $Å^3$	
Z	4	
Density (calculated)	1.266 Mg/m^3	
Absorption coefficient	0.336 mm^{-1}	
F(000)	2536	
Crystal size	0.200 x 0.100 x 0.030 mm^3	
Theta range for data collection	1.71 to 25.35°.	
Index ranges	-17 ≤ h ≤ 18, -23 ≤ k ≤ 22, -25 ≤ l ≤ 25	
Reflections collected	57765	
Independent reflections	11312 [R(int) = 0.0317]	
Completeness to theta = 25.00°	99.2%	
Absorption correction	Multiscan	
Max. and min. transmission	1.0000 and 0.9433	
Refinement method	Full-matrix least-squares on F^2	
Data / restraints / parameters	11312 / 23 / 762	
Goodness-of-fit on F^2	1.033	
Final R indices [I>2sigma(I)]	R1 = 0.0666, wR2 = 0.1759	
R indices (all data)	R1 = 0.0711, wR2 = 0.1807	
Largest diff. peak and hole	2.419 and -0.941 e.$Å^{-3}$	

2.5 References and Notes

[1] For reviews on interlocked molecules assembled about transition metal templates see: (a) Sauvage, J.-P.; Dietrich-Buchecker, C. *Molecular Catenanes, Rotaxanes and Knots*; Wiley-VCH: Weinheim, Germany, 1999. (b) Hubin, T. J.; Busch, D. H.; *Coord. Chem. Rev.* **2000**, *200–202*, 5–52. (c) Collin, J.-P.; Dietrich-Buchecker, C.; Gaviña, P.; Jimenez-Molero, M. C.; Sauvage, J.-P. *Acc. Chem. Res.* **2001**, *34*, 477–487. (d) Menon, S. K.; Guha, T. B.; Agrawal, Y. K. *Rev. Inorg. Chem.* **2004**, *24*, 97–133. (e) Cantrill, S. J.; Chichak, K. S.; Peters, A. J.; Stoddart, J. F. *Acc. Chem. Res*. **2005**, *38*, 1–9.

[2] For catenates assembled around a tetrahedral four-coordinate Cu(I) template, see: (a) Dietrich-Buchecker, C. O.; Sauvage, J.-P.; Kintzinger, J.-P. *Tetrahedron Lett.* **1983**, *24*, 5095–5098. (b) Dietrich-Buchecker, C. O.; Sauvage, J.-P.; Kern, J.-M. *J. Am. Chem. Soc.* **1984**, *106*, 3043–3045. (c) Cesario, M.; Dietrich-Buchecker, C. O.; Guilhem, J.; Pascard, C.; Sauvage, J.-P. *J. Chem. Soc., Chem. Commun.* **1985**, 244–247. (d) Dietrich-Buchecker, C. O.; Guilhem, J.; Khemiss, A. K.; Kintzinger, J.-P.; Pascard, C.; Sauvage, J.-P. *Angew. Chem., Int. Ed. Engl.* **1987**, *26*, 661–663. (e) Dietrich-Buchecker, C. O.; Edel, A.; Kintzinger, J.-P.; Sauvage, J.-P. *Tetrahedron* **1987**, *43*, 333–344. (f) Jørgensen, T.; Becher, J.; Chambron, J.-C.; Sauvage, J.-P. *Tetrahedron Lett.* **1994**, *35*, 4339–4342. (g) Kern, J.-M.; Sauvage, J.-P.; Weidmann, J.-L. *Tetrahedron* **1996**, *52*, 10921–10934. (h) Kern, J.-M.; Sauvage, J.-P.; Weidmann, J.-L.; Armaroli, N.; Flamigni, L.; Ceroni, P.; Balzani, V. *Inorg. Chem.* **1997**, *36*, 5329–5338. (i) Mohr, B.; Weck, M.; Sauvage, J.-P.; Grubbs, R. H. *Angew. Chem., Int. Ed.* **1997**, *36*, 1308–1310. (j) Amabilino, D. B.; Sauvage, J.-P. *New J. Chem.* **1998**, *22*, 395–409. (k) Weidmann, J.-L.; Kern, J.-M.; Sauvage, J.-P.; Muscat, D.; Mullins, S.; Köhler, W.; Rosenauer, C.; Räder, H. J.; Martin, K.; Geerts, Y. *Chem. Eur. J.* **1999**, *5*, 1841–1851. (l) Raehm, L.; Hamann, C.; Kern, J.-M.; Sauvage, J.-P. *Org. Lett.* **2000**, *2*, 1991–1994. (m) Frey, J.; Kraus, T.; Heitz, V.; Sauvage, J.-P. *Chem. Commun.* **2005**, 5310–5312. For catenates assembled around a bis-Cu(I) template see: (o) Hutin, M.; Schalley, C. A.; Bernardinelli, G.; Nitschke, J. R. *Chem. Eur. J.* **2006**, *12*, 4069–4076.

[3] For chiral [2]catenates assembled around tetrahedral four-coordinate Cu(I) templates see: (a) Chambron, J.-C.; Mitchell, D. K.; Sauvage, J.-P. *J. Am. Chem. Soc.* **1992**, *114*, 4625–4631. (b) Kaida, Y.; Okamoto, Y.; Chambron, J.-C.; Mitchell, D. K.; Sauvage, J.-P. *Tetrahedron Lett.* **1993**, *34*, 1019–1022.

[4] For doubly entwined [2]catenates (Solomon knots) assembled around tetrahedral four-coordinate Cu(I) templates see: (a) Nierengarten, J.-F.; Dietrich-Buchecker, C. O.; Sauvage, J.-P. *J. Am. Chem. Soc*. **1994**, *116*, 375–376. (b) Nierengarten, J.-F.; Dietrich-Buchecker, C. O.; Sauvage, J.-P. *New J. Chem.* **1996**, *20*, 685–693. (c) Dietrich-Buchecker, C.; Leize, E.; Nierengarten, J.-F.; Sauvage, J.-P.; Van Dorsselaer, A. *J. Chem. Soc., Chem.*

Commun. **1994**, 2257–2258. For Solomon knots assembled around three Li(I) ions see: (d) Dietrich-Buchecker, C.; Sauvage, J. P.; *Chem. Commun.* **1999**, 615–616. For Solomon knots assembled around a mixed Cu(II)/Zn(II) template see: (e) Pentecost, C. D.; Chichak, K. S.; Peters, A. J.; Cave, G. W. V.; Cantrill, S. J.; Stoddart, J. F. *Angew. Chem., Int. Ed.* **2007**, *46*, 218–222.

[5] For rotaxanes assembled around a tetrahedral four-coordinate Cu(I) template see: (a) Wu, C.; Lecavalier, P. R.; Shen, Y. X.; Gibson, H. W. *Chem. Mater.* **1991**, *3*, 569–572. (b) Chambron, J.-C.; Heitz, V.; Sauvage, J.-P. *J. Chem. Soc., Chem. Commun.* **1992**, 1131–1133. (c) Chambron, J.-C.; Heitz, V.; Sauvage, J.-P. *J. Am. Chem. Soc.* **1993**, *115*, 12378–12384. (d) Diederich, F.; Dietrich-Buchecker, C.; Nierengarten, J.-F.; Sauvage, J.-P. *J. Chem. Soc., Chem. Commun.* **1995**, 781–782. (e) Cárdenas, D. J.; Gaviña, P.; Sauvage, J.-P. *Chem. Commun.* **1996**, 1915–1916. (f) Solladié, N.; Chambron, J.-C.; Dietrich-Buchecker, C. O.; Sauvage, J.-P. *Angew. Chem., Int. Ed. Engl.* **1996**, *35*, 906–909. (g) Armaroli, N.; Diederich, F.; Dietrich-Buchecker, C. O.; Flamigni, L.; Marconi, G.; Nierengarten, J.-F.; Sauvage, J.-P. *Chem. Eur. J.* **1998**, *4*, 406–416. (h) Armaroli, N.; Balzani, V.; Collin, J.-P.; Gaviña, P.; Sauvage, J.-P.; Ventura, B. *J. Am. Chem. Soc.* **1999**, *121*, 4397–4408. (i) Solladié, N.; Chambron, J.-C.; Sauvage, J.-P. *J. Am. Chem. Soc.* **1999**, *121*, 3684–3692. (j) Weber, N.; Hamann, C.; Kern, J.-M.; Sauvage, J.-P. *Inorg. Chem.* **2003**, *42*, 6780–6792. (k) Poleschak, I.; Kern, J.-M.; Sauvage, J.-P. *Chem. Commun.* **2004**, 474–476. (l) Kwan, P. H.; Swager, T. M. *J. Am. Chem. Soc.* **2005**, *127*, 5902–5909.

[6] For a rotaxane dimer assembled around tetrahedral four-coordinate Cu(I) templates see: (a) Jiménez, M. C.; Dietrich-Buchecker, C.; Sauvage, J.-P.; De Cian, A. *Angew. Chem., Int. Ed.* **2000**, *39*, 1295–1298. (b) Jiménez, M. C.; Dietrich-Buchecker, C.; Sauvage, J.-P. *Angew. Chem., Int. Ed.* **2000**, *39*, 3284–3287. (c) Kraus, T.; Buděšínský, M.; Cvačka, J.; Sauvage, J.-P. *Angew. Chem., Int. Ed.* **2006**, *45*, 258–261. (d) Champin, B.; Sartor, V.; Sauvage, J.-P. *New J. Chem.* **2008**, *32*, 1048–1054. (e) Frey, J.; Kraus, T.; Heitz, V.; Sauvage, J.-P. *Chem. Commun.* **2005**, 5310–5312. (f) Collin, J.-P.; Frey, J.; Heitz, V.; Sakellariou, E.; Sauvage, J.-P.; Tock, C. *New J. Chem.* **2006**, *30*, 1386–1389. (g) Frey, J.; Tock, C.; Collin, J.-P.; Heitz, V.; Sauvage, J.-P.; Rissanen, K. *J. Am. Chem. Soc.* **2008**, *130*, 11013–11022.

[7] For knots assembled around tetrahedral four-coordinate Cu(I) templates see: (a) Dietrich-Buchecker, C. O.; Sauvage, J.-P. *Angew. Chem., Int. Ed. Engl.* **1989**, *28*, 189–192. (b) Dietrich-Buchecker, C. O.; Nierengarten, J.-F.; Sauvage, J.-P. *Tetrahedron Lett.* **1992**, *33*, 3625–3628. (c) Dietrich-Buchecker, C. O.; Sauvage, J.-P.; Kintzinger, J.-P.; Maltese, P.; Pascard, C.; Guilhem, J. *New. J. Chem.* **1992**, *16*, 931–942. (d) Dietrich-Buchecker, C. O; Sauvage, J.-P.; De Cian, A.; Fischer, J. *J. Chem. Soc., Chem. Commun.* **1994**, 2231–2232. (e) Perret-Aebi, L.-E.; von Zelewsky, A.; Dietrich-Buchecker, C.; Sauvage, J.-P. *Angew. Chem., Int. Ed.* **2004**, *43*, 4482–4485. For knots assembled around an octahedral template see: (f) Rapenne, G.; Dietrich-Buchecker, C. O.; Sauvage, J.-P. *J. Am. Chem. Soc*. **1999**, *121*, 994–1001.

[8] (a) Fujita, M.; Ibukuro, F.; Hagihara, H.; Ogura, K. *Nature* **1994**, *367*, 720–723. (b) Fujita, M.; Ibukuro, F.; Yamaguchi, K.; Ogura, K. *J. Am. Chem. Soc.* **1995**, *117*, 4175–4176. (c) Piguet, C.; Bernardinelli, G.; Williams, A. F.; Bocquet, B. *Angew. Chem., Int. Ed. Engl.* **1995**, *34*, 582–584. (d) Mingos, D. M. P.; Yau, J.; Menzer, S.; Williams, D. J. *Angew. Chem., Int. Ed. Engl.* **1995**, *34*, 1894–1895. (e) Fujita, M.; Ogura, K. *Bull. Chem. Soc. Jpn.* **1996**, *69*, 1471–1482. (f) Fujita, M.; Ogura, K. *Coord. Chem. Rev.* **1996**, *148*, 249–264. (g) Fujita, M.; Ibukuro, F.; Seki, H.; Kamo, O.; Imanari, M.; Ogura, K. *J. Am. Chem. Soc.* **1996**, *118*, 899–900. (h) Cárdenas, D. J.; Sauvage, J.-P. *Inorg. Chem.* **1997**, *36*, 2777–2783. (i) Cárdenas, D. J.; Gaviña, P.; Sauvage, J.-P. *J. Am. Chem. Soc.* **1997**, *119*, 2656–2664. (j) Fujita, M.; Aoyagi, M.; Ibukuro, F.; Ogura, K.; Yamaguchi, K. *J. Am. Chem. Soc.* **1998**, *120*, 611–612. (k) Whang, D.; Park, K.-M.; Heo, J.; Kim, K. *J. Am. Chem. Soc*. **1998**, *120*, 4899–4900. (l) Try, A. C.; Harding, M. M.; Hamilton, D. G.; Sanders, J. K. M. *J. Chem. Soc., Chem. Commun.* **1998**, 723–724. (m) Fujita, M.; Fujita, N.; Ogura, K.; Yamaguchi, K. *Nature* **1999**, *400*, 52–55. (n) Fujita, M. *Acc. Chem. Res.* **1999**, *32*, 53–61. (o) Jeong, K. S.; Choi, J. S.; Chang, S. Y.; Chang, H. Y. *Angew. Chem., Int. Ed.* **2000**, *39*, 1692–1695. (p) Dietrich-Buchecker, C.; Geum, N.; Hori, A.; Fujita, M.; Sakamoto, S.; Yamaguchi, K.; Sauvage, J.-P. *Chem. Commun.* **2001**, 1182–1183. (q) Padilla-Tosta, M. E.; Fox, O. D.; Drew, M. G. B.; Beer, P. D. *Angew. Chem., Int. Ed.* **2001**, *40*, 4235–4239. (r) Park, K.-M.; Kim, S.-Y.; Heo, J.; Whang, D.; Sakamoto, S.; Yamaguchi, K.; Kim, K. *J. Am. Chem. Soc*. **2002**, *124*, 2140–2147. (s) Kim, K. *Chem. Soc. Rev*. **2002**, *31*, 96–107. (t) McArdle, C. P.; Irwin, M. J.; Jennings, M. C.; Vittal, J. J.; Puddephatt, R. J. *Chem. Eur. J.* **2002**, *8*, 723–734. (u) McArdle, C. P.; Van, S.; Jennings, M. C.; Puddephatt, R. J. *J. Am. Chem. Soc.* **2002**, *124*, 3959–3965 (v) Dietrich-Buchecker, C.; Colasson, B.; Fujita, M.; Hori, A.; Geum, N.; Sakamoto, S.; Yamaguchi, K.; Sauvage, J.-P. *J. Am. Chem. Soc.* **2003**, *125*, 5717–5725. (w) Hori, A.; Kataoka, H.; Akasaka, A.; Okano, T.; Fujita, M. *J. Polym. Sci. Part A: Polym. Chem.* **2003**, *41*, 3478–3485. (x) Mohr, F.; Eisler, D. J.; McArdle, C. P.; Atieh, K.; Jennings, M. C.; Puddephatt, R. J. *J. Organomet. Chem.* **2003**, *670*, 27–36. (y) Mohr, F.; Jennings, M. C.; Puddephatt, R. J. *Eur. J. Inorg. Chem.* **2003**, 217–223. (z) Colasson, B. X.; Sauvage, J.-P. *Inorg. Chem.* **2004**, *43*, 1895–1901. (aa) Hori, A.; Yamashita, K.; Kusukawa, T.; Akasaka, A.; Biradha, K.; Fujita, M. *Chem. Commun.* **2004**, 1798–1799. (bb) Burchell, T. J.; Eisler, D. J.; Puddephatt, R. J. *Dalton Trans.* **2005**, 268–272. (cc) Wong, W. W. H.; Cookson, J.; Evans, E. A. L.; McInnes, E. J. L.; Wolowska, J.; Maher, J. P.; Bishop, P.; Beer, P. D. *Chem. Commun.* **2005**, 2214–2216. (dd) Habermehl, N. C.; Jennings, M. C.; McArdle, C. P.; Mohr, F.; Puddephatt, R. J. *Organometallics* **2005**, *24*, 5004–5014. (ee) Fujita, M.; Tominaga, M.; Hori, A.; Therrien, B. *Acc. Chem. Res.* **2005**, *38*, 369–378. (ff) Blanco, V.; Chas, M.; Abella, D.; Peinador, C.; Quintela, J. M. *J. Am. Chem. Soc*. **2007**, *129*, 13978–13986; (gg) Westcott, A.; Fisher, J.; Harding, L. P.; Rizkallah, P.; Hardie, M. J. *J. Am. Chem. Soc.* **2008**, *130*, 2950–2951.

[9] (a) Leigh, D. A.; Lusby, P. J.; Teat, S. J.; Wilson, A. J.; Wong, J. K. Y. *Angew. Chem., Int. Ed.* **2001**, *40*, 1538–1543. (b) Hogg, L.; Leigh, D. A.; Lusby, P. J.; Morelli, A.; Parsons, S.; Wong, J. K. Y. *Angew. Chem., Int. Ed.* **2004**, *43*, 1218–1221.

[10] For other examples of '3+3' approaches to rotaxanes assembled around octahedral metal centers see: (a) Sauvage, J.-P.; Ward, M. *Inorg. Chem.* **1991**, *30*, 3869–3874. (b) Loren, J. C.; Gantzel, P.; Linden, A.; Siegel, J. S.; *Org. Biomol. Chem.* **2005**, *3*, 3105–3116. For a '4+2' approach see: (c) Mobian, P.; Kern, J.-M.; Sauvage, J.-P. *J. Am. Chem. Soc.* **2003**, *125*, 2016–2017. (d) P. Mobian, J.-M. Kern, J.-P. Sauvage, *Helv. Chim. Acta* **2003**, *86*, 4195–4213. (e) Mobian, P.; Kern, J.-M.; Sauvage, J.-P. *Angew. Chem., Int. Ed.* **2004**, *43*, 2392–2395. (f) Chambron, J.-C.; Collin, J.-P.; Heitz, V.; Jouvenot, D.; Kern, J.-M.; Mobian, P.; Pomeranc, D.; Sauvage, J.-P. *Eur. J. Org. Chem.* **2004**, 1627–1638. (g) F. Arico, P. Mobian, J.-M. Kern, J.-P. Sauvage, *Org. Lett.* **2003**, *5*, 1887–1890. (g) Mobian, P.; Kern, J.-M.; Sauvage, J.-P. *Inorg. Chem.* **2003**, *42*, 8633–8637. (i) Pomeranc, D.; Jouvenot, D.; Chambron, J.-C.; Collin, J.-P.; Heitz, V.; Sauvage, J.-P. *Chem. Eur. J.* **2003**, *9*, 4247–4254. (j) Collin, J.-P.; Jouvenot, D.; Koizumi, M.; Sauvage, J.-P. *Eur. J. Inorg. Chem.* **2005**, 1850–1855. For a '2+2+2' approach to rotaxanes see: (k) Prikhod'ko, A. I.; Durola, F.; Sauvage, J.-P. *J. Am. Chem. Soc.* **2008**, *130*, 448–449. For an example of interlocked molecules assembled using a five-coordinate TM template see: (l) Hamann, C.; Kern, J.-M.; Sauvage, J.-P. *Inorg. Chem.* **2003**, *42*, 1877–1883.

[11] (a) Fuller, A.-M. L.; Leigh, D. A.; Lusby, P. J.; Slawin, A. M. Z.; Walker, D. B. *J. Am. Chem. Soc.* **2005**, *127*, 12612–12619. (b) Fuller, A.-M.; Leigh, D. A.; Lusby, P. J.; Oswald, I. D. H.; Parsons, S.; Walker, D. B. *Angew. Chem., Int. Ed.* **2004**, *43*, 3914–3918. (c) Furusho, Y.; Matsuyama, T.; Takata, T.; Moriuchi, T.; Hirao, T. *Tetrahedron Lett.* **2004**, *45*, 9593–9597. (d) Fuller, A.-M. L.; Leigh, D. A.; Lusby, P. J. *Angew. Chem., Int. Ed.* **2007**, *46*, 5015–5019. (e) Crowley, J. D.; Leigh, D. A.; Lusby, P. J.; McBurney, R. T.; Perret-Aebi, L.-E.; Petzold, C.; Slawin, A. M. Z.; Symes, M. D. *J. Am. Chem. Soc.* **2007**, *129*, 15085–15090.

[12] Goldup, S. M.; Leigh, D. A.; Lusby, P. J.; McBurney, R. T.; Slawin, A. M. Z.; *Angew. Chem., Int. Ed.* **2008**, *47*, 6999–7003.

[13] (a) Dietrich-Buchecker, C.; Sauvage, J.-P.; Kern, J.-M. *J. Am. Chem. Soc.* **1989**, *111*, 7791–7800. (b) Raehm, L.; Kern, J.-M.; Sauvage, J.-P. *Chem. Eur. J.* **1999**, *5*, 3310–3317.

[14] (a) Chambron, J.-C.; Harriman, A.; Heitz, V.; Sauvage, J.-P. *J. Am. Chem. Soc.* **1993**, *115*, 6109–6114. (b) Andersson, M.; Linke, M.; Chambron, J.-C.; Davidsson, J.; Heitz, V.; Hammarström, L.; Sauvage, J.-P. *J. Am. Chem. Soc.* **2002**, *124*, 4347–4362. (c) Bonnet, S.; Collin, J.-P. *Chem. Soc. Rev.* **2008**, *37*, 1207–1217.

[15] (a) Dietrich-Buchecker, C. O.; Kern, J.-M.; Sauvage, J.-P. *J. Chem. Soc., Chem. Commun.*, **1985**, 760–762; (b) Albrecht-Gary, A.-M.; Saad, Z.; Dietrich-Buchecker, C. O.; Sauvage, J.-P. *J. Am. Chem. Soc.* **1985**, *107*, 3205–3209. (c) Albrecht-Gary, A.-M.; Saad, Z.; Dietrich-Buchecker, C.; Sauvage, J.-P. *J. Am. Chem. Soc.* **1988**, *110*, 1467–1472. (d) Leigh, D. A.; Lusby, P. J.; Slawin, A. M. Z.; Walker, D. B. *Angew. Chem., Int. Ed.* **2005**, *44*, 4557–4564.

[16] Arnaud-Neu, F. A.; Marques, E.; Schwing-Weill, M.-J.; Dietrich-Buchecker, C. O.; Sauvage, J.-P.; Weiss, J. *New J. Chem.* **1988**, *12*, 15–20.

[17] (a) Champin, B.; Mobian, P.; Sauvage, J.-P. *Chem. Soc. Rev.* **2007**, *36*, 358–366. (b) Kay, E. R.; Leigh, D. A.; Zerbetto, F. *Angew. Chem., Int. Ed.* **2007**, *46*, 72–191.

[18] For a [2]catenane with Co(II)/Co(III) ions in the framework see: (a) Abedin, T. S. M.; Thompson, L. K.; Miller, D. O. *Chem. Comm.* **2005**, 5512–5514. For a [3]rotaxane with Co(III) in the thread see: (b) Cheetham, A. G.; Claridge, T. D. W.; Anderson, H. L. *Org. Biomol. Chem.* **2007**, *5*, 457–462.

[19] (a) Noveron, J. C.; Olmstead, M. M.; Mascharak, P. K. *Inorg. Chem.* **1998**, *37*, 1138–1139. (b) Chavez, F. A.; Rowland, J. M.; Olmstead, M. M.; Mascharak, P. K. *J. Am. Chem. Soc.* **1998**, *120*, 9015–9027. (c) Noveron, J. C.; Olmstead, M. M.; Mascharak, P. K. *J. Am. Chem. Soc.* **1999**, *121*, 3553–3554. (d) Marlin, D. S.; Olmstead, M. M.; Mascharak, P. K. *Inorg. Chem.* **1999**, *38*, 3258–3259. (e) Tyler, L. A.; Noveron, J. C.; Olmstead, M. M.; Mascharak, P. K. *Inorg. Chem.* **2000**, *39*, 357–362. (f) Chavez, F. A.; Mascharak, P. K. *Acc. Chem. Res.* **2000**, *33*, 539–545. (g) Marlin, D. S.; Mascharak, P. K. *Chem. Soc. Rev.* **2000**, *29*, 69–74. (h) Noveron, J. C.; Olmstead, M. M.; Mascharak, P. K. *J. Am. Chem. Soc.* **2001**, *123*, 3247–3259.

[20] For related Co(III) complexes see: Dwyer, A. N; Grossel, M. C; Horton, P. N. *Supramol. Chem.* **2004**, *16*, 405–410.

[21] ^{1}H NMR and mass spectrometry revealed that all of the purified Co(III) complexes had undergone cation exchange of Et_4N^+ with $Et_3N^+CH_2Cl$. This was most likely formed by reaction of Et_3N with CH_2Cl_2 [Menshutkin, N. Z. *Phys. Chem.* **1890**, *6*, 41–57]. This reaction normally proceeds slowly under ambient conditions [Wright, D. A.; Wulff, C. A. *J. Org. Chem.* **1970**, *35*, 4252] but is accelerated under pressure [Almarzoqi, B.; George, A. V.; Issacs, N. S. *Tetrahedron* **1986**, *42*, 601–607]. It was recently reported [Lee, J. J.; Stanger, K. J.; Noll, B. C.; Gonzalez, C.; Marquez, M.; Smith, B. D. *J. Am. Chem. Soc.* **2005**, *127*, 4184–4185] that macrocyclic hosts containing a tertiary amine and a chloride anion binding cleft react with CH_2Cl_2. In the present case, however, the reaction takes place during the chromatographic purification procedure (silica gel, CH_2Cl_2, acetone, Et_3N).

[22] Initially pristine Co(III) complexes were found to decompose over a period of a few days in both $CDCl_3$ and $(CD_3)_2CO$, however, no decomposition was observed for CD_2Cl_2 solutions of Co(III) complexes.

[23] (a) Belfrekh, N.; Dietrich-Buchecker, C. O.; Sauvage, J.-P. *Inorg. Chem.* **2000**, *39*, 5169–5172. Exploited to yield large macrocycles: (b) Shah, M. R.; Duda, S.; Muller, B.; Godt, A.; Malik, A. *J. Am. Chem. Soc.* **2003**, *125*, 5408–5414.

[24] Creaser, I. I; Harrowfield, J. M.; Herlt, A. J.; Sargeson, A. M.; Springborg, J.; Geue, R. J.; Snow, M. R. *J. Am. Chem. Soc.* **1977**, *99*, 3181–3182.

[25] (a) Cesario, M.; Dietrich-Buchecker, C. O.; Guilhem, J.; Pascard, C.; Sauvage, J.-P. *J. Chem. Soc., Chem. Commun.* **1985,** 244–247. (b) Leigh, D. A.; Moody, K.; Smart, J. P.; Watson, K. J.; Slawin, A. M. Z. *Angew. Chem., Int. Ed. Engl*. **1996**, *35*, 306–310.

[26] Elucidation of the crystal structure revealed that another cation exchange had occurred, with $Et_3N^+CH_2Cl$ being replaced by Et_3N^+H.

[27] During the initial stages of the remetallation reaction, addition of pink crystals of Co(II) to a solution of H_4**L10** and $Et_4N(OAc)$ in THF and EtOH resulted in an immediate color change, giving a green solution indicating spontaneous oxidation of Co(II) to Co(III).

[28] For 'active-metal template' rotaxane synthesis, in which the metal acts as both a template and a catalyst for covalent bond formation and thus generally changes oxidation state, coordination number and/or geometry during the reaction, see: (a) Aucagne, V.; Hänni, K. D.; Leigh, D. A.; Lusby, P. J.; Walker, D. B. *J. Am. Chem. Soc.* **2006**, *128*, 2186–2187. (b) Saito, S.; Takahashi, E.; Nakazono, K. *Org. Lett*. **2006**, *8*, 5133–5136. (c) Berná, J.; Crowley, J. D.; Goldup, S. M.; Hänni, K. D.; Lee, A.-L.; Leigh, D. A. *Angew. Chem., Int. Ed.* **2007**, *46*, 5709–5713. (d) Aucagne, V.; Berná, J.; Crowley, J. D.; Goldup, S. M.; Hänni, K. D.; Leigh, D. A.; Lusby, P. J.; Ronaldson, V. E.; Slawin, A. M. Z.; Viterisi, A.; Walker, D. B. *J. Am. Chem. Soc.* **2007**, *129*, 11950–11963. (e) Crowley, J. D.; Hänni, K. D.; Lee, A.-L.; Leigh, D. A. *J. Am. Chem. Soc*. **2007**, *129*, 12092–12093. (f) Goldup, S. M.; Leigh, D. A.; Lusby, P. J.; McBurney, R. T.; Slawin, A. M. Z. *Angew. Chem., Int. Ed*. **2008**, *47*, 3381–3384. (g) Berná, J.; Goldup, S. M.; Lee, A.-L.; Leigh, D. A.; Symes, M. D.; Teobaldi, G.; Zerbetto, F. *Angew. Chem., Int. Ed*. **2008**, *47*, 4392–4396.

[29] Ashley, J. N.; Barber, H. J., Ewins, A. J.; Newbery, G.; Self, A. D. H.; *J. Chem. Soc.* **1942**, 103-116.

CHAPTER THREE

Active Template Pd(II)-Promoted Michael Addition Synthesis of Rotaxanes

Published as "*Active Template Synthesis of Rotaxanes and Molecular Shuttles with Switchable Dynamics via Four-Component Pd(II)-Promoted Michael Additions*"

Stephen M. Goldup, David A. Leigh, Paul J. Lusby, Roy T. McBurney and Alexandra M. Z. Slawin, *Angew. Chem. Int. Ed.* **2008**, *43*, 3381-3384.

Acknowledgements

The following people are gratefully acknowledged for their contribution to this chapter: Dr. Steve Goldup for assistance with EXSY experiments and calculations; Prof. Alex Slawin solved the X-ray crystal structures of [**L2**Pd(CH_3CN)], [**L2**Pd**L1**] and [**L3**Pd]; Diego Gonzalez-Cabrera, Mark Symes and Juraj Bella for assistance with VT ^{1}H NMR and EXSY studies.

Synopsis

In Chapter Two the template effect of a three dimensional octahedral cobalt(III) ion was successfully utilized for the construction of interlocked architectures. The strategy relied on the metal ion acting to passively gather and organize pyridine-2,6-biscarboxamido ligands in a mutually orthogonal alignment to favor interlocked architecture formation. Chapter Three describes a novel strategy in which a metal ion plays a dual role; acting to both gather and organize the ligands, and also actively catalyze covalent bond formation between two 'half-threads' through the cavity of the macrocycle.

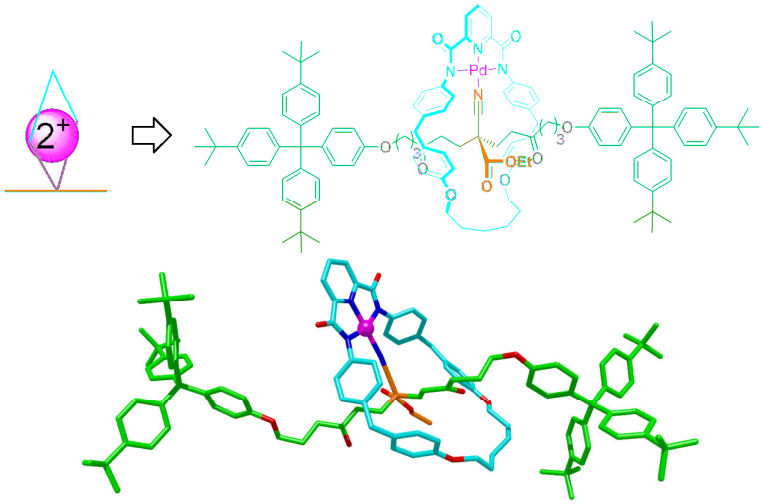

Here a square planar Pd(II) pyridine-2,6-biscarboxamido complex is used to promote Michael addition reactions between cyano ester and vinyl ketone functionalized units to construct a simple rotaxane and a degenerate molecular shuttle. The interlocked nature of the simple rotaxane was confirmed by X-ray crystallography, demonstrating that the nitrile functional group acted as a "station" for the Pd(II)-macrocycle. Incorporation of two nitrile "stations" allowed the synthesis of a [2]rotaxane-based degenerate shuttle. The dynamics of the molecular shuttle were investigated by VT ^{1}H NMR and 2D EXSY ^{1}H NMR and were controlled by reagent addition.

3.1 Introduction

Active template synthesis,[1] in which a substrate acts as both the template for a threaded complex and the catalyst for the covalent bond forming step that captures the interlocked product, is a new addition to the strategies available[2, 3] for the assembly of rotaxanes. Unlike traditional 'passive template' methods,[3] the intercomponent interactions responsible for rotaxane formation in an active template reaction do not normally 'live on' in the final product.[4] Removing the need for permanent recognition features increases the structural diversity that can be introduced into interlocked architectures but also loses one of the key features of rotaxanes that has been so successfully exploited in the early generations of artificial molecular machines.[5] Here we report on the first active template reaction in which the template interactions between macrocycle and thread persist in the resulting rotaxane. A macrocycle-coordinated palladium(II) center promotes the formation of carbon-carbon bonds between three other building blocks by successive Michael additions while positioning the reactants so that the final covalent bond forms through the macrocycle producing [2]rotaxanes in up to 99% yield (Scheme 3.1 and Table 3.1). The Pd-nitrile coordination bond that directs and controls the synthesis is retained in the rotaxane product, enabling the preparation of both degenerate station molecular shuttles (with controllable dynamics, Scheme 3.2) and stimuli-switchable molecular shuttles (Scheme 3.1) through a simple one pot multi-component assembly process.

3.2 Results and Discussion

3.2.1 Rotaxane Synthesis

The basis for the recognition-element-persistent active template reaction lies in a range of tridentate pyrroloimidazolone[6] and bisoxazoline[7] pincer Pd(II) complexes that catalyze asymmetric 1,4-conjugate additions of α-cyano esters to alkyl vinyl ketones in the presence of *N*,*N*-diisopropylethylamine (DIPEA).[8] It seemed that a suitably constructed tridentate macrocycle-Pd(II) complex[9] might promote the

double Michael addition between ethyl cyanoacetate, **L1**, and two suitably derivatized vinyl ketone 'half-threads' (**1**) to generate [2]rotaxanes with the intercomponent recognition motif intact (Scheme 3.1).

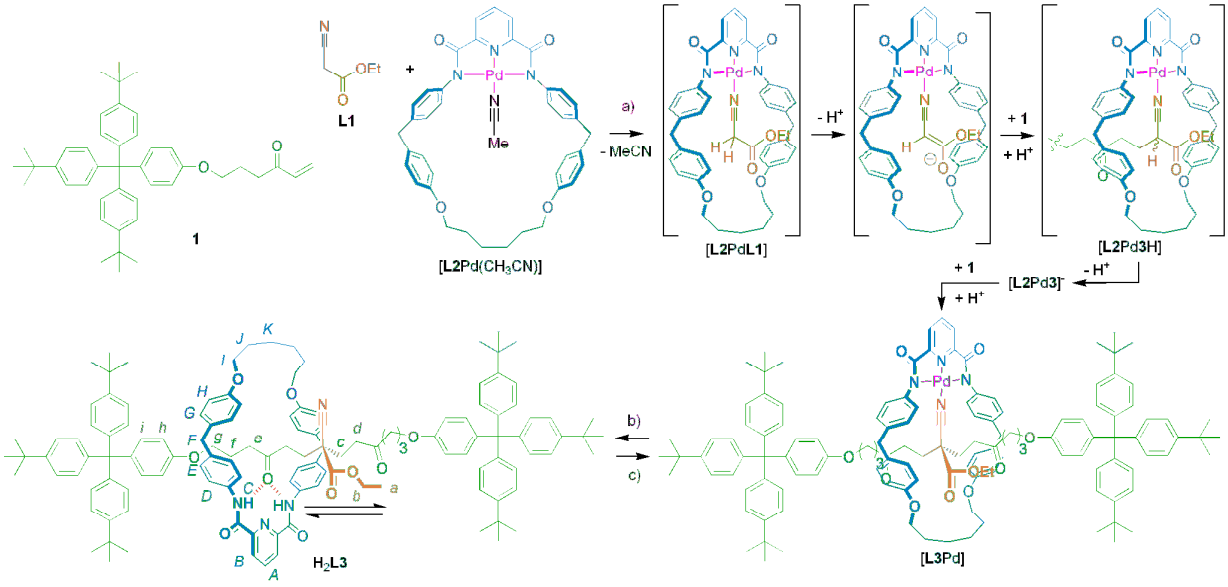

Scheme 3.1. Synthesis of metal-coordinated [2]rotaxane [(**L3**)Pd] by an active template Pd(II)-promoted double Michael addition, and its decomplexation to hydrogen bonded molecular shuttle H_2**L3**. Reagents and conditions: a) DIPEA, CH_2Cl_2 (see Table 3.1 for the effects of reagent stoichiometry on the yield of rotaxane [(**L3**)Pd]); b) 1 M HCl (aq):CH_2Cl_2 (1:1), reflux, 92%. In $CDCl_3$ the macrocycle in H_2**L3** shuttles rapidly on the NMR timescale between the two thread ketone groups; c) $Pd(OAc)_2$ (2.2 equiv.), CH_3CN:CH_2Cl_2 (1:1), 18 h, 313 K, 99%.

Palladium(II)-macrocycle complex [(**L2**)Pd(CH_3CN)] was prepared in five steps from commercially available materials (see Schemes 3.4 and 3.5). Treatment of [(**L2**)Pd(CH_3CN)] with ethyl cyanoacetate in CH_2Cl_2, followed by removal of the solvent and acetonitrile under reduced pressure, afforded complex [(**L2**)Pd(**L1**)], which crystallized from a saturated CH_2Cl_2/Et_2O solution in a form suitable for investigation by X-ray diffraction.[10] The solid state structures of both [(**L2**)Pd(CH_3CN)] (Figures 3.1a and 3.1b) and [(**L2**)Pd(**L1**)] (Figures 3.1c and 3.1d) show that the coordination mode[11] of $\mathbf{L2}^{2-}$ and the shape of the ring holds the nitrile ligand occupying the fourth Pd(II) coordination site centrally within the macrocycle

cavity. The crystal structures suggested that the first alkylation of the α-methylene group should result in one face of the macrocycle being blocked such that the second Michael addition must proceed from the other side, generating a [2]rotaxane.

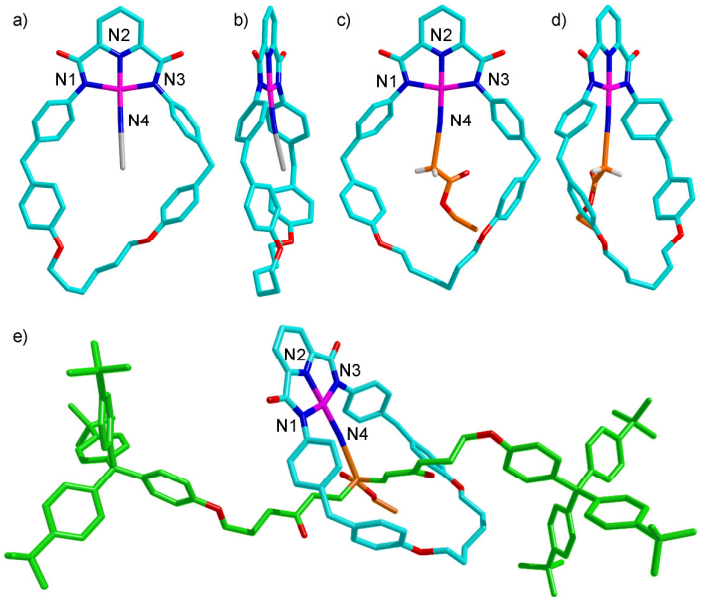

Figure 3.1. X-Ray crystal structures[10] of [(**L2**)Pd(CH_3CN)] from a) face-on and b) side-on views and [(**L2**)Pd(**L1**)] from c) face-on and d) side-on views and e) rotaxane [(**L3**)Pd]. Selected bond lengths [Å] and angles [°]: [(**L2**)Pd(CH_3CN)]: N1-Pd 2.04, N2-Pd 1.92, N3-Pd 2.02, N4-Pd 2.02, N1-Pd-N3 161.4, N2-Pd-N4 176.1. [(**L2**)Pd(**L1**)]: N1-Pd 2.02, N2-Pd 1.92, N3-Pd 2.04, N4-Pd 2.02, N1-Pd-N3 161.7, N2-Pd-N4 177.9. [(**L3**)Pd]: N1-Pd 2.02, N2-Pd 1.92, N3-Pd 2.03, N4-Pd 2.00, N1-Pd-N3 161.8, N2-Pd-N4 178.9.

Pleasingly, the four component assembly of [(**L2**)Pd(CH_3CN)], **1** (x 2) and **L1** at RT in CH_2Cl_2, in the presence of DIPEA, led to [2]rotaxane [(**L3**)Pd], initially in 47% yield (Scheme 3.1 and Table 3.1, entry 1). The assignment of [(**L3**)Pd] as a rotaxane was initially made by mass spectrometry and ^{1}H NMR spectroscopy (for a stackplot of the spectra of [(**L3**)Pd] and the corresponding thread showing upfield shifts of the encapsulated regions of the rotaxane axle,[12] see Figure 3.2). Confirmation of the mechanically interlocked structure came from demetallation of [(**L3**)Pd] (1M HCl (aq):CH_2Cl_2 (1:1), 92%, Scheme 3.1, step b) which gave the weakly hydrogen bonded rotaxane H_2**L3** rather than the de-threaded components. The ^{1}H NMR spectrum shows the macrocycle in H_2**L3** preferentially resides over, and rapidly

shuttles between, the two thread ketone groups in $CDCl_3$. Finally, single crystals of [(**L3**)Pd] were grown from a saturated butanone/methanol solution. The solid state structure[10] (Figure 3.1e) confirms that the Pd-nitrile coordination bond is maintained in the metallated rotaxane and is responsible for holding the macrocycle and thread in the well-defined co-conformation observed in solution.

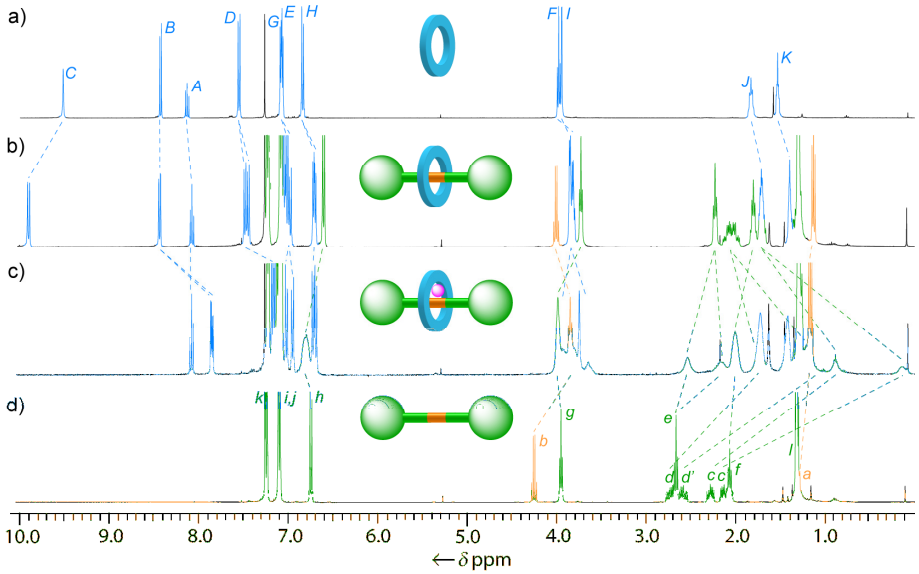

Figure 3.2. ^{1}H NMR (400 MHz, $CDCl_3$, 300 K) spectra of (a) macrocycle H_2**L2** (b) rotaxane H_2**L3** (c) Pd(II)-rotaxane [(**L3**)Pd] and (d) thread **S10**. The assignments correspond to the lettering in Scheme 3.1.

The rotaxane-forming reaction shown in Scheme 1 was optimized in terms of reagent stoichiometry and conditions (Table 3.1). The amount of base was reduced to 10 mol% to minimize the background non-palladium promoted reaction (Table 3.1, entry 2).[13] A concomitant increase in reaction temperature (to 313 K,[14] Table 3.1, entry 3) was then required for the reaction to achieve significant conversion within a reasonable timeframe (76% yield of double Michael addition products after 7 d). Under these conditions and using a modest excess of the thread building blocks (2.5 versus 1.0 equiv.), the yield of [2]rotaxane [**L3**Pd] was increased to >99% (Table 3.1, entry 6). This makes this active template reaction amongst the most efficient, albeit rather slowly proceeding, rotaxane-forming procedures reported to date.

Table 3.1. Optimization of the active template Pd(II)-promoted Michael addition synthesis of rotaxane [(**L3**)Pd].[a]

Entry	Thread components [equiv.][b]	DIPEA [equiv.]	Total conversion [%][c]	Yield of [(**L3**)Pd] [%]
1[d]	1.0	1.0	69	47
2[e]	1.0	0.1	70	53
3[f]	1.0	0.1	76	60
4[f]	1.5	0.1	77	85
5[f]	2.0	0.1	71	96
6[f]	2.5	0.1	67	>99

[a] Reaction conditions: [(**L2**)Pd(CH_3CN)], thread components **1** (x 2) and **L1**, DIPEA, CH_2Cl_2; [b] 2:1 stoichiometry of **1**:**L1**; [c] **L1** + [(**L2**)Pd(CH_3CN)] + 2 x **1** → [(**L3**)Pd] + non-interlocked thread; [d] 5 days at RT; [e] 19 days at RT; [f] 7 days at 313 K.

3.2.2 Molecular Shuttle Synthesis

As the nitrile functionality is preserved in the product of the active template reaction it can in principle be used as a binding site or 'station' for the macrocycle-Pd component in a molecular shuttle. To incorporate two such units into a rotaxane the reaction pattern for formation of the thread was reversed, so that shuttle [(**L4**)Pd] was synthesized by Michael additions of two 'hlaf-thread' *α*-cyano esters, **L5** to *bis*-(vinyl ketone) spacer **2** in the presence of [(**L2**)Pd(CH_3CN)] (Scheme 3.2, step a).

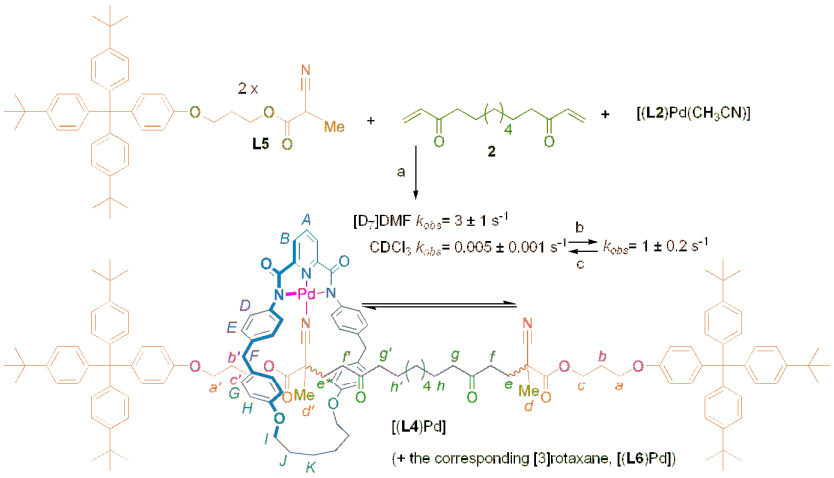

Scheme 3.2. Active template synthesis of a metal-coordinated molecular shuttle, [(**L4**)Pd], with stimuli-responsive dynamics. Reagents and conditions: a) **L5** (2 equiv.), **2** (1 equiv.), [(**L2**)Pd(CH_3CN)] (1 equiv.), DIPEA (0.1 equiv.), CH_2Cl_2, 313 K, 5 days; 27% [2]rotaxane [(**L4**)Pd] and 32% of the corresponding [3]rotaxane, [(**L6**)Pd]; b) pyridine (1 equiv.); c) TsOH (1 equiv.).

There are few examples[15] of metal-complexed molecular shuttles and the investigation of their dynamics is of interest. At room temperature in $CDCl_3$ the exchange of the palladium-coordinated macrocycle between the thread nitrile groups in [(**L4**)Pd] is slow on the NMR timescale. Ligand exchange at Pd(II) centers proceeds predominately *via* associative pathways,[16] possibly through folding at the low concentrations employed here, and no assistance for this mechanism is intrinsically available from non-coordinating solvents such as $CDCl_3$. Two dimensional exchange spectroscopy (2D-EXSY)[17] gave the room temperature pseudo-first-order rate constant $k_{obs} = 5 \times 10^{-3}$ s^{-1}, equivalent to an activation free energy of ~20 kcal mol^{-1} (details of the EXSY kinetic measurements are given in Section 3.3.4). In [D_7]DMF, the separated signals in the ^{1}H NMR spectrum caused by slow shuttling of the macrocycle at room temperature (Figure 3.3b) coalesced at 390 K (Figure 3.3c) (see Section 3.3.3 for VT ^{1}H NMR details, and for a stacked plot of ^{1}H NMR spectra of [(**L4**)Pd] in 10 K intervals from 300 K to 360 K, see Figure 3.4). EXSY experiments at 300 K determined the shuttling rate in [D_7]DMF (k_{obs} = 3 s^{-1}) to be 600x faster than in $CDCl_3$, corresponding to a rate for the bimolecular process involving solvent participation, k_{bi}, of 0.2 M^{-1} s^{-1}.

A bimolecular mechanism could also be made to operate in $CDCl_3$ by simply adding pyridine (Scheme 3.2, step b). EXSY experiments showed that at 300 K addition of just one equiv. of pyridine led to a 200-fold increase in the rate of macrocycle shuttling in [(**L4**)Pd] to 1 s^{-1}, corresponding to a bimolecular rate constant k_{bi} = 95 M^{-1} s^{-1}. In other words, a molecule of pyridine is ~500x more effective at accelerating the shuttling rate in [(**L4**)Pd] than a molecule of DMF.[18] Subsequently neutralizing the added pyridine with one equivalent of TsOH (Scheme 3.2, step c) returned the shuttling rate to its original value in $CDCl_3$, providing powerful and reversible control over the macrocycle dynamics by reagent addition.

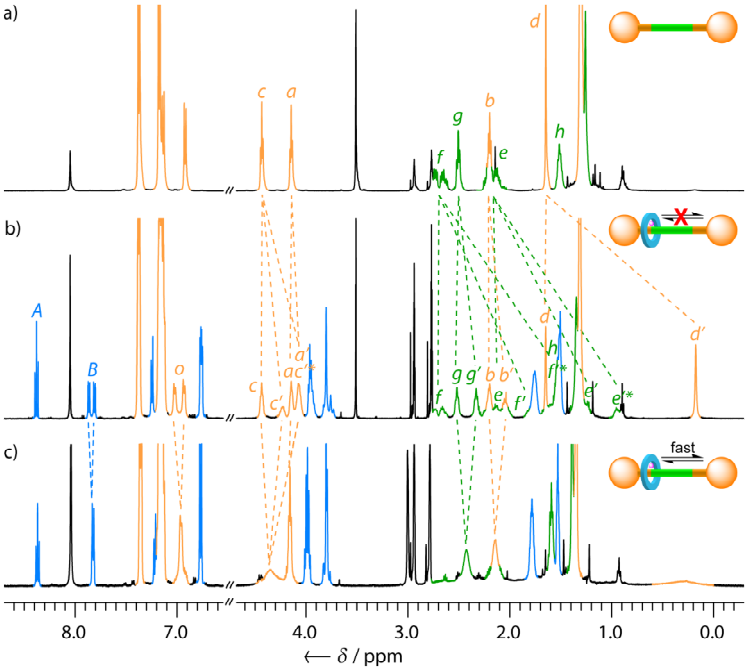

Figure 3.3. Partial ^{1}H NMR (500 MHz, [D_7]DMF) spectra of a) the free thread at 298 K; b) molecular shuttle [(**L4**)Pd] at 298 K; and c) molecular shuttle [(**L4**)Pd] at 390 K. The assignments correspond to the lettering shown in Scheme 3.2. Signals labeled * are parts of sets of diastereotopic protons.

3.3 Conclusions

The Pd(II)-catalyzed Michael addition of α-cyano esters to vinyl ketones provides an exceptionally high yielding multi-component active metal template reaction in which the template motif is retained in the rotaxane product. The reaction is operationally

simple to perform and can generate [2]rotaxanes in essentially quantitative yields with only a modest excess of the thread-forming components. The reaction can be applied to the construction of metal-complexed molecular shuttles in which the dynamics of the shuttling can be controlled by the addition of external reagents. The search for other active template reactions that offer different or improved rotaxane design features compared to existing strategies is ongoing in our laboratory.

3.4 Experimental Section

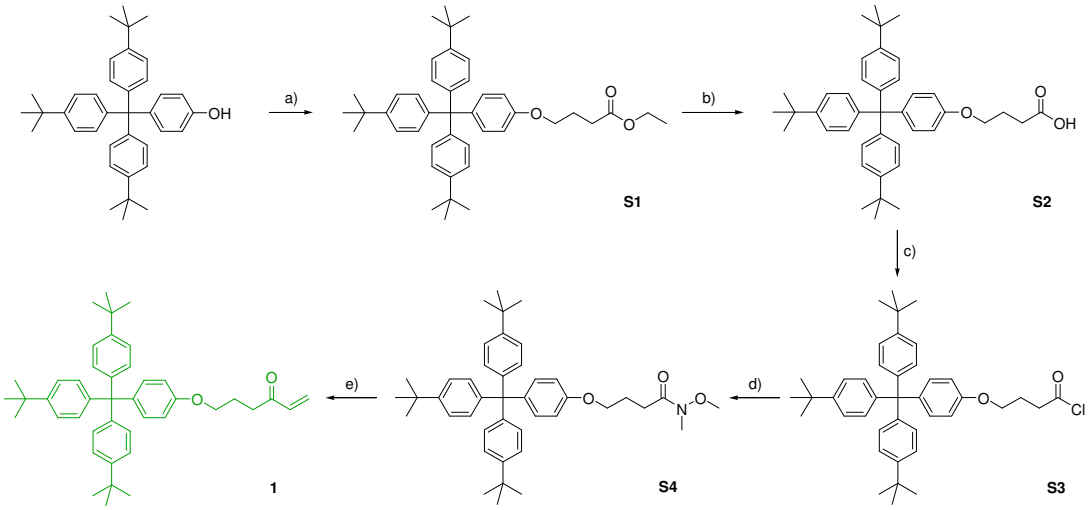

Scheme 3.3. Synthesis of vinyl ketone functionalized "stopper" **1** from 4-[tris(4-*tert*-butylphenyl)methyl]-phenol. Reagents and conditions: a) ethyl 4-bromobutyrate, K_2CO_3, butanone, reflux, 94%; b) LiOH, THF, H_2O, 85%; c) $(COCl)_2$, CH_2Cl_2, DMF (cat.), 96%; d) *N,O*-dimethylhydroxylamine hydrochloride, Et_3N, THF, 0 °C, 95%; e) vinyl magnesium bromide, THF, -78 °C, 92%.

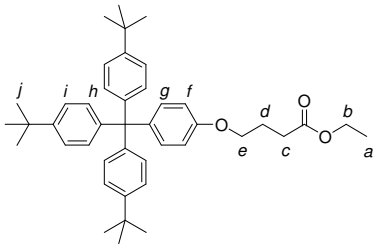

Ethyl 4-(4-(tris(4-*tert*-butylphenyl)methyl)phenoxy)butanoate, S1

To a stirred solution of 4-[tris(4-*tert*-butylphenyl)methyl]-phenol (2.10 g, 4.1 mmol) and ethyl 4-bromobutyrate (0.90 ml, 6.2 mmol) in butanone (50 ml) was added

K_2CO_3 (5.70 g, 41 mmol). The suspension was heated at reflux for 18 h. The solvent was removed under reduced pressure and the residue was redissolved in CH_2Cl_2 (200 ml), washed with H_2O (3 × 100 ml), dried ($MgSO_4$) and concentrated under reduced pressure. The crude residue was purified by column chromatography (CH_2Cl_2:petroleum ether 1:1) to yield the title compound as a colorless powder (2.40 g, 94%). m.p. 212 °C; ^{1}H NMR (400 MHz, $CDCl_3$, 300 K): δ = 1.26 (t, J = 7.1 Hz, 3H, H_a), 1.30 (s, 27H, H_j), 2.09 (m, 2H, H_d), 2.51 (t, J = 7.3 Hz, 2H, H_c), 3.98 (t, J = 6.1 Hz, 2H, H_e), 4.14 (q, J = 7.1 Hz, 2H, H_b), 6.75 (d, J = 8.9 Hz, 2H, H_f), 7.08 (d, J = 8.6 Hz, 8H, H_{g+h}), 7.23 (d, J = 8.6 Hz, 6H, H_i); ^{13}C NMR (100 MHz, $CDCl_3$, 300 K): δ = 14.2, 24.7, 30.9, 31.4, 34.3, 60.4, 63.0, 66.5, 112.9, 124.0, 130.7, 132.2, 139.6, 144.1, 148.3, 156.6, 173.3; LRFAB-MS (3-NOBA matrix): m/z = 618 $[M]^+$; HRFAB-MS (Glycerol matrix): m/z = 618.4096 (calcd. for $C_{43}H_{54}O_3$, 618.4073).

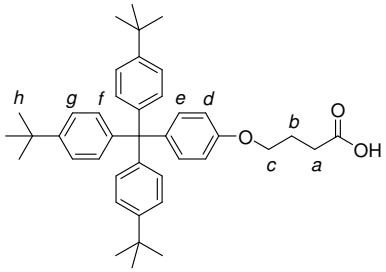

4-(4-(Tris(4-*tert*-butylphenyl)methyl)phenoxy)butanoic acid, S2

A solution of ester **S1** (3.75 g, 6.06 mmol) and LiOH (1.02 g, 24.2 mmol) in THF (45 ml) and H_2O (15 ml) was stirred until **S1** had been consumed, as evidenced by TLC (EtOAc). The reaction mixture was diluted with CH_2Cl_2 (100 ml), washed with 1 M HCl (50 ml), a saturated aqueous solution of $NaHCO_3$ (50 ml) and brine (50 ml). The organic layer was dried ($MgSO_4$), and concentrated under reduced pressure to yield the title compound as a colorless solid (3.03 g, 85%). The product was used without further purification. m.p. 272 °C; ^{1}H NMR (400 MHz, $CDCl_3$, 300 K): δ = 1.30 (s, 27H, H_h), 2.11 (m, 2H, H_b), 2.58 (t, J = 7.3 Hz, 2H, H_a), 4.00 (t, J = 6.0 Hz, 2H, H_c), 6.75 (d, J = 8.75 Hz, 2H, H_d), 7.08 (d, J = 8.7 Hz, 8H, H_{e+f}), 7.23 (d, J = 8.7 Hz, 6H, H_g); ^{13}C NMR (100 MHz, $CDCl_3$, 300 K): δ = 24.4, 30.3, 31.4, 34.3, 63.0, 66.3, 112.9, 124.0, 130.7, 132.3, 139.7, 144.1, 148.3, 156.5, 177.8; LRFAB-MS (3-NOBA

matrix): *m/z* = 590 $[M]^+$; HRFAB-MS (3-NOBA matrix): *m/z* = 590.3752 (calcd. for $C_{41}H_{50}O_3$, 590.3760).

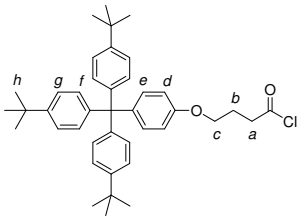

4-(4-(Tris(4-*tert*-butylphenyl)methyl)phenoxy)butanoyl chloride, S3

To a solution of acid **S2** (3.4 g, 5.7 mmol) in CH_2Cl_2 (60 ml) was added dropwise $(COCl)_2$ (2.9 ml, 29 mmol) and DMF (0.1 ml). The solution was stirred for 5 h at which time the solvent was removed under reduced pressure. The crude residue was redissolved in boiling hexane and filtered whilst hot. The filtrate was concentrated under reduced pressure to yield the title compound as a colorless solid (3.30 g, 96%). m.p. 254 °C; ^{1}H NMR (400 MHz, $CDCl_3$, 300 K): δ = 1.30 (s, 27H, H_h), 2.16 (m, 2H, H_b), 3.14 (t, *J* = 7.1 Hz, 2H, H_a), 3.98 (t, *J* = 5.8 Hz, 2H, H_c), 6.74 (d, *J* = 8.9 Hz, 2H, H_d), 7.07 (d, *J* = 8.6 Hz, 6H, H_f), 7.09 (d, *J* = 8.9 Hz, 2H, H_e), 7.23 (d, *J* = 8.6 Hz, 6H, H_g); ^{13}C NMR (100 MHz, $CDCl_3$, 300 K): δ = 24.5, 30.3, 31.4, 34.3, 63.0, 66.3, 112.9, 124.0, 130.7, 132.2, 139.8, 144.1, 148.3, 156.5, 177.6; LRFAB-MS (3-NOBA matrix): *m/z* = 608 $[M]^+$; HRFAB-MS (3-NOBA matrix): *m/z* = 608.3420 (calcd. for $C_{41}H_{49}{}^{35}ClO_2$, 608. 3421).

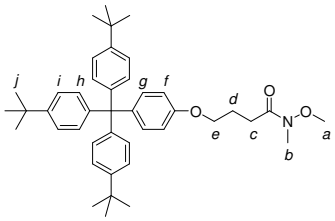

***N*-Methoxy-*N*-methyl-4-(4-(tris(4-*tert*-butylphenyl)methyl)phenoxy)butanamide, S4**

To a solution of *N*,*O*-dimethyl hydroxylamine (0.58 g, 5.9 mmol) and Et_3N (1.7 ml, 12 mmol) in CH_2Cl_2 (60 ml) at 0 °C was added dropwise a solution of acid chloride **S3** (3.3 g, 5.4 mmol) in CH_2Cl_2 (10 ml). The solution was allowed to warm to RT and stirred for 18 h. The reaction mixture was diluted with CH_2Cl_2 (200 ml) and

washed with 1M HCl (100 ml), saturated aqueous $NaHCO_3$ (100 ml) and brine (100 ml). The organic layer was dried ($MgSO_4$) and concentrated under reduced pressure. The residue was purified by column chromatography (CH_2Cl_2) to yield the title compound as a colorless solid (3.27 g, 95%). m.p. 218 °C; ^{1}H NMR (400 MHz, $CDCl_3$, 300 K): δ = 1.30 (s, 27H, H_j), 2.11 (m, 2H, H_d), 2.65 (t, J = 7.0 Hz, 2H, H_c), 3.19 (s, 3H, H_b), 3.67 (s, 3H, H_a), 4.01 (t, J = 6.0 Hz, 2H, H_e), 6.77 (d, J = 8.9 Hz, 2H, H_f), 7.09 (d, J = 8.6 Hz, 8H, H_{g+h}), 7.23 (d, J = 8.6 Hz, 6H, H_i); ^{13}C NMR (100 MHz, $CDCl_3$, 300 K): δ = 24.2, 28.3, 31.4, 32.2, 34.3, 61.2, 63.0, 66.8, 112.9, 124.0, 130.7, 132.2, 139.5, 144.2, 148.3, 156.7, 174.0; LREI-MS: m/z = 634 $[MH]^+$; HRFAB-MS (3-NOBA matrix): m/z = 634.4260 (calcd. for $C_{43}H_{56}NO_3$, 634.4260).

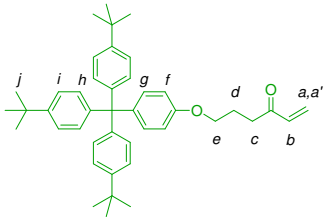

6-(4-(Tris(4-*tert*-butylphenyl)methyl)phenoxy)hex-1-en-3-one, 1

To a solution of Weinreb amide **S4** (1.33 g, 2.1 mmol) in THF (20 ml) at -78 °C was added dropwise vinyl magnesium bromide (1 M in THF, 5.2 mmol, 5.2 ml). The solution was stirred at -78 °C for 30 min, and then allowed to warm to 0 °C for 2 h. The reaction was quenched with a cold solution of saturated aqueous NH_4Cl (50 ml), extracted with CH_2Cl_2 (4 × 50 ml), the combined organic layers were washed with brine (50 ml), dried ($MgSO_4$) and concentrated under reduced pressure. The residue was purified by column chromatography (CH_2Cl_2:petrol 1:1) to yield the title compound as colorless solid (1.13 g, 92%) which was stored under an atmosphere of N_2 in a freezer. m.p. 208 °C; ^{1}H NMR (400 MHz, $CDCl_3$, 300 K): δ = 1.30 (s, 27H, H_j), 2.10 (m, 2H, H_d), 2.82 (t, J = 7.1 Hz, 2H, H_c), 3.98 (t, J = 5.9 Hz, 2H, H_e), 5.84 (d, J = 10.5 Hz, 1H, H_b), 6.25 (d, J = 17.3 Hz, 1H, $H_{a'}$), 6.37 (dd, J = 10.5 Hz, 17.3 Hz, 1H, H_a), 6.75 (d, J = 8.8 Hz, 2H, H_f), 7.08 (d, J = 8.6 Hz, 8H, H_{g+h}), 7.23 (d, J = 8.6 Hz, 6H, H_i); ^{13}C NMR (100 MHz, $CDCl_3$, 300 K): δ = 23.5, 31.4, 34.3, 35.9, 63.0, 66.6, 112.9, 124.0, 128.2, 130.7, 132.3, 136.6, 139.6, 144.1, 148.3, 156.6, 200.2;

LRFAB-MS (3-NOBA matrix): *m/z* = 600 $[M]^+$; HRFAB-MS (3-NOBA matrix): *m/z* = 600.3966 (calcd. for $C_{43}H_{52}O_2$, 600.3967).

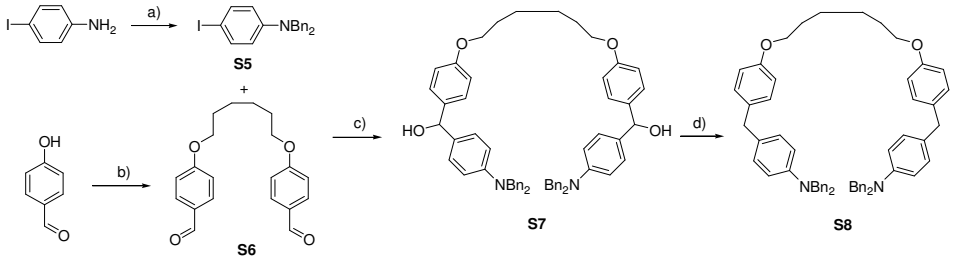

Scheme 3.4. Synthesis of benzyl protected macrocycle precursor **S8** from iodoaniline and 4-hydroxybenzaldehyde. Reagents and conditions: a) BnBr, K_2CO_3, KI, DMF, 97%; b) 1,6-dibromohexane, K_2CO_3, butanone, reflux, 66%; c) i) **S5**, *n*-BuLi, THF, -78 °C, ii) **S6**, THF, -78 °C; d) $NaBH_4$, TFA, CH_2Cl_2, 46% (over 2 steps).

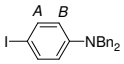

N,*N*-Dibenzyl-4-iodoaniline, S5

To a vigorously stirred solution of 4-iodoaniline (16.1 g, 73.4 mmol), BnBr (18.3 ml, 154 mmol) and KI (2.40 g, 14.7 mmol) in DMF (75 ml) was added K_2CO_3 (24.4 g, 176 mmol). The reaction was stirred for 18 h. CH_2Cl_2 (200 ml) was added and the reaction mixture was washed with H_2O (100 ml), the organic layer was dried ($MgSO_4$) and concentrated under reduced pressure. The crude residue was recrystallized from EtOH (1 L) to yield the title compound as colorless needles (25.5 g, 97%). m.p. 122 °C; ^{1}H NMR (400 MHz, $CDCl_3$, 300 K): δ = 4.54 (s, 4H, $H_{benzylic}$), 6.41 (d, J = 9.1 Hz, 2H, H_A), 7.21 (m, 12H, $H_{B+phenyl}$); ^{13}C NMR (100 MHz, $CDCl_3$, 300 K): δ = 54.2, 77.6, 114.7, 126.4, 127.1, 128.8, 137.7, 137.9, 148.6; LRFAB-MS (3-NOBA matrix): *m/z* = 399 $[M]^+$; HRFAB-MS (3-NOBA matrix): *m/z* = 399.0502 (calcd. for $C_{20}H_{18}IN$, 399.0484).

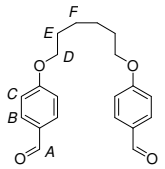

4,4'-Hexanediyldioxy dibenzaldehyde, S6

To a solution of 1,6-dibromohexane (4.4 ml, 29 mmol) and 4-hydroxybenzaldehyde (10.5 g, 85.9 mmol) in butanone (300 ml) was added K_2CO_3 (39.5 g, 286 mmol). The suspension was heated at reflux for 18 h. The solvent was removed under reduced pressure and the crude residue was redissolved in CH_2Cl_2 (500 ml) and washed with H_2O (200 ml). The organic layer was dried ($MgSO_4$) and concentrated under reduced pressure. The crude residue was dissolved in hot MeOH and allowed to cool to RT, the resultant precipitate was collected by suction filtration to yield the title compound as a colorless powder (6.11 g, 66%). m.p. 81-83 °C; ^{1}H NMR (400 MHz, $CDCl_3$, 300 K): δ = 1.57 (m, 4H, H_F), 1.87 (m, 4H, H_E), 4.06 (t, J = 6.4 Hz, 4H, H_D), 6.99 (d, J = 8.8 Hz, 4H, H_C), 7.83 (d, J = 8.8 Hz, 4H, H_B), 9.88 (s, 2H, H_A); ^{13}C NMR (100 MHz, $CDCl_3$, 300 K): δ = 25.8. 29.0, 68.0, 114.7, 129.8, 132.0, 164.1, 190.8; LRFAB-MS (3-NOBA matrix): *m/z* = 327 $[MH]^+$; HRFAB-MS (3-NOBA matrix): *m/z* = 327.1593 (calcd. for $C_{20}H_{23}O_4$, 327.1596).

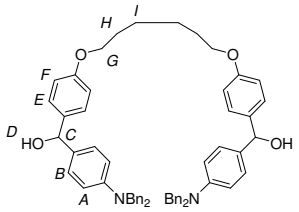

S7

To a solution of iodide **S5** (24.1 g, 60.3 mmol) in THF (200 ml) at -78 °C was added *n*-BuLi (1.6 M in hexane, 36.4 ml, 58.2 mmol) dropwise. The temperature was maintained at -78 °C for 30 min. A solution of aldehyde **S6** (6.55 g, 20.1 mmol) in THF (100 ml) was added dropwise whilst maintaining the temperature at -78 °C. The reaction was allowed to warm to RT over 2 h. The reaction mixture was diluted with CH_2Cl_2 (500 ml) and washed with saturated aqueous NH_4Cl (300 ml) and brine (300 ml). The organic layer was dried ($MgSO_4$) and concentrated under reduced pressure. The product was used without further purification. LRFAB-MS (3-NOBA matrix):

m/z = 872 $[M]^+$; HRFAB-MS (3-NOBA matrix): *m/z* = 872.4553 (calcd. for $C_{60}H_{60}N_2O_4$, 872.4553).

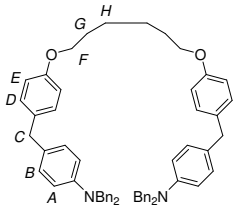

4-(4-(6-(4-(4-(Dibenzylamino)benzyl)phenoxy)hexyloxy)benzyl)-*N*,*N*-dibenzylaniline, S8[19]

To a solution of diol **S7**, obtained from the previous reaction, and TFA (90 ml) in CH_2Cl_2 (120 ml) at 0 ºC was added $NaBH_4$ (7.53 g, 199 mmol) portion-wise. The reaction was stirred for 18 h. The reaction was diluted with CH_2Cl_2 (1 L) and neutralized with 1 M NaOH (1.5 L). The organic layer was washed with brine (500 ml), dried ($MgSO_4$) and concentrated under reduced pressure. The residue was purified by column chromatography (petrol:CH_2Cl_2 3:2) to yield the title compound as a colorless solid (7.82 g, 46% from **S6**). m.p. 105 °C; ^{1}H NMR (400 MHz, $CDCl_3$, 300 K): δ = 1.56 (m, 4H, H_H), 1.83 (m, 4H, H_G), 3.84 (s, 4H, H_C), 3.97 (t, *J* = 6.5 Hz, 4H, H_F), 4.66 (s, 8H, H_{benzyl}), 6.70 (d, *J* = 8.7 Hz, 4H, H_A), 6.84 (d, *J* = 8.6 Hz, 4H, H_E), 7.01 (d, *J* = 8.7 Hz, 4H, H_B), 7.13 (d, *J* = 8.6 Hz, 4H, H_D), 7.33 (m, 20H, H_{phenyl}); ^{13}C NMR (100 MHz, $CDCl_3$, 300 K): δ = 25.9, 29.3, 40.0, 54.3, 67.8, 112.5, 114.5, 126.8, 127.0, 128.3, 129.2, 129.8, 131.3, 138.8, 133.9, 147.5, 157.3; LRFAB-MS (3-NOBA matrix): *m/z* = 841 $[MH]^+$; HRFAB-MS (3-NOBA matrix): *m/z* = 841.4710 (calcd. for $C_{60}H_{61}N_2O_2$, 841.4733).

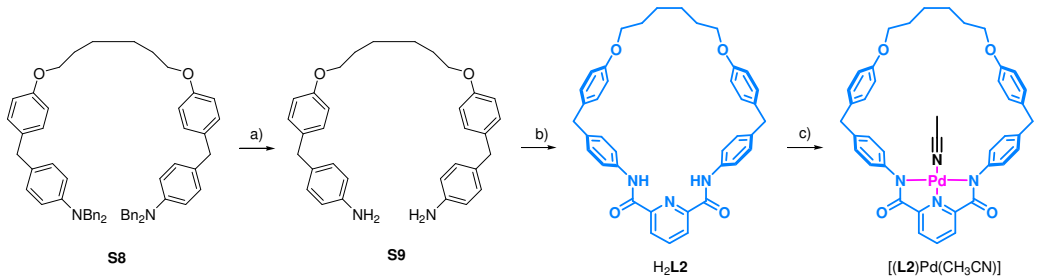

Scheme 3.5. Synthesis of Pd(II) macrocycle complex [(**L2**)Pd(CH_3CN)] from **S8**. Reagents and conditions: a) Pd/C (10% w/w), H_2, THF, EtOH, 78%; b) pyridine-2,6-dicarbonyl dichloride, Et_3N, THF, 30%; b) $Pd(OAc)_2$, CH_3CN, reflux then RT, 88%.

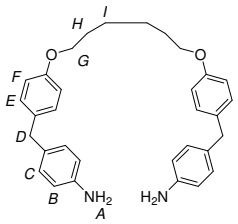

4-(4-(6-(4-(4-Aminobenzyl)phenoxy)hexyloxy)benzyl)aniline, S9

To a solution of benzyl aniline **S8** (7.82 g, 9.30 mmol) in THF (80 ml) and EtOH (20 ml) was added 10% w/w Pd/C (1.56 g). The reaction mixture was initially purged with an atmosphere of N_2 and then purged with H_2 before being stirred for 18 h under an atmosphere of H_2. The reaction mixture was filtered through celite, concentrated under reduced pressure and purified by column chromatography (CH_2Cl_2:MeOH 99.5:0.5) to give the title compound as a colorless solid (3.48 g, 78%). m.p. 120 °C; ^{1}H NMR (400 MHz, $CDCl_3$, 300 K): δ = 1.53 (m, 4H, H_I), 1.80 (m, 4H, H_J), 3.56 (br, 4H, H_A), 3.82 (s, 4H, H_D), 3.94 (t, J = 6.4 Hz, 4H, H_G), 6.63 (d, J = 8.3 Hz, 4H, H_B), 6.82 (d, J = 8.5 Hz, 4H, H_F), 6.98 (d, J = 8.3 Hz, 4H, H_C), 7.08 (d, J = 8.5 Hz, 4H, H_E); ^{13}C NMR (100 MHz, $CDCl_3$, 300 K): δ = 25.9, 29.3, 40.2, 67.8, 114.4, 115.3, 129.6, 129.7, 131.7, 133.9, 144.4, 157.3; LRFAB-MS (3-NOBA matrix): m/z = 480 [M]; HRFAB-MS (3-NOBA matrix): m/z = 480.2765 (calcd. for $C_{32}H_{36}N_2O_2$, 480.2777).

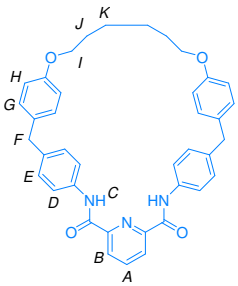

H_2**L2**

To a solution of aniline **S9** (3.363 g, 7.00 mmol) and Et_3N (2.9 ml, 21.0 mmol) in THF (4 L) was added, in one portion, pyridine-2,6-dicarbonyl dichloride (1.429 g, 7.00 mmol), the reaction was stirred for 18 h. The reaction mixture was filtered, concentrated under reduced pressure, and purified first by column chromatography (CH_2Cl_2:MeOH; 99.5:0.5) then recrystallized from acetonitrile (50 ml) to yield the

title compound as colorless powder (1.28 g, 30%). m.p. 325 °C (dec.); ^{1}H NMR (400 MHz, $CDCl_3$, 300 K): δ = 1.52 (m, 4H, H_K), 1.82 (m, 4H, H_J), 3.94 (s, 4H, H_F), 3.97 (t, J = 6.3 Hz, 4H, H_I), 6.83 (d, J = 8.6 Hz, 4H, H_H), 7.07 (d, J = 8.5 Hz, 4H, H_E), 7.08 (d, J = 8.6 Hz, 4H, H_G), 7.55 (d, J = 8.5 Hz, 4H, H_D), 8.15 (t, J = 7.8 Hz, 1H, H_A), 8.44 (d, J = 7.8 Hz, 2H, H_B), 9.52 (s, 2H, H_C); ^{13}C NMR (100 MHz, $CDCl_3$, 300 K): δ = 25.4, 29.1, 40.0, 67.8, 114.7, 119.5, 125.1, 129.3, 130.4, 132.7, 134.8, 139.2, 140.0, 148.7, 157.7, 160.5; LRFAB-MS (3-NOBA matrix): m/z = 612 $[MH]^+$; HRFAB-MS (3-NOBA matrix): m/z = 612.2864 (calcd. for $C_{39}H_{38}N_3O_4$, 612.2862).

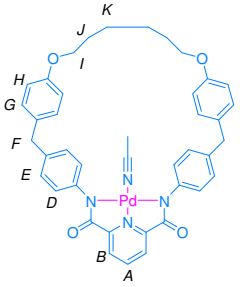

[(**L2**)Pd(CH_3CN)]

A stirred suspension of amide H_2**L2** (1.163 g, 1.90 mmol) and $Pd(OAc)_2$ (0.470 g, 2.094 mmol) in CH_3CN (50 ml) was heated at reflux for 10 mins then stirred at for 18 h. The resulting suspension was filtered and the precipitate was redissolved in CH_2Cl_2 (50 ml) and filtered through celite. The filtrate was concentrated under reduced pressure to yield the title compound as a yellow solid (1.27 g, 88%). m.p. 310 °C (dec.); ^{1}H NMR (400 MHz, $CDCl_3$:CD_3CN 95:5, 300 K): δ = 1.46 (m, 4H, H_K), 1.75 (m, 4H, H_J), 3.79 (s, 4H, H_F), 3.84 (t, J = 6.2 Hz, 4H, H_I), 6.66 (d, J = 8.6 Hz, 4H, H_H), 6.98 (d, J = 8.6 Hz, 4H, H_G), 7.05 (d, J = 8.3 Hz, 4H, H_E), 7.11 (d, J = 8.3 Hz, 4H, H_D), 7.85 (d, J = 7.8 Hz, 2H, H_B), 8.10 (t, J = 7.8 Hz, 1H, H_A); ^{13}C NMR (100 MHz, $CDCl_3$:CD_3CN 95:5, 300 K): δ = 23.6, 26.8, 38.9, 65.9, 112.3, 123.8, 124.5, 126.7, 127.4, 132.8, 136.5, 139.1, 142.9, 151.1, 155.5, 166.4; LRFAB-MS (3-NOBA matrix): m/z = 756 [M]; HRFAB-MS (3-NOBA matrix): m/z = 756.1922 (calcd. for $C_{41}H_{38}N_4O_4{}^{106}$Pd, 756.1928).

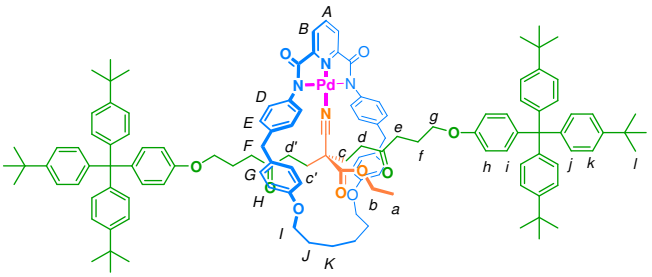

3.4.1 Representative Synthesis of Rotaxane [(L3)Pd]

To a solution of complex [(**L2**)Pd(CH_3CN)] (0.0304 g, 0.0402mmol), ketone **1** (0.1208 g, 0.201 mmol) and ethyl cyano acetate **L1** (10.7 µl, 0.101 mmol) in CH_2Cl_2 (0.4 ml) was added DIPEA (0.698 µl, 0.004 mmol). The solution was stirred for 7 d at 40˚C. The solvent was removed under reduced pressure and the crude residue was purified by column chromatography (CH_2Cl_2 then CH_2Cl_2:MeOH 99:1) to yield rotaxane [**L3**Pd] as a yellow solid (0.081 g, >99%). m.p. 213 °C (dec.); ^{1}H NMR (400 MHz, $CDCl_3$, 323 K): δ = 0.32 (br, 2H, $H_{c'}$), 0.90 (br, 2H, H_c), 1.17 (t, J = 7.1 Hz, 3H, H_a), 1.25 (br, 2H, $H_{d'}$), 1.31 (s, 54H, H_l), 1.44 (br, 4H, H_K), 1.49 (br, 2H, $H_{d'}$), 1.73 (br, 4H, H_J), 2.02 (br, 4H, H_f), 2.36 (br, 4H, H_e), 3.75 (s, 4H, H_F), 3.87 (m, J = 7.1 Hz, 2H, H_b), 3.89 (br, 4H, H_I), 4.00 (t, J = 4.0 Hz, 4H, H_g), 6.71 (dd, J = 8.5 Hz, 16.5 Hz, 4H, H_H), 6.81 (d, J = 8.3 Hz, 4H, H_h), 6.99 (dd, J = 8.5 Hz, 22.7 Hz, 4H, H_G), 7.10 (m, 20H, H_{E+i+j}), 7.19 (d, J = 8.2 Hz, 4H, H_D), 7.23 (d, J = 8.6 Hz, 12H, H_k), 7.83 (dd, J = 3.6 Hz, 7.8 Hz, 2H, H_B), 8.05 (t, J = 7.8 Hz, 1H, H_A); ^{13}C NMR (100 MHz, $CDCl_3$, 300 K): δ = 13.8, 25.3, 25.7, 28.9, 29.4, 31.4, 34.3, 40.9, 48.8, 63.0, 63.5, 66.3, 67.9, 68.1, 112.8, 114.7, 121.5, 124.1, 125.8, 126.3, 128.4, 129.4, 130.7, 132.4, 134.3, 138.7, 139.1, 139.9, 141.1, 144.1, 144.6, 148.3, 152.9, 156.5, 157.5, 165.1, 168.6, 206.3; LRFAB-MS (3-NOBA matrix): m/z = 2030 $[MH]^+$; HRFAB-MS (3-NOBA matrix): m/z = 2030.015 (calcd. for $C_{130}H_{147}N_4O_{10}{}^{106}Pd$, 2030.015).

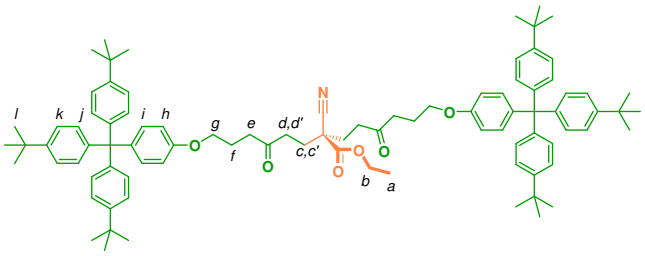

Thread, S10

m.p. 202 °C; ^{1}H NMR (400 MHz, $CDCl_3$, 300 K): δ = 1.32 (s, 57H, H_{a+l}), 2.07 (m, 4H, H_f), 2.13 (ddd, J = 5.1 Hz, 10.3 Hz, 15.8 Hz, 2H, $H_{c'}$), 2.28 (ddd, J = 5.4 Hz, 10.3 Hz, 15.8, 2H, H_c), 2.58 (ddd, J = 5.4 Hz, 10.3 Hz, 17.7 Hz, 2H, $H_{d'}$), 2.66 (t, J = 7.1 Hz, 4H, H_e), 2.74 (ddd, J = 5.1 Hz, 10.3 Hz, 17.7 Hz, 2H, H_d), 3.95 (t, J = 5.9 Hz, 4H, H_g), 4.25 (q, J = 7.1 Hz, 2H, H_b), 6.75 (d, J = 8.9 Hz, 4H, H_h), 7.10 (d, J = 8.7 Hz, 16H, H_{i+j}), 7.24 (d, J = 8.6 Hz, 12H, H_k); ^{13}C NMR (100 MHz, $CDCl_3$, 300 K): δ = 14.1, 22.6, 29.7, 31.4, 34.5, 38.3, 39.3, 48.1, 63.1, 63.2, 66.5, 112.9, 118.5, 124.3, 131.1, 132.6, 139.7, 144.2, 148.3, 156.5, 168.5, 207.3; LRFAB-MS (3-NOBA matrix): m/z = 1314 [M]; HRFAB-MS (3-NOBA matrix): m/z = 1313.846 (calcd. for $C_{91}H_{111}O_6N$, 1313.841).

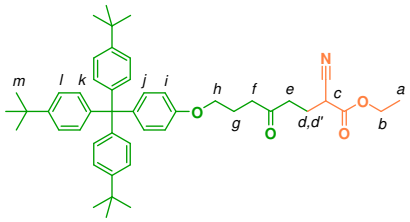

Half thread, S11

m.p. 194 °C; ^{1}H NMR (400 MHz, $CDCl_3$, 300 K): δ = 1.22 (s, 30H, H_{a+m}), 1.98 (m, 2H, H_g), 2.17 (m, 1H, $H_{d'}$), 2.28 (m, 1H, H_d), 2.58 (t, J = 7.1 Hz, 2H, H_f), 2.64 (t, 7.0 Hz, 2H, H_e), 3.62 (dd, J = 6.1 Hz, 8.3 Hz, 1H, H_c), 3.87 (d, J = 5.9 Hz, 2H, H_h), 4.18 (q, J = 7.1 Hz, 2H, H_b), 6.74 (d, J = 8.9 Hz, 2H, H_i), 7.08 (d, J = 8.6 Hz, 8H, H_{j+k}), 7.23 (d, J = 8.6 Hz, 6H, H_l); ^{13}C NMR (100 MHz, $CDCl_3$, 300 K): δ = 14.0, 23.4, 23.5, 31.4, 34.3, 36.4, 38.6, 39.3, 63.0, 63.0, 66.4, 112.9, 116.2, 124.1, 130.7, 132.3, 139.7, 144.1, 148.3, 156.5, 165.7, 208.1; LRFAB-MS (3-NOBA matrix): m/z = 713; HRFAB-MS (3-NOBA matrix): m/z = 713.4442 (calcd. for $C_{48}H_{59}NO_4$, 713.4444).

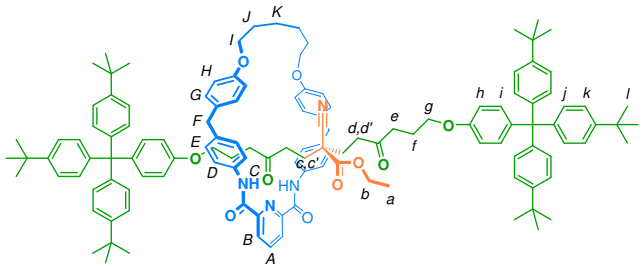

H_2L3

A solution of [(**L3**)Pd] (0.222 g, 0.109 mmol) in CH_2Cl_2 (0.5 ml) and 1M HCl (0.5 ml) was heated at reflux for 18 h. The solution was diluted with CH_2Cl_2 (50 ml) and washed with saturated $NaHCO_3$ (20 ml), brine (20 ml), dried ($MgSO_4$), filtered and concentrated under reduced pressure. The crude residue was purified by column chromatography (CH_2Cl_2:MeOH 99:1) to yield the title compound as a colorless solid (0.194 g, 92%). m.p. 141 ˚C (dec.); ^{1}H NMR (400 MHz, $CDCl_3$, 300 K): δ = 1.13 (t, J = 7.1 Hz, 3H, H_a), 1.30 (s, 56H, $H_{c'+l}$), 1.39 (m, 4H, H_K), 1.71 (m, 6H, H_{J+c}), 1.80 (m, 4H, H_f), 2.00 (m, 2H, $H_{d'}$), 2.06 (m, 2H, H_d), 2.22 (t, J = 7.1 Hz, 4H, H_e), 3.72 (t, J = 5.9 Hz, 4H, H_g), 3.81 (q, J = 4.3 Hz, 6.4 Hz, 4H, H_I), 3.85 (d, J = 4.1 Hz, 4H, H_F), 4.00 (q, J = 7.1 Hz, 2H, H_b), 6.60 (d, J = 8.9 Hz, 4H, H_h), 6.70 (dd, J = 5.3 Hz, 8.5 Hz, 4H, H_H), 7.00 (m, 8H, H_{G+E}), 7.08 (d, J = 8.6 Hz, 16H, H_{i+j}), 7.22 (d, J = 8.6 Hz, 12H, H_k), 7.46 (dd, J = 8.4 Hz, 15.0 Hz, 4H, H_D), 8.07 (t, J = 7.8 Hz, 1H, H_A), 8.43 (d, J = 7.8 Hz, 2H, H_B), 9.89 (d, J = 9.0 Hz, 2H, H_C); ^{13}C NMR (100 MHz, $CDCl_3$, 300 K): δ = 13.9, 23.1, 25.4, 29.1, 30.1, 31.4, 34.3, 37.9, 40.2, 40.4, 47.7, 63.0, 66.3, 67.8, 112.8, 114.7, 118.7, 121.4, 124.1, 125.1, 129.0, 130.1, 130.7, 131.1, 132.3, 133.5, 134.9, 139.3, 139.6, 139.7, 144.1, 148.3, 149.0, 156.4, 157.7, 161.1, 167.7, 207.3; LRFAB-MS (3-NOBA matrix): m/z = 1926 $[MH]^+$; HRFAB-MS (3-NOBA matrix): m/z = 1926.121 (calcd. for $C_{130}H_{149}N_4O_{10}$, 1926.127).

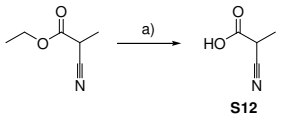

S12

Scheme 3.6. Synthesis of 2-cyanopropanoic acid, **S12**, from ethyl 2-cyanopropionate. Reagents and conditions: a) LiOH, MeOH, H_2O, 89%.

2-Cyanopropanoic acid, S12

To a solution of ethyl 2-cyanopropionate (0.749 g, 5.89 mmol) in MeOH (10 ml) and water (10 ml) was added LiOH (1.24 g, 29.5 mmol). The suspension was stirred for 36 h. The reaction mixture was acidified with 1M HCl (100 ml), saturated with NaCl, the crude product was then extracted with Et_2O (3 x 100 ml), dried ($MgSO_4$) and concentrated under reduced pressure to yield acid **S12** as a colorless liquid (0.521 g, 89%). ^{1}H NMR and ^{13}C NMR data were consistent with the published data.[20]

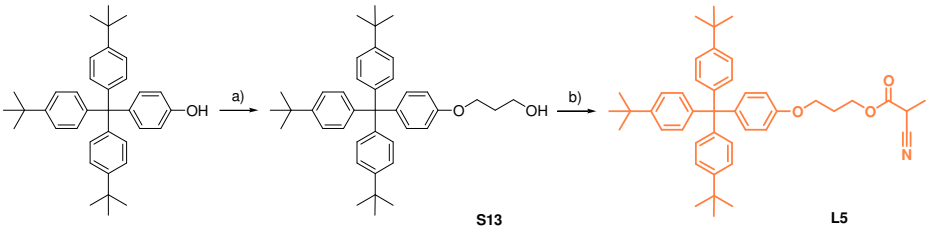

Scheme 3.7. Synthesis of nitrile **L5** from 4-[tris(4-*tert*-butylphenyl)methyl]-phenol. Reagents and conditions: a) 3-bromopropan-1-ol, K_2CO_3, butanone, reflux, 87%; b) **S12**, EDCI, DMAP, CH_2Cl_2, 0 °C → RT, 79%.

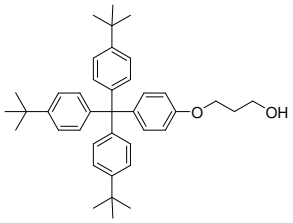

3-(4-(Tris(4-*tert*-butylphenyl)methyl)phenoxy)propan-1-ol, S13

To a solution of 4-[tris(4-*tert*-butylphenyl)methyl]-phenol (2.06 g, 4.08 mmol) and 3-bromopropan-1-ol (0.540 ml, 6.12 mmol) in butanone (40 ml) was added K_2CO_3 (2.82 g, 20.4 mmol), the suspension was heated at reflux for 36 h. The suspension was diluted with CH_2Cl_2 (100 ml) and washed with H_2O (100 ml), the aqueous layer was further extracted with CH_2Cl_2 (100 ml), the combined organic layers were dried ($MgSO_4$), and concentrated under reduced pressure. The crude residue was purified by column chromatography (CH_2Cl_2) to yield the title compound as a colorless

powder (2.00 g, 87%). ^{1}H NMR and ^{13}C NMR data were consistent with the published data.[1e]

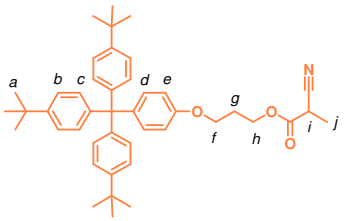

3-(4-(Tris(4-*tert*-butylphenyl)methyl)phenoxy)propyl 2-cyanopropanoate, L5

To a 0 ˚C solution of alcohol **S13** (0.938 g, 1.67 mmol) and 2-cyanopropanoic acid **S12** (0.206 g, 2.08 mmol) in CH_2Cl_2 (20 ml) was added DMAP (0.102 g, 0.835 mmol) and EDCI (0.640 g, 3.34 mmol). The solution was stirred for 18 h. The reaction was diluted with CH_2Cl_2 (100 ml) and washed with 1M HCl (50 ml), $NaHCO_3$ (50 ml) and brine (50 ml). The organic layer was dried ($MgSO_4$), filtered, concentrated under reduced pressure and purified by column chromatography (CH_2Cl_2) to yield the title compound as colorless solid (0.855 g, 79%). m.p. 224 ˚C; ^{1}H NMR (400 MHz, $CDCl_3$, 300 K): δ = 1.30 (s, 27H, H_a), 1.59 (d, J = 7.4 Hz, 3H, H_j), 2.16 (m, 2H, H_g), 3.55 (q, J = 7.4 Hz, 1H, H_i), 4.04 (t, J = 5.9 Hz, 2H, H_f), 4.41 (t, J = 6.3 Hz, 2H, H_h), 6.76 (d, J = 8.9 Hz, 2H, H_e), 7.08 (d, J = 8.9 Hz, 12H, H_c), 7.09 (d, J = 8.6 Hz, 2H, H_d), 7.23 (d, J = 8.6 Hz, 12H, H_b); ^{13}C NMR (100 MHz, $CDCl_3$, 300 K): δ = 15.3, 28.4, 31.4, 31.5, 34.3, 63.0, 63.6, 63.8, 112.9, 117.5, 124.1, 130.7, 132.3, 139.9, 144.1, 148.3, 156.4, 166.5; LRFAB-MS (3-NOBA matrix): *m/z* = 643 [M]; HRFAB-MS (3-NOBA matrix): *m/z* = 643.4070 (calcd. for $C_{44}H_{53}NO_3$, 643.4025).

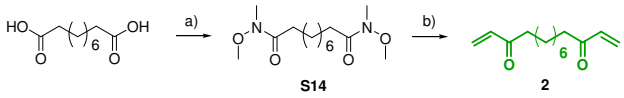

Scheme 3.8. Synthesis of *bis*-vinyl ketone **2** from sebacic acid. Reagents and conditions: a) i) $(COCl)_2$, CH_2Cl_2, DMF (cat.), ii) *N,O*-dimethyl hydroxylamine hydrochloride, Et_3N, CH_2Cl_2, 0 ˚C, 95%; b) vinyl magnesium bromide, THF, -78 ˚C, 75%.

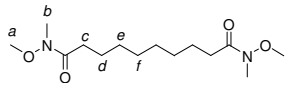

_N_-Methoxy-11-(methoxy(methyl)amino)-_N_-methyl-10-oxoundecanamide, S14

To a suspension of sebacic acid (5.20 g, 25.7 mmol) in CH_2Cl_2 (250 ml) and DMF (0.1 ml) was added dropwise $(COCl)_2$ (22.1 ml, 257 mmol). The suspension was stirred for 16 h. The resulting solution was concentrated under reduced pressure and the residue was redissolved in CH_2Cl_2 (20 ml) and added slowly to a 0 ˚C solution of *N*,*O*-dimethyl hydroxylamine hydrochloride (5.52 g, 56.54 mmol) and Et_3N (14.4 ml, 102 mmol) in CH_2Cl_2 (250 ml). After the addition was complete the reaction was allowed to warm to RT and stirred for 2 h. The reaction was diluted with Et_2O (1 L) and washed with 1M HCl (500 ml), saturated aqueous $NaHCO_3$ (500 ml) and brine (500 ml) before being dried ($MgSO_4$) and concentrated under reduced pressure to give the title compound as a pale oil (7.08 g, 95%). The product was used without further purification. ^{1}H NMR (400 MHz, $CDCl_3$, 300 K): δ = 1.30 (br, 8H, H_{e+f}), 1.60 (m, 4H, H_d), 2.38 (t, J = 7.5 Hz, 4H, H_c), 3.16 (s, 6H, H_b), 3.66 (s, 6H, H_a); ^{13}C NMR (100 MHz, $CDCl_3$, 300 K): δ = 24.6, 24.8, 29.2, 29.4, 32.1, 61.2, 174.8; LRFAB-MS (3-NOBA matrix): *m/z* = 289 $[MH]^+$; HREI-MS (perfluorotributylamine): *m/z* = 288.2043 (calcd. for $C_{14}H_{28}N_2O_4$, 288.2044).

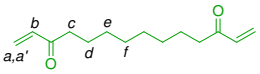

Tetradeca-1,13-diene-3,12-dione, 2

To a solution of Weinreb amide **S14** (6.87 g, 23.8 mmol) in THF (200 ml) at -78 ˚C was added dropwise a 1M solution of vinyl magnesium bromide in THF (119 ml, 119 mmol). The reaction was stirred at -78 ˚C for 30 min, then allowed to warm to 0 ˚C and stirred for 1 h. The reaction was poured into cold saturated NH_4Cl (500 ml) and extracted with Et_2O (2 x 1 L). The combined organic extracts were washed with brine (500 ml), dried ($MgSO_4$) and concentrated under reduced pressure. The crude residue was purified by column chromatography (Et_2O:petrol 1:1) to yield the title compound as a waxy pale solid (3.99 g, 75%). m.p. 60 ˚C (dec.); ^{1}H NMR (400 MHz, $CDCl_3$, 300 K): δ = 1.30 (br, 8H, H_{e+f}), 1.60 (m, 4H, H_d), 2.57 (t, J = 7.4 Hz, 4H, H_c), 5.81 (dd, J = 1.2, 10.5 Hz, 2H, H_b), 6.21 (dd, J = 1.2, 17.7 Hz, 2H, H_a), 6.35 (dd, J =

10.5, 17.7 Hz, 2H, $H_{a'}$); ^{13}C NMR (100 MHz, $CDCl_3$, 300 K): δ = 23.9, 29.2, 29.2, 39.6, 127.9, 136.6, 201.2; LRFAB-MS (3-NOBA matrix): *m/z* = 223 $[MH]^+$; HREI-MS (perfluorotributylamine): *m/z* = 222.1617 (calcd. for $C_{14}H_{22}O_2$, 222.1614).

3.4.2 Synthesis of Molecular Shuttle [(L4)Pd]

To a solution of complex [(**L2**)Pd(CH_3CN)] (0.0305 g, 0.040 mmol), nitrile **L5** (0.0519 g, 0.081 mmol) and vinyl ketone **2** (0.0089 g, 0.040 mmol) in CH_2Cl_2 (0.4 ml) was added DIPEA (0.7 µl, 0.004 mmol). The reaction was stirred at 40 °C for 7 days. The solvent was removed under reduced pressure and the crude residue was purified by column chromatography (CH_2Cl_2 then CH_2Cl_2:MeOH 99:1) to yield rotaxane [(**L4**)Pd] as a yellow solid (0.024 g, 27 %) and [3]rotaxane [(**L6**)Pd] as a yellows solid (0.018 g, 32%).

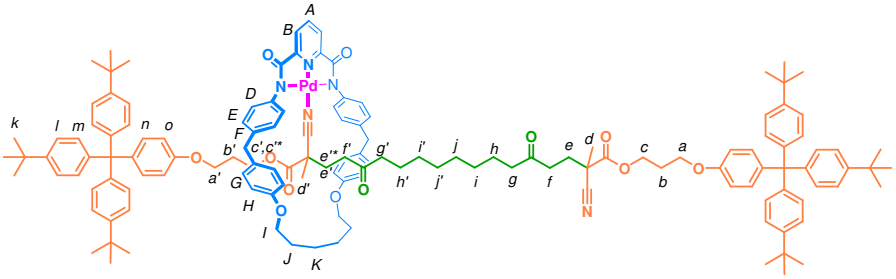

[(**L4**)Pd]**:** ^{1}H NMR (400 MHz, $CDCl_3$, 300 K): δ = 0.00 (s, 3H, $H_{d'}$), 0.94 (m, 1H, $H_{e'*}$), 1.07 (m, 1H, $H_{e'}$), 1.30 (br, 64H, $H_{f+i+i'+j+j'+k}$), 1.45 (br, 4H, H_K), 1.52 (m, 4H, H_h), 1.59 (s, 3H, H_d), 1.74 (br, 4H, H_J), 2.01 (m, 2H, $H_{b'}$), 2.12 (m, 2H, $H_{b'}$), 2.17 (m, 2H, H_b), 2.19 (m, 2H, H_e), 2.40 (t, *J* = 7.4 Hz, 2H, H_g), 2.59 (m, 2H, H_f), 3.72 (m, 4H, H_F), 3.85 (m, 4H, H_I), 3.98 (m, 3H, $H_{a'+c'*}$), 4.04 (t, *J* = 5.9 Hz, 2H, H_a), 4.15 (m, 1H, $H_{c'}$), 4.40 (m, 2H, H_c), 6.64 (m, 4H, H_H), 6.76 (d, *J* = 8.9 Hz, 2H, $H_{o'}$), 6.82 (d, *J* = 8.9 Hz, 2H, H_o), 7.00 (m, 6H, $H_{n,\ G'}$), 7.07 (m, 18H, H_{m+E+G}), 7.14 (dd, *J* = 2.2, 8.6 Hz, 4H, H_D), 7.22 (dd, *J* = 2.5, 8.6 Hz, 12H, H_l), 7.84 (d, *J* = 7.8 Hz, 2H, H_B), 8.07 (t, *J* = 7.8 Hz, 1H, H_A); ^{13}C NMR (100 MHz, $CDCl_3$, 300 K): δ = 21.5, 23.5, 23.6, 23.7, 25.2, 25.4, 28.5, 28.9, 29.2, 29.3, 29.4, 29.7, 31.6, 34.3, 36.8, 38.3, 41.3, 42.7, 42.9, 43.2, 43.6, 63.0, 63.3, 63.6, 63.9, 64.1, 67.7, 68.1, 112.8, 112.9, 114.6, 114.8, 119.5, 121.9, 124.1, 124.1, 125.8, 126.2, 126.4, 128.2, 128.4, 128.8, 129.3, 130.7, 130.7, 132.3, 132.4, 134.0, 134.3, 138.8, 138.9, 139.9, 140.3, 141.1, 144.0, 144.1, 144.6,

144.7, 148.3, 148.4, 152.8, 152.9, 156.2, 156.4, 157.7, 157.7, 166.1, 168.6, 168.9, 207.0, 208.2; LRFAB-MS (3-NOBA matrix): *m/z* = 2224 $[M]^+$; HRFAB-MS (3-NOBA matrix): *m/z* = 2224.148 (calcd. for $C_{141}H_{164}O_{12}N_5{}^{105}Pd$, 2224.142).

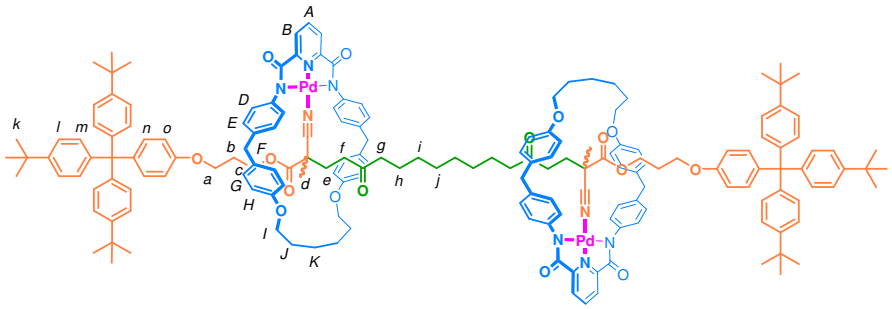

[(**L6**)Pd]**:** m.p. 219 ˚C; ^{1}H NMR (400 MHz, $CDCl_3$, 300 K): δ = 0.00 (s, 6H, H_d), 1.04 (m, 4H, H_e), 1.29 (s, 54H, H_k), 1.38 (m, 10H, $H_{half\ of\ f+i+j}$), 1.46 (m, 8H, H_K), 1.53 (m, 4H, H_h), 1.74 (m, 10H, $H_{half\ of\ f+J}$), 2.01 (m, 4H, H_b), 2.14 (t, *J* = 7.4 Hz, 4H, H_g), 3.73 (m, 8H, H_F), 3.84 (m, 8H, H_I), 3.99 (m, 6H, $H_{half\ of\ c+a}$), 4.16 (m, 2H, $H_{half\ of\ c}$), 6.65 (m, 8H, H_H), 6.82 (d, *J* = 8.9 Hz, 4H, H_o), 7.07 (m, 32H, $H_{m+n+E+G}$), 7.14 (d, *J* = 8.2 Hz, 8H, H_D), 7.22 (d, *J* = 8.6 Hz, 12H, H_l), 7.83 (d, *J* = 7.8 Hz, 4H, H_B), 8.07 (t, *J* = 7.8 Hz, 2H, H_A); ^{13}C NMR (100 MHz, $CDCl_3$, 300 K): δ = 21.5, 23.5, 25.2, 25.2, 28.3, 28.9, 29.5, 31.0, 31.4, 34.3, 36.9, 41.3, 42.7, 43.6, 63.1, 63.3, 64.1, 67.8, 112.8, 114.8, 121.9, 124.1, 125.8, 126.2, 128.4, 129.3, 130.7, 132.4, 134.0, 138.8, 140.3, 141.2, 144.0, 144.6, 148.4, 152.8, 156.2, 157.7, 166.1, 168.6, 207.0; LRFAB-MS (3-NOBA matrix): *m/z* = 2940 $[MH]^+$; HRFAB-MS (3-NOBA matrix): *m/z* = 2944.326 (calcd. for $^{12}C_{176}{}^{13}C_4H_{199}O_{16}N_8{}^{102}Pd{}^{104}Pd$, 2944.326).

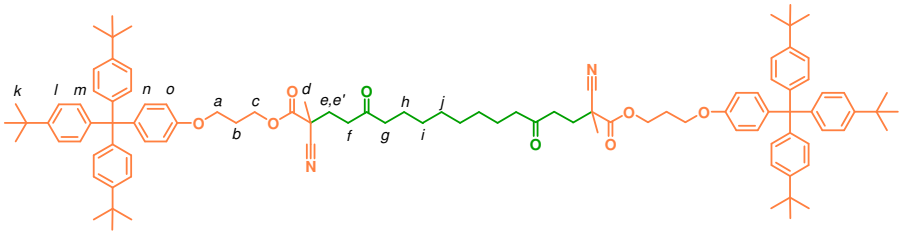

Thread, S15: To a solution of **L5** (0.0554 g, 0.086 mmol), **2** (0.0096 g, 0.043 mmol), benzylic amide Pd-macrocycle[15g] (0.0296 g, 0.043 mmol) in CH_2Cl_2 (0.4 ml) was added DIPEA (7.5 µl, 0.043 mmol). The solution was heated at 40 ˚C for 7 d, the crude residue was concentrated under reduced pressure and purified by column

chromatography (CH_2Cl_2) to yield the title compound as a colorless solid (0.048 g, 74%). ^{1}H NMR (400 MHz, $CDCl_3$, 300 K): δ = 1.26 (br, 8H, H_{i+j}), 1.30 (s, 54H, H_k), 1.54 (m, 4H, H_h), 1.60 (s, 6H, H_d), 2.07 (m, 2H, H_e), 2.17 (m, 4H, H_b), 2.24 (m, 2H, $H_{e'}$), 2.39 (t, J = 7.4 Hz, 4H, H_g), 2.61 (m, 4H, H_f), 4.05 (t, J = 5.9 Hz, 4H, H_a), 4.40 (m, 4H, H_c), 6.76 (d, J = 8.9 Hz, 4H, H_o), 7.09 (m, 16H, H_{m+n}), 7.23 (d, J = 8.6 Hz, 12H, H_l); ^{13}C NMR (100 MHz, $CDCl_3$, 300 K): δ = 23.6, 23.7, 28.5, 29.1, 29.6, 31.2, 31.6, 34.3, 38.2, 42.9, 43.2, 63.0, 63.6, 63.9, 112.9, 119.5, 124.1, 130.7, 132.3, 139.9, 144.1, 148.3, 156.4, 168.9, 208.2. LRFAB-MS (3-NOBA matrix): *m/z* = 1510 $[MH]^+$; HRFAB-MS (3-NOBA matrix): *m/z* = 1509.971 (calcd. for $C_{102}H_{129}O_8N_2$ 1509.975).

3.4.3 Variable Temperature ^{1}H NMR investigation of Degenerate Shuttling Process in [(**L4**)Pd]

Variable temperature ^{1}H NMR experiments allow the estimation of the activation energy for the shuttling process in rotaxane [(**L4**)Pd]. Using a Bruker AVA 600 MHz spectrometer, ^{1}H NMR spectra were taken at 2 K increments from 298 K to 360 K, a stacked plot of ^{1}H NMR obtained at every 10 K from 300 K to 360 K is shown in Figure 3.4. Upon heating the spectra simplified as many of the peaks coalesced, although only a few resonances were usable for interpretation.

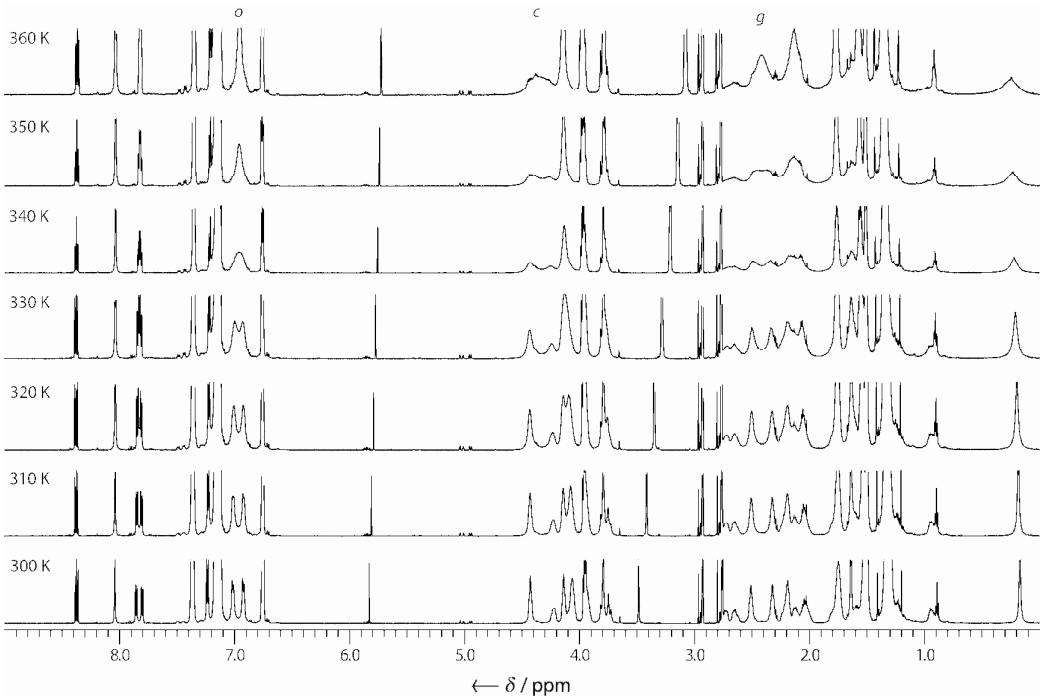

Figure 3.4. ^{1}H NMR (600 MHz, [D_7]DMF) of [(**L4**)Pd] at 10 K intervals from 300 K to 360 K. Resonances *c*, *g* and *o* were used to calculate the kinetic parameters.

Three proton resonances, H_o, H_c and H_g, are useful for interpretation. The coalescence temperature, T_c, for those protons along with the maximum peak separation, $\Delta\nu_o$, and an estimation of both the observed, k_{obs}, and bimolecular, k_{bi}, rates and activation free energy, $\Delta G^{\ddagger}$, at the coalescence temperature are listed in Table S1. $\Delta G^{\ddagger}$ was estimated using a modified Eyring equation:

$$k_{obs} = \frac{\pi \Delta \nu_o}{\sqrt{2}}$$

$$k_{bi} = \frac{k_{obs}}{[Nu]}$$

$$\Delta G^{\ddagger} = -RT \ln \frac{k_{bi} h}{k_B T}$$

(R = 1.9872 *cal* K^{-1} *mol*$^{-1}$, k_B = 3.30 x 10^{-24} *cal* K^{-1}, h = 1.58 x 10^{-34} *cal s*)

Table 3.2. Estimation of kinetic parameters of [(**L4**)Pd] from VT ^{1}H NMR.

	T_c (K)	Δv_o (Hz)	k_{obs} (s^{-1})	k_{bi} (M^{-1} s^{-1})	$\Delta G^{\ddagger}$ (kcal mol^{-1})
H_o	338	55.38	123	9.54	18.4
H_g	353	112.69	250	19.4	18.7
H_c	357	123.42	274	21.3	18.9

3.4.4 Exchange Spectroscopy (2D-EXSY) Investigation of Degenerate Shuttling Process in [(L4)Pd].[17]

2D-EXSY allows investigation of the shuttling process in the degenerate molecular shuttle [(**L4**)Pd]; all spectra were recorded on a Bruker 400 MHz NMR spectrometer at 300 K and the mixing time, τ_m, was 0.3 s. Using the equations shown below, where I_{AA} and I_{BB} are the diagonal peak intensities and I_{AB} and I_{BA} are the cross-peak intensities, we obtain a value for k which is the *sum* of the forward, k_1, and backward, k_{-1}, pseudo-first order rate constants for the shuttling process. As both stations are identical k_1 and k_{-1} are equal and thus the observed pseudo-first order rate constant, k_{obs}, can be determined. It is assumed that the shuttling is mediated by a nucleophile which displaces the palladium complex from the nitrile station in an associative fashion and that this is the rate determining step. If this is not an intramolecular process, the shuttling is a bimolecular process and, where the dominant nucleophile could be determined, k_{obs} was converted to k_{bi} which allows the value of $\Delta G^{\ddagger}$ to be determined using a modified Eyring equation.

$$A + Nu \underset{k_{-1}}{\overset{k_1}{\rightleftharpoons}} A' + Nu$$

$$r = \frac{(I_{AA} + I_{BB})}{(I_{AB} + I_{BA})}$$

$$k = \frac{1}{\tau_m} \times \ln \frac{r+1}{r-1}$$

$$k = k_1 + k_{-1} \qquad (k_1 = k_{-1} = k_{obs})$$

$$k_{bi} = \frac{k_{obs}}{[Nu]}$$

$$\Delta G^{\ddagger} = -RT \ln \frac{k_{bi} h}{k_B T}$$

($R = 1.9872\ cal\ K^{-1}\ mol^{-1}$, $k_B = 3.30 \times 10^{-24}\ cal\ K^{-1}$, $h = 1.58 \times 10^{-34}\ cal\ s$)

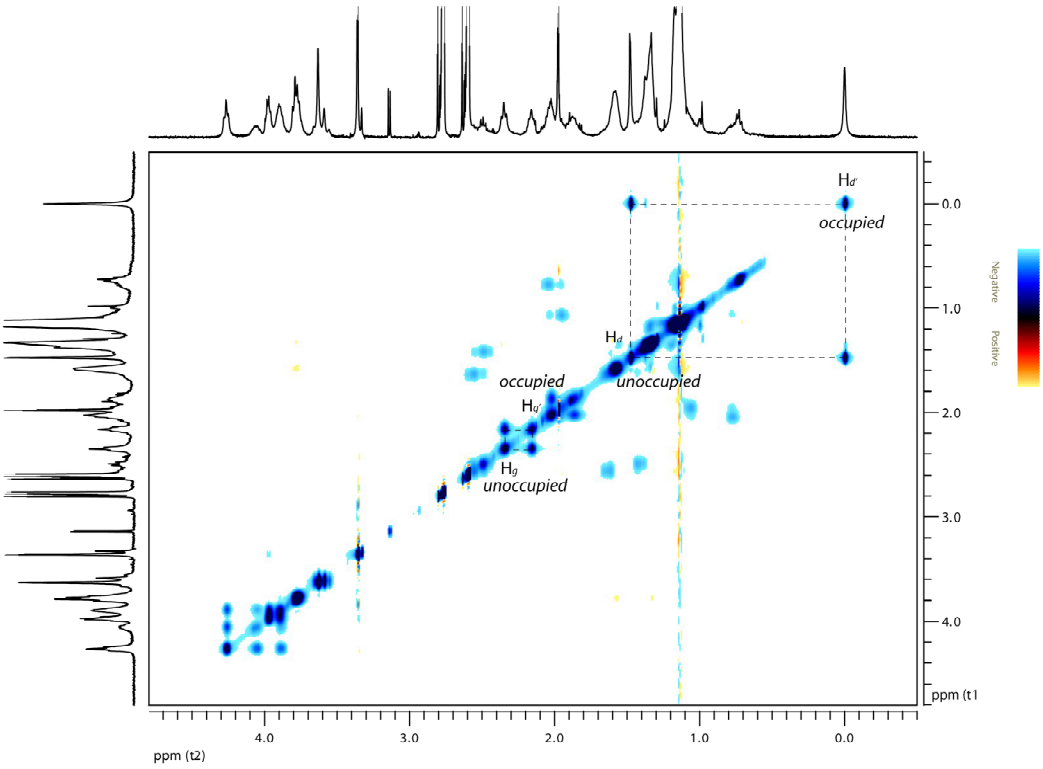

Figure 3.5. Partial 2D-EXSY spectrum of [(**L4**)Pd] (400 MHz, [D_7]DMF, 300 K).

Table 3.3. Kinetic parameters of [(**L4**)Pd] in [D_7]DMF. Concentration of [D_7]DMF in [D_7]DMF is 12.9 mol dm^{-3}. Estimated error in k_{obs} ± 1 s^{-1}.

	I_{AA}	I_{AB}	I_{BB}	I_{BA}	k_{obs} (s^{-1})	k_{bi} ($M^{-1}\ s^{-1}$)	$\Delta G^{\ddagger}$ (kcal mol^{-1})
H_d	1.86	1.00	0.93	1.04	3	0.2	18
H_g	1.80	1.00	1.47	1.04	2	0.2	19

3.4.5 Controlling Shuttling Rates *via* the Addition and Removal of Pyridine

[(**L4**)Pd] (0.023 g, 0.0113 mmol) was dissolved in $CDCl_3$ (0.75 ml) and a 2D-EXSY spectra was obtained. Pyridine (0.92 µl, 0.0113 mmol) was added to the yellow solution and a 2D-EXSY was obtained. *p*-Toluenesulfonic acid (0.0022 g, 0.0113 mmol) was added to the yellow solution and a 2D-EXSY spectra was obtained which showed that the rates had returned to the background level.

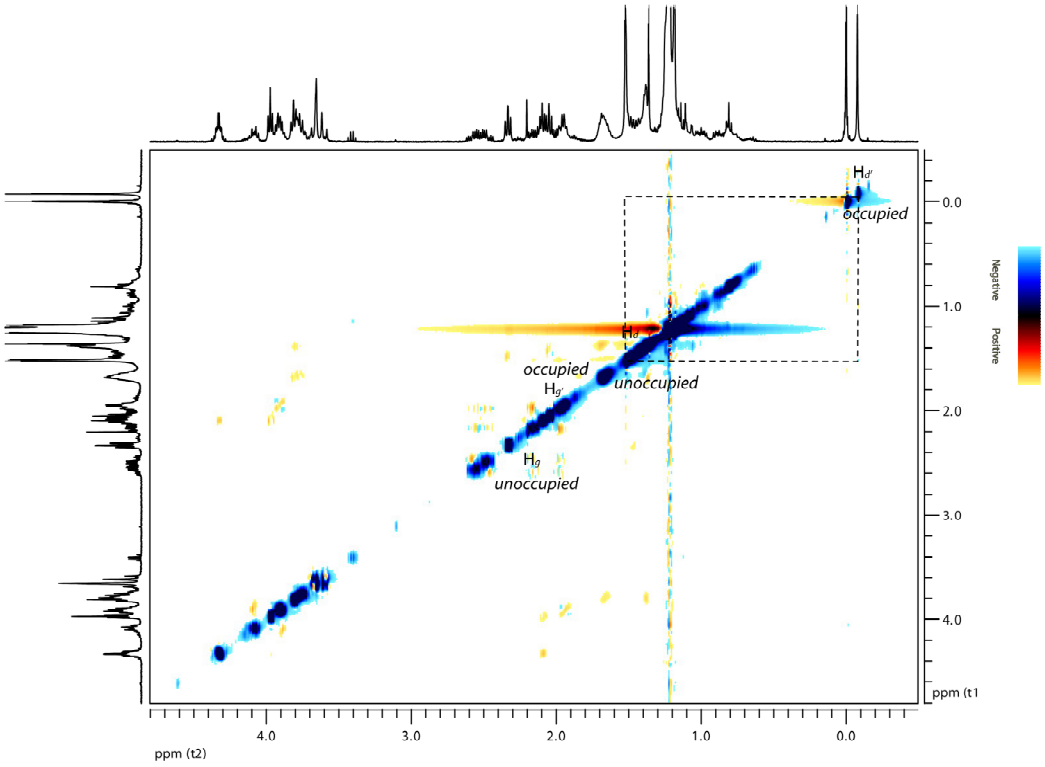

Figure 3.6. Partial 2D-EXSY spectrum of [(**L4**)Pd] (400 MHz, $CDCl_3$, 300 K).

Table 3.4. Kinetic parameters of [(**L4**)Pd] in $CDCl_3$. Estimated error in $k_{obs} \pm 1 \times 10^{-3}$ s^{-1}.

	I_{AA}	I_{AB}	I_{BB}	I_{BA}	k_{obs} (s^{-1})
H_d	1402.72	1.00	436.63	1.10	5×10^{-3}

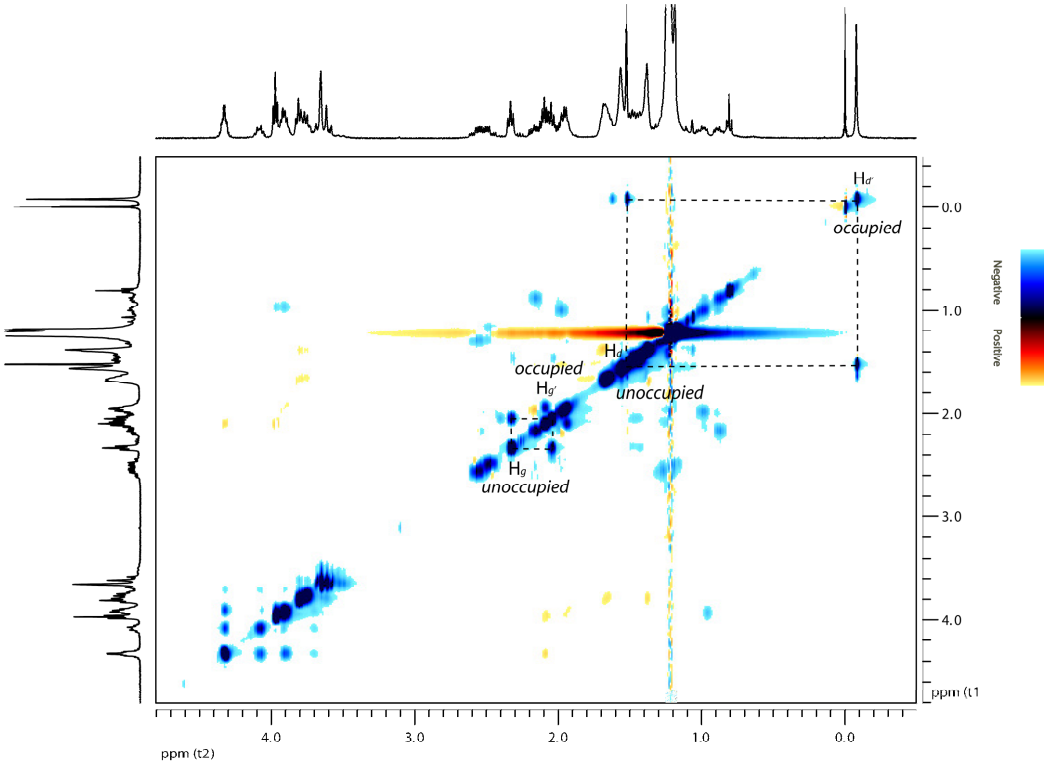

Figure 3.7. Partial 2D-EXSY spectrum of [(**L4**)Pd] plus 1 equiv. of pyridine (400 MHz, $CDCl_3$, 300 K).

Table 3.5. Kinetic parameters of [(**L4**)Pd] in $CDCl_3$ with 1 equiv. of pyridine. Concentration of pyridine present, 0.0119 mol dm^{-3}. Average k_{bi} = 95 M^{-1} s^{-1}. Estimated error in k_{obs} ± 0.1 s^{-1}.

	I_{AA}	I_{AB}	I_{BB}	I_{BA}	k_{obs} (s^{-1})	k_{bi} (M^{-1} s^{-1})	$\Delta G^{\ddagger}$ (kcal mol^{-1})
H_d	4.16	1.00	1.93	1.00	1	96	15
H_g	4.07	1.00	3.01	1.26	1	93	15

Table 3.6. Crystal data and structure refinement for [(**L2**)Pd(CH_3CN)].

CCDC-670786		
Identification code	[(**L2**)Pd(CH_3CN)]	
Empirical formula	$C_{41}H_{38}N_4O_4Pd$	
Formula weight	757.15	
Temperature	93(2) K	
Wavelength	0.71073 Å	
Crystal system	Monoclinic	
Space group	P2(1)/c	
Unit cell dimensions	a = 13.774(3) Å	α = 90°.
	b = 15.345(3) Å	β = 94.23(3)°.
	c = 16.410(3) Å	γ = 90°.
Volume	3459.3(12) $Å^3$	
Z	4	
Density (calculated)	1.454 Mg/m^3	
Absorption coefficient	0.586 mm^{-1}	
F(000)	1560	
Crystal size	0.0800 x 0.0800 x 0.0800 mm^3	
Theta range for data collection	1.48 to 25.44°.	
Index ranges	$-16 \le h \le 16$, $-18 \le k \le 18$, $-16 \le l \le 19$	
Reflections collected	22408	
Independent reflections	6336 [R(int) = 0.0500]	
Completeness to theta = 25.00°	99.7 %	
Absorption correction	Multiscan	
Max. and min. transmission	1.0000 and 0.7573	
Refinement method	Full-matrix least-squares on F^2	
Data / restraints / parameters	6336 / 0 / 453	
Goodness-of-fit on F^2	1.069	
Final R indices [I>2sigma(I)]	R1 = 0.0437, wR2 = 0.0787	
R indices (all data)	R1 = 0.0630, wR2 = 0.0864	
Largest diff. peak and hole	0.966 and -0.866 $e.Å^{-3}$	

Table 3.7. Crystal data and structure refinement for [(**L2**)Pd(**L1**)].

CCDC-670785		
Identification code	[(**L2**)Pd(**L1**)]	
Empirical formula	$C_{45}H_{44}Cl_2N_4O_6Pd$	
Formula weight	914.14	
Temperature	93(2) K	
Wavelength	0.71073 Å	
Crystal system	Monoclinic	
Space group	P2(1)	
Unit cell dimensions	a = 13.658(5) Å	α = 90°.
	b = 10.548(4) Å	β = 95.009(7)°.
	c = 14.508(6) Å	γ = 90°.
Volume	2082.1(14) $Å^3$	
Z	2	
Density (calculated)	1.458 Mg/m^3	
Absorption coefficient	0.628 mm^{-1}	
F(000)	940	
Crystal size	0.2000 x 0.1000 x 0.0500 mm^3	
Theta range for data collection	2.99 to 25.29°.	
Index ranges	$-16 \le h \le 16$, $-12 \le k \le 12$, $-17 \le l \le 17$	
Reflections collected	19257	
Independent reflections	7224 [R(int) = 0.0498]	
Completeness to theta = 25.00°	97.1 %	
Absorption correction	Multiscan	
Max. and min. transmission	1.0000 and 0.8801	
Refinement method	Full-matrix least-squares on F^2	
Data / restraints / parameters	7224 / 1 / 524	
Goodness-of-fit on F^2	1.045	
Final R indices [I>2sigma(I)]	R1 = 0.0384, wR2 = 0.0979	
R indices (all data)	R1 = 0.0387, wR2 = 0.0985	
Absolute structure parameter	0.02(2)	
Largest diff. peak and hole	0.637 and -0.755 $e.Å^{-3}$	

Table 3.8. Crystal data and structure refinement for [(**L3**)Pd].

CCDC-670784		
Identification code	[(**L3**)Pd]	
Empirical formula	$C_{133.50}H_{155}ClN_4O_{11.50}Pd$	
Formula weight	2141.47	
Temperature	93(2) K	
Wavelength	0.71073 Å	
Crystal system	Triclinic	
Space group	P-1	
Unit cell dimensions	a = 10.767(2) Å	α = 82.166(6)°.
	b = 21.409(5) Å	β = 79.665(8)°.
	c = 27.970(6) Å	γ = 86.688(10)°.
Volume	6280(2) $Å^3$	
Z	2	
Density (calculated)	1.132 Mg/m^3	
Absorption coefficient	0.227 mm^{-1}	
F(000)	2278	
Crystal size	0.2000 x 0.1000 x 0.0100 mm^3	
Theta range for data collection	2.09 to 25.36°.	
Index ranges	$-12 \le h \le 12$, $-25 \le k \le 25$, $-33 \le l \le 30$	
Reflections collected	63886	
Independent reflections	22787 [R(int) = 0.0988]	
Completeness to theta = 25.00°	99.4 %	
Absorption correction	Multiscan	
Max. and min. transmission	1.0000 and 0.9554	
Refinement method	Full-matrix least-squares on F^2	
Data / restraints / parameters	22787 / 6 / 1426	
Goodness-of-fit on F^2	1.180	
Final R indices [I>2sigma(I)]	R1 = 0.1256, wR2 = 0.3114	
R indices (all data)	R1 = 0.1606, wR2 = 0.3348	
Largest diff. peak and hole	1.011 and -0.656 $e.Å^{-3}$	

3.5 References and Notes

[1] a) V. Aucagne, K. D. Hänni, D. A. Leigh, P. J. Lusby, D. B. Walker, *J. Am. Chem. Soc.* **2006**, *128*, 2186–2187; b) S. Saito, E. Takahashi, K. Nakazono, *Org. Lett*. **2006**, *8*, 5133–5136; c) J. Berná, J. D. Crowley, S. M. Goldup, K. D. Hänni, A.-L. Lee, D. A. Leigh, *Angew. Chem*. **2007**, *119*, 5811–5815; *Angew. Chem. Int. Ed.* **2007**, *46*, 5709–5713; d) V. Aucagne, J. Berná, J. D. Crowley, S. M. Goldup, K. D. Hänni, D. A. Leigh, P. J. Lusby, V. E. Ronaldson, A. M. Z. Slawin, A. Viterisi, D. B. Walker, *J. Am. Chem. Soc.* **2007**, *129*, 11950–11963; e) J. D. Crowley, K. D. Hänni, A.-L. Lee, D. A. Leigh, *J. Am. Chem. Soc*. **2007**, *129*, 12092–12093; f) T. M. Swager, R. M. Moslin, *Synfacts* **2007**, *11*, 1158.

[2] a) D. B. Amabilino, J. F. Stoddart, *Chem. Rev*. **1995**, *95*, 2725–2828; b) *Molecular Catenanes, Rotaxanes and Knots: A Journey Through the World of Molecular Topology* (Eds.: J.-P. Sauvage, C. Dietrich-Buchecker), Wiley-VCH, Weinheim, 1999.

[3] For some recent innovations in passive template strategies to rotaxanes, see: a) M. S. Vickers, P. D. Beer, *Chem. Soc. Rev.* **2007**, *36*, 211–225; b) S. J. Loeb, *Chem. Soc. Rev*. **2007**, *36*, 226–235; c) B. Champin, P. Mobian, J.-P. Sauvage, *Chem. Soc. Rev*. **2007**, *36*, 358–366; d) P. C. Haussmann, S. I. Khan, J. F. Stoddart *J. Org. Chem*. **2007**, *72*, 6708–6713; e) A. B. Braunschweig, W. R. Dichtel, O. Š. Miljanić, M. A. Olson, J. M. Spruell, S. I. Khan, J. R. Heath, J. F. Stoddart, *Chem.–Asian J.* **2007**, *2*, 634–647; f) J. Wu, K. C.-F. Leung, J. F. Stoddart, *Proc. Natl. Acad. Sci. USA* **2007**, *104*, 17266–17271; g) S.-Y. Kim, Y. H. Ko, J. W. Lee, S. Sakamoto, K. Yamaguchi, K. Kim, *Chem.–Asian J.* **2007**, *2*, 747–754; h) C.-W. Chiu, C.-C. Lai, S.-H. Chiu, *J. Am. Chem. Soc*. **2007**, *129*, 3500–3501; i) H.-B. Yang, K. Ghosh, B. H. Northrop, Y.-R. Zheng, M. M. Lyndon, D. C. Muddiman, P. J. Stang, *J. Am. Chem. Soc.* **2007**, *129*, 14187–14189; j) A. I. Prikhod'ko, F. Durola, J.-P. Sauvage, *J. Am. Chem. Soc.* **2008**, *130*, 448–449; k) A.-M. L. Fuller, D. A. Leigh, P. J. Lusby, *Angew. Chem.* **2007**, *119*, 5103–5107; *Angew. Chem. Int. Ed.* **2007**, *46*, 5015–5019; l) J. R. Johnson, N. Fu, E. Arunkumar, W. M. Leevy, S. T. Gammon, D. Piwnica-Worms, B. D. Smith, *Angew. Chem*. **2007**, *119*, 5624–5627; *Angew. Chem. Int. Ed.* **2007**, *46*, 5528–5531; m) S. Nygaard, B. W. Laursen, T. S. Hansen, A. D. Bond, A. H. Flood, J. O. Jeppesen, *Angew. Chem.* **2007**, *119*, 6205–6209; *Angew. Chem. Int. Ed*. **2007**, *46*, 6093–6097; n) H. W. Daniell, E. J. F. Klotz, B. Odell, T. D. W. Claridge, H. L. Anderson, *Angew. Chem.* **2007**, *119*, 6969–6972; *Angew. Chem. Int. Ed*. **2007**, *46*, 6845–6848; o) T. Sato, T. Takata, *Tetrahedron Lett.* **2007**, *48*, 2797–2801; p) K. Nakazono, T. Oku, T. Takata, *Tetrahedron Lett*. **2007**, *48*, 3409–3411; q) Y. Tokunaga, N. Kawai, Y. Shimomura, *Tetrahedron Lett*. **2007**, *48*, 4995–4998; r) Y. Makita, N. Kihara, T. Takata, *Chem. Lett*. **2007**, *36*, 102–103; s) Y. Makita, N. Kihara, N. Nakakoji, T. Takata, S. Inagaki, C. Yamamoto, Y. Okamoto, *Chem. Lett*. **2007**, *36*, 162–163; t) L. Li, G. J. Clarkson, *Org. Lett.*

2007, *9*, 497–500; u) K. Hirose, K. Nishihara, N. Harada, Y. Nakamura, D. Masuda, M. Araki, Y. Tobe, *Org. Lett*. **2007**, *9*, 2969–2972; v) Y. Suzaki, K. Osakada, *Dalton Trans*. **2007**, 2376–2383; w) A. G. Cheetham, T. D. W. Claridge, H. L. Anderson, *Org. Biomol. Chem*. **2007**, *5*, 457–462; x) D. Castillo, P. Astudillo, J. Mares, F. J. González, A. Vela, J. Tiburcio, *Org. Biomol. Chem.* **2007**, *5*, 2252–2256; y) M. Narita, I. Yoon, M. Aoyagi, M. Goto, T. Shimizu, M. Asakawa, *Eur. J. Inorg. Chem*. **2007**, 4229–4237; z) S. R. Bayly, T. M. Gray, M. J. Chmielewski, J. J. Davis, P. D. Beer, *Chem. Commun*. **2007**, 2234–2236.

[4] The triazole rings introduced during active template CuAAC reactions (refs [1a] and [1d]) can be used as ligands for metals coordinated to the macrocycle.

[5] E. R. Kay, D. A. Leigh, F. Zerbetto, *Angew. Chem.* **2007**, *119*, 72–196; *Angew. Chem. Int. Ed*. **2007**, *46*, 72–191.

[6] a) K. Takenaka, Y. Uozumi, *Org. Lett*. **2004**, *6*, 1833–1835. b) K. Takenaka, M. Minakawa, Y. Uozumi, *J. Am. Chem. Soc*. **2005**, *127*, 12273–12281.

[7] M. A. Stark, G. Jones, C. J. Richards, *Organometallics* **2000**, *19*, 1282–1291.

[8] Other ligands that promote this reaction include bisoxazoline pyrrole Pd(II) complexes [C. Mazet, L. H. Gade, *Chem.–Eur. J.* **2003**, *9*, 1759–1767], bidentate phospino-oxazoline Pt(II) [A. J. Blacker, M. L. Clarke, M. S. Loft, M. F. Mahon, J. M. J. Williams, *Organometallics* **1999**, *18*, 2867–2873] and Ir(I) [D. Carmona, J. Ferrer, N. Lorenzo, F. J. Lahoz, I. T. Dobrinovitch, L. A. Oro, *Eur. J. Inorg. Chem*. **2005**, 1657–1664] catalysts and (salen)Al complexes [M. S. Taylor, D. N. Zalatan, A. M. Lerchner, E. N. Jacobsen, *J. Am. Chem. Soc*. **2005**, *127*, 1313–1317].

[9] The Pd(II) complex of a benzylic amide macrocycle previously successfully employed [a) A.-M. Fuller, D. A. Leigh, P. J. Lusby, I. D. H. Oswald, S. Parsons, D. B. Walker, *Angew. Chem.* **2004**, *116*, 4004–4008; *Angew. Chem. Int. Ed*. **2004**, *43*, 3914–3918; b) A.-M. L. Fuller, D. A. Leigh, P. J. Lusby, A. M. Z. Slawin, D. B. Walker, *J. Am. Chem. Soc*. **2005**, *127*, 12612–12619] in the passive template synthesis of interlocked architectures, efficiently catalyzes the double Michael addition of **1** with **L1** but only affords non-interlocked thread. Molecular modeling and X-ray crystallography show that the benzylic methylene group kinks the tridentate macrocyclic ring away from the nitrile ligand bound to the fourth coordination site of the Pd(II) such that Michael addition can occur out of the plane of the macrocycle rather than through it. Replacing the benzylic groups with anilide spacers changes the shape of the macrocycle (Figure 3.1) such that alkylation of the Pd-coordinated ethyl cyanoacetate is directed through the macrocycle cavity.

[10] The crystal data and experimental details of the structural refinement for [(**L2**)Pd(CH_3CN)] (CCDC-670786), [(**L2**)Pd(**L1**)] (CCDC-670785) and

[(**L3**)Pd] (CCDC-670784) are provided in the Experimental Section. The supplementary crystallographic data for these structures can be obtained free of charge from the Cambridge Crystallographic Data Centre *via* www.ccdc.cam.ac.uk/data_request/cif.

[11] a) D. A. Leigh, P. J. Lusby, A. M. Z. Slawin, D. B. Walker, *Angew. Chem.* **2005**, *117*, 4633–4640; *Angew. Chem. Int. Ed.* **2005**, *44*, 4557–4564. b) D. A. Leigh, P. J. Lusby, A. M. Z. Slawin, D. B. Walker, *Chem. Commun.* **2005**, 4919–4921.

[12] E. R. Kay, D. A. Leigh, *Top. Curr. Chem.* **2005**, *262*, 133–177.

[13] In the absence of [(**L2**)Pd(CH_3CN)] only 4% thread was produced after 7 d (other conditions as for Table 3.1, entry 6), indicating that the uncatalyzed background reaction is slow.

[14] Extended reaction times at higher temperatures (e.g. 333 K for 24 h) led to some decomposition of the Pd(II)-macrocycle complex.

[15] a) P. Gaviña, J.-P. Sauvage, *Tetrahedron Lett.* **1997**, *38*, 3521–3524; b) N. Armaroli, V. Balzani, J.-P. Collin, P. Gaviña, J.-P. Sauvage, B. Ventura, *J. Am. Chem. Soc.* **1999**, *121*, 4397–4408; c) M. C. Jiménez, C. Dietrich-Buchecker, J.-P. Sauvage, *Angew. Chem.* **2000**, *112*, 3422–3425; *Angew. Chem. Int. Ed.* **2000**, *39*, 3284–3287; d) M.C. Jiménez-Molero, C. Dietrich-Buchecker, J.-P. Sauvage, *Chem. Eur. J.* **2002**, *8*, 1456–1466; e) F. Durola, J.-P. Sauvage, *Angew. Chem.* **2007**, *119*, 3607–3610; *Angew. Chem. Int. Ed.* **2007**, *46*, 3537–3540; f) B. A. Blight, X. Wei, J. A. Wisner, M. C. Jennings, *Inorg. Chem.* **2007**, *46*, 8445–8447; g) J. D. Crowley, D. A. Leigh, P. J. Lusby, R. T. McBurney, L.-E. Perret-Aebi, C. Petzold, A. M. Z. Slawin, M. D. Symes, *J. Am. Chem. Soc.* **2007**, *129*, 15085–15090.

[16] a) J. D. Atwood, *Inorganic and Organometallic Reaction Mechanisms*, 2nd Ed., Wiley-VCH, New York, 1997. For a discussion of the mechanisms involved in the exchange of the fourth ligand in analogous Pd-pincer complexes, see: b) W. C. Yount, D. M. Loveless, S. L. Craig, *J. Am. Chem. Soc.* **2005**, *127*, 14488–14496.

[17] C. L. Perrin, T. J. Dwyer, *Chem. Rev.* **1990**, *90*, 935–967.

[18] However, in neat [D_5]-pyridine the palladium is sequestered from the rotaxane.

[19] F. Bellamy, D. Horton, J. Millet, F. Picart, S. Samreth, J. B. Chazan, *J. Med. Chem.* **1993**, *36*, 898–903.

[20] M. Sawamura, H. Hamashima, Y. Ito, *Tetrahedron* **1994**, *50*, 4439–4454.

CHAPTER FOUR

Gold(I) Template Catenane and Rotaxane Synthesis

Published as "*Gold(I) Template Catenane and Rotaxane Synthesis*"

Stephen M. Goldup, David A. Leigh, Paul J. Lusby, Roy T. McBurney and Alexandra M. Z. Slawin, *Angew. Chem. Int. Ed.* **2008**, *47*, 6999-7003.

Acknowledgements

The following people are gratefully acknowledged for their practical contribution to this chapter: Dr. Steve Goldup for synthesis of additional 2,6-*bis*(3-(4-hydroxyphenyl)-propyl)-pyridine; Prof. Alex Slawin solved the X-ray crystal structures of H_2**L2**$(OTs)_2$ and [(**L2**)Au]SbF_6. Dr. James Crowley is thanked for useful discussions.

Synopsis

As discussed in previous chapters, interlocked architectures have been synthesized using templates based on three dimensional and two dimensional metal-ligand coordination geometries. Here we describe the use of a one dimensional, linear, coordination geometry in the construction of catenanes and rotaxanes.

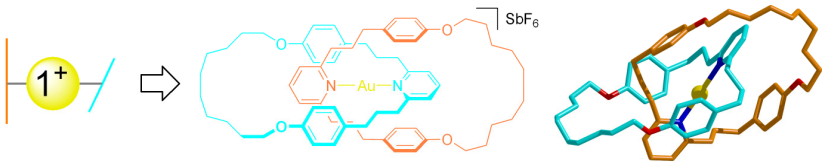

The approach is simple, two monodentate ligands coordinate gold(I), with secondary non-covalent interactions acting to promote a favorable orientation for interlocked architecture formation. The linear coordination geometry of the pyridine-gold(I)-pyridine bond and interlocked topology was demonstrated by an X-ray crystal structure of the gold(I) catenate. The interlocked nature of the rotaxane was proved by ^{1}H NMR spectroscopy.

4.1 Introduction

Metal ions with a range of different 2D and 3D coordination geometries (Figure 4.1a-d) have been used to template the synthesis of catenanes and rotaxanes.[1, 2] The result is a rich tapestry of mechanically interlocked ligands and complexes that have been studied from the point of view of their electrochemistry,[3] photochemistry,[4] reactivity,[5] selectivity,[3b, 6] and as prototypes for molecular machines.[7] Some of these systems can be assembled under thermodynamic control,[8] others kinetic.[3-6, 9] Some use sophisticated ligand systems,[10] others relatively simple ones.[8] Some feature homoleptic complexation modes,[3a, 8a,c, 11, 12] others heteroleptic.[9a,c, 13, 14] All employ at least one multidentate ligand. Here we report on the first use of a 1D (linear) metal-ligand coordination geometry (Figure 4.1e) to template the synthesis of mechanical bonds.[15, 16] The methodology requires only monodentate units on each component (we have used pyridine rings but aryl-Au coordination motifs are also well known[17]) and both homoleptic (suitable for homocircuit catenanes) and heteroleptic (suitable for heterocircuit catenanes and rotaxanes) complexes can be assembled. The approach is exemplified through the gold(I) template synthesis of a catenane and a rotaxane *via* ring closing olefin metathesis (RCM) macrocyclization[8a, 11] protocols.

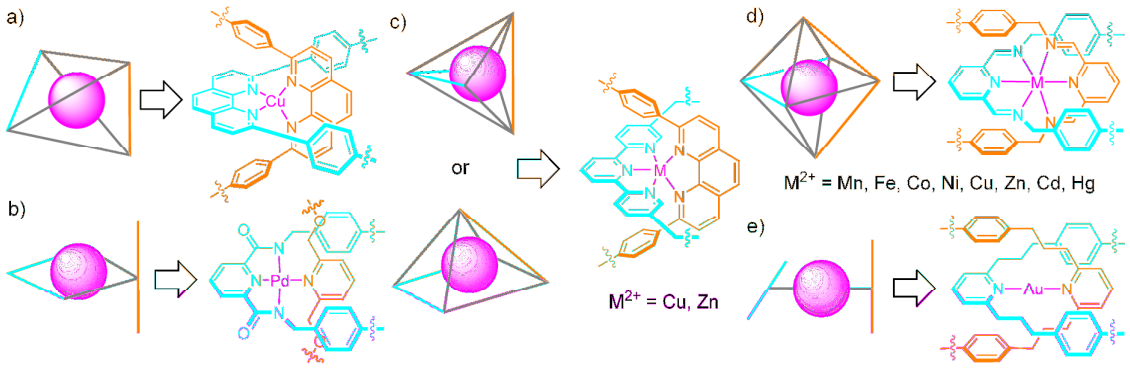

Figure 4.1. Metal coordination geometries successfully utilized in the metal template synthesis of catenanes and rotaxanes. (a) Four coordinate (tetrahedral);[3a, 4e, 5a,b, 6, 8c, 9a,b, 11] (b) four coordinate (square planar);[5d, 9c, 13] (c) five coordinate (square based pyramid/ trigonal bipyramidal);[14] (d) six coordinate (octahedral);[8a,b, 12] and, this work, (e) two coordinate (linear).

4.2 Results and Discussion

4.2.1 Ligand Design

Although square planar gold(III) has previously been used as a template in synthesis (to direct the assembly of aza-macrocycles[18]), to the best of our knowledge two coordinate gold(I) has not, despite it being an integral part of many oligomeric and polymeric supramolecular complexes, helicates and organometallic structures (which often feature multiple gold-gold aurophilic interactions in addition to the metal-ligand interactions).[15, 19] The attractiveness of using a linear coordination mode in synthesis lies in its simplicity and the potential generality of a motif that requires just two monodentate ligands to bind the metal. However, a key design question in any metal-template catenane or rotaxane synthesis is how to promote entwining of the ligands once they are attached to the metal. With gold(I) this is particularly easy to achieve: two 2,6-dialkylpyridine ligands, which are readily accessible *via* metal-mediated cross-couplings with 2,6-dihalopyridines,[20] must necessarily assemble with orthogonal orientations about the gold ion with the 'arms' of each ligand pointing over the other ligand to create the required two cross-over points. For our chosen ligand system (**L1**, Scheme 4.1) we also introduced aromatic rings (Figure 4.1e) at positions equivalent to those found to form efficient intercomponent aromatic stacking interactions in benzylic amide and imine catenanes and rotaxanes (Figure 4.1b, d). The terminal functional groups on each ligand should thus be oriented such that macrocyclization reactions should favor interlocked products over the formation of larger macrocycles, oligomers and polymers.

4.2.2 Catenane Synthesis

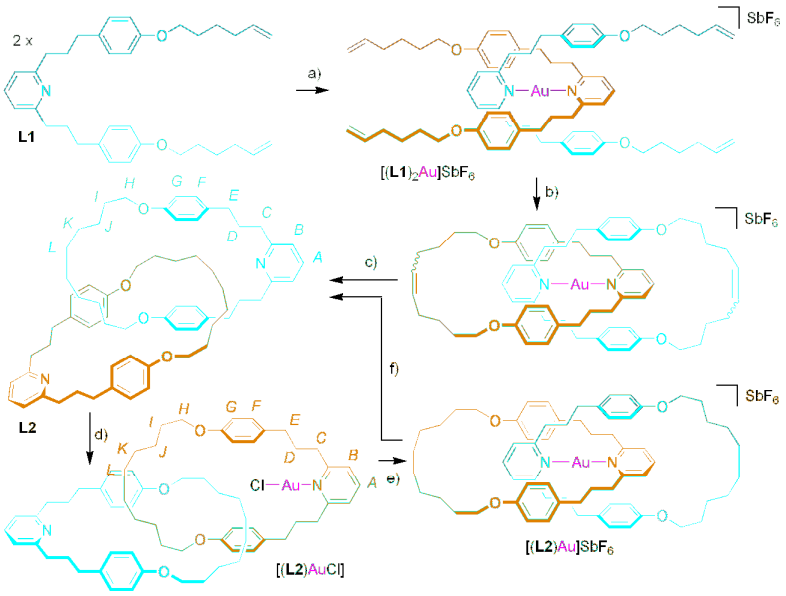

Scheme 4.1. Gold(I) template catenane synthesis and subsequent chemistry. Reagents and conditions: a) 1. $AuCl(SMe_2)$, acetone, 5 min.; 2. $AgSbF_6$, 5 min.; b) $(PCy_3)_2Cl_2Ru$=CHPh, CH_2Cl_2, 2 d; c) 1. 1M HCl(aq.):CH_2Cl_2 (1:1), 40 ˚C, 18 h; 2. H_2, Pd/C, THF:EtOH (1:1), 18 h, **L2** 41% (from **L1**); d) $AuCl(SMe_2)$, acetone, 5 min.; e) $AgSbF_6$, acetone, 5 min. >98%; f) 1M HCl(aq.):CH_2Cl_2 (1:1), 40 ˚C, 18 h or *hν* 400-700 nm (500 W halogen lamp), $CDCl_3$, 6 d, >98%.

Pyridine ligand **L1** was synthesized by alkylation of a known[2d] bis-phenol (see Experimental Section 4.3) and a 2:1 complex with gold(I), $[(\mathbf{L1})_2Au]SbF_6$, was assembled by treating **L1** (2 equiv.) with $AuCl(SMe_2)$ (1 equiv.) followed by anion exchange with $AgSbF_6$ (Scheme 4.1, step a). Ring closing metathesis of $[(\mathbf{L1})_2Au]SbF_6$ ($(PCy_3)_2Cl_2Ru$=CHPh, CH_2Cl_2 (high dilution), 2 days, Scheme 4.1, step b) afforded one major and two minor products, each as a mixture of olefin diastereomers and in both metallated and de-metallated forms. To facilitate purification, the crude product mixture was fully demetallated (1 M HCl(aq):CH_2Cl_2 (1:1), 40 ˚C, 18 h) and the olefins reduced (Pd/C, H_2, 18 h), before being subjected to column chromatography to yield the major product, later confirmed to be the desired catenane **L2**, in 41% yield (from **L1**). Also isolated were the macrocycle resulting from simple cyclization of **L1** (20%) and a larger macrocycle (an isomer of the

catenane) formed from the 1 + 1 cyclization of **L1** (18%). It is not clear whether the non-interlocked products arise from unproductive macrocyclization reactions on the gold(I) template (similar product distributions have been observed in some Pd(II) template catenane syntheses[13c]) or from reactions involving uncomplexed **L1** (a potential disadvantage of using relatively weakly binding monodentate ligands for a template synthesis is that unbound ligand can be present during the reaction).

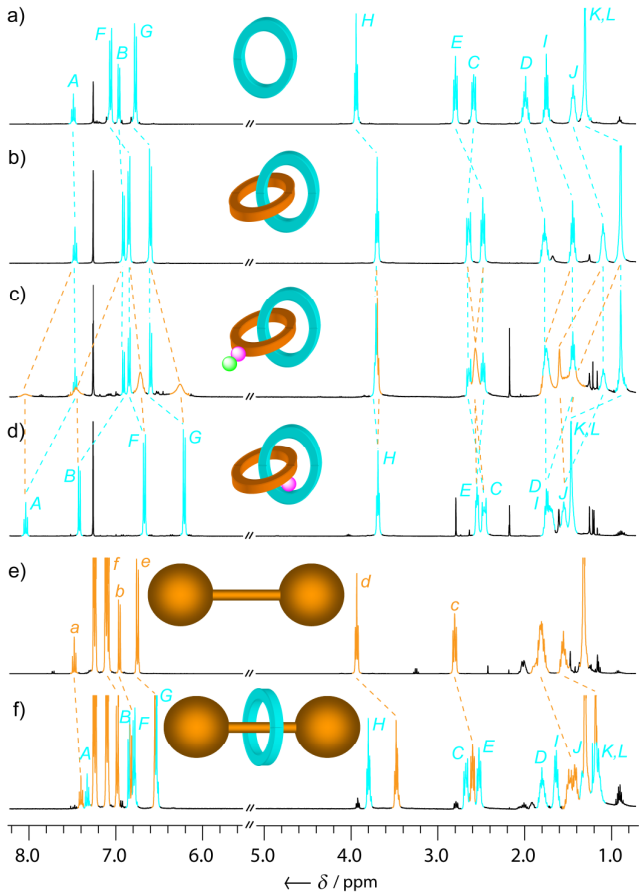

Figure 4.2. ^{1}H NMR spectra (400 MHz, $CDCl_3$, 300 K) of a) non-interlocked macrocycle; b) metal-free catenand **L2**; c) [(**L2**)AuCl]; d) gold(I) catenate [(**L2**)Au]SbF_6; e) thread **L3**, and f) metal-free rotaxane **L4**. The assignments correspond to the lettering shown in Schemes 4.1 and 4.2.

Evidence supporting assignment of the major product as [2]catenane **L2** came initially from mass spectrometry and ^{1}H NMR comparison of the products (*e.g.* Figure 4.2a and 4.2b: the major product (Figure 4.2b) shows shielding effects similar

to those found in other catenanes[8a, b, 13c]). Confirmation of the mechanically interlocked structure was obtained from X-ray crystallography of the *bis-p*-toluenesulfonic acid salt (Figure 4.3), in which the protonated pyridine groups lie to the outside of each catenane, with the alkyl chains of each macrocycle buried through the cavity of the other.

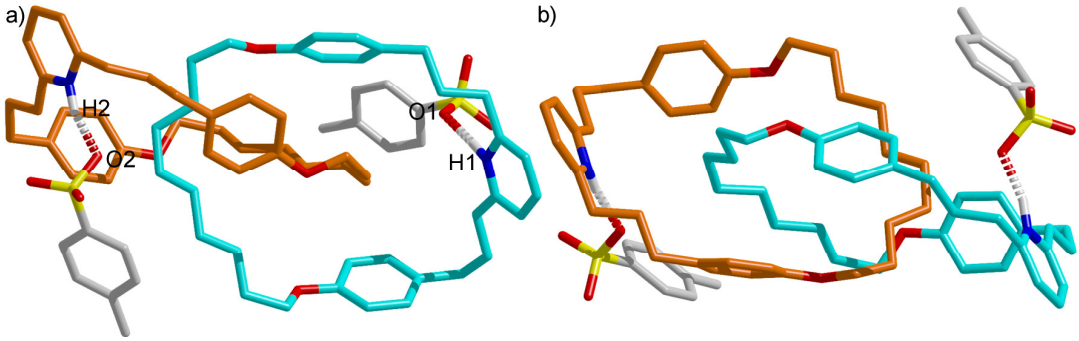

Figure 4.3. Two views of the X-ray crystal structure[21] of *bis*-protonated catenand H_2**L2**$(OTs)_2$ from a single crystal grown by vapor diffusion of diisopropyl ether into a saturated acetone solution. Carbon atoms are shown in light blue for one macrocycle and brown for the other, oxygen atoms red, nitrogen blue, sulfur yellow. Hydrogen bond lengths [Å] and angles [°]: NH1···O1 = NH2···O2 1.76. N1–H1–O1 = N2–H2–O2 163.

Gold(I) could be re-introduced into catenand **L2** in a two step process. Treatment with $AuCl(SMe_2)$ quantitatively generated the interesting complex [(**L2**)AuCl], the ^{1}H NMR of which (Figure 4.2c) shows inequivalent resonances for the two macrocycles indicating that gold is coordinated to just one ring. Subsequent addition of $AgSbF_6$ and filtration through celite generated [(**L2**)Au]SbF_6, whose ^{1}H NMR spectrum (Figure 4.2d) shows only one set of macrocycle resonances, enhanced shielding for aromatic protons H_F and H_G and reduced shielding of the resonances corresponding to the alkyl chain, indicating that a significant co-conformational rearrangement takes place for both rings to bind to the gold. Crystals of the gold(I) catenate suitable for X-ray crystallography were obtained by vapor diffusion of diisopropyl ether into a saturated acetone solution of the complex.[21] The solid state structure of [(**L2**)Au]SbF_6 (Figure 4.4), in which the pyridine groups are now internal to the catenate so that both can bind the metal, with the alkyl chains to the outside, shows the close-to-linear (175.3°) coordination geometry of the pyridine-

gold(I)-pyridine motif and some of the offset intercomponent aromatic stacking interactions introduced to aid catenane formation. The gold ion is fully encapsulated within the organic framework and thus prevented from making aurophilic gold-gold interactions[19] (the shortest Au···Au distance in [(**L2**)Au]SbF_6 in the solid state is more than a nanometer).

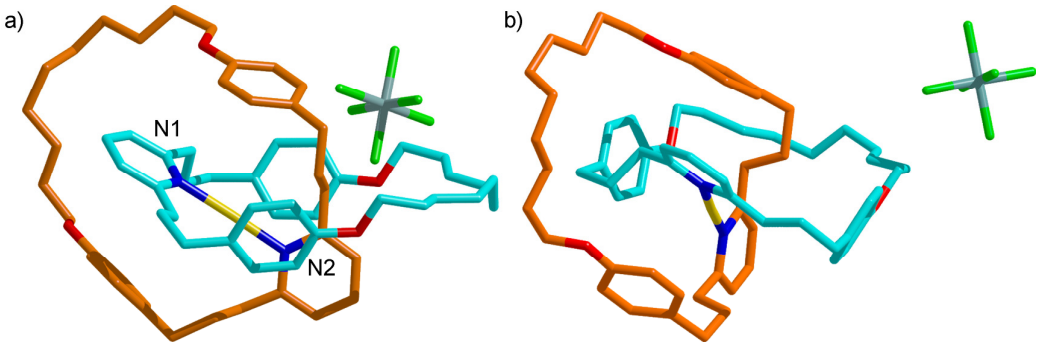

Figure 4.4. X-Ray crystal structure[21] of gold(I) catenate [(**L2**)Au]SbF_6, viewed a) parallel to the N-Au-N bond, b) close to the axis of the N-Au-N bond. Carbon atoms are shown in light blue for one macrocycle and brown for the other, oxygen atoms red, nitrogen blue, gold(I) gold, antimony grey and fluorine green. Selected bond lengths [Å] and angles [°]: N1-Au 2.05, N2-Au 2.06; N1-Au-N2 175.3. Closest Au···Au distance 11.31 Å.

4.2.3 Rotaxane Synthesis

To extend the methodology to rotaxane formation required the assembly of a heteroleptic complex about the gold(I) center (Scheme 4.2). Treatment of **L1** with $AuCl(SMe_2)$ (1 equiv.) followed by $AgSbF_6$ and **L3**, attached both the macrocycle precursor and the thread to the same gold ion, generating [(**L1**)Au(**L3**)]SbF_6 (Scheme 4.2, steps a and b). Subsequent RCM ($(PCy_3)_2Cl_2Ru$=CHPh (0.2 equiv.), CH_2Cl_2, 2 days, Scheme 4.2, step c) captured the interlocked architecture. As with the catenane synthesis, the metal was removed and the double bond hydrogenated prior to purification by column chromatography, which yielded metal-free rotaxane **L4** in 26% yield (from **L1**) together with 14% of catenane **L2** (arising from ligand-scrambling of [(**L1**)Au(**L3**)]SbF_6). The ^{1}H NMR spectrum of rotaxane **L4** (Figure 4.2f) shows shielding with respect to the spectra of its non-interlocked components (macrocycle, Figure 4.2a, and thread, Figure 4.2e) similar to that observed for catenane **L2** (Figure 4.2b).

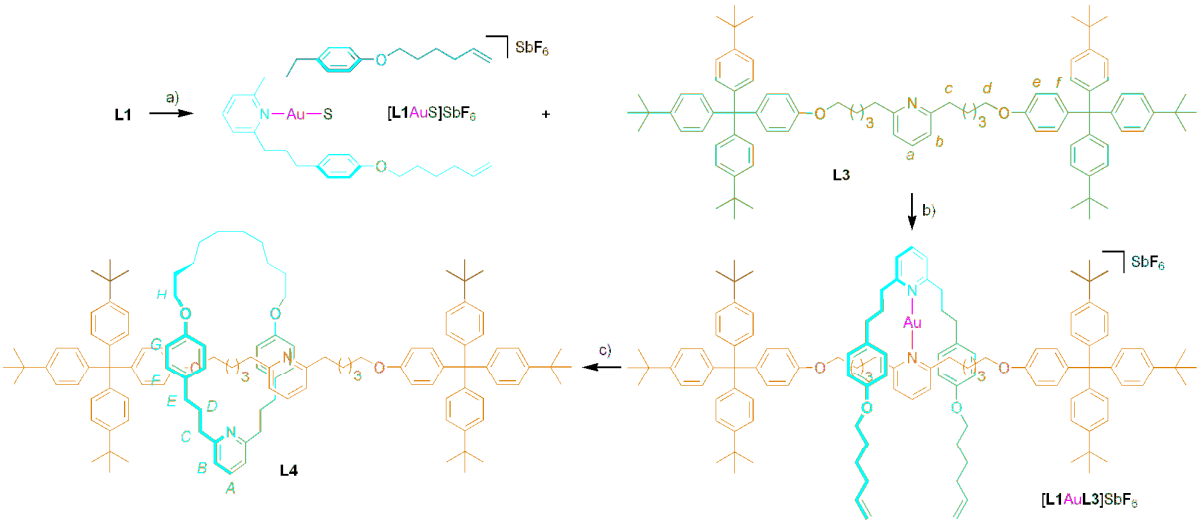

Scheme 4.2. Gold(I) template rotaxane synthesis. Reagents and conditions: a) 1. $AuCl(SMe_2)$, acetone, 5 min.; 2. $AgSbF_6$, acetone, 5 min.; b) acetone, 5 min.; c) 1. $(PCy_3)_2Cl_2Ru{=}CHPh$, CH_2Cl_2, 2 d; 2. 1M HCl(aq):CH_2Cl_2 (1:1), 40 ˚C, 18 h; 3. H_2, Pd/C, THF:EtOH (1:1), 18 h, **L4** 26% (from **L1**).

4.3 Conclusions

It is easy to forget that prior to Sauvage's original Cu(I) template synthesis[9a] the construction of mechanically interlocked molecules was a task of almost Herculean proportions.[22] A quarter of a century on, the gold(I) template synthesis of [2]catenane **L2** and [2]rotaxane **L4** marks the last of the simple metal coordination geometries (linear) to join the family of metal-ligand arrangements that can direct the formation of mechanical bonds. The ability to form both homoleptic and heteroleptic complexes, and the simplicity of the monodentate ligands required, suggests that gold(I) could prove to be a particularly versatile template for the synthesis of interlocked molecular structures.

4.3 Experimental Section

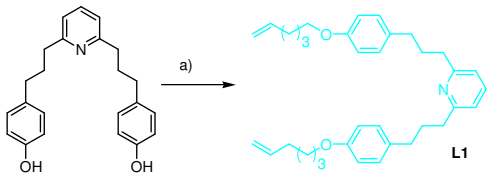

Scheme 4.3. Synthesis of ligand **L1** from 2,6-bis(3-(4-hydroxyphenyl)-propyl)-pyridine.[2c] Reagents and conditions: a) 2,6-*bis*(3-(4-hydroxyphenyl)-propyl)-pyridine, 6-bromohex-1-ene, K_2CO_3, DMF, 48 h, 80%.

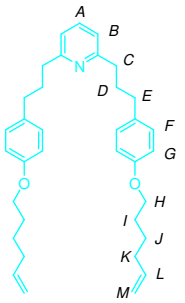

2,6-*Bis*(3-(4-(hex-5-enyloxy)phenyl)propyl)pyridine - L1

To a solution of 2,6-*bis*(3-(4-hydroxyphenyl)propyl)pyridine[2c] (1.01 g, 2.92 mmol) and 6-bromohex-1-ene (1.20 ml, 8.75 mmol) in DMF (30 ml) was added K_2CO_3 (4.04 g, 29.2 mmol). The suspension was heated at 80 ˚C for 48 h. The reaction mixture was diluted with CH_2Cl_2 (100 ml) and washed with H_2O (50 ml), the organic layer was dried ($MgSO_4$), then purified by column chromatography (CH_2Cl_2:PE 1:1 then CH_2Cl_2) to yield the title compound as a colorless waxy solid (1.19 g, 80%). m.p. 45 ˚C; ^{1}H NMR (400 MHz, $CDCl_3$, 300 K): δ = 1.56 (m, 4H, H_J), 1.79 (m, 4H, H_I), 2.00 (m, 4H, H_D), 2.12 (m, 4H, H_K), 2.61 (m, 4H, H_E), 2.79 (m, 4H, H_C), 3.93 (t, J = 6.5 Hz, 4H, H_H), 5.00 (m, 4H, H_M), 5.83 (m, 2H, H_L), 6.80 (d, J = 8.5 Hz, 4H, H_G), 6.93 (d, J = 7.7 Hz, 2H, H_B), 7.09 (d, J = 8.5 Hz, 4H, H_F), 7.48 (t, J = 7.7 Hz, 1H, H_A); ^{13}C NMR (100 MHz, $CDCl_3$, 300 K): δ = 25.3, 28.8, 32.1, 33.5, 34.7, 38.0, 67.7, 114.3, 114.7, 119.8, 129.3, 134.2, 136.5, 138.6, 157.2, 161.5; LRFAB-MS (3-NOBA matrix): *m/z* = 512 $[MH]^+$; HRFAB-MS (3-NOBA matrix): *m/z* = 512.3506 (calcd. $C_{35}H_{46}NO_2$ 512.3523).

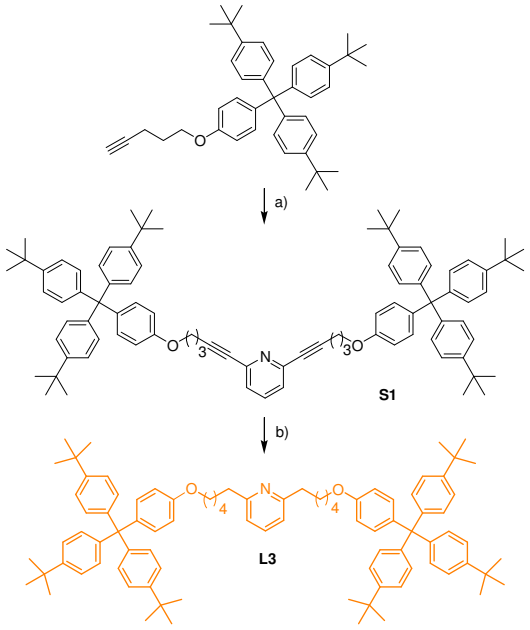

Scheme 4.4. Synthesis of thread **L3** from 1-(*bis*(4-*tert*-butylphenyl)(4-(pent-4-ynyloxy)phenyl)methyl)-4-*tert*-butylbenzene.[2c] Reagents and conditions: a) 2,6-dibromopyridine, $PdCl_2(PPh_3)_2$, CuI, Et_3N, THF, 85% ; b) Pd/C, THF, EtOH, 18 h, 77%.

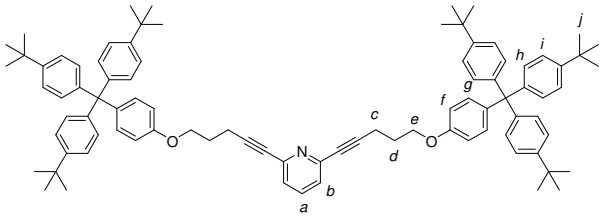

2,6-*Bis*(5-(4-(tris(4-*tert*-butylphenyl)methyl)phenoxy)pent-1-ynyl)pyridine – S1

To a solution of 1-(*bis*(4-*tert*-butylphenyl)(4-(pent-4-ynyloxy)phenyl)methyl)-4-*tert*-butylbenzene[2c] (2.1 g, 3.7 mmol) and 2,6-dibromopyridine (0.29 g, 1.2 mmol) in THF (15 ml) and Et_3N (15 ml) was added copper(I) iodide (0.046 g, 0.12 mmol) and $PdCl_2(PPh_3)_2$ (0.084 g, 0.12 mmol). The resulting mixture was stirred at RT for 18 h. The solvent was removed under reduced pressure and the residue was redissolved in CH_2Cl_2 (100 mL) and washed with a saturated aqueous solution of NH_4Cl (3 × 50 mL) and brine (100 mL). The organic layer was dried ($MgSO_4$), the solvent removed under reduced pressure and the crude residue purified by column chromatography on silica (CH_2Cl_2) to yield the title product as a yellowish solid (1.27 g, 85%). m.p. 159 ˚C (dec.); ^{1}H NMR (400 MHz, $CDCl_3$, 300 K): δ = 1.30 (s,

54H, H_j), 2.08 (m, 4H, H_d), 2.63 (t, J = 7.0 Hz, 4H, H_c), 4.06 (t, J = 6.0 Hz, 4H, H_e), 6.79 (d, J = 8.9 Hz, 4H, H_f), 7.08 (d, J = 8.6 Hz, 16H, H_{g+h}), 7.23 (m, 14H, H_{b+i}), 7.52 (t, J = 7.8 Hz, 1H, H_a); ^{13}C NMR (100 MHz, $CDCl_3$, 300 K): δ = 16.2, 28.2, 31.4, 34.3, 63.0, 66.1, 80.5, 90.2, 113.0, 124.0, 125.6, 130.7, 132.2, 136.3, 139.6, 143.8, 144.1, 148.3, 156.6; LRFAB-MS (3-NOBA matrix): m/z = 1217 $[MH]^+$; HRFAB-MS (3-NOBA matrix): m/z = 1216.791 (calcd. $C_{89}H_{102}NO_2$, 1216.791).

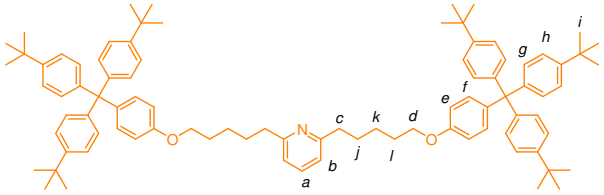

Thread – L3

After the addition of 10% w/w Pd/C (0.310 g) to a solution of **S1** (1.55 g, 1.27 mmol) in THF (15 ml), the mixture was repeatedly degassed and purged, first with N_2 and then with H_2, before being stirred for 18 h at RT under a constant atmosphere of H_2. The reaction mixture was then filtered through celite, the solvent removed under reduced pressure and the crude residue purified by column chromatography to yield the title compound as a colorless solid (1.19 g, 77%). m.p. 127 °C; ^{1}H NMR (400 MHz, $CDCl_3$, 300 K): δ = 1.32 (s, 54H, H_i), 1.55 (m, 4H, H_k), 1.82 (m, 8H, H_{j+l}), 2.81 (m, 4H, H_c), 3.93 (t, J = 6.4 Hz, 4H, H_d), 6.75 (d, J = 8.9 Hz, 4H, H_e), 6.96 (d, J = 7.7 Hz, 2H, H_b), 7.10 (m, 16H, H_{f+g}), 7.24 (d, J = 8.6 Hz, 12H, H_h), 7.48 (t, J = 7.7 Hz, 1H, H_a); ^{13}C NMR (100 MHz, $CDCl_3$, 300 K): δ = 25.2, 28.8, 29.4, 31.2, 34.1, 39.3, 63.1, 67.7, 113.0, 119.8, 124.0, 130.8, 132.2, 136.5, 139.4, 144.2, 148.2, 156.9, 161.6; LRFAB-MS (3-NOBA matrix): m/z = 1225 $[M]^+$; HRFAB-MS (3-NOBA matrix): m/z = 1224.853 (calcd. $C_{88}{}^{13}CH_{109}NO_2$, 1224.849).

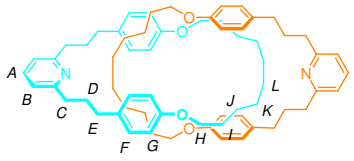

Catenane - L2

To a solution of **L1** (0.178 g, 0.348 mmol) in acetone (5 ml) was added $AuCl(SMe_2)$ (0.0513 g, 0.174 mmol), the solution was stirred. After 5 min $AgSbF_6$ (0.0598 g, 0.174 mmol) was added and the grey-blue suspension was stirred for a further 5 min before filtration through a pad of celite and removal of the solvent under reduced pressure. The crude residue was redissolved in CH_2Cl_2 (100 ml) and Grubbs' 1st generation olefin metathesis catalyst (0.058 g, 0.070 mmol) was added and the purple solution was stirred for 2 d with a stream of nitrogen bubbled directly through the solution. The solvent was removed under reduced pressure, the crude residue was redissolved in CH_2Cl_2 (10 ml) to which was added 1M HCl(aq) (10 ml) followed by heating at 40 ˚C for 18 h. The reaction mixture was neutralized with saturated aqueous sodium bicarbonate (100 ml) then extracted with CH_2Cl_2 (3 × 100 ml). The combined organic layers were washed with brine (50 ml), dried ($MgSO_4$) and concentrated under reduced pressure. The crude residue was dissolved in THF (5 ml) and EtOH (5 ml) then 10% w/w Pd/C (0.070 g) was added. The reaction vessel was repeatedly degassed and purged with N_2, then repeatedly degassed and purged with H_2 and left to stir for 18 h under an atmosphere of H_2. The reaction mixture was filtered through a pad of celite, concentrated under reduced pressure and then purified by column chromatography (0% to 10% EtOAc in CH_2Cl_2 gradient elution) to yield catenane **L2** (0.069 g, 41%) as a colorless oil which solidified on standing, mono-pyridine macrocycle (0.034 g, 40% w.r.t. **L1**) and bis-pyridine macrocycle (0.030 g, 18 % w.r.t. **L1**) as a colorless solid. The ^{1}H NMR and ^{13}C NMR spectra of the mono-pyridine macrocycle were consistent with the published data.[2c]

L2: m.p. 66 ˚C; ^{1}H NMR (400 MHz, $CDCl_3$, 300 K): δ = 0.91 (br, 16H, H_{K+L}), 1.11 (br, 8H, H_J), 1.50 (m, 8H, H_I), 1.78 (m, 8H, H_D), 2.49 (m, 8H, H_E), 2.65 (m, 8H, H_C), 3.71 (t, J = 6.4 Hz, 8H, H_H), 6.61 (d, J = 8.5 Hz, 8H, H_G), 6.86 (d, J = 8.5 Hz, 8H, H_F), 6.92 (d, J = 7.7 Hz, 4H, H_B), 7.47 (t, J = 7.7 Hz, 2H, H_A); ^{13}C NMR (100 MHz,

$CDCl_3$, 300 K): δ = 25.6, 28.4, 28.7, 29.6, 32.7, 35.4, 38.4, 67.1, 114.5, 119.6, 129.2, 134.0, 136.4, 157.0, 161.6; LRFAB-MS (3-NOBA matrix): *m/z* = 486 $[MH_2]^{2+}$; HRFAB-MS (3-NOBA matrix): *m/z* = 486.3387 (calcd. $C_{66}H_{88}N_2O_4$ 486.3367).

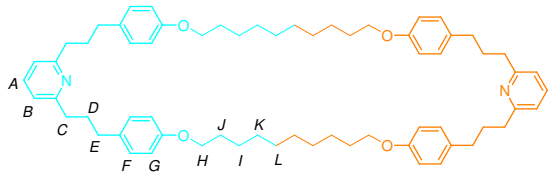

Bis-pyridine macrocycle: m.p. 69 ˚C; ^{1}H NMR (400 MHz, $CDCl_3$, 300 K): δ = 1.33 (br, 16H, H_{K+L}), 1.45 (br, 8H, H_J), 1.76 (m, 8H, H_I), 2.01 (m, 8H, H_D), 2.62 (m, 8H, H_E), 2.79 (m, 8H, H_C), 3.92 (t, *J* = 6.5 Hz, 8H, H_H), 6.81 (d, *J* = 8.5 Hz, 8H, H_G), 6.93 (d, *J* = 7.7 Hz, 4H, H_B), 7.09 (d, *J* = 8.5 Hz, 8H, H_F), 7.48 (t, *J* = 7.7 Hz, 2H, H_A); ^{13}C NMR (100 MHz, $CDCl_3$, 300 K): δ = 22.6, 25.8, 29.4, 31.6, 32.1, 34.7, 38.0, 68.0, 114.3, 119.8, 129.3, 134.2, 136.4, 157.3, 161.5; LRFAB-MS (3-NOBA matrix): *m/z* = 486 $[MH_2]^{2+}$; HRFAB-MS (3-NOBA matrix): *m/z* = 486.3371 (calcd. $C_{66}H_{88}N_2O_4$ 486.3367).

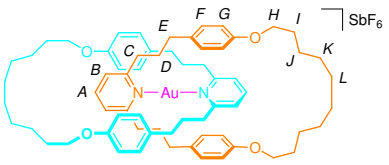

Catenate - [(**L2**)Au]SbF_6

To a solution of **L2** (0.157 g, 0.162 mmol) in acetone (2 ml) was added $AuCl(SMe_2)$ (0.0476 g, 0.162 mmol), the solution was stirred for 5 min to give [(**L2**)AuCl] [from which an aliquot was taken for analysis: ^{1}H NMR (400 MHz, $CDCl_3$, 300K): δ = 1.09 (br, 8H, H_{k+l}), 1.09 (br, 4H, H_j), 1.44 (m, 12 H, H_{i+K+L}), 1.60 (br, 4H, H_J), 1.76 (m 12H, $H_{d+D+\ I}$), 2.57 (m, 16H, $H_{c+C+e+E}$), 3.70 (m, 8H, H_{h+H}), 6.27 (br, 4H, H_G), 6.60 (d, *J* = 8.5 Hz, 4H, H_g), 6.72 (br, 4H, H_F), 6.85 (d, *J* = 8.5 Hz, 4H, H_f), 6.91 (d, *J* = 7.7 Hz, 2H, H_b), 7.47 (m, 3H, H_{a+B}), 8.06 (br, 1H, H_A)]. $AgSbF_6$ (0.0557 g, 0.162 mmol) was added and the resulting grey-blue suspension was stirred for 5 min before being filtered through a pad of celite. The solvent was removed under reduced pressure to yield the title compound as a colorless solid (0.225 g, 99%). Single crystals suitable for investigation by X-ray crystallography were grown by vapor

diffusion of diisopropyl ether into a solution of [(**L2**)Au]SbF_6 in acetone. ^{1}H NMR (400 MHz, $CDCl_3$, 300 K): δ = 1.47 (br, 16H, H_{K+L}), 1.55 (m, 8H, H_J), 1.73 (m, 16H, H_{D+I}), 2.47 (m, 8H, H_C), 2.55 (m, 8H, H_E), 3.69 (t, J = 5.9 Hz, 8H, H_H), 6.21 (d, J = 8.5 Hz, 8H, H_G), 6.67 (d, J = 8.5 Hz, 8H, H_f), 7.42 (d, J = 7.8 Hz, 4H, H_B), 8.04 (t, J = 7.8 Hz, 2H, H_A); ^{13}C NMR (100 MHz, $CDCl_3$, 300 K): δ = 26.4, 28.9, 29.0, 29.5, 32.0, 34.2, 39.5, 67.0, 113.5, 123.3, 129.6, 132.3, 141.0, 157.1, 162.6.

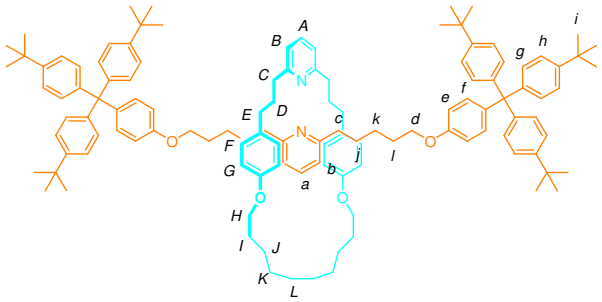

Rotaxane - L4

To a solution of **L1** (0.0810 g, 0.158 mmol) in acetone (2 ml) was added $AuCl(SMe_2)$ (0.0467 g, 0.158 mmol), the solution was stirred for 5 min. $AgSbF_6$ (0.0543 g, 0.158 mmol) was added and the grey-blue suspension was stirred for 5 min before filtration through a pad of celite into a receiver flask that contained a solution of **L3** (0.193 g, 0.158 mmol) in acetone (5 ml). The solvent was removed under reduced pressure. The crude residue was redissolved in CH_2Cl_2 (100 ml), Grubbs' 1st generation olefin metathesis catalyst (0.026 g, 0.32 mmol) was added and the purple solution was stirred for 2 d with a stream of nitrogen bubbled directly through the solution. The solvent was removed under reduced pressure, the crude residue was redissolved in CH_2Cl_2 (10 ml) to which was added 1M HCl(aq) (10 ml) followed by heating at 40 ˚C for 18 h. The reaction mixture was neutralized with saturated aqueous sodium bicarbonate (100 ml) then extracted with CH_2Cl_2 (3 × 100 ml). The combined organic layers were washed with brine (50 ml), dried ($MgSO_4$) and concentrated under reduced pressure. The crude residue was redissolved in THF (5 ml) and EtOH (5 ml) then 10% w/w Pd/C (0.055 g) was added. The reaction vessel was repeatedly degassed and purged with N_2, then repeatedly degassed and purged with H_2 and left to stir for 18 h under an atmosphere of H_2. The reaction mixture was filtered through a pad of celite, concentrated under reduced

pressure and then purified by column chromatography (0% to 10% EtOAc in CH_2Cl_2 gradient elution) to yield rotaxane **L4** (0.070 g, 26%) as a colorless solid, and catenane **L2** (0.021 g, 14%) as a colorless solid. Analytical data for **L4**: m.p. 100 ˚C (dec.); ^{1}H NMR (400 MHz, $CDCl_3$, 300 K): δ = 1.19 (, 12H, H_{k+K+L}), 1.31 (m, 58H, H_{i+J}), 1.42 (m, 4H, H_l), 1.49 (m, 4H, H_j), 1.63 (m, 4H, H_I), 1.80 (m, 4H, H_D), 2.53 (m, 4H, H_E), 2.60 (m, 4H, H_c), 2.68 (m, 4H, H_C), 3.48 (t, J = 6.7 Hz, 4H, H_d), 3.80 (t, J = 6.5 Hz, 4H, H_H), 6.54 (m, 8H, H_{e+G}), 6.79 (d, J = 8.5 Hz, 4H, H_F), 6.84 (m, 4H, H_{b+B}), 6.98 (d, J = 8.9 Hz, 4H, H_f), 7.10 (d, J = 8.6 Hz, 12H, H_g), 7.24 (d, J = 8.6 Hz, 12H, H_h), 7.33 (t, J = 7.7 Hz, 1H, H_A), 7.40 (t, J = 7.6 Hz, 1H, H_a); ^{13}C NMR (100 MHz, $CDCl_3$, 300 K): δ = 25.7, 25.8, 28.8, 29.1, 29.6, 29.7, 29.8, 31.4, 32.9, 34.3, 34.3, 35.3, 38.5, 63.0, 67.1, 67.4, 113.0, 114.3, 119.6, 119.6, 124.0, 129.1, 130.7, 132.0, 133.8, 133.9, 136.2, 136.5, 139.0, 144.3, 148.2, 156.8, 156.9, 161.6; LRFAB-MS (3-NOBA matrix): *m/z* = 1710 $[MH]^+$; HRFAB-MS (3-NOBA matrix): *m/z* = 1711.184 (calcd. $C_{120}{}^{13}C_2H_{152}N_2O_4$ 1711.182).

Table 4.1. Crystal data and structure refinement for [(**L2**)Au]SbF_6.

CCDC-680077		
Identification code	[(**L2**)Au]SbF_6	
Empirical formula	$C_{66}H_{86}AuF_6N_2O_4Sb$	
Formula weight	1404.08	
Temperature	93(2) K	
Wavelength	1.54178 Å	
Crystal system	Orthorhombic	
Space group	Pbca	
Unit cell dimensions	a = 17.008(2) Å	α = 90°.
	b = 19.798(2) Å	β = 90°.
	c = 36.675(5) Å	γ = 90°.
Volume	12349(3) $Å^3$	
Z	8	
Density (calculated)	1.510 Mg/m^3	
Absorption coefficient	8.418 mm^{-1}	
F(000)	5696	
Crystal size	0.1000 × 0.1000 × 0.0300 mm^3	
Theta range for data collection	2.41 to 68.61°.	
Index ranges	$-19 \le h \le 19$, $-23 \le k \le 23$, $-44 \le l \le 43$	
Reflections collected	159948	
Independent reflections	11303 [R(int) = 0.0996]	
Completeness to theta = 66.50°	99.7%	
Absorption correction	Multiscan	
Max. and min. transmission	1.0000 and 0.6555	
Refinement method	Full-matrix least-squares on F^2	
Data / restraints / parameters	11303 / 4 / 722	
Goodness-of-fit on F^2	1.213	
Final R indices [I>2sigma(I)]	R1 = 0.0794, wR2 = 0.1818	
R indices (all data)	R1 = 0.0984, wR2 = 0.1958	
Largest diff. peak and hole	0.688 and -1.777 $e.Å^{-3}$	

Table 4.2. Crystal data and structure refinement for H_2**L2**$(OTs)_2$.

CCDC-682689	
Identification code	H_2**L2**$(OTs)_2$
Empirical formula	$C_{80}H_{106}N_2O_{12}S_2$
Formula weight	1351.79
Temperature	93(2) K
Wavelength	0.71073 Å
Crystal system	Monoclinic
Space group	C2/c
Unit cell dimensions	a = 38.606(5) Å $\alpha = 90°$.
	b = 10.9310(13) Å $\beta = 108.412(8)°$.
	c = 19.303(3) Å $\gamma = 90°$.
Volume	7729.0(17) $Å^3$
Z	4
Density (calculated)	1.162 Mg/m^3
Absorption coefficient	0.128 mm^{-1}
F(000)	2912
Crystal size	0.200 × 0.200 × 0.100 mm^3
Theta range for data collection	1.94 to 25.35°.
Index ranges	$-45 < h \leq 45$, $-13 \leq k < 13$, $-21 \leq l \leq 23$
Reflections collected	33273
Independent reflections	6961 [R(int) = 0.1880]
Completeness to theta = 25.00°	98.9%
Absorption correction	Multiscan
Max. and min. transmission	1.0000 and 0.9223
Refinement method	Full-matrix least-squares on F^2
Data / restraints / parameters	6961 / 3 / 448
Goodness-of-fit on F^2	1.243
Final R indices [I>2sigma(I)]	R1 = 0.2011, wR2 = 0.3766
R indices (all data)	R1 = 0.2128, wR2 = 0.3831
Extinction coefficient	0.0018(3)
Largest diff. peak and hole	0.586 and -0.533 $e.Å^{-3}$

4.4 References and Notes

[1] For reviews on the metal template synthesis of mechanically interlocked molecules, see: a) *Molecular Catenanes, Rotaxanes and Knots: A Journey Through the World of Molecular Topology* (Eds.: J.-P. Sauvage, C. Dietrich-Buchecker), Wiley-VCH, Weinheim, **1999**; b) T. J. Hubin, D. H. Busch, *Coord. Chem. Rev*. **2000**, *200–202*, 5–52; c) J.-P. Collin, C. Dietrich-Buchecker, P. Gaviña, M. C. Jiménez-Molero, J.-P. Sauvage, *Acc. Chem. Res*. **2001**, *34*, 477–487; d) S. K. Menon, T. B. Guha, Y. K. Agrawal, *Rev. Inorg. Chem*. **2004**, *24*, 97–133; e) S. J. Cantrill, K. S. Chichak, A. J. Peters, J. F. Stoddart, *Acc. Chem. Res.* **2005**, *38*, 1–9.

[2] For "active" metal template rotaxane synthesis, in which the metal acts as both a template and a catalyst for covalent bond formation and thus generally changes oxidation state, coordination number and/or geometry during the reaction, see: a) V. Aucagne, K. D. Hänni, D. A. Leigh, P. J. Lusby, D. B. Walker, *J. Am. Chem. Soc.* **2006**, *128*, 2186–2187; b) S. Saito, E. Takahashi, K. Nakazono, *Org. Lett*. **2006**, *8*, 5133–5136; c) J. Berná, J. D. Crowley, S. M. Goldup, K. D. Hänni, A.-L. Lee, D. A. Leigh, *Angew. Chem*. **2007**, *119*, 5811–5815; *Angew. Chem. Int. Ed*. **2007**, *46*, 5709–5713; d) V. Aucagne, J. Berná, J. D. Crowley, S. M. Goldup, K. D. Hänni, D. A. Leigh, P. J. Lusby, V. E. Ronaldson, A. M. Z. Slawin, A. Viterisi, D. B. Walker, *J. Am. Chem. Soc.* **2007**, *129*, 11950–11963; e) J. D. Crowley, K. D. Hänni, A.-L. Lee, D. A. Leigh, *J. Am. Chem. Soc*. **2007**, *129*, 12092–12093; f) S. M. Goldup, D. A. Leigh, P. J. Lusby, R. T. McBurney, A. M. Z. Slawin, *Angew. Chem*. **2008**, *120*, 3429–3432; *Angew. Chem. Int. Ed*. **2008**, *47*, 3381–3384; g) J. Berná, S. M. Goldup, A.-L. Lee, D. A. Leigh, M. D. Symes, G. Teobaldi, F. Zerbetto, *Angew. Chem*. **2008**, *120*, 4464–4468; *Angew. Chem. Int. Ed*. **2008**, *47*, 4392–4396.

[3] a) C. O. Dietrich-Buchecker, J.-P. Sauvage, J.-M. Kern, *J. Am. Chem. Soc.* **1984**, *106*, 3043–3045; b) C. Dietrich-Buchecker, J.-P. Sauvage, J.-M. Kern, *J. Am. Chem. Soc*. **1989**, *111*, 7791–7800; c) N. Armaroli, V. Balzani, J.-P. Collin, P. Gaviña, J.-P. Sauvage, B. Ventura, *J. Am. Chem. Soc.* **1999**, *121*, 4397–4408; d) L. Raehm, J.-M. Kern, J.-P. Sauvage, *Chem.–Eur. J.* **1999**, *5*, 3310–3317.

[4] a) J.-C. Chambron, A. Harriman, V. Heitz, J.-P. Sauvage, *J. Am. Chem. Soc.* **1993**, *115*, 6109–6114; b) M. Andersson, M. Linke, J.-C. Chambron, J. Davidsson, V. Heitz, L. Hammarström, J.-P. Sauvage, *J. Am. Chem. Soc*. **2002**, *124*, 4347–4362; c) P. Mobian, J.-M. Kern, J.-P. Sauvage *Angew. Chem.* **2004**, *116*, 2446–2449; *Angew. Chem. Int. Ed.* **2004**, *43*, 2392–2395; d) J.-P. Collin, D. Jouvenot, M. Koizumi, J.-P. Sauvage *Eur. J. Inorg. Chem.* **2005**, 1850–1855; e) P. H. Kwan, T. M. Swager, *J. Am. Chem. Soc*. **2005**, *127*, 5902–5909; f) S. Bonnet, J.-P. Collin, *Chem. Soc. Rev.* **2008**, *37*, 1207–1217.

[5] a) C. O. Dietrich-Buchecker, J.-M. Kern, J.-P. Sauvage, *J. Chem. Soc., Chem. Commun.*, **1985**, 760-762; b) A.-M. Albrecht-Gary, Z. Saad, C. O. Dietrich-Buchecker, J.-P. Sauvage, *J. Am. Chem. Soc.* **1985**, *107*, 3205–3209. c) A.-M. Albrecht-Gary, Z. Saad, C. Dietrich-Buchecker, J.-P. Sauvage, *J. Am. Chem. Soc.* **1988**, *110*, 1467–1472. d) D. A. Leigh, P. J. Lusby, A. M. Z. Slawin, D. B. Walker, *Angew. Chem.* **2005**, *117*, 4633-4640; *Angew. Chem. Int. Ed.* **2005**, *44*, 4557–4564.

[6] F. A. Arnaud-Neu, E. Marques, M.-J. Schwing-Weill, C. O. Dietrich-Buchecker, J.-P. Sauvage, J. Weiss, *New J. Chem.* **1988**, *12*, 15–20.

[7] a) B. Champin, P. Mobian, J.-P. Sauvage, *Chem. Soc. Rev.* **2007**, *36*, 358–366; b) E. R. Kay, D. A. Leigh, F. Zerbetto, *Angew. Chem.* **2007**, *119*, 72–196; *Angew. Chem. Int. Ed.* **2007**, *46*, 72–191.

[8] a) D. A. Leigh, P. J. Lusby, S. J. Teat, A. J. Wilson, J. K. Y. Wong, *Angew. Chem.* **2001**, *113*, 1586–1591; *Angew. Chem. Int. Ed.* **2001**, *40*, 1538–1543; b) L. Hogg, D. A. Leigh, P. J. Lusby, A. Morelli, S. Parsons, J. K. Y. Wong, *Angew. Chem.* **2004**, *116*, 1238–1241; *Angew. Chem. Int. Ed.* **2004**, *43*, 1218–1221; c) M. Hutin, C. A. Schalley, G. Bernardinelli, J. R. Nitschke, *Chem.–Eur. J.* **2006**, *12*, 4069–4076.

[9] a) C. O. Dietrich-Buchecker, J.-P. Sauvage, J.-P. Kintzinger, *Tetrahedron Lett.* **1983**, *24*, 5095–5098; b) J.-P. Sauvage, *Acc. Chem. Res.* **1990**, *23*, 319–327; c) A.-M. L. Fuller, D. A. Leigh, P. J. Lusby, *Angew. Chem.* **2007**, *119*, 5103–5107; *Angew. Chem. Int. Ed.* **2007**, *46*, 5015–5019.

[10] a) M. C. Jiménez, C. Dietrich-Buchecker, J.-P. Sauvage, *Angew. Chem.* **2000**, *112*, 3422–3425; *Angew. Chem. Int. Ed.* **2000**, *39*, 3284–3287; b) M. C. Jiménez-Molero, C. Dietrich-Buchecker, J.-P. Sauvage, *Chem.–Eur. J.* **2002**, *8*, 1456–1466.

[11] B. Mohr, M. Weck, J.-P. Sauvage, R. H. Grubbs, *Angew. Chem.* **1997**, *109*, 1365-1367; *Angew. Chem., Int. Ed. Engl.* **1997**, *36*, 1308–1310.

[12] a) J.-P. Sauvage, M. Ward, *Inorg. Chem.* **1991**, *30*, 3869–3874; b) C. Piguet, G. Bernardinelli, A. F. Williams, B. Bocquet, *Angew. Chem.* **1995**, *107*, 618–621; *Angew. Chem., Int. Ed. Engl.* **1995**, *34*, 582–584; c) P. Mobian, J.-M. Kern, J.-P. Sauvage, *J. Am. Chem. Soc.* **2003**, *125*, 2016–2017; d) F. Arico, P. Mobian, J.-M. Kern, J.-P. Sauvage, *Org. Lett.* **2003**, *5*, 1887–1890; e) J.-C. Chambron, J.-P. Collin, V. Heitz, D. Jouvenot, J.-M. Kern, P. Mobian, D. Pomeranc, J.-P. Sauvage, *Eur. J. Org. Chem.* **2004**, 1627–1638.

[13] a) A.-M. Fuller, D. A. Leigh, P. J. Lusby, I. D. H. Oswald, S. Parsons, D. B. Walker, *Angew. Chem.* **2004**, *116*, 4004–4008; *Angew. Chem. Int. Ed.* **2004**, *43*, 3914–3918; b) Y. Furusho, T. Matsuyama, T. Takata, T. Moriuchi, T. Hirao, *Tetrahedron Lett.* **2004**, *45*, 9593–9597; c) A.-M. L. Fuller, D. A.

Leigh, P. J. Lusby, A. M. Z. Slawin, D. B. Walker, *J. Am. Chem. Soc*. **2005**, *127*, 12612–12619.

[14] C. Hamann, J.-M. Kern, J.-P. Sauvage, *Inorg. Chem*. **2003**, *42*, 1877–1883.

[15] Multiple Au···Au interactions have been used to drive the assembly of catenanes in which gold ions form an integral part of each ring: a) D. M. P. Mingos, J. Yau, S. Menzer, D. J. Williams, *Angew. Chem.* **1995**, *107*, 2045–2047; *Angew. Chem. Int. Ed. Engl.* **1995**, *34*, 1894–1895; b) C. P. McArdle, M. J. Irwin, M. C. Jennings, R. J. Puddephatt, *Angew. Chem.* **1999**, *111*, 3571–3573; *Angew. Chem. Int. Ed.* **1999**, *38*, 3376–3378; c) M. R. Wiseman, P. A. Marsh, P. T. Bishop, B. J. Brisdon, M. F. Mahon, *J. Am. Chem. Soc.* **2000**, *122*, 12598–12599; d) W. W. H. Wong, J. Cookson, E. A. L. Evans, E. J. L. McInnes, J. Wolowska, J. P. Maher, P. Bishop, P. D. Beer, *Chem. Commun.* **2005**, 2214–2216; e) S. S.-Y. Chui, R. Chen, C.-M. Che, *Angew. Chem.* **2006**, *118*, 1651–1654; *Angew. Chem. Int. Ed.* **2006**, *45*, 1621–1624.

[16] Gold(III) porphyrins have been used as 'stopper' units in rotaxanes, see: J.-C. Chambron, V. Heitz, J.-P. Sauvage, *J. Chem. Soc., Chem. Commun.* **1992**, 1131–1133.

[17] For recent examples of aryl-Au constructs, see: a) D. V. Partyka, M. Zeller, A. D. Hunter, T. G. Gray *Angew. Chem*. **2006**, *118*, 8368–8371; *Angew. Chem. Int. Ed*. **2006**, *45*, 8188–8191; b) W. Y. Heng, J. Hu, J. H. K. Yip, *Organometallics*, **2007**, *26*, 6760–6768.

[18] a) S. A. Brawner, I. J. B. Lin, J.-H. Kim, G. W. Everett, *Inorg. Chem*. **1978**, *17*, 1304–1308; b) J.-H. Kim, G. W. Everett, *Inorg. Chem*. **1979**, *18*, 3145–3149; b) J.-H. Kim, G. W. Everett, *Inorg. Chem*. **1981**, *20*, 853–856.

[19] a) *Gold: Progress in Chemistry, Biochemistry, and Technology* (Ed.: H. Schmidbaur), Wiley-VCH, Chichester, **1999**; b) V. W.-W. Yam, E. C.-C. Cheng, *Angew. Chem*. **2000**, *112*, 4410–4412; *Angew. Chem. Int. Ed*. **2000**, *39*, 4240–4242; c) S.-Y. Yu, Q.-F. Sun, T. K.-M. Lee, E. C.-C. Cheng, Y.-Z. Li, V. W.-W. Yam, *Angew. Chem*. **2008**, *120*, 4627–4630; *Angew. Chem. Ed.***2008**, *47*, 4551–4554**.**

[20] *Metal-Catalyzed Cross-Coupling Reactions*, *Vol. 1*, Completely Revised and Enlarged, 2nd ed. (Eds.: A. de Meijere, F. Diederich), Wiley-VCH, Weinheim, **2004**.

[21] The crystal data and experimental details of the structural refinement for [(**L2**)Au]SbF_6 and H_2**L2**$(OTs)_2$ are provided in the Supporting Information. CCDC-680077 and CCDC-682689 contain the supplementary data for this paper. These data can be obtained free of charge from the Cambridge Crystallographic Data Centre via www.ccdc.cam.ac.uk/data_request/cif.

[22] G. Schill, *Catenanes, Rotaxanes and Knots*, Academic Press, New York, **1971**.

Appendix

Published Papers

"Active metal template synthesis of rotaxanes, catenanes and molecular shuttles", James D. Crowley, Stephen M. Goldup, Ai-Lan Lee, David A. Leigh and Roy T. McBurney, *Chem. Soc. Rev.*, **2009**, DOI: 10.1039/b804243h.

"Getting Harder: Cobalt(III)-Template Synthesis of Catenanes and Rotaxanes", David A. Leigh, Paul J. Lusby, Roy T. McBurney, Alessandra Morrelli, Alexandra M. Z. Slawin, Andrew R. Thomson and D. Barney Walker, *J. Am. Chem. Soc.* **2009**, *131*, 3762-3771.

"Active Template Synthesis of Rotaxanes and Molecular Shuttles with Switchable Dynamics via Four-Component Pd(II)-Promoted Michael Additions", Stephen M. Goldup, David A. Leigh, Paul J. Lusby, Roy T. McBurney and Alexandra M. Z. Slawin, *Angew. Chem. Int. Ed.* **2008**, *43*, 3381-3384.

Cover picture: "*Gold(I) Template Catenane and Rotaxane Synthesis*", Stephen M. Goldup, David A. Leigh, Paul J. Lusby, Roy T. McBurney and Alexandra M. Z. Slawin, *Angew. Chem. Int. Ed.* **2008**, *47*, 6925.

"*Gold(I) Template Catenane and Rotaxane Synthesis*", Stephen M. Goldup, David A. Leigh, Paul J. Lusby, Roy T. McBurney and Alexandra M. Z. Slawin, *Angew. Chem. Int. Ed.* **2008**, *47*, 6999-7003.